The Influence of Anthropogenic Climate Change on the 2015–2017 Hydrological Drought in the South-Western Cape, South Africa.

by

Andrew Hall

Supervised by:

Professor Mark New

Dr Piotr Wolski

A dissertation submitted in fulfilment of the requirements for

the degree of

Master of Science

in the
Department of Environmental and Geographical Science
Faculty of Science
University of Cape Town
September 2020

DECLARATION

I know the meaning of plagiarism and declare that all of the work in the dissertation, save for that which is properly acknowledged, is my own.

Signature: Signed by candidate

Date: 7 September 2020.

ACKNOWLEDGEMENTS

This dissertation would not have been possible without the support and guidance of a number of people whose contributions I thankfully acknowledge. First and foremost, I would like to sincerely express my gratitude and thanks to my supervisors Professor Mark New and Dr Piotr Wolski, for their patience, unwavering support, guidance, and extensive expertise throughout this dissertation. I would also like to thank the National Research Foundation of South Africa and the AXA chair in African climate risks for the funding provided throughout this dissertation.

A huge thank you to all of the African Climate and Development Initiative (ACDI) staff and a special thanks to Zoe Boshoff, Roland Hunter and Rabia Karriem for all the motivation, support and opportunities provided. To my lab partners: Nivedita, Luleka, Sesethu, Makeya, Lavinia and the AXA climate risk research team based at the University of Cape Town: Petra, Romaric, Joyce, and Tiro thank you for all the knowledge shared and support.

I would like to thank my family Julian and Michelle and, Geneviev for their unwavering love, support and encouragement throughout this dissertation.

This dissertation is dedicated to my Father and Mother, who have driven and encouraged me to continuously improve myself through education.

TABLE OF CONTENTS

LIST OF ACRONYMS

AAO Antarctic Oscillation

AR5 Fifth Assessment Report

BRC Berg River catchment

CMIP5 Coupled Model Intercomparison Project 5

CoCT City of Cape Town

CRU Climate Research Unit-Timeseries

ENSO El Niño Southern Oscillation

FAR Fractional attributable risk

GCM Global climate model

GEV Generalized extreme value

GHG Greenhouse gas

GMST Global mean surface temperature

IPCC Intergovernmental Panel on Climate Change

ITCZ Inter-tropical Convergence Zone

MAE Mean annual evaporation

MAP Mean annual precipitation

MAR Mean annual runoff

NSE Nash and Sutcliffe Efficiency

NWA National Water Act

P_0 Pre-industrial world

P_1 Current world

PBIAS Percent bias

PDF Probability density function

PDSI Palmer Drought Severity Index

PEA Probability event attribution

RCP Representative Concentration Pathway

RR Risk ratio

SAM South Annular Mode

SAWS South African Weather Services

SDGs Standard Development Goals

SIOD Subtropical Indian Ocean Dipole

SPEI Standard Precipitation Evapotranspiration Index

SPI Standardized Precipitation Index

SRES Special Report on Emissions Scenario

SST Sea-Surface Temperature

SWC South-Western Cape

WCWSS Western Cape Water Supply System

WR, 2012 Water Resources, 2012 study

LIST OF FIGURES

LIST OF TABLES

ABSTRACT

The Western Cape Province in South Africa recently experienced below-average rainfall during the period 2015−2017, this resulted in a three-year compound hydro-meteorological drought event in the Province. The 2015−2017 Western Cape hydro-meteorological drought was the worst drought event since 1904 and caused severe unprecedented water shortages throughout the Western Cape region, with many municipal water supply systems close to failure by the first quarter of 2018; most especially the Western Cape Water Supply System that serves Cape Town. The drought gained a lot of interest from the public, media and climate scientists alike. The main aim of this study was to assess the extent to which human influence on climate from fossil fuel emissions has changed the likelihood of a hydro-meteorological drought event with the magnitude of that experienced in 2015−2017 in the South-Western Cape.

The Pitman hydrological model was set up for the Berg River catchment in a way that enabled multiple simulations with different rainfall inputs so that attribution experiments could be undertaken. The key differences to the standard Pitman model set up included: (i) constant abstractions, return flows, and land use conditions; (ii) reservoir and dam storages were set to reflect current storage volumes; and (iii) extending the observed rainfall inputs to include the drought period. A hydrological model evaluation was then undertaken, using updated streamflow gauging station data, to assess the ability of the Pitman model to realistically simulate runoff in the Berg River catchment. The model was deemed suitable for the purposes of this study in simulating runoff.

To generate the climate attribution experiments, Coupled Model Intercomparison Project Phase 5 historical simulations (1861−2010) were merged with the Representative Concentration Pathway 8.5 greenhouse gas scenario simulations (2011−2100) of rainfall from 77 simulations From 42 models to create a long-term (150 years) time series. Attribution experiments were constructed by considering the average conditions in the 31 year period centred on the years of the event, i.e. 2002−2031 to represent current climate conditions and the period 1861−1890 to represent pre-industrial climate conditions. Five 150-year long stochastic time series of rainfall for each individual simulation were then generated conditioned on observed rainfall characteristics this was done to increase the sample size of the models available. These stochastic rainfall time series were then used as input to the Pitman model to generate outputs/realisations of runoff for a pre-industrial and current world; thus generating impact attribution experiments.

To determine the role of anthropogenic climate change on the 2015−2017 hydro-meteorological drought in the South-Western Cape the risk-based approach was applied to the rainfall and runoff attribution outputs. The 2015−2017 meteorological/hydrological drought event was defined in terms of three-year mean annual rainfall/runoff received in the Berg River catchment and its individual 12 quaternary catchments. This event definition was used as a rainfall/runoff threshold in the attribution analysis for the 2015−2017 meteorological/hydrological drought in the South-Western Cape. The three-year minimum averages of rainfall/runoff were identified in each of the 150-year stochastic time series generated from the 77 simulations; resulting in 385 values for both current and pre-industrial climates for rainfall and runoff. A normal distribution was then fitted to the 385 values of the current and pre-industrial rainfall/runoff. From this distribution, the probability of the current rainfall/runoff occurring, based on the defined threshold, was identified and compared to the pre-industrial time series to calculate the risk ratios of the Berg River catchment and its 12 quaternary catchments.

Results show that the risk of the meteorological drought event occurring in the Berg River catchment was increased by a factor of 28.5, 95% confidence interval: 26.0−32.4, (but ranged from 11.5−41.0 in the individual quaternary catchments) due to anthropogenic climate change. The occurrence of the hydrological drought event in the Berg River catchment was found to be increased by a factor of 12.9, 95% confidence interval: 11.3−13.5 (2.7−61.0 in the quaternary catchments) due to anthropogenic

climate change. The risk ratio for runoff was higher than for rainfall in the wetter southern quaternary catchments, while it was lower than for rainfall in the drier more northern quaternary catchments. Thus, the human influence on meteorological drought appears to have been amplified in those catchments most important to the Western Cape Water Supply System.

CHAPTER 1: INTRODUCTION AND BACKGROUND TO THE STUDY

1.1 Introduction

Extreme climate events are of great societal interest as they have a substantial adverse effect on people and property (Sheperd, 2016). Globally, droughts are one of the most devastating natural disasters (Seneviratne et al., 2012; Dai, 2013). According to the International Disaster Database (EM-DAT, 2017), global drought events have resulted in the deaths of more than 11.7 million people and affected nearly 2.7 billion people between 1900–2017. The number of deaths caused by droughts globally has increased in recent times from 2 118 (1996–2005) to 20 177 (2006–2015) (CRED, 2016). Socio-economic impacts of drought tend to be more severe in regions that receive rainfall of 500 mm annually and less (WRC, 2015). Annually, global gross domestic product (GDP) losses due to drought events are estimated at an average of US$ 109 billion (WRG, 2012). Developing economic regions, such as southern Africa, are particularly vulnerable to the impacts of drought as a wide range of socio-economic activities depend greatly on rain-fed agriculture, water resources and hydropower, and business (Meque and Abiodun, 2015; Gannon et al., 2018). South Africa has an annual rainfall amount of 480 mm, making the country particularly prone to severe drought events and the resultant socio-economic impacts (WRC, 2015). During the 2013/2014 financial year, extreme climatic-related events cost the insurance industry in South Africa over R1 billion (Uys, 2014). The frequency and the magnitude of drought, other extreme climate events and high wind velocities are projected to increase in South Africa in the next century as a result of projected increases in temperature, changes in rainfall and future climate variability (Schulze, 2012; DEA, 2013; El Chami and El Moujabber, 2016). The year 2015 experienced unprecedentedly dry and hot weather, the driest weather experienced in over a century across different regions of South Africa (SAWS, 2015a; SAWS, 2015b).

Drought is usually characterised by a decrease in seasonal or annual rainfall and may result in crop loss and failure, economic inflation, power outages and several other adverse effects within a region (Boken et al., 2005). The Western Cape Province in South Africa has recently experienced one of the worst droughts in recorded history. By the end of the 2017 rainfall season (the end of October) the cumulative volume of the six major dams, which make up 96.6% of stored water resource in the Western Cape Water Supply System (WCWSS), were at 38.4% (2017); in comparison to 60.3% (2016), 77.1% (2015), and 97.0% (2014) (CoCT, 2017). Due to the extremity of the drought, the City of Cape Town (CoCT) began to prepare for what it termed “Day-Zero”: a failure of the city’s entire water system. The Western Cape Province is particularly susceptible to several climate-related risks, including: i) droughts; ii) floods; iii) heavy rain; iv) storms; and v), wildfires, which are naturally occurring features of the Western Cape climate. Climate change projections for the Province indicate an increased risk of more frequent and intense extreme climatic events that drive these risks (WCDoA, 2016). Between 2003 and 2008, direct damage related to climatic extreme events cost the Western Cape Province an estimated 3.16 billion Rand (Pharoah, et al., 2016).

Currently, addressing the impacts associated with a changing climate is one of the most crucial challenges globally for human society, particularly that of anthropogenic climate change (Stott et al., 2016; Easterling et al., 2016). Drought and other extreme climate events are rare by definition and are a naturally occurring part of the climate system; however, a continual change in climate presents a change in risks, either increasing or decreasing, related to climate extremes (Otto et al., 2015; Easterling et al., 2016). Reducing the risks associated with climate change requires consideration of vulnerability, exposure and sensitivity to climate-related hazards (Stott et al., 2016).

According to the Synthesis Report (2014) of the Intergovernmental Panel on Climate Change (IPCC), the influence of anthropogenic climate change on the climate system is clear and changes in the

number of extreme weather and climate events have been detected since 1950. According to Seneviratne et al. (2012: 111), an extreme event is defined as 'the occurrence of a value of a weather or climate variable above (or below) a threshold value near the upper (or lower) ends of the range of observed values of the variable'.

There is a great desire to attribute the occurrence of extreme events to anthropogenic climate change. However, attributing the occurrence of an event solely to climate change can be misleading as both anthropogenic climate change and the climate system's natural variability are invariably contributing factors to the occurrence and magnitude of a given extreme event (Trenberth et al., 2015; Stott et al., 2016). Extreme event attribution is a relatively new field of science. According to Hergerl et al (2010: 2), attribution is 'the process of evaluating the relative contributions of multiple causal factors to a change or event with an assignment of statistical confidence'. Several types of general attribution studies exist, such as: attribution of trends in climate variables; attribution of changes in extremes; attribution of weather or climate events; attribution of climate-related impacts (Knutson et al., 2017).

Event attribution studies aim to quantify the extent to which anthropogenic or natural forcing has affected the likelihood or magnitude of a given extreme climate event, such as a hydrological drought (Stott et al., 2016). Attribution of anthropogenic climate change involves evaluating the causes of observed changes in the climate system or to a unique climatic event using a methodical comparison of climate models and observations through the use of different statistical approaches (Easterling, 2016; Knutson et al., 2017).

In the southern Africa region, there is medium confidence that the projected duration and intensity of hydrological drought events will increase in some regions as a result of climate change (Seneviratne et al., 2012). Many continental- and global-scale studies of observed and potential changes on hydro-meteorological drought indicators have been done, yet, very few studies have been undertaken on measures of water resources drought or drought impacts, and even fewer that attempt to attribute the causes of drought or its impacts (Handmer et al., 2012).

Globally, the impacts of recent regional climate change on both natural and human systems have been well documented (Cramer et al. 2014). However, there is a lack of studies that explicitly link these observations to anthropogenic forcing of the climate (Hansen and Stone, 2016). Impact attribution studies investigate the connection between attribution sciences to observed impacts to inform risk management (Hansen and Stone, 2016; Herring et al., 2016).

This study aims to help fill the knowledge gap and understanding in impact attribution science in the southern African region and is the first to investigate hydrological impact attribution of a compound drought event in southern Africa. This will be done by evaluating the role of anthropogenic climate change in the rainfall and runoff amounts received in the Berg River catchment (BRC), which is a key source of water in the WCWSS, during the 2015–2017 drought. This study attempts to quantify only the impact of human induced climate change impact on the hydrological system. This is done by the use of a hydrological model; by using a hydrological model it is possible to keep human activities that affect runoff constant and only analyse the impact of climate change on runoff. In this sense, the study can be considered an impact attribution study. For drought attribution to climate change, very few attribution studies exist that use a combination of large multiple model ensembles and full hydrologic model simulations (NSM, 2016).

1.2 Aim

The aim of this study was to determine the extent to which anthropogenic climate change has contributed to the likelihood of the 2015–2017 hydro-meteorological drought event in the South-

Western Cape (SWC). As such this study is one of the first to do an end-to-end (i.e. emissions to runoff) multi-step attribution analysis of a multi-year drought event in South Africa, and indeed globally.

I. The study asks the following specific research question: To what extent has human interference on the climate changed the risk of the 2015–2017 hydro-meteorological drought in the SWC?

1.3 Objectives

To answer the above research question, the study has the following step by step specific objectives:

I. To set up the Pitman hydrological model to realistically simulate hydrological responses in the BRC driven by attribution experiment data from global climate model (GCM) simulations.
II. To generate attribution inputs for the model from GCM simulations.
III. To implement attribution experiments with the Pitman model setup for the BRC.
IV. To analyse the attribution outputs and assess possible reasons for variation in risk ratio across the Berg River quaternary catchments.

1.4 Structure of the Dissertation

The remainder of this dissertation is structured as follows: the literature review (Chapter 2), encompasses a synthesis of the literature on drought and climate change, event attribution and methodologies, hydrological modelling, downscaling and, uncertainties in hydrological and GCM's. This is followed by Chapter 3 which describes the study area, data and, methodologies used in the study. Chapter 4 goes on to analyse and discuss rainfall and runoff during the drought event, evaluation of the hydrological model, and the attribution results produced. This leads into the final chapter, Chapter 5, which provides a summary along with conclusions and discussion of limitations of the study.

CHAPTER 2: LITERATURE REVIEW

This chapter presents an overview of the types of drought, drought indices and metrics, and the current issues linked to global and national water resources as a result of climate change. The chapter also provides a detailed description of the current water security issues caused by drought and its associated impacts; focusing on previous drought events in South Africa and the 2015–2017 Western Cape drought. A detailed description of the projected hydrological impacts of climate change in South Africa, and particularly in the SWC, is provided by reviewing previously undertaken national and regional studies in South Africa. The Chapter goes on to describe attribution, from a general sense, before focusing on the status of event attribution in Africa and impact attribution, as well as methodologies of extreme event attribution. A brief introduction of hydrological models and types of hydrological models is also provided. The chapter then goes on to describe the uncertainties linked to the use of running hydrological models with GCM data, and a brief overview of the evaluation of hydrological models and GCM's in climate impact studies.

2.1 Global Water Resources and Climate Change

Water has a central role in human societies and is critical for human health, development and well-being (Grey and Sadoff, 2007; du Plesis, 2017). Beyond the function of water within the hydrological cycle of the Earth's system, the resource has social, economic and environmental value, and is necessary for sustainable development (UNESCO, 2011). Two of the 17 Sustainable Development Goals (SDGs), adopted by the United Nations in 2015, focus on water (Hering et al., 2016). This includes Goal 6, which aims to ensure access to water and sanitation for everybody; and Goal 14, which calls for conservation and sustainable use of the oceans, seas and marine resources (UN, 2017). Water is used as an input to almost all production in: agriculture, energy, industry and transport sectors (Grey and Sadoff, 2007). Water is distributed unevenly across the globe and the availability of the resource is becoming an increasingly great concern; particularly in North Africa and the Middle East (du Plesis, 2017). Global change has a significant impact on the quality and quantity of water resources, the main drivers of global change are population growth, urbanisation, climate change, infrastructure development, migration, land changes and pollution (UNESCO, 2011). The aforementioned drivers of global change contribute to increasing demands and pressure on freshwater resources (UNESCO, 2011; WEF, 2014). In 2016, the World Economic Forum ranked global water crises as the highest risk and one of the greatest threats facing mankind within the next decade (WEF, 2016).

Water scarcity emerges as a combination of hydrological variability and high human consumption (UN, 2017). Several regions around the world are already experiencing the effects of global change drivers, particularly on water resources, which has led to aquifer depletion, water pollution, food insecurity, water stress and ecological vulnerability among other negative impacts (UNESCO, 2011). Water is at the centre of the resource nexus, there is an ever-increasing gap between freshwater availability and water demand in many developing rapidly growing economies globally (WRG, 2012). Under a business as usual water management scenario, the world is projected to face a 40% global water deficit by 2030 (WRG, 2012).

The term water security is of substantial international and political significance, as it is directly linked to SDG 6 (Steyn et al., 2019). According to the UN-Water (2013:2), water security is defined as 'the capacity of a population to safeguard sustainable access to adequate quantities of acceptable quality water for sustaining livelihoods, human well-being, and socio-economic development, for ensuring protection against water-borne pollution and water-related disasters, and for preserving ecosystems in a climate of peace and political stability'.

Water security is considered a major challenge for both science and society (Garrick and Hall, 2014). Arid and semi-arid regions face the greatest stress to deliver and manage freshwater resources across the globe (UNESCO, 2011). Water insecurity presents a threat to human well-being and ecosystem health (Garrick and Hall, 2014). Projections indicate that by 2050 an additional 2.3 billion people will live in severely water-stressed regions, particularly in north and southern Africa and, Central Asia (OECD, 2012).

2.2 Drought

This section provides a general introduction to drought, the types of drought as well as the propagation from meteorological through to agricultural droughts, with a focus on hydrological drought. Drought metrics and major drought indices are described in detail. A brief description of how climate change will change drought risk and affect water security is presented as well as a description of climatic and non-climatic drivers of drought. Understanding the differences between various types of drought and measures of severity using drought metrics and indices is important as different types of droughts and their associated severity has varying environmental and socio-economic impacts. Noting the non-climatic drivers of drought are important in attribution studies as only mentioning climatic factors that could potentially increase the frequency and magnitudes of drought events provides an incomplete picture of current and future water security.

Drought is a complex recurring natural phenomenon brought about by an extended period of dry weather due to below-average moisture levels (e.g. mean monthly rainfall, mean annual streamflow below a critical threshold or mean seasonal soil moisture) that result in critical water shortages in a region (Schulze, 2003; Gamble, 2017). Unlike aridity, which is a permanent characteristic of low rainfall regions, droughts are a temporary anomaly that can occur in both low and high rainfall regions (Gihle, 2008). Drought events are predominantly affected by precipitation and evaporation - which is a function of temperature, wind speed, solar radiation, and air humidity (Sheffield, 2012). Drought is also affected by non-atmospheric conditions which include land surface and antecedent soil moisture conditions of a region (Dai, 2011a). Unlike other natural disasters, such as floods, tropical cyclones, volcanic eruptions, earthquakes or tornados; drought is a slowly developing, or “slow onset” natural hazard and can have persistent impacts even after the drought period has ended (Vogt et al., 2011). According to Kogan (1997), nearly half of the Earth’s surface is susceptible to drought.

2.2.1 Types of Drought

By employing a working definition of drought, three main physical drought types were established: meteorological, hydrological and agricultural, as described below, (Wilhite 2000; NOAA, 2008; Gamble, 2017). Figure 1 illustrates the relationships between these three types of drought.

Meteorological drought is characterised by a departure of observed precipitation below the average amount of rainfall on a monthly, seasonal, or annual timescale (i.e. precipitation deficiencies). Generally, drought onset occurs during a meteorological drought.

Hydrological drought events typically manifest following extended periods of below-average precipitation that affect water supply. A hydrological drought represents a decrease in surface or sub-surface (streamflows, lakes, reservoirs and groundwater levels) water resources as a result of below-average seasonal rainfall, which has a direct effect on services and other human activity. A common example of a hydrologic drought is the dry conditions that lead to a decrease in urban water supply from water resources.

Agricultural drought links features of meteorological or hydrological drought to impacts on agriculture. This type of drought is characterized by deficiencies in soil moisture and/or rainfall that impact crop production and livestock.

Hydrological droughts differ significantly from both meteorological and agricultural droughts, which typically directly affect only the specific region over which they occur; in contrast, a hydrological drought can affect areas downstream of where the meteorological drought occurred, and even areas outside of the catchment, through water transfer schemes and hydropower impacts. The differences of hydrological drought in comparison to other types of drought is described further below (Schulze, 2012):

- Hydrological drought events can occur over a specific sub-catchment, however, because water flows downstream the total effect of a drought upstream of a catchment will be felt downstream of that catchment as well;
- Relatively small rainfall episodes have the potential to break both agricultural and meteorological droughts whereas a threshold of rainfall must occur before any significant runoff or groundwater recharge is produced for a hydrological drought to be broken;
- The onset of hydrological drought is slower than meteorological and agricultural drought events as streamflows are partially made up of sustained baseflows which may reach a stream a few months after the groundwater zone has been recharged; and
- During times of high flows, streamflows can be stored in reservoirs and released during times of low flow, whereas soil moisture cannot.

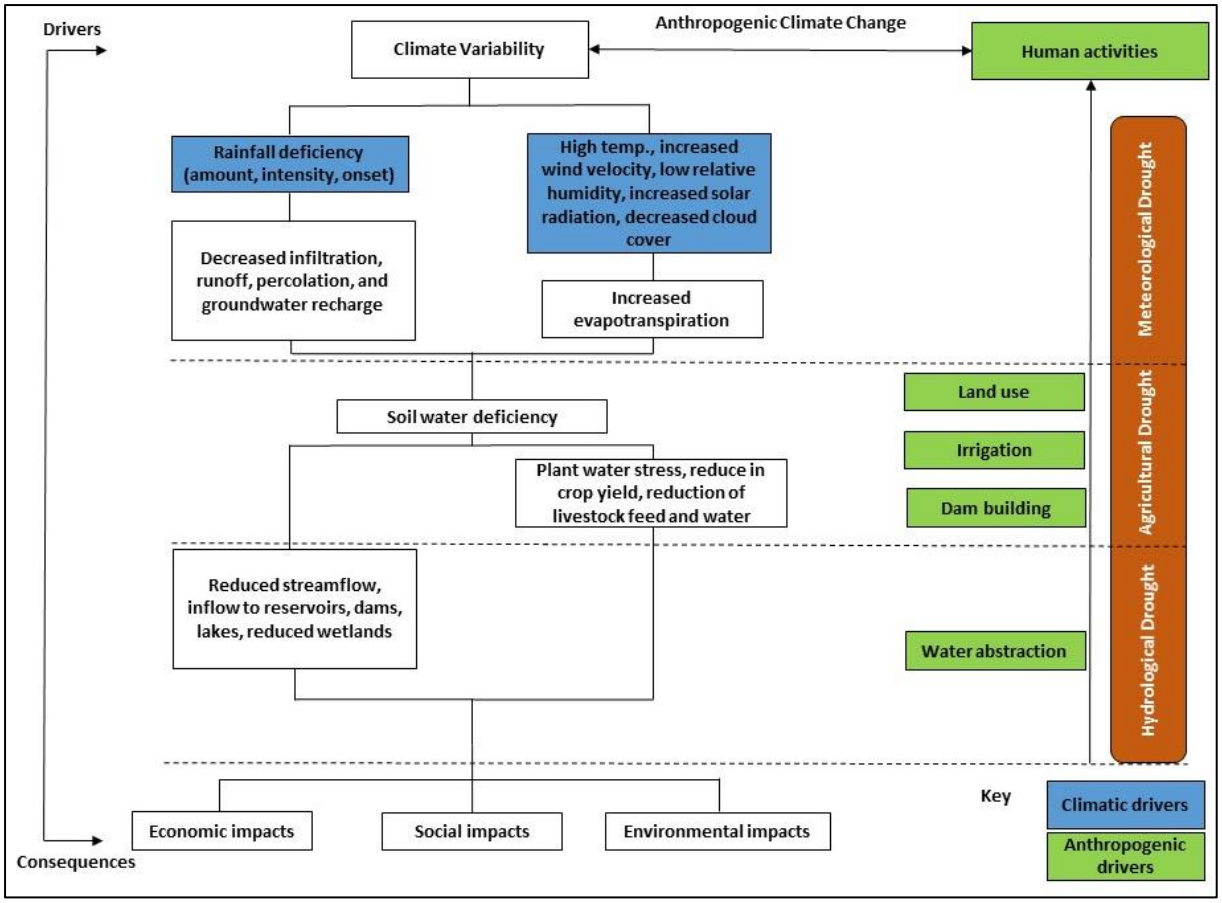

Figure 1. Propagation from meteorological to hydrological drought. (adapted from NOAA, 2008; Van Loon et al., 2016).

Large-scale decreases in precipitation, streamflow and soil moisture are often used to quantify, respectively, hydrological, agricultural and meteorological drought (Dai, 2011a). The use of different drought indices tends to result in different change patterns, particularly on small scales (Burke, 2011).

2.2.2 Drought Metrics

Owing to the complex nature of drought, a universal definition has not been agreed upon (Meque and Abiodun 2015). However, several drought indices have been developed (Heim, 2002; Dai, 2011a). Drought indices are quantitative measures that distinguish drought levels by integrating data from a single or several indicators, such as rainfall and evapotranspiration data into a single numerical value (Zargar et al., 2011). Assimilating these data variables allows for a more readily useable value as opposed to raw indicator data (Hayes, 2007). Drought indices consider several conditions and events, such as: climate dryness anomalies, soil moisture loss, and decreased reservoir levels (Zargar et al., 2011). The most widely used drought index is the Standardized Precipitation Index (SPI) developed by Mckee et al. (1993); this is due to its simplicity, as it only takes precipitation into account (Mishra et al., 2009) and is recommended by the World Meteorological Organization as the standard drought monitoring index (Hayes et al., 2011).

According to Salas (1993), droughts are typically characterized by the following dimensions:

***Duration*:** Duration of drought events, depending on the region, can range from one week to a few years. Due to the complex nature of drought, a region can simultaneously experience dry and wet spells when considering different periods.

Magnitude: The total deficit of water (i.e. rainfall, runoff, or soil moisture) below a given threshold within a drought period.

Intensity: The ratio of drought magnitude to the duration of the drought.

Severity**:** The extent of the lack of rainfall or the extent of impacts as a result of the deficit.

Geographic extent: The areal extent of the drought event. The area can include one or numerous pixels, catchments or regions.

Frequency*:* This is described as the average time between drought events that have a severity that is larger than or equal to a predefined threshold.

Along with precipitation deficit, other variables such as streamflow and evapotranspiration are used to comprehensively characterize drought (Zargar et al., 2011). Drought indicators (hydrological, meteorological, or supply-and-demand) are used in combination with various water balance or hydrological models, to develop a drought index (Zargar et al., 2011).

Effectively, drought indices serve the following purposes (Niemeyer, 2008):

- Drought detection as well as real-time monitoring;
- Declaring the onset or end of a drought period;
- Enabling disaster managers to declare drought levels and prompt response measures to regions most vulnerable; and
- Drought assessment.

Major Operational Drought Indices

Multiple drought indices exist that are frequently used for drought analysis (Zargar et al., 2011; Shukla, et al., 2011). Drought indices are typically categorized based on the type of impacts they relate to, as well as on the variables they relate to (Steinemann and Cavalcanti, 2006). Several drought indices explicitly reflect a single impact or application, while others can be designed to correspond to different impacts and therefore drought types (Zargar et al., 2011).

Standardized Precipitation Index (SPI) (McKee et al., 1993): SPI, is a common meteorological drought index that is based solely on precipitation data (Zargar et al., 2011). SPI is considered one of the most robust and reliable drought indicators (Heim, 2002). SPI is a statistical monthly indicator that compares cumulated rainfall during a period of n-months against the long-term cumulated rainfall distribution for a given location and accumulation period (McKee et al., 1993). SPI accounts for inconsistencies that occur as a result of using a non-standardized distribution by transforming the distribution of the precipitation observations to a standardized distribution (Edwards and McKee, 1997). The mean value is set to zero and resultantly, values higher than zero specify wet periods and values below zero specify dry periods (McKee et al., 1993). SPI values can be determined for any period but are frequently applied for 3-, 6-, 12-, 24-, and 48-month periods (Zargar et al., 2011).

Table 1. Phenomena reflected by specific time duration SPI and their applications (adapted from McKee et al., 1993; NDMC, 2006).

SPI duration	Phenomena reflected	Application
1-month SPI	Short term moisture conditions.	Measuring short-term impacts on soil moisture, streamflow of small rivers and crop water stress (particularly during the growing season).
3-month SPI	Short-to-medium moisture conditions.	A seasonal approximation of rainfall.
6-month SPI	Medium-term trends in rainfall.	Likely to effectively illustrate the rainfall over different seasons.
9-month SPI	Rainfall patterns over an average timescale.	Given $SPI_9 < -1.5$, then it is a good indication that significant impacts can occur in the agricultural sector.
12-month SPI	Long-term rainfall patterns.	Measuring long-term impacts on streamflow, and groundwater and reservoir levels.

Palmer Drought Severity Index (PDSI) (Palmer, 1965): PDSI, is a frequently used meteorological drought index, particularly in the United States (Zargar, 2011). The PDSI concept is based on water-supply-and-demand as opposed to a precipitation anomaly. Importance is placed on irregularities in moisture deficiencies rather than climatic anomalies (Guttmann, 1999). PDSI uses precipitation, temperature, and the regional available water content data for soil (Zargar, 2011). PDSI uses these inputs to compute; evapotranspiration, runoff, soil recharge, and moisture (Palmer, 1965).

Standard Precipitation Evapotranspiration Index (SPEI) (Vicente-Serrano et al., 2010): SPEI, is a modification of SPI that accounts for the effects of evapotranspiration (Vicente-Serrano et al., 2010). The SPEI calculates potential evapotranspiration by use of the Thornthwaite equation, as it only requires temperature and latitudinal data (Thornthwaite, 1948). SPEI is calculated at different temporal scales based on the non-exceedance probability of rainfall and potential evapotranspiration variances (Botai et al., 2016). Similarly, to SPI, SPEI can be computed at different temporal scales, with 1-, 3-, 6-, 12- and 24-months being the most commonly used (Chen et al., 2013).

Table 2. Summary of selected major operational drought indices (Zargar et al., 2011; WMO and GWP, 2016; UCAR, 2017).

	Inputs	Drought		
SPI (McKee et al., 1993)	Precipitation	Meteorological, Hydrological, Agricultural	**Advantages**	• Simplicity- SPI relies solely on precipitation data; • SPI can be used to monitor both agricultural and hydrological drought, as it can be used in the analysis of drought at different time scales; • It is possible to compare the departure of precipitation from the norm for different regions with a highly variable climate; and • Both wet and dry climates are equally represented, thus can be used for monitoring wet periods.
			Disadvantages	• As SPI only considers precipitation, it poorly represents ground conditions such as temperature; • Precipitation data has several limitations including; accuracy of measurements, number of gauging stations and length of historical record; • Requires understanding and knowledge of local climatology; and • Lacks the capability to identify regions prone to drought.
PDSI (Palmer, 1965)	Temperature and Precipitation	Meteorological	**Advantages**	• More comprehensive than indices that only consider precipitation, as evapotranspiration and soil moisture are also considered; • Can use basic data for computation; • Most effective where impacts are sensitive to soil moisture; and • Factors in antecedent conditions.
			Disadvantages	• Random selection of both beginning and end intensity values and processes; • Less transparency due to sophisticated calculations; • Limited applicability, as it is calibrated for the United States Great Plains' conditions; • Differing performance across regions and timescales; and • Neglects the lag between rainfall and runoff.
SPEI (Vicento-Serrano et al., 2010)	Precipitation, Temperature and Evapotranspiration	Meteorological, Hydrological, Agricultural	**Advantages**	• Accounts for the impact of temperature on drought, as both temperature and precipitation data are considered; • Requires only climatological data without assumptions about the characteristics of the underlying system; • Output is applicable for all climate systems, as results are standardized; and • Use of temperature data makes SPEI ideal when analysing the impact of climate change in model output under different future scenarios.
			Disadvantages	• Data-intensive; • Sensitive to the method used to calculate potential evapotranspiration; and • May not be able to identify rapidly developing drought events as it is a monthly index.

2.2.3 Climate Change, Drought and Water Security

Climate change will have varying consequences on the future availability of freshwater resources and amplify existing challenges related to water security throughout the world (UNESCO, 2011; Jiménez Cisneros, 2014). Climate change is projected to significantly reduce both renewable surface and groundwater resources in mid-latitude and dry subtropical regions of the world, while water resources in high-latitudes are projected to increase (Jiménez Cisneros, 2014).

According to van Vliet at al. (2013), global projections of daily river streamflow and water temperature under the Special Report on Emissions Scenarios (SRES) A2 and B1 future emission scenarios indicate an increase in the seasonality of streamflow (an increase in high flow and a decrease in low flow) for an estimated one-third of global land surface area for 2071-2100 in comparison to 1971−2000. For both the SRES A2 and B1 scenarios for 2071−2100 relative to 1971−2000, global average and high (95th percentile) river water temperatures are estimated to increase on average by 0.8−1.6 °C. The greatest increases in river water temperature are projected for Europe, the United States, eastern China, certain parts of Southern Africa and, Australia. The sensitivity of these regions is intensified by decreases in projected low flows, which reduces thermal capacity. The study concluded that significant increases in river temperature, as well as decreases in low flows, are projected for; Europe, the south-eastern United States, Europe, eastern China, Southern Africa and, Southern Australia.

Climate change may also significantly affect water quality; for example, the quality of surface water bodies such as lakes used for water supply can be compromised by the presence of algae producing toxins (Jiménez Cisneros, 2014). Climate change adds to the uncertainty associated with the future

availability and variability of freshwater resources and could lead to long-lasting desertification in certain regions of the world. (UNESCO, 2011).

Apart from climate change, non-climatic drivers will also have an impact on the future of freshwater systems such as: demographic, socio-economic, technological drivers and, lifestyle changes (Jiménez Cisneros, 2014). Changes in land use are also expected to have an impact on the availability and distribution of freshwater resources (Jiménez Cisneros, 2014). These impacts come in the form of increased flood hazards and a decrease in groundwater recharge, due to increasing urbanization (Döll, 2009). The impact of future agricultural land use on freshwater systems is of particular importance, as irrigation accounts for an estimated 90% of water use globally (Döll, 2009). As a result of primarily population and economic growth, as well as climate change, irrigation is projected to increase significantly in the future (Jiménez Cisneros, 2014).

Observational records of precipitation, streamflow and drought indices indicate increased aridity since the 1950s over several regions (Dai, 2011a; Dai, 2011b). Assessment of modelled soil moisture (Wang, 2005; Sheffield and Wood, 2008), drought indices (Rind et al., 1990; Burke and Brown, 2008; Dai, 2011a) and precipitation (minus evaporation) (Seager et al., 2007) indicate an increased risk of drought and water shortages in the 21st century (Dai, 2013). Groundwater is becoming increasingly relied upon as a primary source of water and can be used as a potential buffer during drought (WWF-SA, 2016). However, groundwater levels of many aquifers globally have shown a decrease in the last few decades as a result of exploitation exceeding groundwater recharge rates (du Plesis, 2017).

2.3 Water Security in South Africa

This section begins by providing an overview of the status of water security (or lack thereof) in South Africa. The impacts of drought in the southern African region is discussed as well as a brief timeline of droughts in the region and the respective events sectoral impacts, highlighting that droughts have the highest economic costs when compared with other natural disasters. A detailed description of both the recent South African (2014−2016) drought as well as the 2015−2017 Western Cape drought is presented, highlighting the devastating impacts on the agricultural sector as well as the "Day-Zero" danger, as dams in the Western Cape were near depletion. The section also presents a descriptive overview of drought causing mechanisms in South Africa and the Western Cape and the impacts of climate change on water security in the Western Cape Province.

South Africa is a generally largely semi-arid water-scarce country (Jury, 2019). This is due to a low mean annual precipitation (MAP) value of 490mm, ranging from <50 to >3300mm (see Fig. 2), as well as the high atmospheric demand (evaporation) over the country (Lynch, 2004; Schulze, 2012).

MAP is important as it characterizes the long-term volume of water available in a region. MAP is not only important as a general statistic, but it is also possibly the one climatic variable best known to hydrologist and to which it is possible to relate various other hydrological responses (Schulze, 2012).

Precipitation in South Africa is highly variable, both spatially and temporally, with the greatest variability occurring in the dry interior region of the country (WWF-SA, 2016). A general characteristic of the distribution of MAP over South Africa is a decreasing trend from the eastern and southern escarpments across the interior plateau, see Fig. 2 (Schulze, 2012). An estimated 20% of the country receives <200mm per annum, and 47% receives <400mm per annum, while 9% of South Africa receives >800mm per annum (Lynch, 2004).

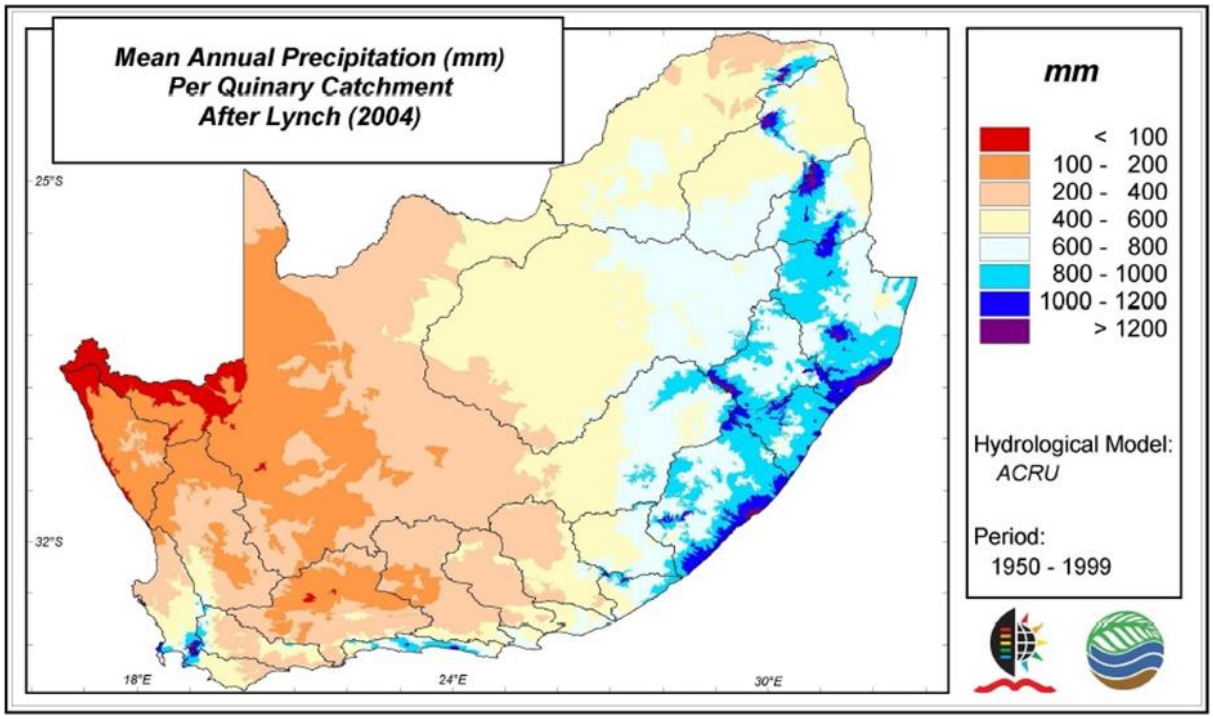

Figure 2. MAP over South Africa (Schulze, 2012).

Out of 193 countries, South Africa is ranked as the 30th driest country in the world with an average volume of 843 m^3 of water per person per year (DWA, 2013). The limited water resources of the country are further stressed through weather extremes brought about by climate variability and change (WRC, 2015).

According to Schulze (2012), four key issues in the setting of climate change and water security that need to be considered in South Africa are:

- The presently overall stressed state of the country's water resources;
- The country's complex water engineered systems;
- Complications associated with transboundary waters; and
- Issues linked to the country's ageing water infrastructure.

South Africa's water security is dependent on the sustained supply from the country's water resources (WWF-SA, 2016). South Africa's primary input to water resources is rainwater (WWF-SA, 2016). Natural mean annual runoff (MAR) in South Africa is 49 billion m^3/annum, of which 10.24 billion m^3/annum of this is accessible at the 98% assurance level (DWS, 2015a). The country presently has a reliable yield from its water infrastructure, at 98% assurance supply, of 15 billion m^3/annum (68% surface water, 13% groundwater, 13% return flows, and 6% miscellaneous sources (DWS, 2015a). Water demand in South Africa is projected to increase by 2030 by 32% to 17.7 billion m^3 due to an increasing population and industrial development, whilst supply is expected to decline (WRG, 2012; WWF-SA, 2016). According to the DWS (2015b), water usage exceeds reliable water yield, which means that in the event of drought the country will experience severe water restrictions on a large scale. Unlocking the potential of groundwater is critical to addressing current and future national water shortages (WWF-SA, 2016).

South Africa's water resources are governed by both the Water Services Act of 1997 and the National Water Act (NWA) of 1998. The Acts provide a complementary framework that enables sustainable

water resource management and improved service delivery (WWF-SA, 2016). The NWA is founded on the belief that all water is part of a single interdependent hydrological cycle and should be controlled under a consistent set of rules. The NWA ensures that South Africa's water resources are: protected, used, developed, conserved, controlled and, managed sustainably and equitably for both humans and the environment (NWA, 1998).

2.3.1 Impacts of Drought in southern Africa

Compared to other climate-related events in southern Africa, during 1980–2016, droughts have caused the highest economic cost (US$ 1.4 billion) and have affected a larger percentage of the region's inhabitants (EM-DAT, 2017; Davis-Reddy and Vincent, 2017). Impacts of drought are non-structural and challenging to measure (Murthy et al., 2009) as they can be social, economic or environmental (see Fig. 3). The dominance of rain-fed subsistence agriculture, as well as a great dependence on water-intensive maize, makes agriculture and livestock production in southern African particularly susceptible to drought, as food security throughout the region is intricately linked to the amount of seasonal rainfall received (Wilhite, 2016). Drought shocks, however, are not only confined to agriculture and livestock but also have a direct effect on: energy security, industry, urban development and, domestic public health (Wilhite, 2016). The economic impacts of drought vary and depend on the economic structure of a country (Benson and Clay, 1994). Low-income countries with a high proportion of the population in subsistence farming, such as Malawi and Zambia, are significantly affected by drought, with a great risk of famine (Wilhite, 2016). Intermediate to complex economies, such as South Africa, will be less severely affected, in terms of famine risk (Wilhite, 2016).

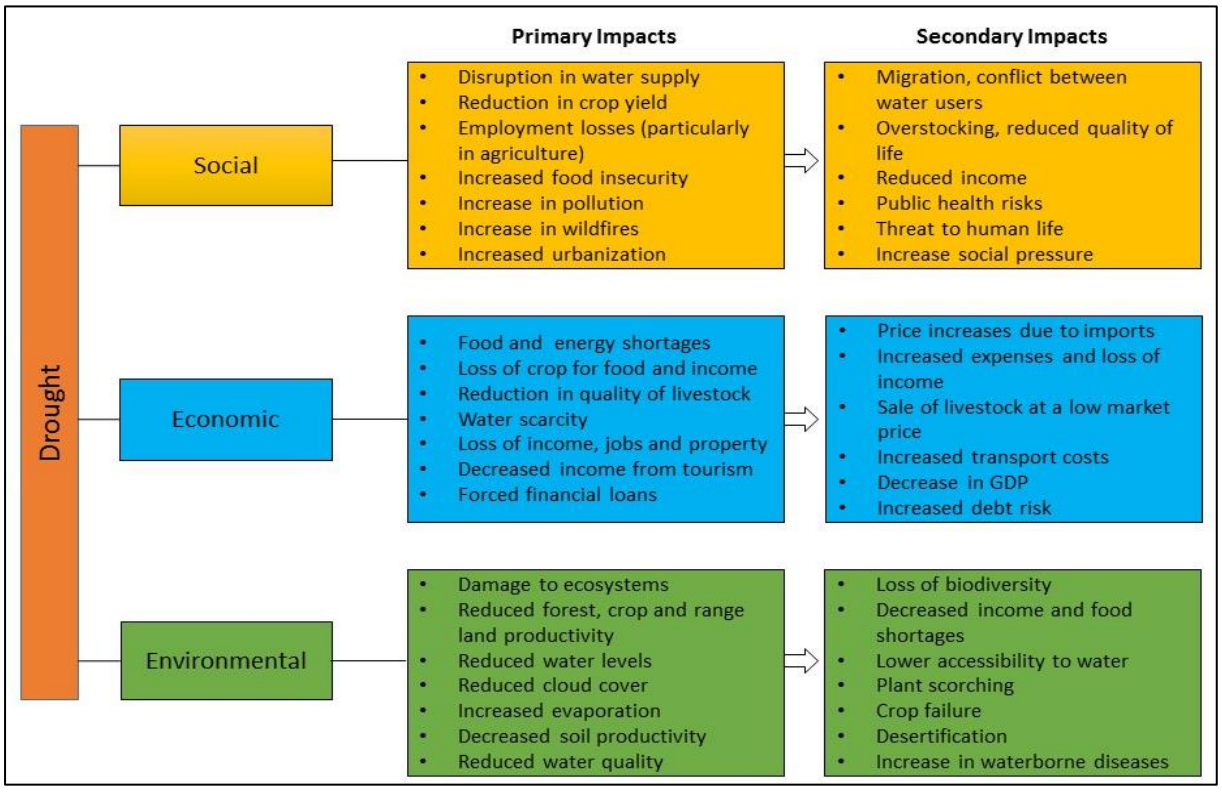

Figure 3. Primary and secondary impacts associated with drought in southern Africa (adapted from Vogel et al., 1999).

2.3.2 Droughts in southern Africa and South Africa

Water deficits in the southern African region are due to the strong seasonality of rainfall and persistently high rates of evapotranspiration (Chikoore, 2016). The rainfall of southern Africa varies

greatly, ranging from <20mm along the western regions of Namibia to highs of >3 000mm in the highland regions of Malawi (Nicholson et al., 1988). The highly variable southern African climate is partly due to a wide range of climate systems, including: i) quasi-stationary high-pressure systems; ii) movement of the Inter-tropical Convergence Zone (ITCZ); iii) varying regional topography; and iv) the effect of the warm Indian Ocean on the east coast (higher rainfall) and the cold Atlantic Ocean on the west coast (lower rainfall) (Nicholson, 2000).

The strong temporal seasonality of rainfall over southern Africa is dominated by the north-south seasonal movement of tropical rain belts, mainly the ITCZ (Christensen et al., 2007; Chikoore, 2016). The ITCZ is located in the equatorial trough and is an area of convergence of trade winds associated with cumulonimbus convection and high rainfall (Chikoore, 2016). The ITCZ is the primary rainfall producing system in southern Africa (Chikoore, 2016)

It has been noted that climate change is increasing the risk associated with extreme events such as drought in southern Africa and is already altering the magnitude and frequency of extreme weather events (Meadows 2006; Shongwe et al., 2009; DEA, 2014). However, despite progress on integrated climate change and disaster risk frameworks, the focus remains primarily on short-term disaster relief as opposed to risk reduction and adaptation strategies for long-term resilience (Midgley and Methner, 2016).

Frequent severe droughts are a major climatic disaster across the southern African region (Wilhite, 2016). Between 1980 and 2016, the southern African region experienced 88 drought events which affected ~107 million people, of which within the same period eight of those drought events occurred in South Africa, affecting 22 million people (EM-DAT, 2017). Evidence suggests that drought events have become more severe and extensive in southern Africa (Fauchereau et al., 2003; New et al., 2006; Masih et al., 2014). Severe droughts occurred in the early 1900s, 1920s, 1930s; the late 1940s, 1960s and the early 1980s (Tyson, 1987). More recent severe drought events, such as those in: 1991–1992, 1994–1995, 2001–2003, and 2014–2015 affected the southern Africa region and resulted in devastating impacts on: water resources, agriculture, industry, national economies, and, the environment (Vogel et al., 2010; Wilhite, 2016). In between these major drought events, many other local droughts occurred as well, which had significant economic implications, particularly for developing countries (Wilhite, 2016).

The 1991–1992 drought was one of the most devastating prolonged droughts in the southern African region which resulted in extensive dry conditions across the entire region (Vogel and Drummond, 1993). The drought affected a large portion of southern Africa and left many rural communities without access to potable water (Calow et al., 2010). The drought caused extensive crop failure (70% of the region's total crop), particularly in South Africa and Zimbabwe, and resulted in significant agricultural and economic losses across the region (FAO, 2004; Holloway 2000; Calow et al., 2010). Landlocked countries such as: Malawi, Zambia and Zimbabwe anticipated reductions in food production ranging between 50−75% (Holloway, 2000). An estimated 20 million people were directly at risk of starvation (SADC, 1992). The drought decreased both surface and groundwater sources and as a result, people began to make use of traditional sources of contaminated water which caused outbreaks of various waterborne diseases such as cholera and dysentery (Calow et al., 2010). During the summer months of 1992, more than 90% of small inland dams in the eastern region of southern Africa dried up; as a result of a 50% decrease in MAP in: Botswana, Namibia, South Africa and Zimbabwe (Unganai and Kogan 1998; Jury and Mwafulirwa, 2002). In South Africa, the drought resulted in an estimated GDP loss of US$ 500 million (Pretorius and Smal, 1992) and nearly 50 000 jobs in the agricultural sector and an additional loss of 20 000 jobs linked to agriculture (Mniki, 2009).

The 2001−2003 drought, although less devastating than the 1991−1992 drought had a significant impact in South Africa. According to Theunissen (2004), wheat yield was 39% lower, water levels were 25% lower in 2003 than in 2004 and, grazing pastures were at 30% of their normal capacity.

2.3.3 The 2015--2017 Drought in South Africa

Recently, South Africa experienced one of the worst droughts on record since 1930 (de Jager, 2016) due to two consecutive below-average rainfall seasons since early 2015 and 2016, which is linked to an acute El Niño phase (SADC, 2016; Brink, 2016). In 2016, South Africa declared drought emergencies in all provinces apart from Gauteng (SADC, 2016). Out of the 40 million people affected by the drought in the Southern African Development Community, nearly 36% (14.4 million) of those people resided in South Africa (SADC, 2016). The rest of the country received some relief from the drought in 2017, in the form of rainfall, but major dam levels in the Western Cape continued to decline, due to a third year of below-average rainfall. (CoCT, 2017).

The country-wide drought hit the agricultural sector the hardest, particularly: maize, sugarcane, wheat, beef and, sheep production (Davis-Reddy and Vincent, 2017), and resulted in food shortages, and stalled the country's economic growth (Midgley and Methner, 2016). Many other southern African countries (Botswana, Lesotho, Namibia and Swaziland) that rely on food imports from South Africa were also affected by the national drought (SADC, 2016).

South Africa exports nearly one million tonnes of food to these countries (UNOCHA, 2016). The drought caused a significant decline in crop-yield, specifically during 2016 and had turned South Africa into a net importer of crops (Agri SA, 2016). The total cereal deficit for the southern African region for 2015−2016 was estimated at 7.9 million tonnes (WFP, 2016). South Africa estimated that 5–6 million tonnes of cereal imports were needed for 2015−2016 (Agri SA, 2016).

2.3.4 The 2015–2017 Western Cape Hydrological Drought

The 2015−2017 hydrological drought that occurred in the Western Cape is considered a rare event with a return period of 1 in 150 years for the meteorological drought (Otto et al., 2018). It was a three-year compound drought and the result of three well-below average rainfall seasons in: 2015, 2016 and 2017 (see Fig. 4 & 5), rainfall was particularly low between March−May and August−October (Otto et al., 2018). The below-average rainfall was exacerbated by other factors contributing to the recent hydrological drought, such as high consumption of water and a lack of investment in increasing water supply capacity (Wolski, 2018). According to a study by Sousa et al. (2018), the 2015–2017 Western Cape drought was largely due to a poleward change in the moisture corridor over the South Atlantic Ocean.

This resulted in an acute drawdown of water supply without sufficient time to recover and the possibility of what the CoCT termed as "Day Zero" (Otto et al, 2018). Day Zero, simply put, was the projected day that the WCWSS system would fail, and water would have been distributed to the city's population through communal standpipes limited to 25 litres per person per day (CoCT, 2018a).

The rainfall anomaly was greatest in the areas encompassing the six major dams that supply water to the CoCT (Otto et al., 2018). Within the local Cape Town region, the rainfall deficit can be considered an extremely rare event with a return period >300 years in comparison to a return period of an event of such magnitude occurring once in 150 years over the greater Western Cape region (Otto et al., 2018).

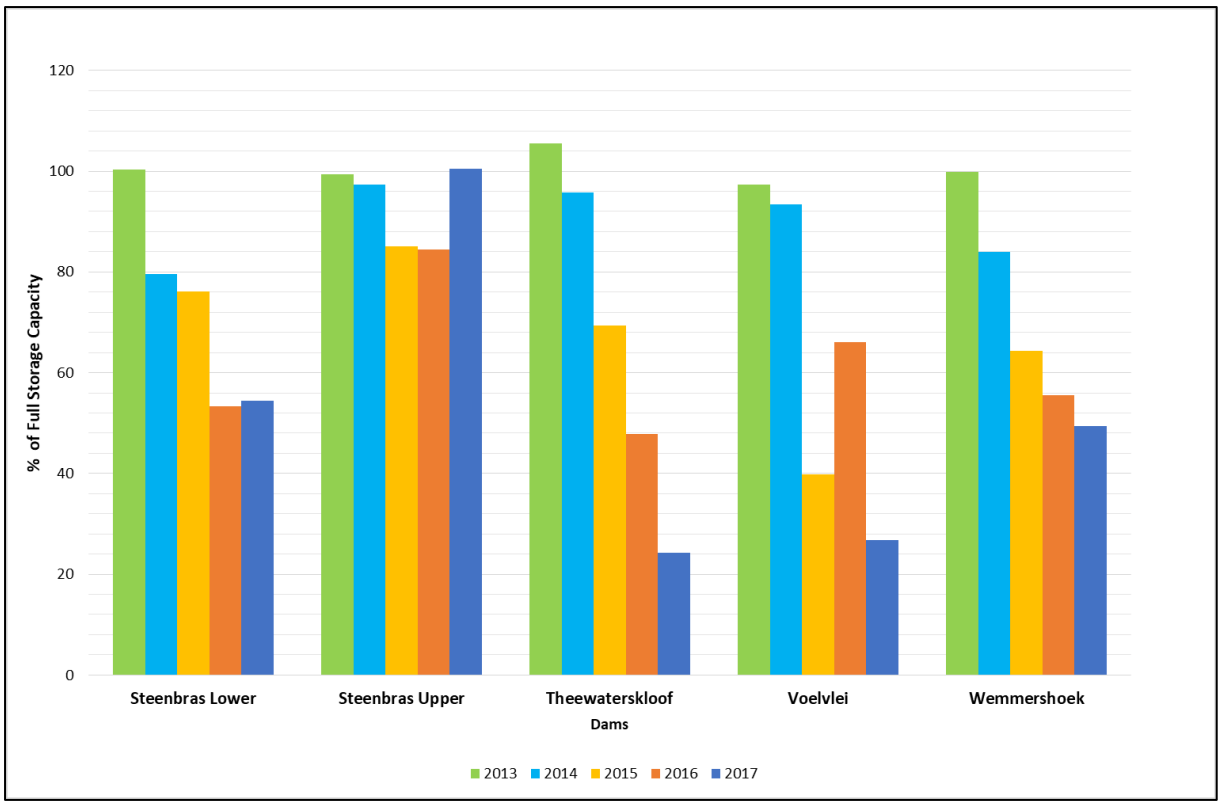

Figure 4. Major Dam levels in the Western Cape as a percentage of full storage capacity at the end of the rainfall season (CoCT, 2018b).

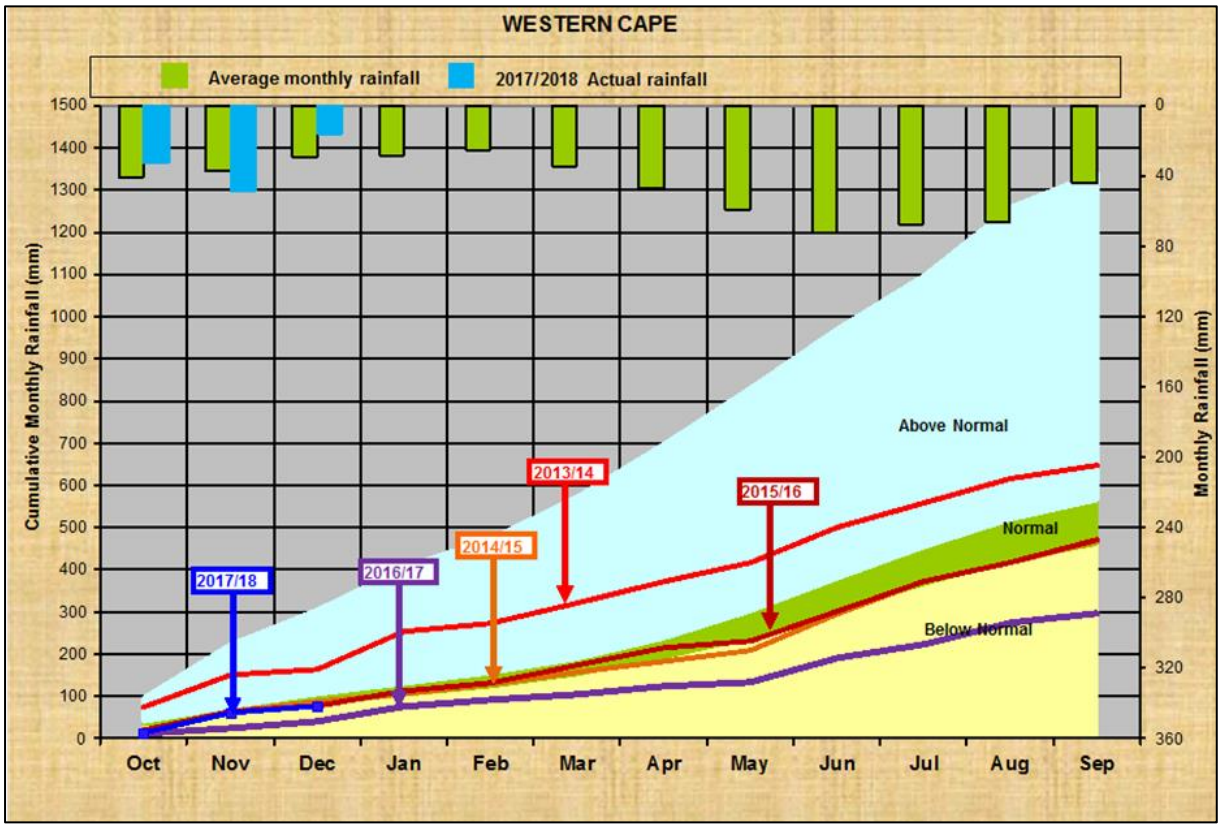

Figure 5. Provincial cumulative monthly and total monthly rainfall of the Western Cape Province from 2013/2014 to 2016/2017 (DWS, 2018).

The drought led to the CoCT progressively implementing water restrictions from Level 2 (20% reduction in urban water use) in January 2016 to level 6B (50 litres of municipal provided water per person) in February 2018 to avoid Day Zero. As of October 2018, the Level 6B water restrictions were relaxed to level 5 (87 litres of municipal provided water per person) (CoCT, 2018a).

Agricultural water usage was restricted by the Department of Water and Sanitation during October 2017−November 2018 by an average of 60% compared to the previous year, from 144 Mm^3 to 58 Mm^3 (CoCT, 2018c). Water restrictions imposed on the agricultural sector varied throughout the WCWSS, from 50% in the Breede Valley, 60% in the Berg River and Riviersonderend region, and 87% in the lower Olifants River Valley (WWF-SA, 2018).

The drought in the Western Cape has had extensive adverse impacts on many of the country's sectors including agriculture, food security, livelihoods, livestock, health, water, sanitation and hygiene (SADC, 2016).

Economic losses in the agricultural sector in the Western Cape were roughly R5.9 billion, resulting in 30 000 job losses and a drop-in export of 13−20% (BFAP, 2018). Droughts tend to have a severe impact on livestock farmers: as a result of the drought, the Western Cape's provincial cattle herd was reduced by 15% and the provincial sheep flock by 11% and had caused meat prices to increase in 2017 (WCG, 2017).

Table 3. Total crop production in the Western Cape 2016−2017 and 2017−2018 winter season (BFAP, 2018; DAFF, 2018).

Crop	2016 Yield (tons)	2017 Yield (tons)	Decrease in Production (%)
Wheat	1 098 200	586 800	47
Malting Barley	355 000	307 064	14
Canola	105 000	93 468	11
Wine Grapes	1 599 728	1 279 782	20
Table Grapes	186 772	153 000	18
Pome Fruit	1 376 279	1 256 773	9
Stone Fruit	319 424	293 887	8

2.3.5 Mechanisms That Cause Drought in South Africa

According to Tyson and Preston-Whyte (2000), drought in South Africa is generally caused by the high variability in precipitation and temperature. This means that droughts are linked to high temperatures (which theoretically increase evaporation) and low rainfall, the severity of the drought, however, is dependent on the degree of change in each of these variables (Tallaksen and van Lanen, 2004).

Atmospheric Circulation: Drought events in the southern African region are primarily associated with large-scale intense anticyclones, of which the Botswana High is the most persistent (Lindesay, 1998; Chikoore, 2016). The Botswana High is an anticyclone in the mid-troposphere that is usually centred over Botswana or Namibia and induces widespread subsidence, particularly during late-summer (January-March) (Driver and Reason, 2017). Anticyclones inhibit vertical cloud development and result in dry spells over southern Africa (Chikoore, 2016). Driver and Reason (2017), found that in the northern South African region the Botswana High has a higher correlation to dry spell frequency than that between the El Niño Southern Oscillation (ENSO) and dry spell frequency.

Drought processes typically act to impede convection as well as displacing primary rain-producing systems (Mulenga et al., 2003). A study conducted by Cook et al. (2004) investigating wet and dry

spells over South Africa, determined that dry summers are linked to an equatorward displacement of the ITCZ.

Sea Surface Temperatures (SST): Variations in SST in the Indian Ocean are known to affect the inter-annual rainfall fluctuations at a regional scale over South Africa (Reason, 2001). The dominant climate mode in the Indian Ocean is the Subtropical Indian Ocean Dipole (SIOD), which was first described by Behera and Yamagata (2001). The SIOD oscillates between negative and positive phases and is significant at the inter-annual scale during the austral summer (Reason 2001; Hermes and Reason, 2005). A positive SIOD phase occurs when the south-western Indian is anomalously warm and the south-eastern Indian Ocean is anomalously cold, during a negative phase the reverse occurs, during the austral summer (Behera and Yamagata 2001). During a negative SIOD event, there is an observed decrease in rainfall over the south-eastern region of South Africa which is influenced by low-level divergence (Reason, 2001).

ENSO: Drought cycles across southern Africa are often linked to El Niño– a naturally occurring warm phase of an irregularly periodical difference in winds and SSTs over the eastern Pacific Ocean (Nicholson and Kim, 1997). The ENSO has a large influence on South Africa, which is a predominantly summer rainfall region, with the exception of the Western Cape, in which there exists a negative correlation between ENSO and precipitation (Ratnam et al., 2014; Dieppois et al., 2015), most significantly since the late 1970s (Richard et al., 2001). ENSO events are interactions between the global atmosphere and the Pacific Ocean (Holloway et al., 2012). Resultantly, events that occur in the Pacific Ocean influence the: temperature, rainfall, wind and pressure over South Africa, such that 30% of South Africa's rainfall variability can be attributed to El Niño phases (Tyson and Preston-Whyte, 2000). The 2015−2016 El Niño that affected South Africa is the third super El Niño in just over three decades, which has reduced the occurrence of the phenomenon from 20- to 10-year cycles, climatologists are in debate about whether these conditions have intensified due to a warming planet (Pearce, 2016).

2.3.6 Climate Change, Drought and the Western Cape

The Cape Town region is situated on the south-western border of South Africa and its winter rainfall greatly depends on the transport of moisture from oceanic regions to the west of the city (Sousa et al., 2018). The majority of Cape Town's winter rainfall is produced by cold fronts, while cut off lows occasionally contribute significantly to the region's rainfall (Reason et al., 2002; Singleton and Reason, 2007). Mechanisms that cause drought in the Western Cape are discussed below:

Intense prolonged droughts in Mediterranean climates are linked to large and continuous disturbances of the westerly flow and resultant anomalies in the storm-track (Sousa et al., 2018). Previous studies have related the variability of rainfall in the greater Cape Town area to anomalies in South Atlantic SST and sea ice (Reason et al., 2002; Reason and Jagadheesa, 2005; Blamey and Reason 2007), the South Annular Mode (SAM) (Reason and Rouault, 2005; Gillet et al., 2006) and ENSO (Phillippon et al., 2012). The SWC climate is sensitive to several large-scale drivers, the most common in all of these is the shift of the westerly storm track and associated moisture fluxes towards the region (Sousa et al., 2018).

SST and Sea Ice: Reason et al. (2002), present evidence that upstream SST in the mid-latitude South Atlantic and sea-ice anomalies in the South Atlantic region of the Southern Ocean is related to year-to-year winter rainfall in the SWC. During years with high winter rainfall, the jet upstream of the SWC is strengthened and large cyclonic anomalies from the south-west Atlantic extend over the region.

SAM: Sometimes referred to as the Antarctic Oscillation (AAO), refers to the north-south movement of the South Westerly wind belt (Reason and Roualt, 2005). A negative SAM phase is, characterized by higher pressure over Antarctica relative to mid-latitudes, and is frequently linked with the eddy-driven jet that is located 50 °S shifting towards the equator. A positive phase is characteristic of lower pressure over Antarctica in comparison to the mid-latitudes and shifts the Southern Hemisphere storm track poleward (Mahlalela et al., 2018).

The SAM is thought to have a significant role in the variability of winter precipitation; because it is the main mode of tropospheric circulation variability in the extra-topics of the Southern Hemisphere (Hartmann and Lo, 1998; Thompson and Wallace, 2000; Marshall, 2003). A study by Reason and Rouault (2005), established that a negative phase of SAM is likely to bring about wet conditions over the SWC during winter months, while a positive phase induced dry conditions over the region.

ENSO: The relationship between ENSO and the winter rainfall region of South Africa is complex. Some El Niño events have been assumed to be associated with increased precipitation over the Western Cape winter (June-August) rainfall region (i.e SWC) (Phillipon et al., 2012). The signal is significantly less distinct than the October-December and January-March seasons, the peak and developed phases of ENSO respectively, when the summer rainfall regions of South Africa tend to experience extensive below-average rainfall during ENSO (Reason et al., 2000; Cook, 2001; Lyon and Mason, 2007).

The SWC being a winter rainfall region is particularly vulnerable to the impacts of climate change (WCDEDP, 2014), due to the expansion of subtropical highs and accompanying retreat of cold fronts, resultantly, decreasing rainfall over the Western Cape (Chikoore, 2016). A study carried out by Botai et al. (2017), analysed drought characteristics using SPI 3-, 6- and 12-month values derived from several different rainfall stations distributed throughout the Western Cape Province for 1985–2016. Results indicate the Western Cape has been experiencing recurrent mild meteorological, agricultural and hydrological drought conditions for the period analysed. Of which, drought conditions tend to increase towards the southern-Cape regions, which covers the Central Karoo and Eden districts. Given that these regions are year-round rainfall areas, the results indicate that the region has been receiving inadequate rainfall throughout the year. Furthermore, results suggest that the Overberg, Cape Winelands and West Coast districts experienced largely mild drought conditions. These regions are predominantly winter rainfall areas, indicating that the drought conditions spread to the winter months.

Climate change predictions for the Western Cape Province indicate (adapted from: Sinclair-Smith and Winter, 2019):

- Increased likelihood of severe drought events (Otto et al., 2018);
- Temperature increases in the range of 1–3 °C, the largest increases are expected to occur over the inland regions while lower increases are projected over the coast (Midgley et al., 2005; Tadross and Johnston, 2012);
- Decreased annual rainfall (Tadross and Johnston, 2012), by 2050, precipitation in the Western Cape is projected to decrease by a projected 30% as a result of climate change (WCG, 2012);
- Increased evaporation as a result of increases in temperature, reducing overall effective rainfall (Tadross and Johnston, 2012);
- Changes in seasonality of rainfall, more late summer rainfall and less early and late winter rainfall (Midgley et al., 2005; Tadross and Johnston, 2012);
- Increased rainfall in mountainous and eastern regions and a decrease in rainfall in lowland areas and the SWC (Midgley et al., 2005); and

- Decreased frequency of rainfall events and increases in abnormal rainfall, more intense rainfall events are expected to occur over the mountainous and eastern regions during mid-to-late summer (Midgley et al., 2005; Tadross and Johnston, 2012).

The above-mentioned changes in climatic variables are set to impact water security within the Western Cape Province (Sinclair-Smith and Winter, 2018). Uncertainty still exists on how future climate change will impact rainfall in the Western Cape, there is a relatively high level of confidence, supported by various climate models and historical trends (Midgley et al., 2005; Tadross and Johnston, 2012), that climate change will result in increased temperatures in the region (Sinclair-Smith and Winter, 2018). Increases in temperature will increase the frequency of heatwaves, exacerbate extended dry spells, increase the frequency and intensity of wildfires; rainfall projections suggest reduced average winter rainfall and more frequent and severe drought events (WCDoA, 2016). Furthermore, the combined effect of projected increases in temperature, increased evapotranspiration rates and an expected decrease in effective rainfall are likely to increase irrigated agricultural water use (Sinclair-Smith and Winter, 2018).

Increases in water demand may also be exacerbated by a range of other predicted changes, such as: projected increased drying in numerous areas, shorter winter rainfall season, less frequent but more intense rainfall events (Sinclair-Smith and Winter, 2018).

2.4 Climate Change and Hydrology in South Africa

This section presents a detailed overview of the impacts of climate change on the hydrological cycle. Beginning with a general description of the projected impact climate change will have on the hydrological cycle with a focus on South Africa. The two major climate variables projected to impact water resources are evaporation and precipitation, as an increase in the former and a decrease in the latter in certain regions of the country are projected to decrease the country's water resources. A review of studies on observed changes of both temperature and precipitation provides evidence that certain regions of the country are getting hotter and drier, particularly the SWC. Observed changes in the Western Cape in evapotranspiration and streamflow show increases in the former and decreases in the latter, a similar trend is projected for the future of the SWC.

Globally, climate change is predicted to have a significant negative impact on the hydrological cycle and freshwater resources (Bates et al., 2008). The assessment of climate change impacts on hydrological events, such as drought, requires an evaluation of projected changes of critical climate variables, particularly precipitation and evaporation and how these two variables, in interaction with one another, influence the terrestrial hydrological cycle (Kusangaya et al., 2013).

Changes in temperature and rainfall directly affect the quantity of evapotranspiration, quantity and quality of runoff and, depletion of both ground and water resources (Kusangaya et al., 2013; El Chami and El Moujabber, 2016). South Africa has a low rainfall-runoff conversion rate, due to the spatial and temporal variation of rainfall, which averages 9% for the entire country (Whitmore, 1971). It is likely that the conversion rate of rainfall to runoff will increase in regions where rainfall is projected to increase under future climate scenarios. It is in regions where rainfall is projected to decrease that the conversion to runoff is expected to decline greatly as the runoff : rainfall relationship is non-linear and any changes in rainfall will be amplified in its response (Schulze, 2012).

South Africa has a respectable network of rainfall and temperature observation stations in comparison to the rest of the African continent (New et al., 2006) making it possible to analyse variability and trends over many decades (DEA, 2013). In-depth projections of climate change scenarios over South Africa began during the 1990s founded on comprehensive work over the preceding decades by Tyson

et al. (1975) on the climatology of South Africa. Tyson et al. (1975) explored the effect of atmospheric and oceanic drivers on regional and local climate and the pattern of decadal and multi-decadal climate variability. Long-term trend analysis of several atmospheric variables such as: temperature, precipitation and evapotranspiration have been widely used as proxies for detecting a change in climate as described further below.

2.4.1 Observed and Projected Changes in Temperature

Observed Changes in Temperature: Temperature changes have a significant influence on the spatial and temporal availability of water resources (Kusangaya et al., 2013). Apart from heatwaves, increases in temperature can result in several other extreme events, such as wildfire and drought (NSM, 2016). These events are strongly linked to the drying effect related to an increase in temperatures when evapotranspiration is moisture-limited, and this depends greatly on the nature of the land cover in the region (Seneviratne et al., 2016). Long-term trends in temperature indices are clearer than trends in rainfall indices (DEA, 2013). Globally, mean temperatures have increased over the last century as a result of anthropogenic greenhouse gas (GHG) emissions (IPCC, 2014). Several temperature studies have been undertaken in South Africa as detailed in table 4.

Table 4. Observed temperature changes for South Africa (adapted from DEA, 2013).

Time period	Temperature change observed	Source
1950–1993	An increase in annual mean maximum temperature and extensive increases in annual mean minimum temperature. Furthermore, an increase in diurnal temperature for much of South Africa.	Easterling et al. (1997)
1901–1995	Cooling in the coastal areas, and a decrease in diurnal temperature over the country during the 1950s and 1960s. A decrease of mean annual temperature of between 1 °C and 0.5 °C in the SWC.	Hulme et al. (2001)
1960–2003	Apart from a few stations, most stations in South Africa have observed several increases in annual mean temperatures, the most significant warming having been reported in the interior and in the autumn months. Stations showed a mix of results concerning diurnal temperature, having shown no clear regional pattern of change. Significant increases in annual maximum and minimum temperatures as well as annual mean temperature in the SWC.	Kruger & Shongwe (2004)
1961–2000	Varied results for changes in diurnal temperature, however, a tendency for the cold extremes of minimum temperature to change more significantly than that of cold extremes of maximum temperature is shown. Additionally, a general increase in hot extremes over South Africa was observed and a significantly decreasing trend in diurnal temperature for the SWC.	New et al. (2006)
1962–2009	Significant changes in the exceedances of the extreme percentile values for minimum temperature and maximum temperature were observed for many of the stations. Overall results illustrated a decreased frequency of cold extremes and an increased frequency of hot extremes, of which the stronger increases occurring in the western and northern interior regions. Significant increases in daily maximum and minimum temperatures in the SWC.	Kruger & Sekele (2013)
1974–2005	Significant and steady increases in both minimum temperature and maximum temperature in the Western Cape winter rainfall region, by values of 0.89 °C and 0.58 °C, respectively.	Hoffman et al. (2011)
1960–2010	A significant warming trend in maximum temperature for SA. Strongest Regionally averaged increase in maximum temperature occurred during autumn in the central interior. The Western Cape region shows a significant increase in and maximum temperature (0.015−0.027 °C/year), with the strongest warming occurring in the last 10−12 years, in all seasons. Significant increases, in all seasons excluding winter, for minimum temperature (0.011−0.021 °C/year).	MacKellar et al. (2014)

Projected Changes in Temperature: Under the unmitigated emission scenarios SRES A2 and Representative Concentration Pathway (RCP) 8.5 (based on statistical and dynamical downscaling), climate change projections for South Africa up to 2050 and beyond project warming as high as 5−8 °C

(RCP 8.5) over the South African interior, over the coastal regions this warming is somewhat less (DEA, 2013).

Table 5. Key messages at near-, mid-, and far-future projections under the SRES A2 and RCP 8.5 scenarios for temperature in South Africa's six hydrological zones, relative to a baseline period of 1975–2005 (adapted from DEA, 2013).

Period	(Limpopo/Olifants/ Inkomati)	(Pongola/Umzimkulu)	Vaal	Orange	Mzimvubu-Tsitsikamma	Breede-Gouritz/Berg
2015-2035	Near-future annual temperature anomaly projections reach up to ~2 °C under A2 and RCP 8.5 towards the end of the period.	Near-future annual temperature anomaly projections are between 1-2 °C under A2 and RCP 8.5 scenarios.	Near-future annual temperature anomalies under A2 and RCP 8.5 scenarios are between 1-2.5 °C.	Near-future annual temperature anomalies under A2 and RCP 8.5 reach values of up to ~2.5 °C.	Near-future annual temperature anomalies under the A2 and RCP 8.5 reach values in excess of ~2 °C.	Near-future annual temperature anomalies under the A2 and RCP 8.5 scenarios reach values of ~1.5 °C.
2040-2060	Mid-future projections of temperature anomalies are between 1-3°C (2-5 °C) under the A2 scenario (RCP 8.5).	Mid-future annual temperature anomalies of 1-3 °C (1-4 °C) are projected under the A2 scenario (RCP 8.5).	Mid-future annual temperature anomalies of 1-3 °C (2-5 °C) are projected under the A2 scenario (RCP 8.5).	Mid-future annual temperature anomalies of 1-3 °C (2-4 °C) are projected under the A2 scenario (RCP 8.5).	Mid-future annual temperature anomalies of 1-2 °C (1-3.5 °C) are projected under the A2 scenario (RCP 8.5).	Mid-future annual temperature anomalies of 1-2 °C (1-2.5 °C) are projected under the A2 scenario (RCP 8.5).
2080-2100	Far-future projections show annual average temperature increases of 3-6 °C (4-7 °C), relative to the baseline period, under the A2 scenario (RCP 8.5) for Limpopo.	Far-future projections show annual average temperature increases of 3-5 °C (4-6.5 °C), relative to the baseline period, under the A2 scenario (RCP 8.5) for Pongola-Umzimkulu.	Far-future projections show significant increases in annual average temperature relative to the baseline period, 3-6.5 °C (5-8 °C) under the A2 scenario (RCP 8.5).	Far-future projections show significant increases in average annual temperature of 3-5.5 °C (4-7.5 °C) for zone 4 (as well as a large part of the Northern Cape), relative to the baseline period, under the A2 scenario (RCP 8.5)	Far-future projections show significant increases in annual average temperature of 2-5 °C (4-6 °C) for the Eastern Cape, relative to the baseline period, under the A2 scenario (RCP 8.5).	Far-future projections show annual average temperature increases of 2-4 °C (2-5 °C) for the south-Western Cape, relative to the baseline period, under the A2 scenario (RCP 8.5).

The increases mentioned in table 5 in the SWC region for the A2 and RCP 8.5 scenarios for the far-future projections are well above the natural temperature variability of the region. Temperature projections under the constrained emission RCP 4.5 scenario for the SWC region imply significantly reduced temperature increases, with annual anomalies of <3 °C.

2.4.2 Observed and Projected Rainfall Changes in South Africa

Observed Changes in Rainfall: South Africa's observed historical annual rainfall pattern differs from < 100 mm per annum in the west and >1500 mm in the east (El Chami and El Moujabber, 2016). Several studies on South African rainfall have shown that rainfall in the country is characterised by high inter-annual variability (Kusangaya et al., 2013). Kane (2009) suggested that annual rainfall has significant yearly fluctuations (50−200% of the mean), whilst five-year running means illustrated long-term fluctuations (75−150% of the mean). Due to the high variability of South Africa's MAP (Jury, 1997), a small number of statistically noteworthy trends have been detected in South Africa's MAP (DEA, 2013), models tend to be inconsistent in predicting the effect of climate change on rainfall (Mantel et al., 2015). However, more important than the MAP is the annual distribution of rainfall, including the onset and end of the rainy season, the average duration of wet and dry periods and the occurrence of higher rainfall events (DEA, 2013). Observed climate trends over the last five decades (1960−2012) indicate a shift in rainfall seasonality and an increase in rainfall intensity (DEA, 2013). Changes in South Africa's observed rainfall as a result of climate change is detailed in the table below:

Table 6. A review of observation-based rainfall studies conducted in South Africa (adapted from DEA, 2013).

Time period	Rainfall trend detected	Source
1931–1990	An increase in excess of 10% in the intensity of 10-year high rainfall events during 1961–1990 compared to 1931–1990 over most of the country. A decrease in intensity of 10-year high rainfall events in the SWC.	Mason et al., (1999)
1906–1997	An increase in the annual frequency of extreme rainfall events over the Eastern region of SA.	Groisman et al. (2005)
1950–1999	Rainfall increases particularly in regions where orography has a strong influence, as well as increases in late summer dry spell duration for most of the summer rainfall regions in South Africa.	Hewitson and Crane (2005)
20th century	An increase in extreme rainfall over Eastern and south-western parts of SA during the majority of the 20th century.	Easterling et al. (2000)
1950–2000	An increase in early-season rainfall detected accompanied by a decrease in late-season rainfall in the north-west region of KZN. Seasonal shifts in Limpopo, late onset of rainfall season accompanied by less rainy days and increases dry spells.	Thomas et al. (2007)
1955–2000	A shift in seasonality in KwaZulu-Natal, Drakensberg. No significant change in MAP was observed, however, whilst there was an increase in summer rainfall, autumn and winter rainfall decreased resulting in a shorter wet season and a more distinct seasonal cycle.	Nel (2009)
1961–2000	Evidence for an increase in extreme rainfall over parts of SA.	New et al., (2006)
1910–2004	Increases in extreme rainfall indices in the southern Free state and parts of the Eastern Cape. An increase in the duration of dry spells apparent for most of the Free State and Eastern Cape, as well as decreases in wet spells for parts of the Eastern Cape and north-eastern regions of SA. Some significant decreases in rainfall along the southern Cape Coast.	Kruger (2006)
1960–2010	Observed statistically significant decreases in rainfall and the number of rainy days over the central and north-eastern parts of the country in the autumn months, as well as significant increases in the number of rainy days in the southern-Drakensberg region, were observed in spring and summer. Significant decrease in rainy days during summer and autumn (overall annual mean decreases of 11.3 days) over the Western Cape region.	MacKellar et al. (2014)

Projected Changes in Rainfall: An overall trend of a risk of drier conditions is projected for the west and south of the country, while projections for the east of the country indicate a risk of wetter conditions (DEA, 2013). However, many of the projected changes are within the domain of historical natural variability (DEA, 2013). Dynamical downscaling for the SWC in the near future under the A2 scenario indicate that strong drying is likely (DEA, 2013). However, these results contrast B1 and A2 statistical downscaling, which indicate moderate to substantial increases in rainfall within the winter rainfall zone of the region for autumn to spring, and for both near- and mid- futures (DEA, 2013). Thermodynamic considerations may be the mechanism behind the statistically downscaled projections indicating wetter futures for the winter rainfall region (DEA, 2013). Under the RCP 4.5 and RCP 8.5, the signal of wetter futures is less pronounced, a wetting signal is only present for winter and spring (DEA, 2013).

On a national level, the future climate of South Africa up to 2050 and beyond has been described using four climate change scenarios as a basis, which consider different degrees of change and likelihood that incorporate the impacts of global mitigation and the passing of time, which are described below (DEA, 2013):

1. ***Warmer (<3 °C above 1961–2000) and wetter***, with an increased frequency of extreme rainfall events.
2. ***Warmer (<3 °C above 1961–2000) and drier***, with an increased frequency of drought events and a relatively higher frequency of extreme rainfall events.
3. ***Hotter (>3 °C above 1961–2000) and wetter***, with a significantly higher frequency of extreme rainfall events.
4. ***Hotter (>3°C above 1961–2000) and drier***, with a significant increase in the frequency of drought events and a higher frequency of extreme rainfall events.

Table 7. Climate scenarios under possible future conditions up to 2050 and beyond from evidence of climate models for South Africa's six hydrological zones (adapted from DEA, 2013).

Scenario	Limpopo/Olifants/ Inkomati	Pongola/Umzimkulu	Vaal	Orange	Mzimvubu-Tsitsikamma	Breede-Gouritz/Berg
1: warmer/wetter	An increase in spring and summer rainfall.	An increase in spring rainfall.	An increase in spring and summer rainfall.	An increase of rainfall in all seasons.	An increase of rainfall in all seasons.	A decrease in autumn rainfall and an increase in winter and spring rainfall.
2: warmer/drier	A decrease in summer, spring and autumn rainfall.	A decrease in spring rainfall and a strong decrease in summer and autumn rainfall.	A decrease in summer and spring rainfall and a strong decrease in autumn rainfall.	A decrease in summer, autumn and spring rainfall.	A decrease of rainfall in all seasons, a particularly strong decrease in summer and autumn.	A decrease of rainfall in all seasons, a particularly strong decrease in the west.
3: hotter/wetter	A strong increase in spring and summer rainfall.	A strong increase in spring rainfall.	An increase in summer and spring rainfall.	An increase in rainfall in all seasons.	A strong increase of rainfall in all seasons.	A decrease in autumn rainfall, and a decrease in winter and spring rainfall.
4: hotter/drier	A strong decrease in summer, spring and autumn rainfall.	A decrease in spring rainfall and a strong decrease in summer and autumn rainfall.	A decrease in summer and spring rainfall and a strong decrease in autumn rainfall.	A decrease in summer, autumn and spring rainfall.	A decrease in rainfall in all seasons and a significant decrease in summer and autumn rainfall.	A decrease in rainfall in all seasons, significantly to the west.

For the SWC region, the consensus from the GCMs is that rainfall is projected to decline considerably and become highly variable by 2050. In contrast, rainfall for the remainder of the country may on average remain relatively unchanged but is likely to become more variable. Decreases in rainfall in the Western Cape will have a significant negative impact on surface water and groundwater resources in the region. Increases in rainfall variability in the SWC are likely to result in increases in prolonged and severe drought events (DEA, 2013).

2.4.3 Projected and Observed Changes in Evaporation

Potential evaporation is an important aspect of the hydrological cycle and is one of the primary climatic drivers controlling freshwater resources (Schulze, 2012; Jiménez Cisneros et al., 2014). According to Jiménez Cisneros et al. (2014), changes in evaporation, as a result of temperature, illustrate similar trends to that of precipitation, with slight increases over a large part of the globe, particularly in higher-latitudes; with decreases of soil moisture (scenario-dependant) particularly in: central and southern Europe, south-western North America, Amazonia and southern Africa. According to a study by Hoffman et al. (2011), A-Pan evaporation during 1974–2004 decreased significantly in the winter rainfall region of the Western Cape from 2117 to 1845mm per annum (an average of 12.8%).

Historical analysis by Schulze (2012) show that mean annual evaporation (MAE) (1950–1999) from open water surface bodies and wetlands in primary catchments is between < 100 million m^3 and >2 500 million m^3. Under the A2 scenario, near-future (2046–2065) projections, relative to the baseline period (1971–1990), show enhanced evaporation of <10 million m^3 to >350 million m^3, of which the largest increases are displayed over the interior and most of the Northern Cape. Far-future projections (2081– 2100) exhibit significant increases in additional evaporation over much of the country,

particularly: over the interior, the Northern Cape, and the north coast of the country. Additionally, it is shown that enhanced evaporation, relative to the baseline period, from open water bodies in the SWC, is projected to increase by <10 million m^3 and between 60−100 million m^3 for mid-and far-future projections, respectively.

Based on GCM projections used by Schulze (2012), there is a reduction in severe soil water stress days over much of South Africa in the mid-future (2046−2065), excluding the West Coast where very moderate changes are projected. However, in the far-future (2081−2100), the SWC exhibits increases in severe soil water stress days, while about 95% of South Africa displays a reduction in the number of days per year experiencing severe soil water stress.

2.4.4 Projected and Observed Changes in Streamflow and Runoff in South Africa

Assessing the effects of climate change on sectoral impacts of water has primarily been undertaken using hydrological models with downscaled climate projections (Perks et al., 1999; Schulze, 2003; Warburton et al., 2010). Changes in hydrological processes, such as runoff, occur as a result of changes in rainfall, temperature and carbon dioxide emissions (DEA, 2013).

The hydrological cycle is a dynamic system, and changes in climate may cause unanticipated hydrological responses in a model, which may be beyond the models' ability range for which processes have been tested and verified against observational records (Warburton et al., 2010).

Several studies have concluded that streamflow in the southern African region is projected to decrease by 2050. For example, streamflow in Swaziland is projected to decrease by 40% (Matondo, 2012), by 20% in the Zambezi catchment (Beck and Bernauer, 2011) and, a projected decrease of up to 18% for the Thukela catchment in South Africa (Andersson et al., 2006).

Observed changes in daily runoff for South Africa (see Fig. 6), displays increases of runoff between 0.5−1.5mm/day across most of the interior and significant increases of between 3−8.5mm/day in the extreme western parts of the country. Northern parts of the country show decreases of between 0.3−0.5mm/day, while the SWC region shows decreases of 1.5−3mm/day (Dai, 2011a).

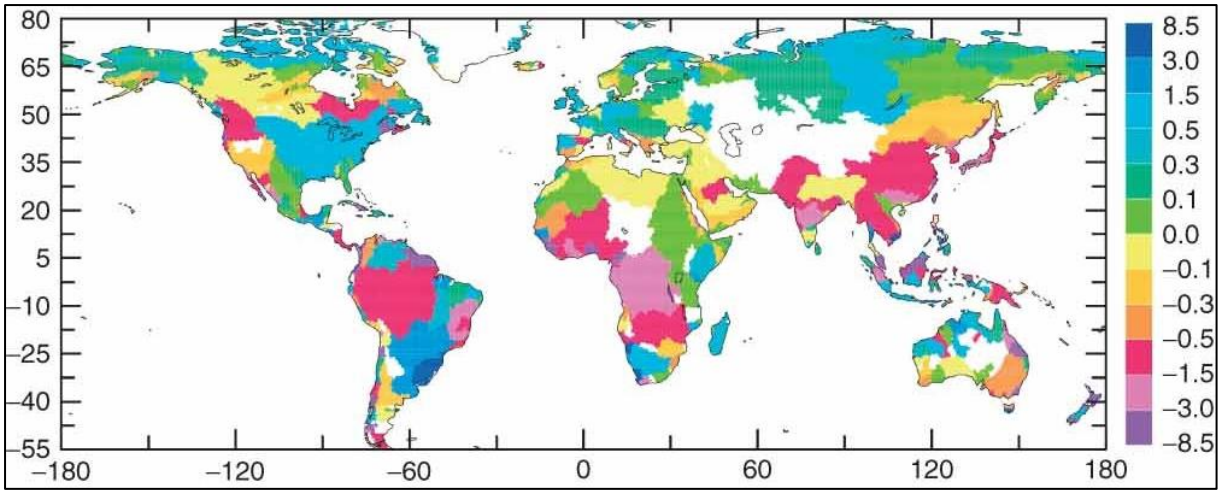

Figure 6. Trend map for observed annual runoff (0.1mm/day/50years) inferred from streamflow data for 1948–2004 (Dai, 2011a).

Future climate scenarios considered by the Long-term Adaptation Scenarios project an increase in the occurrence or magnitude of both drought and flood events in South Africa (DEA, 2013). Projections for runoff in South Africa, under a wide range of scenarios, predict between 20% decrease to 60% increase by 2050 assuming a business as usual emissions pathway, while under a constrained

emissions scenario, runoff projections are estimated to range from 5% decreases to 20% increases (DEA, 2013).

The impacts of climate change on MAR vary greatly throughout the country (see Fig. 7). Significant increases in runoff are projected for: Kwazulu-Natal, parts of Mpumalanga and the Eastern Cape, while significant decreases in runoff are projected for south-western parts of the country, the central-western areas and to a lesser extent the extreme north.

Analysis of multiple GCMs by Schulze (2012), show increases in MAR between 20−30% over large portions of South Africa. In contrast, the SWC region shows projected reductions in average annual runoff under climate change, particularly in the wet years when dams are filled. The runoff reductions in the SWC are more prevalent in the far-future (2071–2100) and are projected to occur particularly in the 35 years between the mid-future (2046–2065) and the far-future. Additionally, the variability of streamflow in the SWC is projected to decrease, particularly into the far-future.

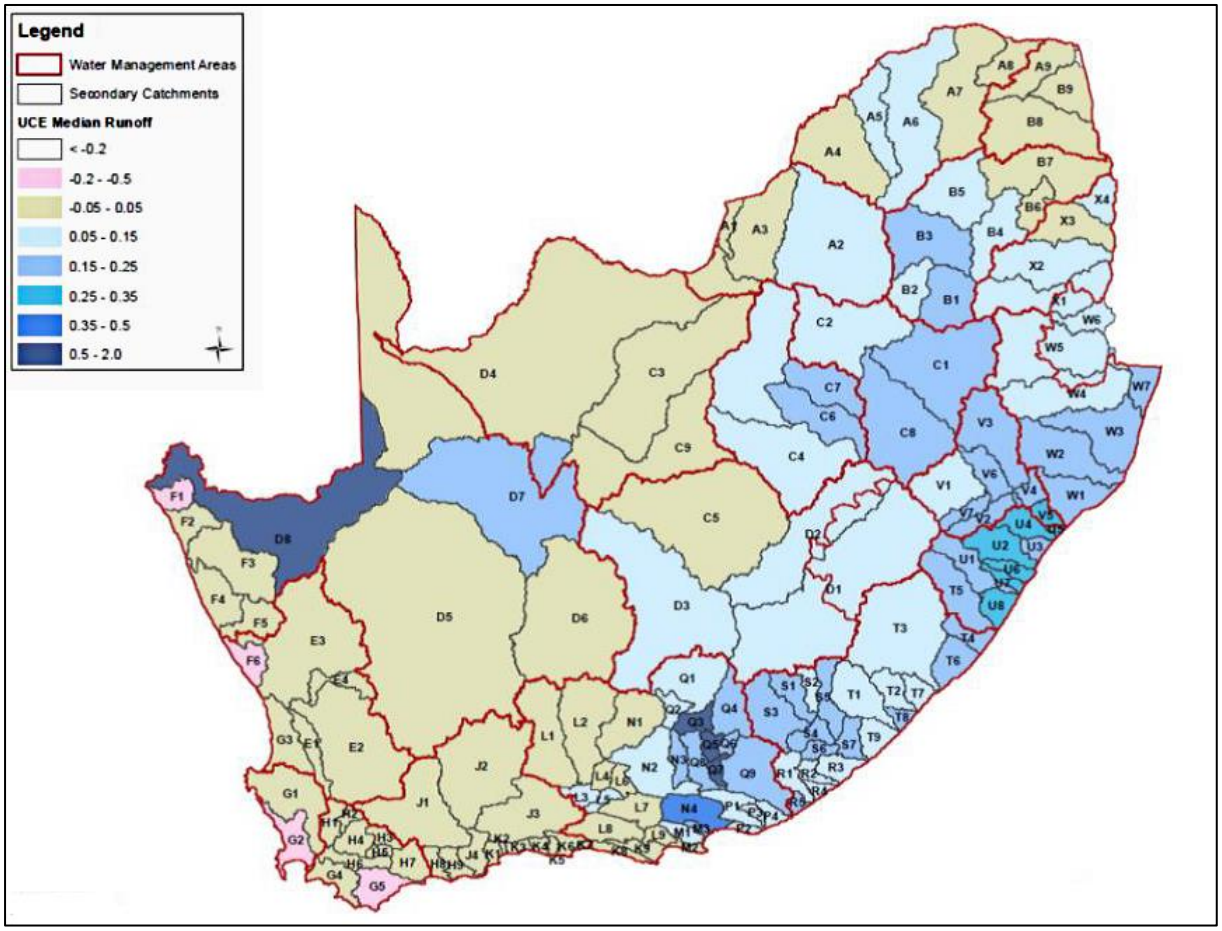

Figure 7. Projected median changes in the average annual runoff for South Africa under an unconstrained emission scenario (Cullis et al., 2015).

2.5 General Climate Change Attribution

This section introduces climate change attribution referring to studies that have analysed changes in temperature over time which can be linked to increased GHG emissions as well as natural variability. Increases in the Earths average temperature as a result of anthropogenic activities have been shown to alter the Earth's climate and hydrological cycle.

The recent warming of the earth's climate system is undeniable and is predominantly due to anthropogenic (GHG) emissions, although the implications for regional climates are less clear (IPCC, 2014). Each of the preceding three decades has been marked by consecutively warmer surface temperatures than any decade since 1850, of which 2016 marked the hottest year on record (NOAA, 2017).

Past GHG emissions can be directly linked to large-scale warming and associated slow-onset events such as sea-level rise and desertification (Bindoff et al., 2013). The consistency of modelled and observed changes throughout the climate system include: warming of the atmosphere and ocean, sea-level rise, ocean acidification, and changes in the hydrological cycle, the cryosphere, and climate extremes. This points to large-scale warming resulting mainly from human-induced increases of GHG concentrations in the atmosphere (Bindoff et al., 2013). GHG's have likely contributed between 0.5 °C and 1.3 °C to global mean surface warming during 1951–2010, with contributions from other anthropogenic forcings likely to be between -0.6 and 0.1 °C, from natural forcing likely to be between -0.1 and 0.1 °C, and lastly from internal variability likely to be in the range of -0.1 and 0.1 °C. These contributions sum up to be consistent with the observed warming of approximately 0.6 °C during 1951–2010 (Bindoff et al., 2013).

The climate of the Earth has experienced changes caused by both natural and human factors (Bindoff et al., 2013). Natural factors include: volcanic eruptions, solar variability, and interactions within the climate system (Bindoff et al., 2013). Human factors that influence the climate include changes in the composition of the atmosphere (i.e. increases in the concentration of GHG and aerosols) as a result of industrial and social activities, and land-use and coverage changes (Bindoff et al. 2013). Attribution studies involving long-term trends in observed records have been carried out regularly since the 1995 IPCC report (Otto et al., 2015).

2.6 The Science of Attributing Extreme Events

This section introduces the basis and underlying methodology for attributing extreme events to anthropogenic climate change, as well as the steps undertaken in extreme event attribution studies.

It has been noted that there is strong evidence for anthropogenic influence on some extreme events and little evidence for anthropogenic influence on others (Liu and Allan, 2013; Herring et al., 2015). However, due to the variability of weather, it is problematic to determine for any specific event if the event would have occurred in the absence of human influence on climate (Otto et al., 2014). Both global and regional studies of drought project a higher likelihood of drought by the end of the 21st century, with a significant increase in the number of drought days (Hirabayashi et al., 2008; Feyen and Dankers, 2009).

Probabilistic event attribution (PEA) is an emerging science that allows for a quantitative assessment of the degree to which human-induced climate change affects localised weather patterns (Pall et al., 2011; Otto et al., 2012). PEA aims to quantify whether and to what extent past emissions have contributed to the probability of the occurrence of an extreme event (Otto et al., 2014). This is done mainly using many climate model experiments, known as ensembles (Otto et al., 2014). A large ensemble size is required, for any given experiment, to assess the change in frequency of extreme climatic events (Otto et al., 2014).

PEA studies aim to compare the frequency at which an extreme event occurs within a model experiment representing the world with anthropogenic influence (factual scenario) on climate against the frequency that the same extreme event would occur without the human factor (counterfactual scenario) on the climate system, see Fig. 8 (Stott et al., 2016).

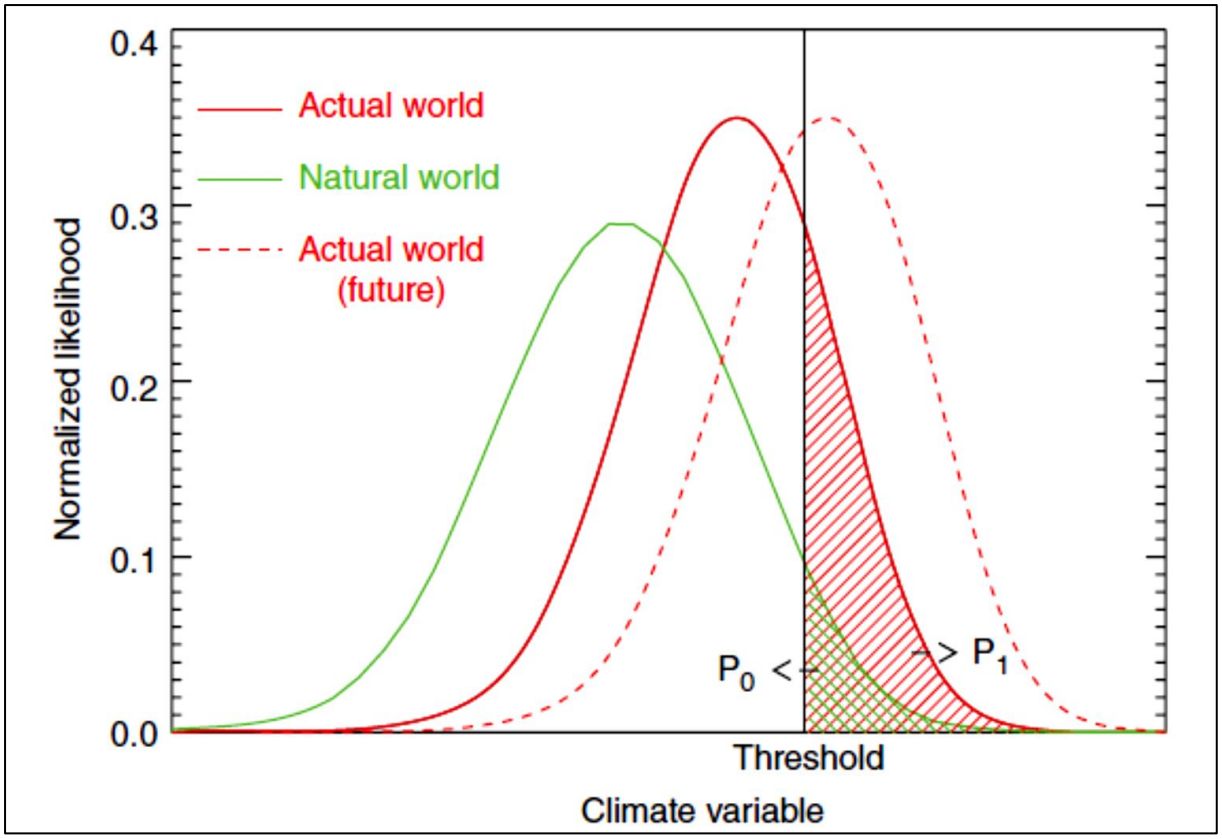

Figure 8. An illustration of the probability density functions (PDFs) of a climate variable with the factual world (solid red line) and the counterfactual world (green line). The corresponding probabilities exceeding a pre-specified threshold (P_1 and P_0) are represented by the enclosed areas of the same colour. The red-dashed line illustrates how climate change may affect the actual world in the future (Stott et al., 2016).

The science of PEA is a rapidly growing field, with the first studies having been conducted less than two decades ago (Stott, et al., 2004). The concept of fractional attributable risk (FAR) of individual extreme climate events had not been considered until the theoretical possibility was described by Allen (2003), and applied to the European heatwave event of 2003 which was the first attempt of an event attribution study that provided a direct connection between anthropogenic climate change and a single extreme event (Stott et al., 2004). The attribution study carried out on the 2003 heatwave concluded that anthropogenic influence had very likely (probability > 90%) increased the likelihood of a record-warm summer by more than two-fold (Stott et al., 2004). Using what is known as the risk-based approach, having determined the probabilities of the event in the factual world (P_1) and the counterfactual world (P_0) the results can be expressed as a risk ratio (RR) as P_1/P_0. Results can also be expressed as an FAR as $1- P_0/P_1$. An FAR value of > 0.5 indicates the probability of the event has more than doubled (Stott et al., 2016).

Attribution studies contain several uncertainties and challenges related to the availability of long-term meteorological data and the accuracy of climate model simulations of climatic conditions that are conducive for extreme weather events (Otto et al., 2014). Variations also exist between regions in the capacity to attribute events, due to differences in regional climate and weather patterns, availability of observational data, and modelling ability. Confidence in attribution studies can be improved where independent methods lead to similar results (Stott et al., 2016).

Assessing the influence of anthropogenic climate change on extreme events has potential importance for policy that is intended to address present and future climate change impacts (Otto et al., 2015).

Given that many extreme events occurred before significant human-induced changes on the climate system had been detected, an oversimplified attribution to anthropogenic causes could be detrimental (Stott et al, 2016). By assessing how human influence on the climate is affecting extreme events such as flooding or drought presently, it may be possible to deliver guidance on whether to expect increases or decreases in the intensity or frequency of extreme events, such as drought, in the near-future and therefore inform and aid in adaptation planning. (Otto et al., 2015; Stott et al., 2016).

According to Sheperd (2016), the risk-based approach involves three steps described below:

- The first step is defining the event under investigation. Extreme events are unique and should be abstracted to a class of event agreeable to statistical analysis. This step requires a selection of physical variables and spatial and temporal averaging used to define the event.
- The second step is the construction of the distribution (P_1) of the factual world. This step is typically carried out using a climate model. The challenge in this step is that estimating the probability of an extreme event requires many years of simulation. A general rule of thumb is the more extreme the event the larger the number of years that need to be simulated. To do so, the model must be computationally low-cost to run.
- The final step is the construction of the counterfactual likelihood distribution (P_0). One of the issues associated with this step is that counterfactual observations to evaluate the model's results do not exist. Historical observations may be used but are limited and unreliable in certain regions of the globe.

2.7 Drought Events and Attribution

The attribution of drought events to anthropogenic climate change can be somewhat problematic in comparison to other climatic events, as described in this section. A review of methodologies and key findings of drought attribution studies undertaken in different regions of the globe is discussed. The review of studies illustrates the complexities involved with drought attribution as well as conflicting results in different regions.

Due to the complex nature of droughts and the various climatic factors that influence a given drought, it is challenging to quantitatively define and detect long-term changes in drought likelihood (IPCC, 2013). Adding to the complication of attribution of drought events are the non-meteorological factors (i.e. increases in population, land-use and poor water resource management) that also contribute to the magnitude and frequency of drought events (NSM, 2016). Confidence in the attribution of extreme climatic events, such as drought, is directly proportional to an increase in the understanding of the influence of climate change on the event type (see Fig. 9). There is low confidence in attributing changes in drought over global land areas since the mid-20th century due to observational inconsistencies as well as difficulties differentiating decadal-scale variability from long-term patterns (Bindoff et al., 2013).

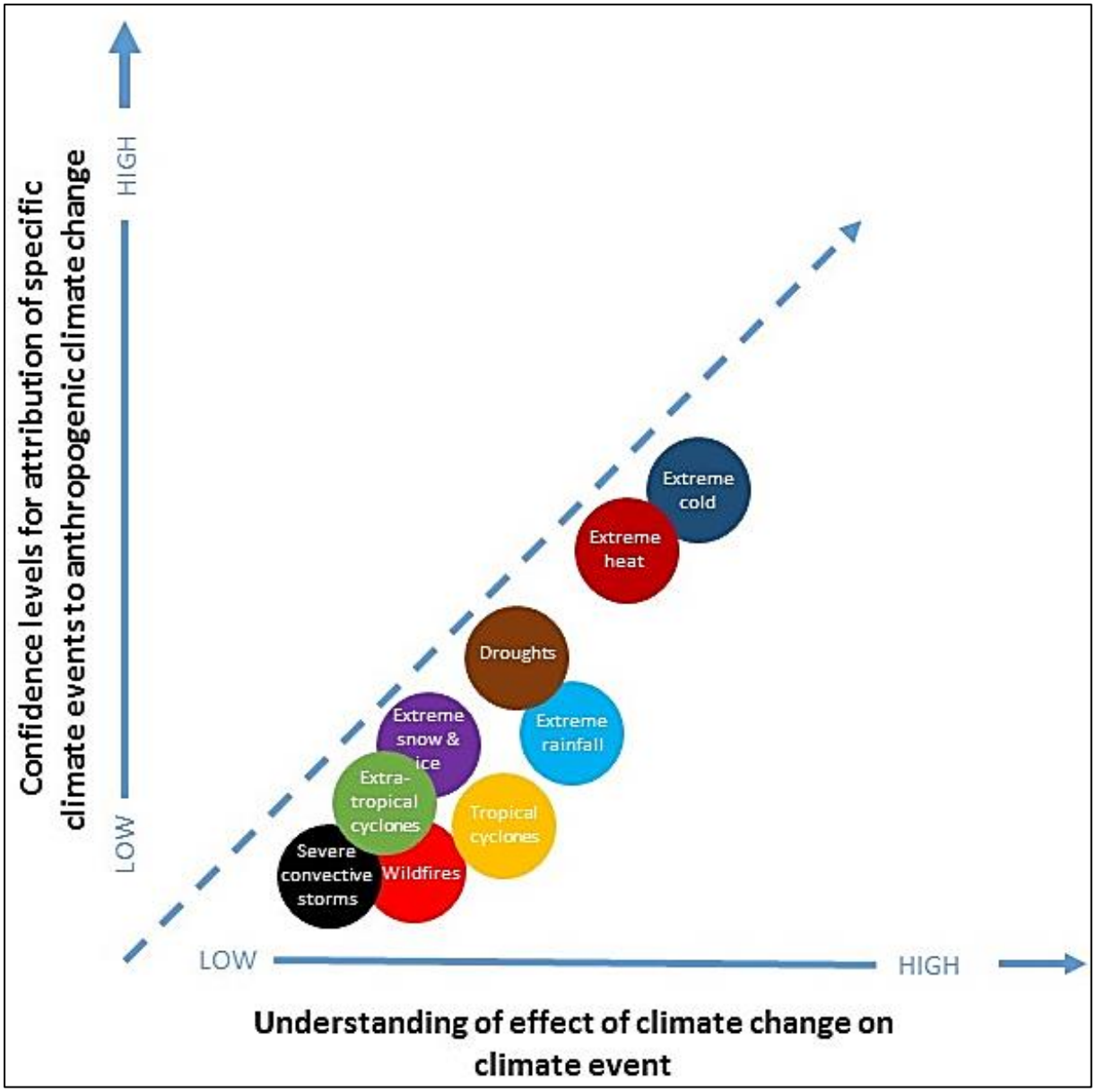

Figure 9. Schematic depiction of the state of attribution studies for various extreme climatic events (adapted from: NSM, 2016).

Several attribution studies have been conducted in the past, which evaluate the influence of anthropogenic climate change on drought events. Gudmundsson and Seneviratne (2016), assessed whether human-induced climate change has changed drought risk in Europe. Focusing on precipitation and quantifying how the probability has changed in response to climate change in the last century. The study employed a framework for meteorological drought risk assessment that can be applied to both model simulations and observational records to increase the confidence in the results. The study found that the consistency of both observational and model-based assessments indicate that it is very likely (> 90%) a changed drought risk is a result of anthropogenic climate change in northern Europe and the Mediterranean region where drought risk is expected to increase. Results from the observational and model-based assessment in the Central Europe region, however, were conflicting and inconclusive. The observed decrease of drought risk in northern Europe is consistent with regional (Bhend and von Storch, 2009), hemispheric (Min et al., 2008) and global studies (Zhang et al., 2007) that attribute an increase in annual rainfall in high-latitudes to human-induced climate

change. The study, however, falls short in that it only considers precipitation neglecting other variables such as soil moisture and atmospheric conditions, nor did the study attempt to quantify the effect of climate change or the change in the probability of drought.

An attribution study undertaken by Diffenbaugh et al. (2015), assessed the record-setting drought in California that began in 2012 which included: the lowest 12-month precipitation, highest annual temperature and the most extreme drought indicators for 2015. The drought led to severe water shortages, critically low streamflow and an increase in wildfire risk. The study undertook both an observational and model-based approach using Coupled Model Intercomparison Project 5 (CMIP5) for historical and natural forcing experiments. The results of the study suggest that precipitation deficits in California were more than twice as likely to bring about drought years if they occurred under warm conditions. The study found that even though there had not been a significant change in the probability of both negative and moderately negative rainfall anomalies in recent decades, the occurrence of drought events has been higher in the two preceding decades than in the previous century. Furthermore, there is an evident increase in the probability that rainfall deficits coincide with that of warm conditions as well as an increase in the probability that rainfall deficits produce droughts. Climate model experiments in a factual and counterfactual world reveal that anthropogenic climate change has increased the likelihood that low rainfall years in California are also warm years. The study concluded that based on findings human-induced warming has increased the likelihood of co-occurring warm-dry conditions.

2.8 Event Attribution in Africa

This section describes the importance of event attribution studies on the African continent. Although the GHG emissions of Africa are one of the lowest in comparison to other continents, Africa is set to feel the greatest impacts of climate change. There is a lack of event attribution work on the African continent, as the focus has been mainly on high profile events as well as various other challenges, as discussed further below.

Africa is often regarded as the most vulnerable continent to the impacts of a changing climate and as such, understanding the change of risk associated with extreme events is particularly important for the continent (Boko, et al., 2007). However, African climate has received very little research attention, particularly research related to extreme event attribution (Washington et al., 2006; Otto et al., 2015). PEA studies undertaken thus far have been focused on high profile extreme events (Stott et al., 2004; Pall et al., 2011; Otto et al., 2012; Peterson et al., 2013), predominantly in mid-latitude regions (Otto et al., 2015), with a limited number of extreme event attribution studies being conducted in Africa (Lott et al., 2013; Funk et al., 2013; Otto et al., 2013). Limited research combined with high vulnerability highlight the need for exploring PEA research in Africa (Otto et al., 2015). Defining the most suitable attribution question to ask is not one that should be a scientific decision but that should be made in dialogue with the various stakeholders that will use the results and information (Otto et al., 2015). This is particularly true for studies carried out in tropical regions, thus a working relationship between: scientists, policymakers and, individuals at ground-level is imperative in Africa (Otto et al., 2015).

Undertaking PEA analyses in Africa presents various challenges that include:

- Long-term observations, required for model validation and to identify extreme events, are limited in many countries across the continent (Washington et al., 2006);
- Existing PEA studies commonly employ atmospheric models forced with SSTs, which may have different implications for tropical precipitation, which is strongly influenced by large scale teleconnection patterns, particularly in Africa (Giannini et al., 2008); in contrast to mid-

latitude regions that are dominated by synoptic precipitation and influenced more by internal variability than remote SSTs; and

- Inter-annual precipitation variability is greater in African countries than in mid-latitude climates (Giannini et al., 2008), which could present challenges in distinguishing the anthropogenic signal from internally generated variability (Otto et al., 2013).

Debatably, the first PEA study conducted in Africa was undertaken by Lott et al. (2013), which analysed the 2011 East African drought which caused severe food crises in Djibouti, Ethiopia, Kenya and Somalia. The drought was caused by the failure of two successive rainy seasons, which typically occur from October to December (short rains), and March to June (long rains), respectively (Hastenrath et al., 2011). The study calculated the attributable increase in the risk of extreme low precipitation in the two rainy seasons before the 2011 drought in East Africa. The study determined that in a world without anthropogenic climate change there would be no significant changes in precipitation during the 2010 short rains and that the dry conditions could be a result of the prevailing La Niña conditions earlier in the year. However, evidence was found for an increased risk of failure of the long rains in 2011 as a result of human-induced climate change. Along with the framing of the attribution statement, the methodology employed in the attribution study is a determinant of the results.

2.9 Methodologies of Event Attribution

This section describes methods used in extreme event attribution divided into methods that use observations and methods that use models, the latter being the most frequently used in attribution studies. This is due to the lack of long-term observational data in many global climate records. Along with how the attribution question is framed, the methodology employed in the attribution study is an influence on the findings.

Several methods have been undertaken in event attribution studies, differing on the use of observational historical records and models as well as in the framing of the attribution question being investigated (Stott et al., 2016). Advances in event attribution have arisen for two main reasons being: i) An increase in the understanding of climate mechanisms that result in extreme events; and ii) Rapid progress that has been achieved in the methodologies used for event attribution (NSM, 2016). Approaches in event attribution work carried out can be divided into two categories (NSM, 2016):

- Attribution that relies on historical observation records to calculate changes in likelihood or magnitude of extreme climate events; and
- Attribution work that relies on model simulations to compare the occurrence of an event in a factual and counterfactual world.

Modelling studies typically use observations to verify the accuracy of the models to reproduce the event of interest, whereas observational studies may rely on models for attribution of the observed changes (NSM, 2016).

2.9.1 Methods Based on Observations

To a certain extent, all event attribution approaches use observations (NSM, 2016). Methods that use observations to analyse extreme events provide limited realisations i.e. establishing their frequency is problematic, particularly for limited observation records (Hegerl, 2015). Using observations in extreme event attribution requires a careful application of statistics (Hegerl, 2015), either by estimating the shape of the distribution tail (Smith, 1989) or statistically modelling record-setting extreme climate events (Meehl et al., 2009). Furthermore, variations in the frequency of extreme climate events are only partially due to human influence and occur for several other reasons, hence the use of climate

model data is a more appealing option in extreme event attribution as much larger ensembles can be provided which will be described in the next section (Hegerl, 2015).

In practice, a statistically confident decision of a change in the frequency or magnitude of an extreme event is only possible for a subset of event types, the most common being temperature extremes, because long observational records and well-observed statistics are required to detect changes in frequency and magnitude of an event (NSM, 2016). Detection of trends in observational records is always challenging because of the limitations of observational records in terms of record length and quality (NSM, 2016). Trend detection is complicated further by unforced natural variability which may result in trends that can last for years (NSM, 2016). These limitations suggest that event attribution should often depend on an understanding of the long-term changes in variables that have a close physical relationship to the event under investigation and are predicted to affect the intensity or the frequency of that event (NSM, 2016).

Statistical Analysis of Observations: In the absence of climate models, statistical analysis of observations can be used to quantify the changing likelihood of specific events (NSM, 2016). The benefit of this approach is that results do not depend on the reliability of a climate model nor the model's ability to simulate the event under investigation, however, as previously mentioned statistical analysis of observations strongly relies on the availability of long-term high-quality data (NSM, 2016). Furthermore, observation-based analysis requires a statistical analysis that can quantify changes in extreme events within a specified period (NSM, 2016).

This method aims to characterise the distribution of a type of event that is similar to a particular event observed by the use of historical observations this would usually exclude the particular event in question to avoid selection bias (NSM, 2016). To address the human influence a trend or covariate in observed data that may be related to human influence is identified. This approach is only permissible if supporting evidence exists that links the covariate to human influence (NSM, 2016).

Examples of work that have used this approach are King et al. (2015), which analysed the annual recordings within the Central England Temperature meteorological dataset and Oldenborgh et al. (2015) where a generalized extreme value (GEV) distribution was applied to seasonal and daily winter minimum temperatures from historical data in Chicago, Netherlands and De Bilt, the study excluded the extreme event under investigation and allows the GEV location parameter to change with a change in climate which is represented by global mean temperature. This approach allows for a comparison of the return time of an extreme event between the present climate and the climate of the 1950s. Results produced indicate that warm events will occur more frequently, and cold events have become considerably rare.

In summary, attribution using statistical analysis of observed time series works best for temperature, or variables closely linked to temperature, as global and regional results are available that approximate the contribution of human influence to long-term temperature change (NSM, 2016).

2.9.2 Methods that Use Models

Climate models in extreme event attribution studies are an important tool (NSM, 2016). The type and configuration of the model are dependent on the type of extreme event being analysed, most studies make use of global atmospheric models (NSM, 2016). Attribution studies also tend to make use of one or more coupled climate models, for example, models used in CMIP5 (Taylor et al., 2012; NSM, 2016). Extreme events are not sufficiently represented by global models due to the low spatial resolution of coupled and atmosphere-only models (NSM, 2016). To resolve this issue downscaling is employed (NSM, 2016). Downscaling is the use of additional models, which are embedded within the global

models to provide large-scale environmental characteristics to represent extreme events (NSM, 2016). Downscaling is commonly used to represent scales at a finer resolution than the global models in which they are embedded (NSM, 2016).

Advantages of using climate models in attribution work include (NSM, 2016):

- Models can utilise input conditions such as: SST, aerosols, and levels of atmospheric CO_2;
- The ability to compare results between simulations with different input scenarios such as comparing a factual world with climate change to a counterfactual world scenario that does not incorporate climate change; and
- Model simulations have the ability to produce quantitative estimations of the extent to which extreme climate event magnitudes or frequencies differ in the factual world compared to what would have happened counterfactual world.

GCMs: GCMs are a three-dimensional representation of the various processes that occur in the atmosphere, oceans and over land surfaces (Jacob and van der Hurk, 2009). GCMs represent the Earth's surface as horizontal and vertical areas through grid cells (see Fig. 10). Within each grid cell, GCMs calculate: water vapour and cloud atmospheric interactions, effects of aerosols on radiation and rainfall, storage of heat in oceans and soils, surface changes of moisture and the large-scale transfer of heat and moisture by the oceans and atmosphere (Wilby et al., 2009).

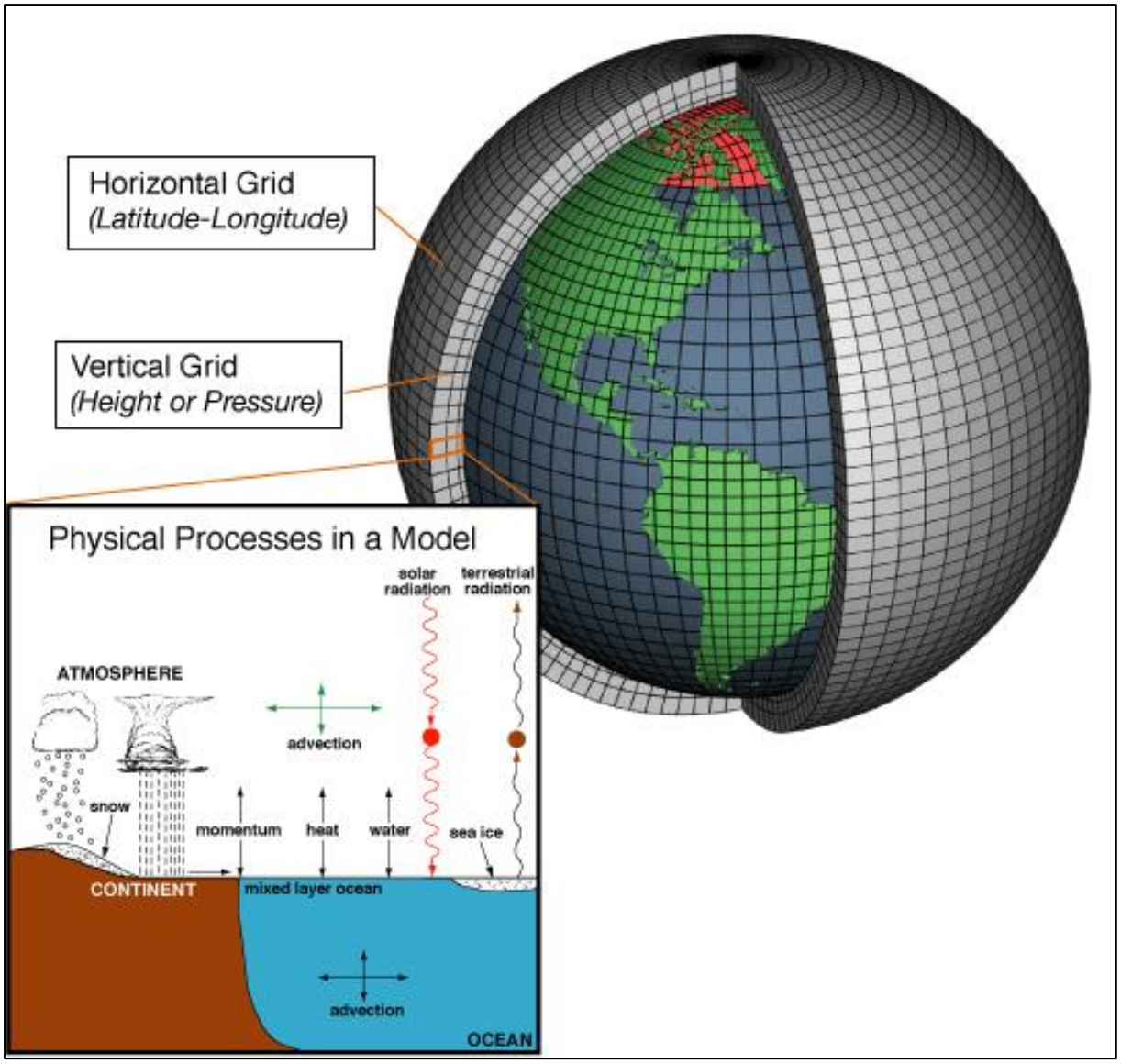

Figure 10. Conceptual schematic structure of a GCM (NOAA, 2012).

GCMs often include: interactive representations of the ocean, sea ice, biological and chemical processes of the atmosphere and land surface, as well as the carbon cycle (NSM, 2016; Stott et al., 2016). Coupled GCMs offer the most complete simulation of the climate system and its processes (Stott et al., 2016). Data from past modelled experiments with various scenarios of forcing combinations are available from the archive of the World Climate Research Programmers CMIP5 (Taylor et al., 2012) and can be used in the analysis of extreme climate events (NSM, 2016; Stott et al., 2016). Generally, this involves the pooling of data from multi-model ensembles of simulations with and without anthropogenic influences and generating large samples of the applicable climate variable (e.g. temperature will be of importance when investigating a heatwave) (Stott et al., 2016). The distribution of the variable in the actual and the counterfactual world can, therefore, be constructed, from which estimates of the RR and FAR for the extreme event being analysed can be determined (Stott et al., 2016). A lot of work has been done using this approach in Australia where recent temperature and rainfall extreme events were analysed (Lewis et al., 2013; Knutson et al., 2013; Perkins et al., 2014). The studies illustrate that anthropogenic forcing has caused multiple increases in the likelihood of Australian heatwaves, however, the influence of anthropogenic forcing on rainfall

extremes is less clear. For such attribution investigations, the models used in studies must be thoroughly evaluated against historical observations (Perkins et al., 2007).

Coupled model approaches are typically used to provide fast-track assessments which are available as soon as an extreme event occurs (Stott et al., 2016). The changing probability of extreme events is determined with reference to pre-specified thresholds (Stott et al., 2016). By pre-computing these estimates over an array of thresholds, attribution information becomes readily available when a new event is observed (Stott et al., 2016). This attribution approach has been applied to the attribution of extreme events related to certain features of the climatic conditions present at the time of the event under investigation (Stott et al., 2016). Such as studies investigating how anthropogenic influence under La Niña conditions affected the likelihood of extreme rainfall experienced during 2011-2012 over south-Eastern Australia (King et al., 2013) and the likelihood of the extreme drought observed in 2011 over Texas (Hoerling et al., 2013).

***SST Forced Atmosphere Only Model Approaches**:* Another method of conditioning results on characteristics of present climatic conditions of extreme events is to make use of an atmospheric GCM in which the anomalies of observed SSTs and the extent of sea ice is specified in an atmosphere climate model (NSM, 2016; Stott et al., 2016). These models are typically coupled with a land model (NSM, 2016). This modelling approach has the ability to impose specific patterns of SSTs and GHG's, applying a degree of conditioning on the results, which cannot be achieved using the CMIP5 model (NSM, 2016). Atmosphere-only based models have smaller biases than that of coupled models and are relevant for looking at local weather events and ignore ocean-atmosphere feedbacks (NSM, 2016). The number of ensemble members in these types of models can range from a few runs of large-scale events (Wilcox et al., 2015) to large ensembles with over 100 simulations (Christidis and Stott, 2012).

Perturbations for generating ensemble members: A common characteristic of studies that use a large number of ensemble members is that they tend to be limited to a single model, furthermore, they tend to make use of a large number of simulations in the range of one-10 years as opposed to a smaller number of longer or multi-decadal simulations (NSM, 2016). There are three types of perturbations that are important for producing ensemble members as described below (NSM, 2016):

- **Initial Condition Ensembles**

The model is run with several varying initial conditions in the start, initial condition ensembles are used in nearly all model-based event attribution studies to produce the replication required to quantify the frequency of events or distribution of event magnitudes.

- **Model Physics**

Perturbed physics experiments are generally not used in attribution studies – primarily because with a prescribed SST design, perturbations that do not degrade the model climatology significantly have also been established to have very little impact on variables of significance, however, they could be. The prospect for this kind of perturbation arises because processes in the models that take place at scales smaller than that of the resolved scale are typically determined using information from resolved-scale fields such as: temperature, wind and, geopotential. These approximations include adjustable parameters with values estimated based on empirical studies and are usually fixed for all model simulations. An example of a process that occurs at spatial scales of a few kilometres is atmospheric convection, this process must be parameterized in models that have resolutions that are too coarse to allow atmospheric convection to be accurately simulated on the model grid. According to Stainforth et al. (2005), simulations using specific parameter combinations are evaluated to determine the realism of the simulated climate in comparison to the observed climate.

- **SST's**

In attribution studies, SST perturbations are used to simulate the counterfactual world as well. As opposed to using control simulations such as in the CMIP5, experiments that use SSTs include "counterfactual" SSTs in which the anthropogenic contribution to modern SST patterns is deducted from the observed SSTs, such as the method used by Pall et al. (2011). Perturbations to the SST patterns are conducted to determine the sensitivity or quantify uncertainty in event attribution results to the selected counterfactual SST.

2.10 Climate Impact Detection and Attribution

This section describes the current state of climate impact detection and attribution, as well as the difficulties involved in conducting these experiments. Impact attribution of anthropogenic climate change is an important, less studied, branch of attribution science as discussed further on in this section. There is a lack of end-to-end impact attribution studies, particularly on the impacts of climate change on water resources in Africa.

There is an increasing interest in attributing the risk of detrimental climatic-related events to anthropogenic climate change (Hegerl al., 2007). The impacts of recent regional climatic changes on biophysical and human systems have been documented globally, however, there is a lack of studies explicitly linking these observations to anthropogenic forcing of the climate (Hansen and Stone, 2016). Assessing whether recent climate change has caused observable damage entails assessments done within a rigorous detection and attribution framework, as impacts include: physical, biological, social and, ecological systems, the framework of assessment needs to cover a vast range of methods to collect and evaluate evidence (Stone et al., 2013). Detection and attribution of impacts of climate change provide the most robust and consistent analysis possible of the cause-effect chain, combining all possible sources of information in a logical evaluation (Hansen and Stone, 2016).

Detection and attribution of impacts assess whether biophysical and human systems are changing as a result of climate change, both are described in more detail below:

Detection of impacts of climate change addresses the question of whether a natural or human system is changing beyond a specified baseline that describes its behaviour in the absence of climate change (Stone et al., 2013). The specified baseline may be stationary or non-stationary and must be clearly defined. This definition focuses unequivocally on the impact of climate change and not on trends as a result of climate change in combination with other factors (Cramer et al., 2014). The detection of impact statements is binary (i.e. an impact has or has not been detected in a system) (Cramer et al., 2014).

Attribution of impacts addresses the question of the extent of the contribution of climate change to a change in a given system (Cramer et al., 2014). In practice, an attribution statement specifies the degree of the observed change which is a result of climate change with an associated statement of confidence (Cramer et al., 2014). Therefore, impact attribution requires the evaluation of external drivers that contribute to change in a given system (Cramer et al., 2014).

Employing a systems analytical perspective, the Earth can be divided into human systems, natural (non-climatic) systems and the climate system (see Fig. 11). Each system, through various mechanisms, can be affected by the other two systems (Stone et al., 2013). From the point of view of the impacted system, these mechanisms are termed *external drivers* (Hegerl et al., 2010). Identifying the explicit role of these external drivers is the fundamental core of impact detection and attribution (Stone et al., 2013). As natural systems are impacted by a variety of other different forcings, of which

many are unrelated to climate change, the term *confounding factor* is often used to describe this particular class of drivers (Stone et al., 2013).

Human activities have the potential to affect other systems through climate change drivers (red arrows in Fig. 11). Humans also affect natural systems, in ways not connected to climate, through activities such as urbanization and water resource management among others (blue arrows in Fig. 11). Sequentially, natural systems and the climate system may impact each other and/or human systems. However, a number of these drivers may be linked directly to an anthropogenic driver of climate change (dashed red arrows in Fig. 11). In contrast, there are external natural forcings, such as volcanic eruptions, which can be regarded as completely independent of these three systems which can also affect climate (grey arrows in Fig. 11).

Performing an impact detection and attribution study involves conceptually isolating the system of interest (shaded circles in Fig. 11), resultantly, all of the incoming drivers affecting the system can be considered external for the purpose of the study (Stone et al., 2013). The analysis then comprises evaluating how the observed behaviour of the isolated system compares against what would be expected if all external drivers were removed (Stone et al., 2013).

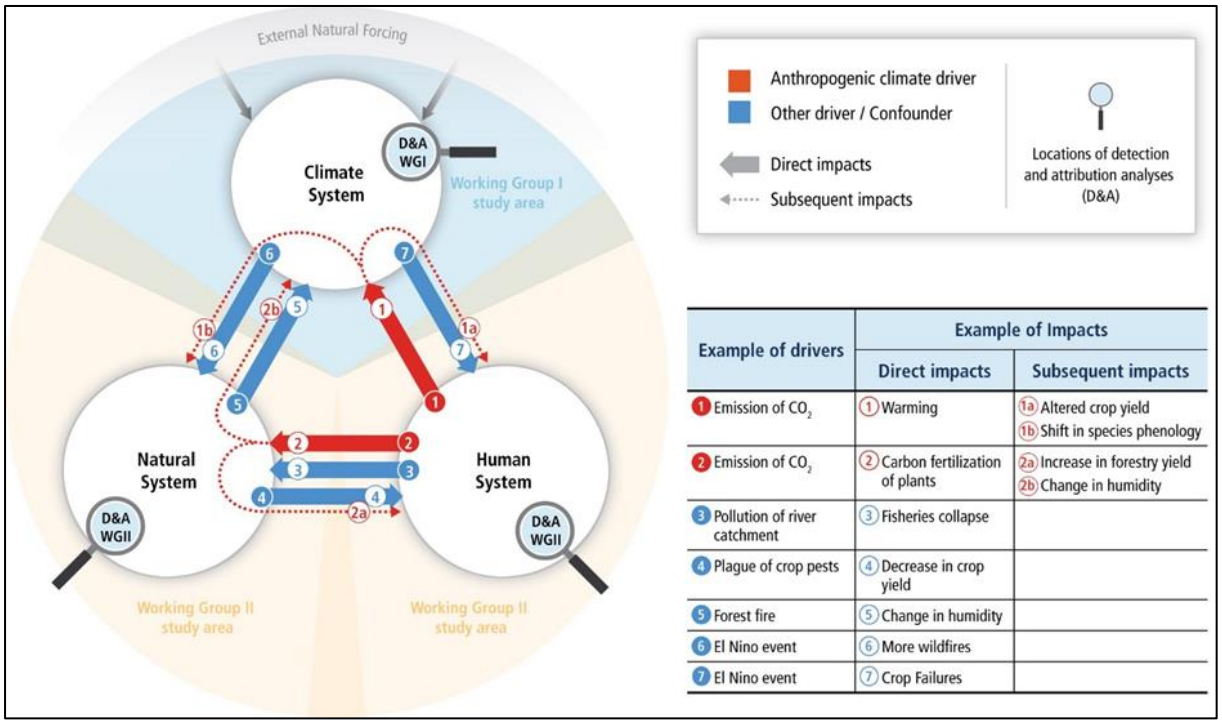

Example of drivers	Example of Impacts	
	Direct impacts	Subsequent impacts
1 Emission of CO_2	1 Warming	1a Altered crop yield 1b Shift in species phenology
2 Emission of CO_2	2 Carbon fertilization of plants	2a Increase in forestry yield 2b Change in humidity
3 Pollution of river catchment	3 Fisheries collapse	
4 Plague of crop pests	4 Decrease in crop yield	
5 Forest fire	5 Change in humidity	
6 El Nino event	6 More wildfires	
7 El Nino event	7 Crop Failures	

Figure 11. Schematic depiction of the interactions in the world as viewed in the detection and attribution analysis (Cramer et al., 2014).

Two approaches exist in impact attribution and detection studies, the single-step and multi-step approach as described by Hegerl et al. (2010), see Fig. 12. The single-step approach makes use of a single modelling setup to link changes in drivers to changes in a particular aspect of a climate, natural or human system. In contrast, a multi-step approach relates separate single-step approaches into an overall attribution assessment. For example, one single-step analysis may link the retreat of a European glacier to local summer warming, while another single-step analysis will link the annual warming over Europe to anthropogenic emissions. A multi-step analysis would combine the aforementioned studies into an analysis of the impact of anthropogenic emissions on that particular glacier.

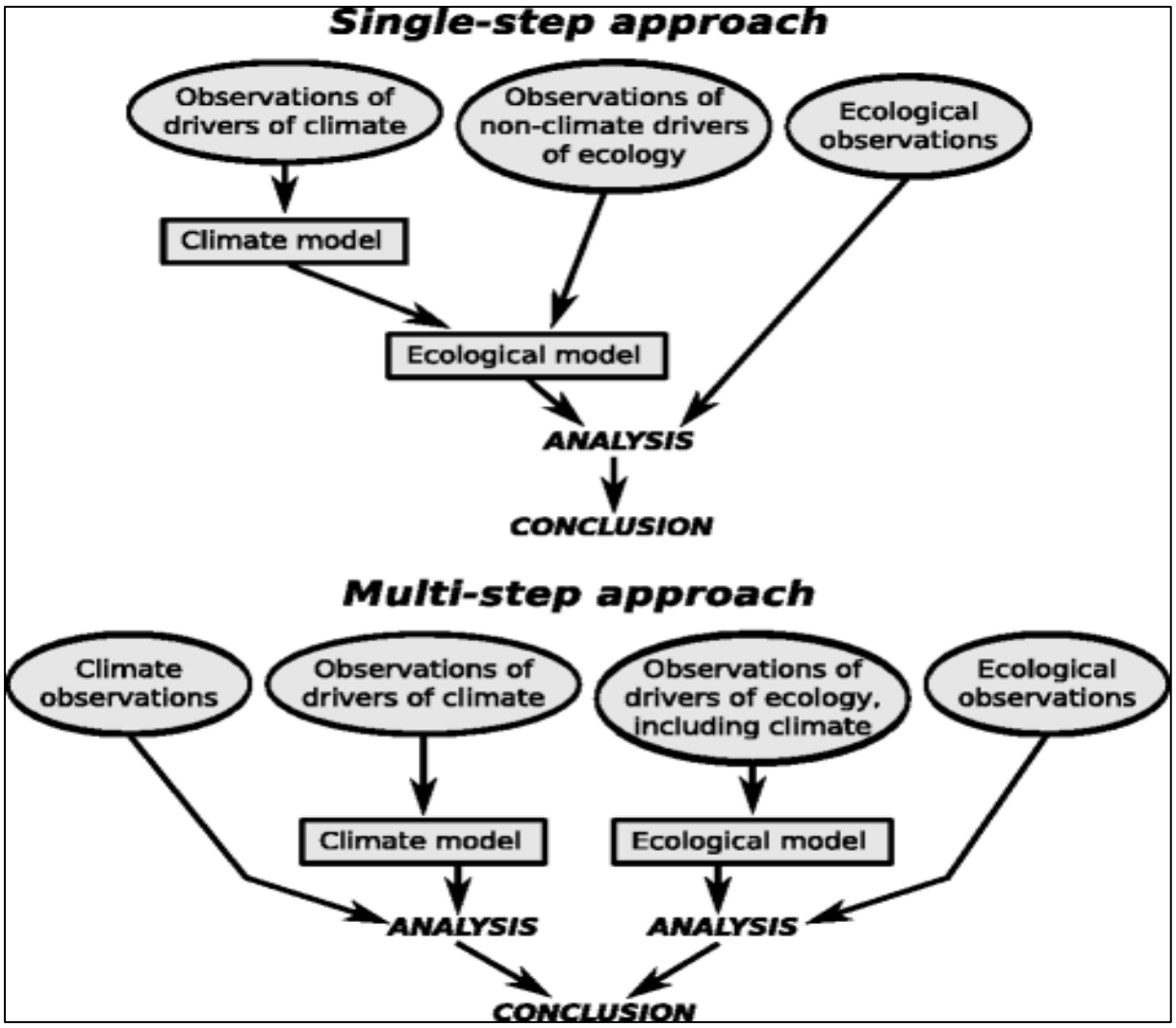

Figure 12. Techniques for single-step and multi-step approaches to attribution of an ecological system (Stone et al., 2013).

Globally, the impacts of climate change have been observed on the hydrological system, particularly on freshwater resources, with varying characteristics of change, in different regions of the world (Cramer et al., 2014). Confidence of detection and attribution tends to be higher for frozen components of freshwater systems, while components, such as streamflow, affected by non-climatic drivers tend to have lower confidence levels (see Fig. 13).

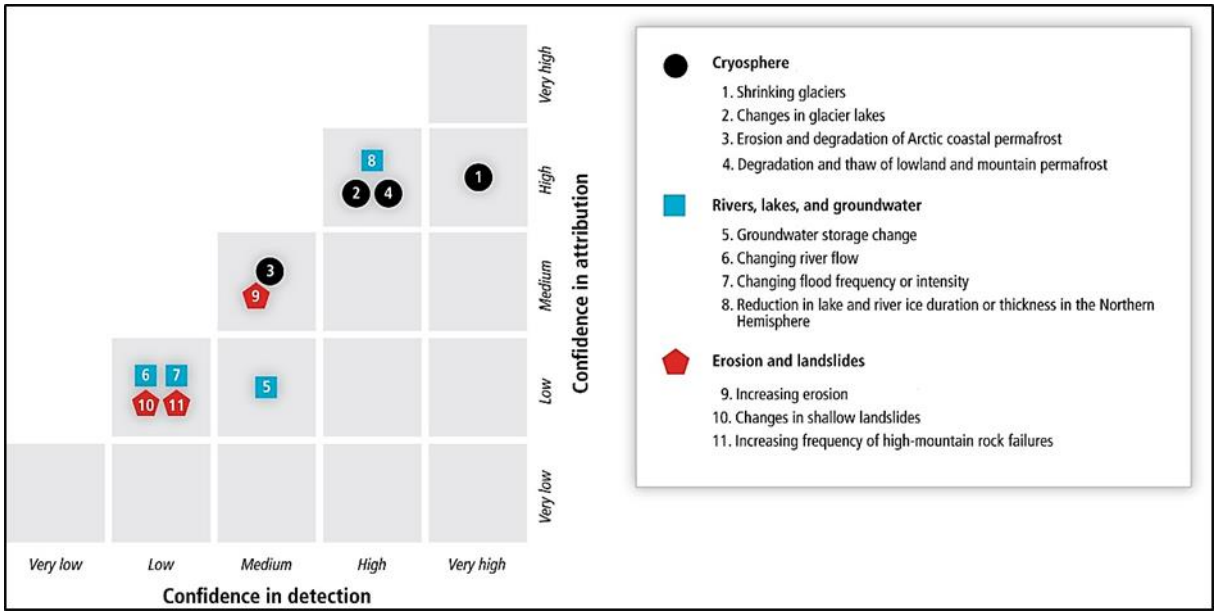

Figure 13. Assessment of confidence in the detection of observed climate change impacts in global freshwater systems over several decades, with confidence in attribution of a major contribution of climate change (adapted from Cramer et al., 2014).

Significant challenges exist in the detection and assessment of the impacts of climate change on biophysical and human systems (Cramer et al., 2014). Fundamentally, all such systems are affected by factors other than climate change (Cramer et al., 2014). Therefore, separating the impacts of climate change requires controlling for the impacts of other factors in the systems (Cramer et al., 2014). Further challenges in impact attribution arise through the ability of many of the systems to adapt to a changing climate (Cramer et al., 2014).

Hansen and Stone (2016), assessed the contribution of anthropogenic climate change for the varying impacts of regional climate trends reported in the IPCC AR5. According to their analysis, nearly two-thirds of the impacts linked to ocean and atmospheric temperatures can be confidently attributed to anthropogenic forcing. In comparison, evidence linking precipitation changes and their relevant impacts to human influence is still low.

End-to-end attribution studies, such as Hansen and Stone (2016) and this study, of anthropogenic climate change impacts on water resources, i.e. from emissions to runoff impacts, is generally not undertaken, as it requires experiments with climate models where the anthropogenic and external natural forcing is "switched off" (Kundzewicz et al., 2018). Apart from this, climate models currently do not simulate the hydrological cycle at a sufficiently fine resolution for the attribution of catchment-level hydrological impacts to that of anthropogenic climate change (Kundzewicz et al., 2018). In the future, it is expected that climate models and impact models will become more integrated (Kundzewicz et al., 2018).

2.11 Hydrological Modelling

Hydrological models are powerful tools in climate impact studies for assessing the effects of climate change on the hydrological cycle, discussed in detail later in this dissertation. The various types of hydrological models and their abilities are discussed as the choice of model will have a direct effect on the findings of an attribution study. It is always best to choose a model that has already been set up and validated for the region of interest, as these models would only require the extension of climatological data.

Hydrological models are simplified mathematical representations of the complex interlinked dynamic and nonlinear conversion of climate variables (i.e. precipitation, evaporation and temperature) into outputs (i.e. runoff, groundwater content and soil moisture) (Beven, 1989; Xu, 1999; New et al., 2002). Modelling hydrological processes that occur at a catchment scale such as: evaporation, infiltration, transpiration, soil-water redistribution, surface, sub-surface and groundwater flows are accounted for in conjunction with the process-based mathematical equations that are centred on established scientific principles (Hesse et al., 2008; Wheater, 2008). Initially, hydrological models were developed to assess catchment response to different hydrological settings (Xu and Singh, 1998). However, in response to current developmental trends, hydrological models have also been used for various other purposes. Uses of hydrological models include (Xu, 2002):

- Assessing the spatial and temporal distribution of water supply;
- Evaluating the impacts of climate change and land-use on water resources;
- Reconstructing a catchment hydrological regime;
- Forecasting water resources yield;
- Producing runoff records for ungauged catchments; and
- Classifying regions based on hydrology and climate.

2.11.1 Types of Hydrological Models

Typically, modellers attempt to set up the simplest model that has the potential to effectively address the given issue (Watts, 2011). This approach has several benefits such as; the development of the model is less time consuming, computation time is greatly decreased and, interpreting the results of the model is simpler (Watts, 2011). For any particular hydrological problem, the main control on the choice of a hydrological model is considered to be the availability of base hydrological data, but also greatly depends on the availability of future climate data, the complexity of the physical water-supply system, the type and scale of the problem and, catchment characteristics (Watts, 2011; Tirivarombo, 2012).

Perceptual models (White box models) are a summary of the modeller's perceptions of how a given catchment would respond to rainfall under different settings (Beven, 2005). These models have a logical structure that is analogous to that of the real-world system and may be useful under changing conditions in a catchment (Xu, 2002). The perceptual model of a given catchment is important because the mathematical descriptions which may be used for generating predictions will be simplifications of the perceptual model, which in some cases could be extreme simplifications that are still sufficient to provide acceptable predictions (Beven, 2005).

Conceptual models (Grey-box models) are a mathematical description that allows for quantitative predictions (Beven, 2005). They account for hydrological physical laws in a highly simplified form (Xu, 2002). These models range in complexity, from employing simple mass balance equations to represent components of storages in a catchment to joint nonlinear partial differential equations (Beven, 2005).

Empirical models (Black-box models) do not aid in the physical understanding of the hydrological process (Xu, 2002). These models contain hydrological parameters which may not have much direct physical significance and can only be determined using concurrent measurements of inputs and outputs (Xu, 2002).

The distinction between deterministic and stochastic models*:* Models are usually divided into deterministic and stochastic sub-classes (Jewitt and Gorgens, 2000). Deterministic models allow for a single outcome from a simulation with only one set of input and parameter values (Beven, 2005). Deterministic models tend to be complex, and may not accurately predict the estimation of water resources, primarily due to inadequate model representations of catchment processes as well as a poor representation of spatial variability of rainfall-runoff processes (Hughes, 1995). Stochastic models permit a degree of randomness or uncertainty in the possible outputs as a result of uncertainty in input variables, model parameters or boundary conditions (Beven, 2005). To a large extent, the majority of models implemented in rainfall-runoff modelling are used in a deterministic way (Beven, 2005).

The distinction between distributed and lumped models: For spatial discretization, lumped models consider the catchment as a homogenous whole. Semi-distributed or distributed models attempt to calculate contributions of flow in distinct areas which are considered homogenous within themselves. Whilst, in distributed models the entire catchment region is divided into unit areas similar to that of a grid net and in which flows pass from one node to another as water is drained through the catchment (Xu, 2002).

2.12 Downscaling Techniques

This section describes and weighs up the pros and cons of statistical and dynamical downscaling. Downscaling climate data from GCMS is important in regional climate change attribution studies in achieving the most realistic simulation of the climate variable being analysed for the spatial and temporal scale at which the variable is being inputted into an impact model. The method chosen to downscale is dependent on the needs of the study and available resources.

Assessing the risk of climate change and its impacts often require climate information at a national to a local scale (USAID, 2014). Downscaling has been developed to produce climate information at a finer scale of local interest than that of GCMs (USAID, 2014), which typically have a spatial resolution of 100s of km or 2.5° latitude/longitude grid cells. Downscaling can be categorised into two classes, statistical and dynamical (Hughes et al., 2014). Typically, any information that is at a spatial scale finer than 100 x 100 kilometres and a finer temporal scale than monthly values have gone undergone some form of downscaling (USAID, 2014).

When interpreting downscaled information from GCMs it is important to consider the following (USAID, 2014):

- Downscaling techniques assume that regional climate is a combination of large-scale climatic features (i.e. global, hemispheric, continental and regional) and local conditions (water bodies, topography, and land surface properties);
- Representation of local conditions is typically beyond the potential of GCMs; and
- Downscaling climate data from GCMs to local scales involves several steps. Each step involves several assumptions and estimates, resulting in uncertainties in climate data.

Statistical downscaling can be described as an empirical approach that forms relationships between GCM outputs and local-scale variables, such as precipitation and temperature (Hewitson and Crane, 1996, Fowler, 2007). Once a validated relationship has been established, future large-scale atmospheric conditions produced by GCMs are employed to project future regional climate features (USAID, 2014). Statistical downscaling techniques have been extensively applied across the African continent in comparison to dynamical downscaling (e.g. Conway and Hulme, 1996; Yates and Strzepek, 1998; Hewitson and Crane, 2006; Brown et al., 2008).

Dynamical downscaling a fine-scale RCM that can provide greater detail of physiographic data is nested within a coarse GCM (Leung et al., 2004). The aim of dynamical downscaling is to extract local scale data from large-scale data within a GCM (Tirivarombo, 2012). Lateral boundary conditions and SSTs from a GCM are forced onto an RCM. High-resolution RCMs have a spatial resolution of 10 to 50 km or 0.5° and simulate climate processes dynamically by use of the temporal variation of atmospheric conditions at the boundary of a given domain (Tirivarombo, 2012). Variables simulated by GCMs (i.e. temperature, wind and vapour) are superimposed at different levels on the boundary of the RCM at various horizontal and vertical points (Xu 1999; Wilby, 2007). The RCM then manipulates the GCM data in a way that the patterns of climate change differ from that of the GCM (Tirivarombo, 2012).

Table 8. A summary of dynamical and statistical downscaling processes (STARDEX, 2005; Fowler et al., 2007; Wilby et al., 2009; Daniels et al., 2012; USAID, 2014).

	Dynamical downscaling	**Statistical downscaling**
Provides	• Information at 20-50 km grid cells; • Data at sites with no historical data; • Daily time-series; • Monthly time-series; and • Scenarios for extreme climate events.	• Any scale, to station-level data; • Some methods provide daily time-series; • Monthly time-series; • Some methods provide scenarios for extreme climate events; and • Scenarios for any constant observed variable.
Requirements	• High expertise and computational capacity; • Large amount of data inputs; and • Reliable global climate model simulations.	• Low-medium computational capacity; • Low-medium amount of data inputs; • Adequate volume of high-quality observational data; and • Reliable global climate model simulations.
Advantages	• Based on constant physical mechanism; • Not limited by observational records, such that novel scenarios can be replicated; and • Experiments that involve an ensemble of regional climate models are being made available for analysis of uncertainty.	• Computational requirements are low-cost and competent, which allows for many emissions scenarios to be run; • Methods can range from simple to complex and are flexible enough to accommodate specific purposes; • A single method can be applied in a regional or global scenario, which enables comparisons of different case studies; • Depends on historical climate for as a basis for future projections; and • Tools are available at no cost and implemented and interpreted with ease.
Disadvantages	• Computationally demanding; • As a result of computational requirements, regional climate models are generally driven by a single emission scenario; • Very limited number of regional climate models are available and model results for many parts of the globe do not exist; • Could require additional downscaling as well as bias correction of RCM outputs; and • Results dependant on RCM assumptions.	• Good quality historical data may not be available for several regions and/or variables; • Assumes that interactions between local and large-scale processes remain unchanged for future projections; and • Simple methods could only provide resolutions at a monthly scale.
Applications	• Country or regional scale analysis with substantial government support and resources; • Future planning by government organisations across various sectors; and • Impact assessments across many geographic areas.	• Weather generators in extensive use for crop-yield and water resource modelling and management; and • Delta method for adaptation activities.

2.13 Uncertainties in Climate and Hydrological Models

Both climate and hydrological models are important tools in attribution impact studies, however, it is impossible to simulate the climatological and hydrological processes with a degree of high confidence, resultantly uncertainties will exist. However, it is possible to evaluate the respective model against available observed data, to assess the model's ability to satisfactory simulate the variable of interest.

By definition, a numerical model is never a complete depiction of a real-world system (Fung et al., 2011). The incomplete understanding of the climate system, the lack of ability to describe all known processes of a model as well as the restrictions in the context of resolution and computational ability all suggest that the modelling of the climate system is flawed (Fung et al., 2011). The uncertainties related to climate inputs such as precipitation and evaporative demand in hydrological models will always be great, particularly in southern Africa due to the relative sparseness of historical data (Hughes 1995; Sawunyama and Hughes, 2007).

The uncertainties that accompany GCMs and the downscaling approaches used for regional or local hydrological models tend to result in inconsistencies in projections of future water resources availability (Hughes et al., 2014). Although it is often put forward that climate change will have the most severe impact on the availability of water resources (Bates et al., 2008), a significant degree of uncertainty remains associated with GCMs and methods used to downscale the inputs of hydrological models (Hewitson and Crane, 1996; Segui et al., 2010; Chen et al., 2013).

A study by Jian et al. (2007) using six hydrological models showed that simulated runoff differed between the models by up to 20% under an increase in temperature (4 °C) and a decrease in precipitation (-20%). Bae et al. (2011), employed three semi-distributed hydrological models to investigate the uncertainty associated with the hydrologic model structure using 13 GCM simulations with three GHG emission scenarios. The study showed that monthly and seasonal simulated runoff change by a single hydrological model is in the range of $\pm$10% of a multi-model ensemble result, apart from low season flows.

A share of this uncertainty stems from the various structures and initial conditions that different GCMs assume, various model inter-comparison studies have illustrated that there can be significant variations in the outputs that represent both present climate (Reichler and Kim, 2008) and future-climate (Hughes et al., 2011). According to Hughes et al. (2014), the notion behind the use of multi-model ensembles is possibly based on the fact that inherent errors exist in all models (mostly due to the need to simplify the complexity of atmospheric physics) as well as that the use of multi-model ensembles provides increased coverage of potential climate outputs. However, it has been noted that the use of single-model ensembles is equivalent to disregarding the uncertainties and in contrast to the trend in hydrological sciences that attempt to account for all uncertainties (Pappenberger and Beven, 2006).

The output of GCMs is often considered inadequate for use within hydrological models applied at a catchment scale because the spatial resolution is not fine enough (Hughes et al., 2014). It is, therefore, necessary to use a downscaling approach (Bouwer et al., 2004; Fowler et al., 2007; Segui et al., 2010; Frost et al., 2011). Whilst downscaling addresses spatial scale issues it tends to introduce a set of different uncertainties into predictions (Buytaert et al., 2010). For hydrological and water resources analysis, GCMs must have the ability to produce realistic patterns of rainfall seasonality, persistence and extremes. If GCMs are not able to reproduce these characteristics adequately under present-day forcing conditions, then the confidence in their ability to reproduce future forcing conditions is greatly reduced (Hughes et al., 2014).

2.13.1 GCM Evaluation in Impact Studies

Attribution methods frequently depend on determining event distributions or probabilities of event magnitudes from simulations of climate models (NSM, 2016). As such, the confidence in attribution results depends largely on the ability of the model to simulate the given event, under factual and counterfactual climate scenarios (NSM, 2016).

Attribution of extreme events rely on the model's capacity to reliably simulate the climate conditions which generate the extreme weather event of interest, the model does not necessarily need to have predictive skill, i.e. the model needs the ability to forecast the correct frequency of events as opposed to the exact time of event occurrence (Otto et al., 2015).

It has been argued that a comprehensive event attribution is possible even when only climatology is well simulated by a given model (Christidis et al., 2013). The quality of a model's ability to represent a given event or the climatology of an event type is best done by assessing the factual simulations, as these are expected to agree most closely to that of the observed climate (NSM, 2016). However, in many cases, observational data is limited for extreme events (NSM, 2016).

Evaluations are necessary; however, they are not an adequate representation of a model's ability to simulate the climate (NSM, 2016). The quantitative correspondence of ordinal statistics of variables such as precipitation or temperature between observations and model output does not necessarily suggest that the mechanisms which produce extremes and variability are represented well in the model (NSM, 2016). Assessments of models need to go beyond the traditional quantitative comparison that accounts for sampling uncertainty, the main processes that lead to or increase a given event need to be assessed (NSM, 2016).

Evaluating the quality of a model under a counterfactual scenario can be difficult and is typically determined from the evaluation of model performance under other forcing scenarios of which observational data exists (NSM, 2016).

This assessment includes the evaluation of the quality of the model for the factual world with anthropogenic forcing encompassing the last several decades, which may be based on observational data for periods before anthropogenic influence on the climate or using paleoclimatic reconstructions of the past climatic conditions (NSM, 2016).

At the regional scale coupled models exhibit substantial biases in mean climate and variability in comparison to observations (NSM, 2016). Systematic errors in model output data are corrected by a means of bias correction, the validity of this corrected data must then be established through a model evaluation (NSM, 2016). Typically, model output is bias corrected by calculating anomalies, subtracting or by dividing by a climatological mean and, adjusting the variance (NSM, 2016). Representing drought events are challenging as they depend on precipitation over land, which is a general challenge for models, as well as land surface feedbacks (Seneviratne et al., 2010).

Improving event attribution studies requires increasing the understanding of the model characteristics that are required to reliably simulate extreme climatic events of different types and scales (NSM, 2016).

2.13.2 Hydrological Model Evaluation in Impact Studies

Hydrological models have a significant role in climate change impact assessments as they can be applied to simulate climate change impacts on the terrestrial water cycle as well as to project future hydrological processes (Teutscbein et al., 2011; Velazquez et al., 2013). Reliable information on climatological variables (precipitation, evaporation, temperature etc.) as well as their temporal and

spatial distribution in a catchment, are required to drive a typical rainfall-runoff hydrological model (Teutscbein et al., 2011). GCMs can provide this information, however, for regional hydrological impact studies, the GCM output must be downscaled to derive high-resolution climate parameters for hydrological modelling, for climate impact studies (Teutscbein et al., 2011).

No best model exists for the assessment of climate change impacts in water resources studies (Watts, 2011). However, empirical or statistical hydrological models have the least confidence in their results, due to the models' limited predictive ability (Watts, 2011). The majority of water availability assessments make use of lumped or semi-distributed hydrological models with a daily time step (Watts, 2011). These models provide the best compromise between complexity and practically, however, they may perform unpredictably outside of their calibration range (Watts, 2011).

Several mature water supplies throughout the World are already represented by existing hydrological models, these models are usually extended to consider the hydrological impact of climate change (Watts, 2011). This approach requires a careful review of the hydrological model, usually by an objective function or model performance indices. Commonly used measures of hydrological model evaluation include Nash and Sutcliffe efficiency (NSE), percent bias (PBIAS), residual variation, and coefficient of determination (Krysanova et al., 2016)

In hydrological model evaluations, the most useful variable is runoff, as it reflects the integrated response of a variety of hydrological processes that occur within a catchment (Fekete et al., 2012). Additionally, runoff observations are readily available for many catchments globally (Hannah et al., 2011).

Climate change impact assessments on water resources have increased understanding of the interactions between climate and hydrological processes (Velazquez et al., 2013). The impacts of climate change have been assessed on runoff (Bergström et al., 2001), on flood frequencies (Cameron, 2006), on groundwater levels (Goderniaux, 2009), soil moisture (Mavromatis, 2012), water quality (Wilby et al., 2006) and on evaporation (Kay and Davies, 2008). A large number of hydrological studies focus on climate change impacts at a rather large-spatial scale or on projections at a low temporal resolution (Teutscbein et al., 2011). In contrast, a limited number of studies on regional impacts or extreme events exist, such as flood peaks and droughts (Teutscbein et al., 2011).

There is a lack of scientifically accepted standard procedures to post-process outputs of climate models for hydrological impact assessments, which is a fundamental problem in climate impact and attribution studies (Teutscbein et al., 2011). Additionally, the uncertainty associated with hydrological simulations has yet to be fully evaluated (Teutscbein et al., 2011).

2.14 Summary

The interest in the role of human-induced climate change on recent extreme events has grown in recent years. Attribution aims to address the question of whether something has changed and to assess the causes of that observed change; in this case the 2015−2017 SWC drought to that of anthropogenic influence.

Droughts have a significant impact on all sectors in a region, water resources are imperative for human health, food security and economic growth; the implications of a major agricultural and economic hub such as the SWC running out of water is severe.

The recent SWC drought caused severe water shortages throughout the region; particularly the CoCT. The drought gained a lot of interests from the public, media and climate scientists alike; particularly

as to the contribution of anthropogenic climate change having in a drought of such magnitude occurring.

The WCWSS is very sensitive as it depends almost entirely on the rainfall-runoff conversion, to fill up key reservoirs. As water resources in the SWC are projected to be further constrained in the near-future by anthropogenic climate change (among non-climatic other factors) as a result of rainfall decreases reducing the amount of runoff that flows into the regions reservoirs during the winter rainfall period. Thus, understanding the impacts of an altered hydrological system is important for water resources planning, to avoid another Day Zero situation.

Although attribution is a relatively new field of science, the role of human-induced climate change in the intensity and frequency has been proven for a wide range of extreme climatic events at both the global and regional scale. However, due to the complex nature of drought, the role of anthropogenic climate change on drought events is less clear than that of other extreme climatic events.

Human-induced climate change has been shown to impact natural and human systems, yet not much work has been done to explicitly link these impacts to human-induced climate change and quantitatively assess the role of human-induced climate change on extreme events.

Climate impact attribution studies on water resources on a multi-year drought on a regional scale, like this one, are less common as the focus has been primarily on climate attribution, in which results can be produced more rapidly than that of end to end (climate to impact) attribution studies. Very few multi-step end to end attribution studies on extreme climatic events exist in the literature, particularly on the response of runoff to a change in precipitation using a hydrological model.

CHAPTER 3: DATA AND METHODOLOGY

This chapter begins by providing an overview of climatology, hydrology, and geology among other aspects of the study area. This is followed by a detailed description of the processes and structure of the Pitman hydrological rainfall-runoff model. The rainfall stations used to run the Pitman hydrological model and their correlation to the WR, 2012 study data is presented. This is followed by the streamflow gauging stations and the quantitative objective functions used in the evaluation of runoff simulation in the BRC by the Pitman model are listed and described. The chapter then goes on to describe how the meteorological/hydrological 2015−2017 SWC drought event is defined for the attribution analysis. The methodology, undertaken by Dr Piotr Wolski, used to bias correct the CMIP5 attribution rainfall experiments' 150-year long time series is then presented and described. This is followed by the impact attribution approach used in this study and a description of the analysis of the attribution results for rainfall/runoff.

3.1 Study Area

The BRC in the Western Cape will be used to analyse the effects of anthropogenic climate change on drought in the SWC. The BRC is located north/north-east of Cape Town, in the Western Cape Province of South Africa (see Fig. 15). The BRC covers an area of roughly 9 000 km^2 (Midgely et al., 2014). The BRC is characterized by a Mediterranean climate with warm dry summers and cool wet winters, the rainy season of the catchment is from April to October (DWAF, 2007). The BRC catchment has a mean temperature of 16 °C, with a minimum daily temperature of 4.5 °C (usually occurs in July) and a maximum daily temperature of 29.4 °C (usually occurs in January) (DWAF, 1994). Rainfall in the catchment is concentrated during the cool winter months, with a steep gradient from the south-eastern upper catchment >1200 mm per year to <300mm per year at the north-western area of the catchment (see Fig. 16). Precipitation is generally in the form of frontal rain approaching from the north-west (DWAF, 2007). These frontal rains are a result of the interaction of air masses with different moisture content, temperature and density (DWAF, 2007). The Upper BRC is underlain by Table Mountain Sandstone while the Malmesbury Shale dominates the catchment downstream of Paarl (WCG, 2012).

The WCWSS is comprised of a total of 14 dams with a cumulative capacity of an estimated 900 000 Ml, the majority of this storage capacity is provided by six large dams: The Berg River, Steenbras (Upper and Lower), Theewaterskloof, Voëlvlei, and Wemmershoek dams. Out of the aforementioned large dams, the BRC contains the 2nd (Voëlvlei), 3rd (Berg River Dam) and 4th (Wemmershoek) largest dams in the WCWSS comprising an estimated 39.2% of the total collective capacity of the big six dams (CoCT, 2018d).

Major water users within the BRC include irrigated agriculture (mainly vineyards, fruit trees and wheat fields), processing and treating of crop produce, urban water supply, wastewater treatment and industry, see Fig. 14 (Midgley et al., 2014). Roughly 75% of crop produced in the BRC is exported to the European Union and the United Kingdom (WCG, 2012). The BRC is heavily impacted by both urban and agricultural development and is particularly important for domestic, agricultural, industrial and environmental water security for the CoCT (WCG, 2012). The catchment modifications over the past 50 years are particularly important and offer a high chance of detecting anthropogenic climate change influence on catchment processes (New, n.d.). The Berg River has 19 tributaries (see Fig. 15) with a total annual runoff amounting to 931 million m^3 (DWA, 2007).

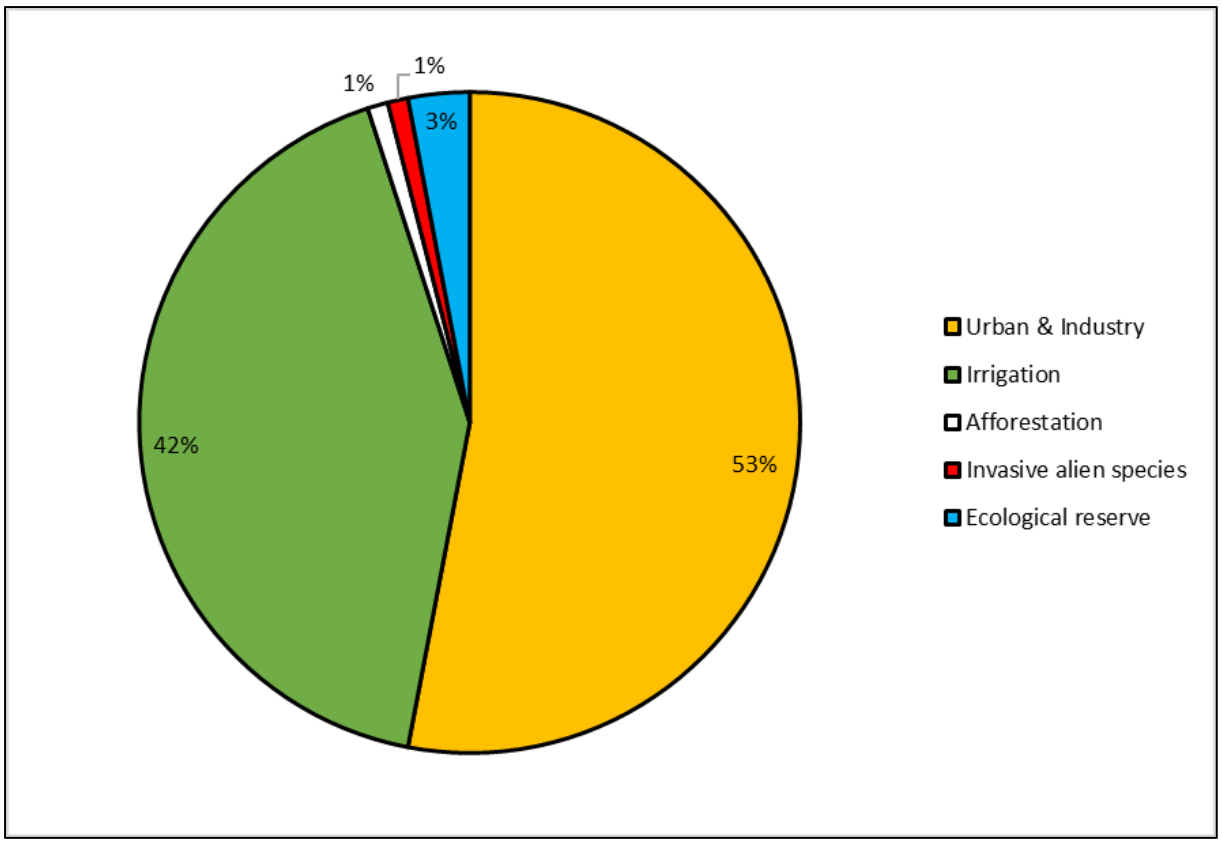

Figure 14. Major water users in the Berg Water Management Area (DEADP, 2013).

The BRC is considered an excellent illustration of an economically significant regional system under great resource extractive pressure at the nexus of water quantity and quality, food production within the context of rich biodiversity and intensive land-use (DWAF, 2004). Major future risks of the BRC include *inter alia* (Midgley et al., 2014):

- A reduction in water supply due to the impacts of climate change and/or basin mismanagement (increasing water resource constraints would result in higher pricing);
- Increasing demand for water due to an increasing population in Cape Town;
- Crop water requirement increases due to climate change (higher temperatures would increase evapotranspiration); and
- A decrease in water quality for agriculture due to increased pollution in the catchment.

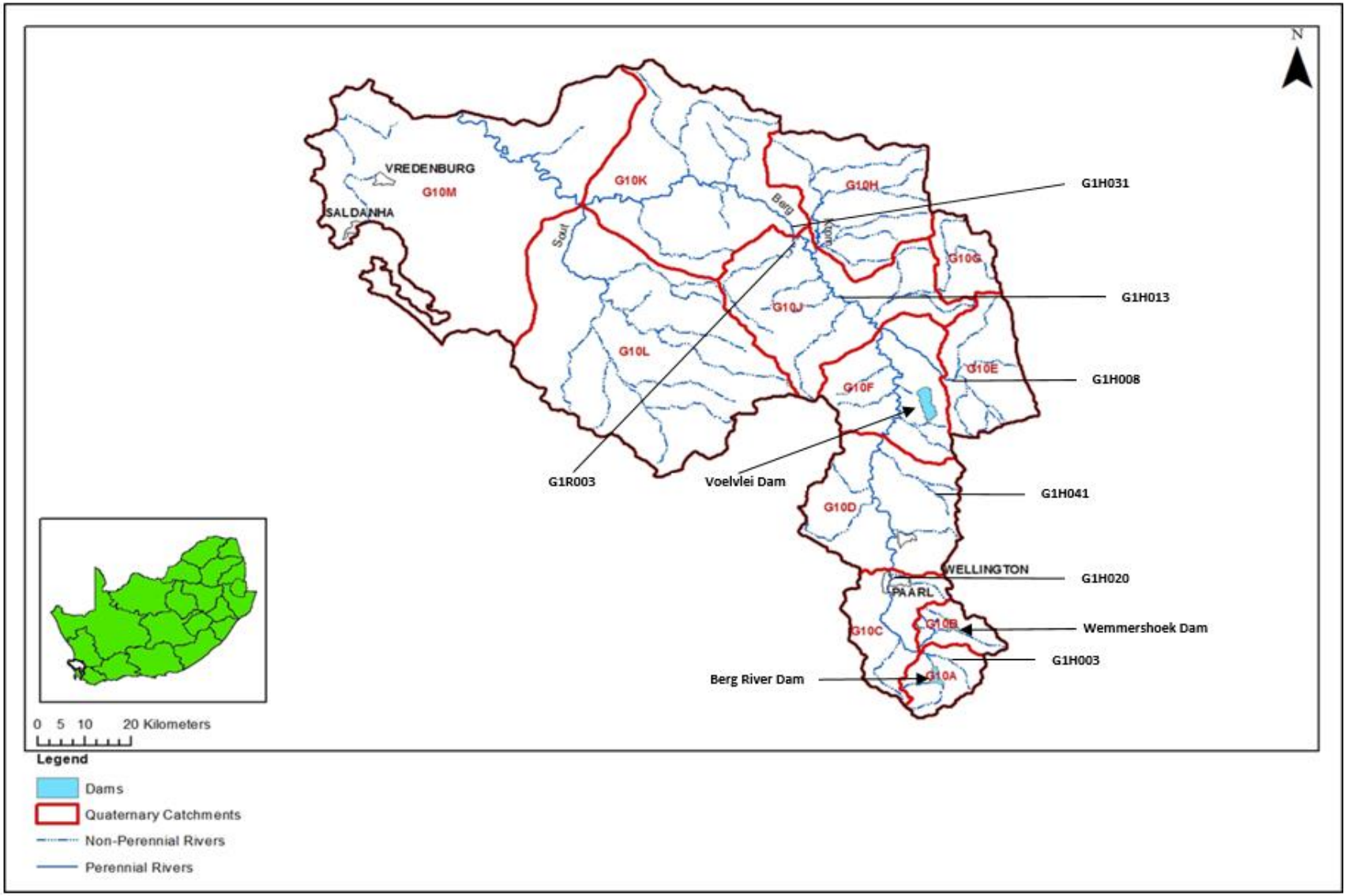

Figure 15. Delineated BRC (Water Resources 2012 study data: WR, 2012).

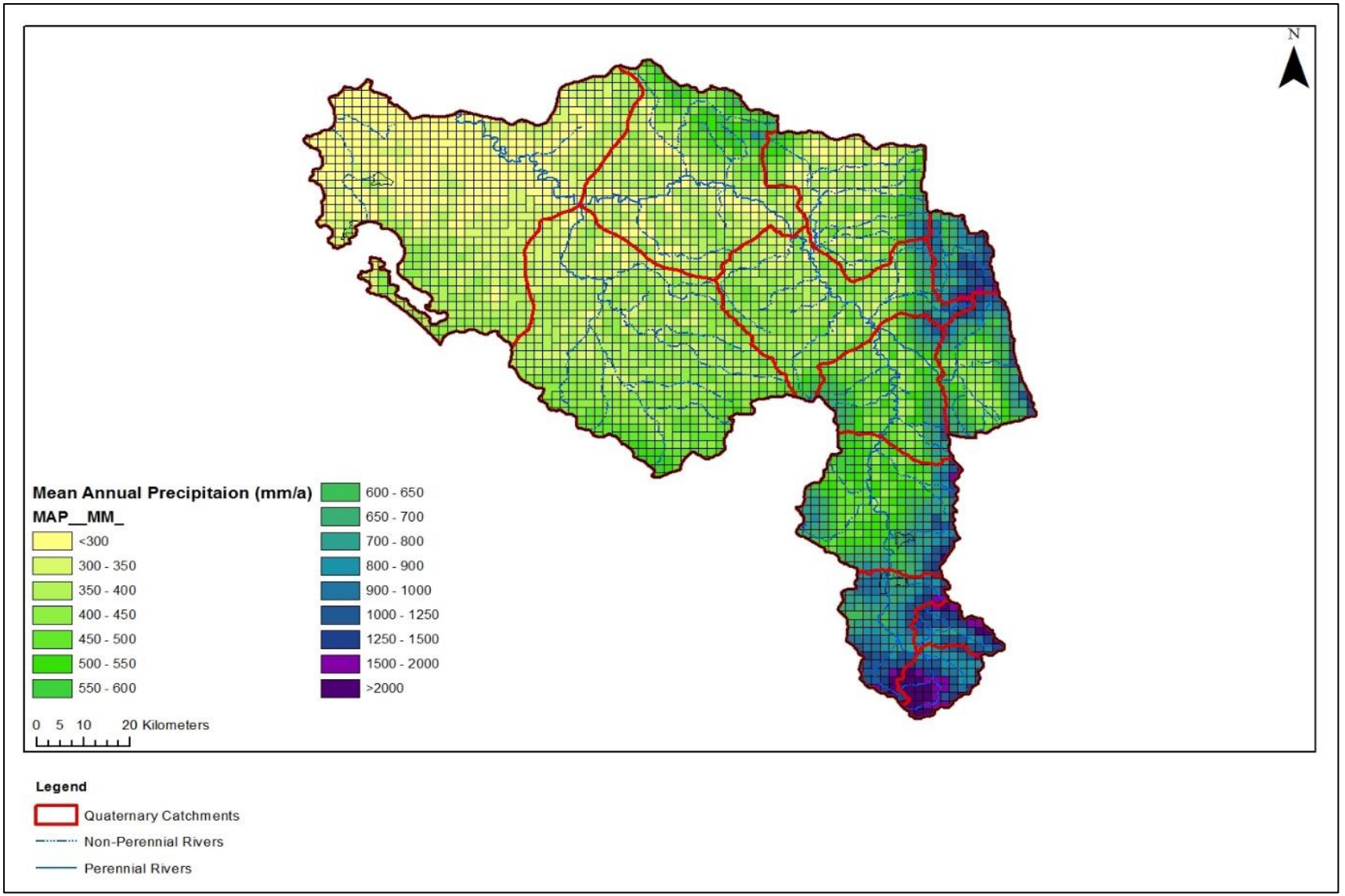

Figure 16. MAP in the BRC (Water Resources 2012 study data: WR, 2012).

3.2 Hydrological Modelling

The simulation of rainfall-runoff in the BRC was carried out using the Pitman model. Rainfall data, streamflow data, and Pitman model data files were updated up to 2017 September to include the three-year SWC drought event and run under the in-built model parameters for present-day catchment conditions. Hydrological years are different to normal calendar years. The South African summer hydrological year is established as from October to September, but also works for the winter rainfall regime in the SWC as October marks the end of the rainfall season in the dominantly winter rainfall SWC. As such, hydrologically speaking the analysis of the 2015−2017 drought, is from 2014 October to 2017 September, for ease of reference, this will be referred to as 2015−2017 for the remainder of this dissertation.

3.2.1 The Pitman Model

The Pitman model, developed in 1973 in South Africa is a conceptual, semi-distributed, monthly time-step rainfall-runoff model (Tanner and Hughes 2013; Tumbo and Hughes, 2015). The Pitman model in its various forms has been extensively applied in hydrological studies throughout southern Africa for purposes of research and hands-on assessments of water resources (Hughes, 1997; Hughes and Metzler, 1998; Mazvimavi et al., 2005; Hughes, 2006; Tsheko, 2006; Ndiritu, 2009; Tshimanga et al., 2011; Wolski et al., 2014). The Pitman model has contributed greatly to the water resources assessment field across southern Africa, particularly in South Africa, and is the basis of water resources assessments in the country (Pitman et al., 1981; Midgley et al., 1994; Bailey and Pitman 2005; WR, 2012).

The Pitman model is comprised of three conceptual storages (soil moisture, interception and groundwater) and mimics infiltration excess flow, overland flow, saturation-excess flow and groundwater flow (Tanner and Hughes, 2013) which are linked by functions to represent various hydrological processes at a catchment scale (Kapangaziwiri, 2010).

The Pitman model has undergone several developments since its initial construction that attempt to account for challenges related to data availability and to improve the ability of the model to quantify hydrological processes at a catchment scale (Kapangaziwiri, 2010).

3.2.2 Structure and Parameters of the Pitman Model

A brief overview of the main inputs, processes and their parameters in the Pitman model is described below taken from Bailey and Pitman, 2016. Figure 17 (below) illustrates the structure, processes and steps in the Pitman model.

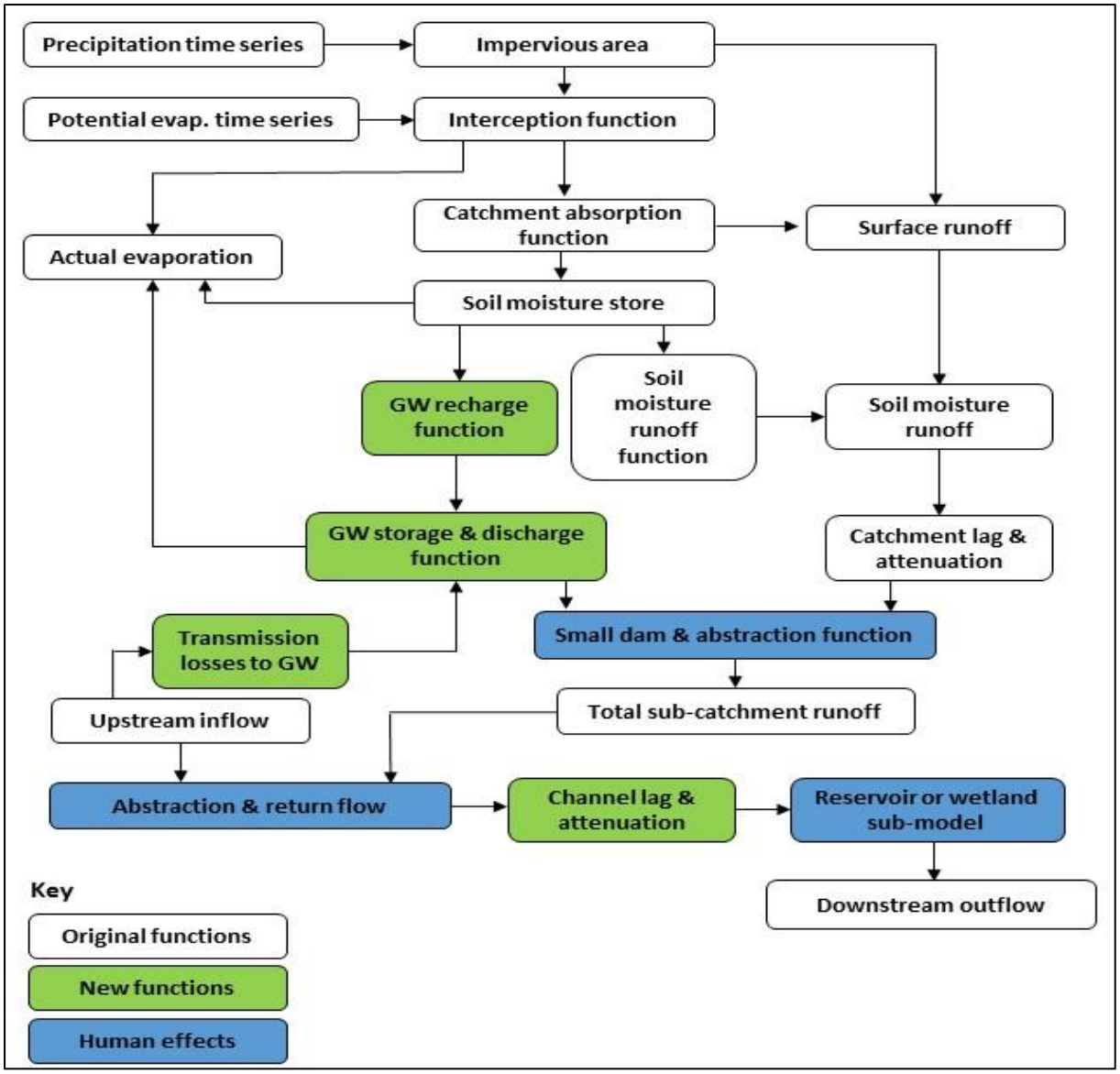

Figure 17. Structure of the Pitman model (adapted from Hughes, 2013).

Catchment Rainfall

Monthly catchment rainfall data are one of the primary inputs for the Pitman model as runoff is simulated using a monthly time-step. The Pitman model averages rainfall records in a given rainfall zone to avoid bias, particularly when dealing with mountainous catchments where isohyetal gradients are steep. This process is done in the model itself using the below equation (Bailey & Pitman, 2016):

$$PC = 100 \times \frac{[(\frac{Pn}{Mn})]}{N} \quad \text{.....Equation 1}$$

Where:

PC = Catchment rainfall expressed as a %

P_n = Monthly rainfall for rain station number in millimetres (n)

M_n = MAP for rain station number in millimetres (n)

N = Sum of rain stations used in the averaging process

Interception

The Pitman model accounts for interception through the parameter PI. To estimate total interception losses for any given month, the following two assumptions are made:

- The total amount of rainfall on any given rainy-day results from a single rain event only; and
- The amount of water retained in interception storage has time to evaporate between consecutive rain-days.

The two assumptions make it possible to derive monthly interception losses for a number of daily rainfall records, by means of the following equation:

$I = a(1 - e^{bp})$……*Equation 2*

Where:

I = Total monthly interception;

P = Total monthly precipitation; and

a, b = Constants

Surface Runoff

The model derives surface runoff generated from impervious areas and runoff from rainfall that is not absorbed by the soil. Runoff from impervious areas is calculated by multiplying catchment rainfall by the impervious area of the catchment. To compute the runoff from rainfall not absorbed by the soil, it is assumed that infiltration varies throughout the catchment from a minimum rate to a maximum rate, with a symmetrical, triangular frequency distribution throughout a catchment. The variables that describe the distribution rate of absorption are:

Zmin = Minimum absorption rate (mm/month)

Zmax = Maximum absorption rate (mm/month)

Zave = mean absorption rate (mm/month) = (Zmin + Zmax)/2

Let r = rainfall (mm), and

Surf = Surface runoff (mm)

Case 1

r <Zmin then Surf = 0

Case 2:

Zmin < r< Zave then Surf = $2(r.Zmin)^3 / 3(Zmax - Zmin)^2$

Case 3:

Zave < r < Zmax then Surf = $r - Zave + 2(Zmax - r)^3 / 3(Zmax - Zmin)2$

Case 4:

r > Zmax then Surf = r – Zave

Sub-surface runoff

Sub-surface runoff is directly proportional to soil moisture given by the following equation:

$$Q = FT\left[\frac{S-SL}{ST-SL}\right]POW$$ .....*Equation 3*

Where:

SL = Soil moisture below which no runoff occurs

ST = Total soil moisture capacity (mm)

FT = Runoff at soil moisture equal to ST

S = Actual soil moisture status

POW = Power of Q - S curve

Time Delay Runoff

The parameter TL is used as a sub-basin routing parameter to represent the runoff lag time as it related to both the surface and soil moisture runoff components. The parameter is defined by the Muskingum routing equation.

Evaporation from Soil Moisture Store

Catchment evapotranspiration (E), is assumed to be equal to potential evapotranspiration (PET), when soil moisture (S), is at full capacity (ST). The relationship between E and S is assumed to be with a minimum S when E is zero. The slopes of the E-S lines lie between two limits defined by the variable R. R is used to describe the relationship between both; the ratio of actual evapotranspiration to potential evapotranspiration (PE) and the current level of soil moisture storage. R ranges between the values 0 and 1. At low values of R, more effective evapotranspiration is lost which is associated with deep-rooted vegetation.

E = bS + c.....*Equation 4*

Where:

S is Soil moisture

b = PE/[ST(1-R(1-PE/PEMAX))]

c = PE-PE/[1-R(1-PE/PEMAX)]

Table 9. Description of the Pitman model calibration parameters.

Acronym	Description	Units
POW	Power in the soil moisture/ subsurface flow equation	-
GPOW	Power in the soil moisture recharge equation	-
ST	Soil moisture storage capacity	mm
FT	Subsurface flow at full moisture capacity	mm/month
HGGW	Maximum soil moisture recharge	mm/month
ZMIN	Minimum catchment absorption rate	mm/month
ZMAX	Maximum catchment absorption rate	mm/month
PI	Interception storage	mm/day
TL	Lag of low, excluding groundwater	months
R	Coefficient on the evaporation/ soil moisture equation	-

3.3 Rainfall Data

Daily rainfall data for 1979 Oct-2017 Sep (for ease of reference this period will be referred to as (1980−2017) were obtained from South African Weather Services (SAWS) for eight rainfall stations, which the Pitman model uses to calculate distributed rainfall in five rainfall zones in the BRC to calculate runoff.

The SAWS data was then converted to monthly rainfall data and correlated using Pearson's coefficient with the Water Resources (WR), 2012 study rainfall data. The WR, 2012 is a website that describes the water resources of South Africa. It is the culmination of several water resource appraisals that have been carried out over the previous four decades undertaken by the South African Water Research Commission. The website provides rainfall station study data up to 2010, as such rainfall station data were needed to update the study to include the 2015−2017 SWC drought.

The Pearson's coefficient was calculated for each rainfall station to determine the validity of extending the WR, 2012 study data up to 2017 with the collected SAWS data to include the 2015−2017 SWC drought (see Table 10 and Appendix A). Missing daily rainfall values in each of the SAWS rainfall station data records were deemed to be insignificant to patch and were ignored in totalling the monthly sum.

Monthly SAWS data was then used to create catchment rainfall zone files (E1A, G1A, G1B, G1C and G1D) for the period 1980 – 2017 for the BRC and used to run the Pitman model.

Table 10. SAWS rainfall stations used to create catchment rainfall zones files and their correlation with the WR 2012 study data.

Rainfall Station	Station Code	Hydrological Year	Altitude (m)	MAP (mm)	% of Missing Daily Record	Correlation Coefficient of WR2012 vs SAWS
Remhoogte	0042281	1980−2017	371	903	1	0.96
Boksveldskloof*	0042582	1980−2017	1035	716	1	1
Vrugbaar	0022038	1980−2017	175	771	0	1
Franschhoek Robertsvlei	0022148	1998−2017	256	1550	1	0.99
Porterville	0041871	1980−2017	142	476	6	0.94
Tulbagh	0042227	1997−2017	163	469	3	1
Hopefield	0040604	1980−2017	40	315	1	1
Laangebaan	0040035	1980−2017	14	329	1	0.94

**The Water Resources, 2012 study data for this rainfall station ends in 2004, however, the station is still in operation, as such, the regression analysis period was done for 1980−2004.*

3.4 Streamflow Gauging Station Data

Reliable gauging station data are important in evaluating the performance of the hydrological model against simulated data. Well validated hydrological models are important as they form the very basis of water resource planning management decisions. Historical monthly streamflow data were obtained from seven gauging stations (see table 11) from the Department of Water and Sanitation website for the relevant modelling period in the BRC to evaluate the performance of the Pitman model in simulating runoff.

Table 11. Streamflow gauging stations located in the BRC to evaluate the performance of the Pitman model.

Station Code	River	Place	Catchment Area (km^2)	Length of Data Record
G1H003	Franschhoek	La Provence	47	1980–2017
G1H020	Berg	Noorder Paarl	628	1980–2017
G1H041	Kompanjies	De Eikeboomen	121	1980–2017
G1H008	Little Berg	Nieuwekloof	393	1980–2017
G1H013	Berg	Drieheuwels	2936	1980–2017
G1H031	Berg	Misverstand	3984	1980–2017
G1R003	Misverstand	Misverstand Dam	3972	1980–2017

3.5 Pitman Model Evaluation

The Pitman model was set up to reflect the current hydrological conditions of the BRC. All anthropogenic abstractions considered in the Pitman model that affect runoff were constant in each respective quaternary catchment throughout the model run in the BRC. As abstractions are still present, these are indeed real flows.

Evaluation of the Pitman model to simulate runoff for a constant abstraction setup was carried out for 1980−2017 using the following two quantitative objective functions:

NSE is a commonly used normalized statistic in hydrological modelling that estimates the relative degree of the modelled residual variance against observed data variance (Nash and Sutcliffe, 1970). Values of NSE range between –∞ and 1. When NSE = 1, it indicates a perfect match between observed and simulated. Ranges for NSE values that are considered satisfactory in monthly data are shown in table 12. NSE is calculated as shown in equation 5:

$$NSE = 1 - \left[\frac{\sum_{i=1}^{n}(Y_i^{obs} - Y_i^{sim})^2}{\sum_{i=1}^{n}(Y_i^{obs} - Y^{mean})^2}\right] \quad \textit{Equation 5}$$

Where:

Y_i^{obs} is observed discharge

Y_i^{sim} is simulated discharge

Y^{mean} is the mean value of observed runoff

n is the total number of observations

PBIAS measures the mean magnitude of which the simulated data are greater or less than the observed data (Gupta et al., 1999). Lower magnitude values indicate accurate model simulation, with 0.0 being the optimal desired value (Moriasi et al., 2007). Negative values indicate model overestimation bias, positive values indicate a model underestimation bias (Gupta et al., 1999), see table 12. PBIAS is calculated as shown in equation 6:

$$PBIAS = \left[\frac{\sum_{i=1}^{n}(Y_i^{obs} - Y_i^{sim}) \times 100}{\sum_{i=1}^{n}(Y_i^{obs})}\right] \quad \textit{Equation 6}$$

Table 12. Recommended model performance rating for NSE and PBIAS for monthly streamflow values (after Moraisi et al., 2007).

Performance Rating	NSE	PBIAS (%)
Very Good	$0.75 \leq NSE < 1$	$\|PBIAS\| < 10$
Good	$0.65 \leq NSE < 0.75$	$10 \leq \|PBIAS\| < 15$
Satisfactory	$0.50 \leq NSE < 0.65$	$15 \leq \|PBIAS\| < 25$
Unsatisfactory	$NSE < 0.5$	$\|PBIAS\| \geq 25$

3.6 Meteorological and Hydrological Drought Event Definition

As described in the literature review, one of the key steps in an attribution study is defining the event to produce a threshold value for the actual attribution. The BRC is divided into 12 quaternary catchments (known as sub-basins or sub-catchments outside of South Africa) (see Fig. 15), which have varying catchment-specific hydrological parameters. To analyse the influence of regional climate change on the meteorological and hydrological drought, event definitions are calculated for all of these catchments as well as the entire analysed region of the BRC as described below:

Meteorological Drought Event Definition

To define the magnitude of the meteorological drought event for 2015−2017 in each quaternary catchment the MAP for 2015−2017 for each of the 12 quaternary catchments was calculated using the extended WR, 2012 data. As the Pitman model breaks up the BRC into rainfall zones and expresses rainfall as a percentage anomaly as its input, the MAP of each of the 12 quaternary catchments was multiplied with the percentage of the respective rainfall zone it belongs to, for the years 2015−2017.

The area-weighted three-year averages of the 12 quaternary catchments that make up the entire BRC was calculated and used to define the magnitude of the event over the entire analysed region. This three-year average was identified as the lowest three-year average rainfall in the observed analysed record (1979−2017).

Hydrological Drought Event Definition

The 2015−2017 hydrological drought event was defined as MAR received in each of the individual 12 quaternary catchments and for the entire analysed BRC during the three-year drought period. This was done by calculating the three-year averages of simulated runoff from the outflows of each individual quaternary catchment (known as routes within the Pitman model), as shown in table 13.

The runoff routes differ from streamflow, as streamflow is runoff routed through the channel network without abstractions, diversions, and storages. As such, removing physical human influence on runoff and only considering the climatological impacts on runoff. The event definition for the entire BRC was then calculated as the sum of all these three-year averages from the quaternary catchments.

Table 13. Quaternary catchment module routes of the Pitman model used to calculate MAR for drought event for the BRC.

Catchment	Route
G10A	G1RQ1; G1RQ2; G1RQ22; G1RQ100
G10B	G1RQ31; G1RQ41; G1RQ42
G10C	G1RQ51; G1RQ52
G10D	G2ARQ1; G2ARQ2; G2ARQ21; G2ARQ22; G2ARQ31; G2ARQ32
G10E	G2BRQ41; G2BRQ42
G10F	G3RQ51; G3RQ52; G3RQ57
G10G	G3RQ1
G10H	G3RQ21; G3RQ22
G10J	G3RQ31; G3RQ32; G3RQ41; G3RQ42
G10K	G4RQ1; G4RQ2; G4RQ9
G10L	G4RQ31; G4RQ32
G10M	G4RQ41; G4RQ42
G10 (BRC)	Summation of all routes listed above

3.7 Bias Correction of Rainfall for Attribution Experiments

A stochastic delta-factor method was used for bias correction in GCM rainfall data as described below (Wolski et al. in preparation)

This method incorporates a change in first-order statistics, namely: mean and standard deviation, with autocorrelation, are incorporated into a stochastic generator of monthly rainfall totals. This approach permits a more realistic assessment of low-frequency events, such as drought events, in comparison to deterministic methodologies such as bias correction or the change factor method. This is because the stochastic approach is stationary in time and provides a larger sample of data allowing for the sampling of events from the tail of the distribution that is less dependent on idiosyncrasies of a particular model or observations time series.

The basis of this approach is to apply a change factor in a stochastic manner, where GCM simulations are used to derive changes of the aforementioned first-order statistics from the given model's rainfall time series. These changes are then used to perturb the statistics of the observational data, and the perturbed statistics are used in the stochastic rainfall generator to produce a stochastic ensemble reflecting possible states of monthly total rainfall.

The parameters of the stochastic rainfall generator included mean monthly rainfall, month-on-month correlation of monthly anomalies, and year-on-year correlation of annual anomalies. Monthly uncorrelated anomalies were parametrized by the use of a gamma distribution. In the case where a number of spatially correlated time series are to be taken into consideration (i.e. several neighbouring catchments), a spatial cross-correlation concerning each time series is included. Each of the rainfall generator parameters can be altered derived from analyses of the GCM projection data.

The monthly stochastic rainfall generator is grounded on the Thomas-Fiering (1962) approach. Such that, the observed rainfall time series is disaggregated into three components: climatology; persistent anomaly; and random component, which are parameterized at a monthly interval. Combining these three components for successive time steps generates the monthly stochastic rainfall time series, with stochastic effects arising owing to the random component. The benefit of this approach is that it preserves time series characteristics, such as mean and variance, both at monthly, and at an inter-

annual time scale. Obtaining autocorrelation at the inter-annual time scale is done by rearranging individual years of the given monthly time series.

Single Series of Monthly Totals

A given monthly rainfall is derived as:

$P_t = A_t \ . \ \sigma_m + \bar{P}_m$ ……*Equation 7*

Where:

A_t is the standardized rainfall anomaly (assuming a normal distribution)

σ_m is the standard deviation of monthly rainfall

$\bar{P}_m$ is mean monthly rainfall

t is a consecutive month in the generated time series

m is a calendar month that corresponds to month *t*

$\bar{P}_m$ and σ_m are descriptive of the climatological component of the time series.

The standardized rainfall anomaly is derived using the following equation:

$A_t = r_m . A_{t-1} + \gamma_t$ ……*Equation 8*

Where:

r_m is Pearson's correlation of monthly rainfall anomalies in months *m* and *m – 1*

γ_t is a stochastic noise component

$r_m . A_{t-1}$ element expresses the persistent anomaly component of the time series

The random, non-serially co-related component of the series is expressed by γ_t, and is derived by sampling from a gamma distribution with parameters determined on the calendar month basis:

$\gamma_t = gamma(c_m, \lambda_m)$ ……*Equation 9*

The time series produced based on equations 7–9 maintain the imposed statistics, $\acute{P}_m$ and σ_m, r_m and c_m, λ_m on a monthly basis, but fails to replicate characteristics at an inter-annual time scale.

Multiple cross-correlated series

To account for characteristics at the inter-annual time scale. A spatial correlation is described using a correlation matrix derived for each of the calendar months from the time series of standardized monthly anomalies at each of the locations. The matrix is then used through the Choleski decomposition to produce a set of random correlated numbers ranging between 0 and 1. These numbers are then used as quantiles for which γ_t is determined from equation 9 at a given time step. The noise component then becomes spatially or cross-correlated. Cross-correlation characterizes the final generated time series, as the noise component is the only random component of the rainfall time series. Cross-correlation is done so that dry years occur at all stations in the same years with some form of random noise, such that the sub-catchment hydrological responses correlate.

3.7.1 Application of the Approach to Generate Data for Attribution of the 2015−2017 SWC Drought

The approach described above was applied by **Dr Piotr Wolski** to generate rainfall data for hydrological attribution of the 2015−2017 SWC drought, as described in the procedure below:

1. Attribution experiments were based on multi-model data from the CMIP5 ensemble, with attribution experiments constructed by considering the average conditions in the 31-year period centred on the years of the event, i.e. spanning 2002−2031 to represent current or "factual" conditions, and the period of 1861−1890 to represent the "counterfactual" conditions.
2. Data from 77 CMIP5 simulations under RCP8.5 GHG emission scenario spanning the period of 1861−2100 were downloaded from the KNMI Explorer website, and monthly rainfall totals were derived for the region representing the southern part of the so-called winter rainfall region, bounded by: -34.5 - 32.5°S, 18.00 − 20.00°E.
3. Catchment-specific parameters of the monthly stochastic rainfall model (monthly means, standard deviations, month-on-month serial correlation, year-on-year serial correlation, and parameters of gamma distribution describing month-on-month regression residuals) and spatial cross-correlation of monthly totals, were derived based on 1980−2010 rainfall data for 12 quaternary catchments taken from the WR2012 study website.
4. Change factors for each of the following parameters of the stochastic rainfall model were derived for each of the 77 GCM rainfall time series:
    - Monthly mean rainfall;
    - Standard deviation of monthly rainfall; and
    - Year-on-year autocorrelation

    Change factors were derived as a ratio of a given parameter in the "factual" period to that in the reference period (the period overlapping with the period for which WR2012 data were analysed), i.e. 1980−2010. Similarly, change factors were derived for the "counterfactual" period (again, against the 1980−2010 reference period).

    These change factors were derived as:

    $$D_{x,n,factual}=X_{n,factual}/X_{n,reference} \quad \text{Equation 10}$$

    $$D_{x,n,counterfactual}=X_{n,couterfactual}/X_{n,reference} \quad \text{Equation 11}$$

    Where:

    D denotes the change factor

    X denotes a parameter

    n denotes a given GCM scenario

    factual, counterfactual and reference denotes respective time periods

5. The change factors for each of the parameters were then used to modify the respective parameters of the stochastic rainfall model, and the model with modified parameters was used to generate a stochastic series of rainfall. For each of the 77 ensemble members, and for each of the attribution "experiments", a time series of 150 years of rainfall values were generated. These data were then used to run the Pitman model in attribution mode.

3.8 Attribution Experiments

The attribution approach used in this study considers continuous long-term time series generated by each of the 77 model simulation experiments from the CMIP5 ensemble. Each time series is obtained by merging historical CMIP5 simulations spanning 1861−2010 (1861−1890 was selected to represent the pre-industrial conditions), with RCP 8.5 GHG emission scenario simulations spanning 2011−2100 (2002−2031 was selected to represent the current world scenario). This approach assumes that changes in precipitation observed in time represent the influence of anthropogenic climate change. This attribution approach has similarly been used in studies by van Oldenborgh et al. (2019) for a heatwave; Otto et al. (2018) for a flood, cold wave, extreme rainfall and drought; and Jones et al. (2013) for surface temperature, among other studies, particularly by the World Weather Attribution Group. That similarity is in the fact that in both approaches, attribution experiments are based on transient simulations with climate models spanning current and pre-industrial, or near-pre-industrial conditions. Such an approach is appropriate as it is based on simulations with coupled ocean-atmosphere general circulation models.

The risk-based approach was used to analyse the data produced from the attribution experiments. The risk-based approach (described in section 6 of chapter 2) to event attribution is principally probabilistic and was used to compare the likelihood of the event occurring in the pre-industrial climate to that of the current climate, by means of two measures of change in probability of an event-the RR and FAR, which are calculated below as:

$RR = P_1/P_0$ ..... *Equation 12*

$FAR = 1- P_0/P_1$ ..... *Equation 13*

Where:

P_0 is the probability of the event in the counterfactual (in this case pre-industrial) world

P_1 is the probability of the event in the factual world (in this case current)

Attribution studies often use the well-established bootstrap technique to quantify uncertainties associated with sampling variance in RR and FAR values (Stone and Allen 2005; Pall et al., 2011; Christidis et al., 2013; Sheperd, 2016). Bootstrapping is a technique that estimates the sampling distribution of a statistic (Davison and Hinkley, 1997). Bootstrapping involves selecting, at random, a subset of data from the original data. This sampling distribution is then used to determine a confidence interval (CI).

3.8.1 Attribution Model Runs and Data Analysis

The Pitman model was automated, to allow for many runs to take place in a short period of time. The monthly rainfall time series produced by stochastic bias correction of the CMIP5 model data were then used as inputs for the Pitman model.

The model was run with each of the five stochastic rainfall time series' generated for each of the 77 CMIP5 climate model simulations. Each time series spanned 150 years and included data for each of the five rainfall zones covering the studied area. In total, the model was run 770 times (385 times each for current and pre-industrial) to produce a 150-year time series of current and pre-industrial modelled runoff and an attribution analysis was undertaken as described below.

For this study the following approach was used to determine the RR and FAR for rainfall/runoff attribution experiments undertaken in the quaternary catchments that make up the BRC:

- A threshold for rainfall/runoff was defined for each of the individual 12 quaternary catchments that make up the BRC and, the entire BRC based on observed rainfall/modelled runoff received during the 2015−2017 drought event (see section 3.6).
- The three-years of minimum MAP/MAR were identified in each of the 150-year time series (as they do not reflect a real-world time series but rather possibilities of three-year averages of lowest rainfall/runoff) of rainfall/runoff from each of the individual 385 simulated runoff time series, separately for the current and pre-industrial rainfall/runoff in each of the 12 quaternary catchments and the BRC.
- Once the minimum three-year average of rainfall/runoff in each of the 150-year rainfall/simulated runoff time series for current and pre-industrial climate scenarios were identified from the 385 climate model/simulated runoff time series.
- Although the three lowest years were selected from each of the time series a normal distribution was fitted to the 385 data points of rainfall/runoff as opposed to a GEV distribution. This was because a large number of models were analysed together, as opposed to a single model, introducing model uncertainty. As such, the distribution of 385 values is affected by both the distribution of extreme values in each of the models climate, and by the distribution of model uncertainty. Thus, assumptions can no longer be made in regard to the shape of the distribution.
- From this distribution the probability of the three-year observed drought event occurring in the current and pre-industrial rainfall/runoff is determined by calculating cumulative probability from the fitted distribution, corresponding to the level of the actual observed event.
- The probability of the current climate rainfall/runoff three-year average occurring was then compared to the paired pre-industrial time series to determine the likelihood of this threshold change using the risk-based approach.
- The uncertainty intervals for the distribution of rainfall and runoff RRs for each quaternary catchment and the greater BRC were then determined by bootstrapping the distribution 1000 times at a CI of 0.95.

3.9 Analysis of the Effect of Hydrological Parameters on RRs

RRs varied greatly across the 12 quaternary catchments located in the BRC and quaternary catchments with the highest rainfall RRs did not always correspond to those with the highest RRs for runoff. Thus, further analysis was conducted to understand the relationship and variation between rainfall RRs and runoff RRs and to determine which model parameters influenced this variation. To determine the effect of hydrological parameters used in the Pitman model for the BRC (see table 14) and rainfall RRs, a stepwise regression was undertaken.

Stepwise regression builds the best regression equation by adding the variable that accounts for the greatest amount of the remaining unexplained variation (i.e. in R^2) at each step.

A simple correlation was done to determine the catchment hydrological parameter that has the highest correlation with RR, this was the first parameter added to the regression equation. The second catchment parameter added to the equation was the catchment parameter that explains the largest part of variance that remained unexplained after adding the first parameter. At each step, all the hydrological catchment parameters in the equation were examined for significance and discarded if they no longer explain a significant variation in the regression equation. This process was repeated until all the hydrological catchment parameters excluded from the regression equation were found to be insignificant ($p < 0.1$) and variables in the equation significant ($p > 0.1$).

Akaike Information Criteria (AIC; Akaike, 1973), is a model selection criterion and was used to select the best regression model based on the stepwise linear regression equations built. AIC is based on in-sample fit to estimate the goodness-of-fit of the approximating model with the given dataset without overfitting of variables. In practice, the best model is the one with the lowest AIC value. Once the AIC values were computed for all the regression equations built, the model with the lowest AIC value was selected. The AIC is computed as:

$AIC = -2ln(L) + 2k$……Equation 14

Where:

L is the value of the likelihood

k is the number of estimated parameters

Table 14. Parameters used in the BRC by the Pitman model to simulate runoff.

Quaternary Catchment	MAP (mm)	MAE (mm)	FT (mm/month)	HGGW (mm/month)	TL (months)	Zmin (mm/month)	Zmax (mm/month)	ST (mm)
G10A	1610	1475	30	5	0.25	50	450	375
G10B	1306	1515	80	5	0	0	350	235
G10C	877	1500	55	2	0	60	750	340
G10D	691	1595	48	5	0.17	25	483	338
G10E	764	1635	25	2	0	50	420	285
G10F	582	1615	25	0.6	0.25	50	650	250
G10G	997	1645	5	2	0.25	100	600	465
G10H	404	1615	5	2	0	80	360	160
G10J	494	1605	5	2	0.25	88	700	558
G10K	317	1520	0	1	0.25	15	450	200
G10L	306	1485	0	1	0.25	15	450	200
G10M	225	1460	0	1	0.25	15	450	200

CHAPTER 4: RESULTS AND DISCUSSION

This chapter presents the results and findings produced using the methods described in the preceding chapter. It begins with the findings of the evaluation undertaken on the Pitman hydrological model followed by a description of rainfall and runoff during the drought event in the greater BRC, and its 12 quaternary catchments. This is followed by an analysis of model input rainfall and modelled runoff during the hydrological drought. Event definitions for the 2015−2017 meteorological and hydrological SWC drought are presented, followed by the climate impact-attribution experiment results for each of the 12 quaternary catchments and the BRC. Lastly, the parameters found to be most significant and influential on RRs produced are presented and their influence on RR values described.

4.1 Streamflow and Hydrological Model Evaluation

This section focuses on the results obtained from the Pitman hydrological model. A graphical and statistical evaluation of the Pitman model's performance in reproducing observed runoff within the BRC at several operational streamflow stations located in the catchment is presented.

The performance of the Pitman model driven by observed rainfall in simulating the streamflow at gauging stations is illustrated in Table 15. NSE values for monthly streamflow range from 0.45-0.75. Based on the model evaluation guidelines, presented in section 3.5, the Pitman model simulated streamflow with accuracy varying between individual catchments from unsatisfactory, to satisfactory to good and very good. The PBIAS values varied from -15.16% to 3.24%, falling within the satisfactory, good and very good categories.

Overall, the Pitman model simulation of streamflow was satisfactory to very good, based on average magnitude (PBIAS), and trends (NSE); apart from one indication of unsatisfactory model performance based on the NSE value at streamflow gauge station G1H041 located in catchment G10D. G1H041 is a complicated gauge; there is an offtake above the gauge for the Voëlvlei dam; additionally, there is a lot of upstream farm dams in the Tulbagh area that store quite a bit of the water that the Pitman model assumes is being generated. The unsatisfactory performance at gauge G1H041 could also be attributed to rainfall data, as rainfall data is from in the Tulbagh valley and might not be representative of the rainfall of the surrounding mountains.

Simulated runoff during the hydrological drought event, 2015−2017, is overestimated by the model; but the model does simulate a significantly lower runoff volume during the drought period and the simulated flows follow a similar pattern to that of the observed streamflow (see Fig. 18 & 19).

Table 15. Performance statistics of the Pitman model in the BRC for 1980−2017 at gauging stations located along the Berg River and its tributaries (colours refer to the performance of the Pitman model; green: very good, blue: good, yellow: satisfactory, red: unsatisfactory).

Gauge	River	Period	MAR (mcm/a)		MAR DIFFERENCE		NSE
			Observed	Simulated	(mcm/a)	Bias (%)	
MAINSTREAM							
G1H020	Berg River	1980–2017	331.14	325.65	-5.49	1.70	0.70
G1H013	Berg River	1980–2017	568.05	553.39	-14.66	2.60	0.70
G1R003	Berg River at Misverstand Dam	1980–2017	565.65	577.90	12.25	-2.16	0.67
G1H031	Berg River downstream of Misverstand Dam	1980–2017	502.18	566.43	64.25	-12.79	0.74
TRIBUTARIES							
G1H003	Franschoek River	1980–2017	25.18	28.99	3.81	-15.13	0.64
G1H041	Kompanjies River	1980–2017	26.47	25.61	-0.86	3.20	0.75
G1H008	Klein Berg River	1980–2017	69.26	73.00	3.74	-5.40	0.45

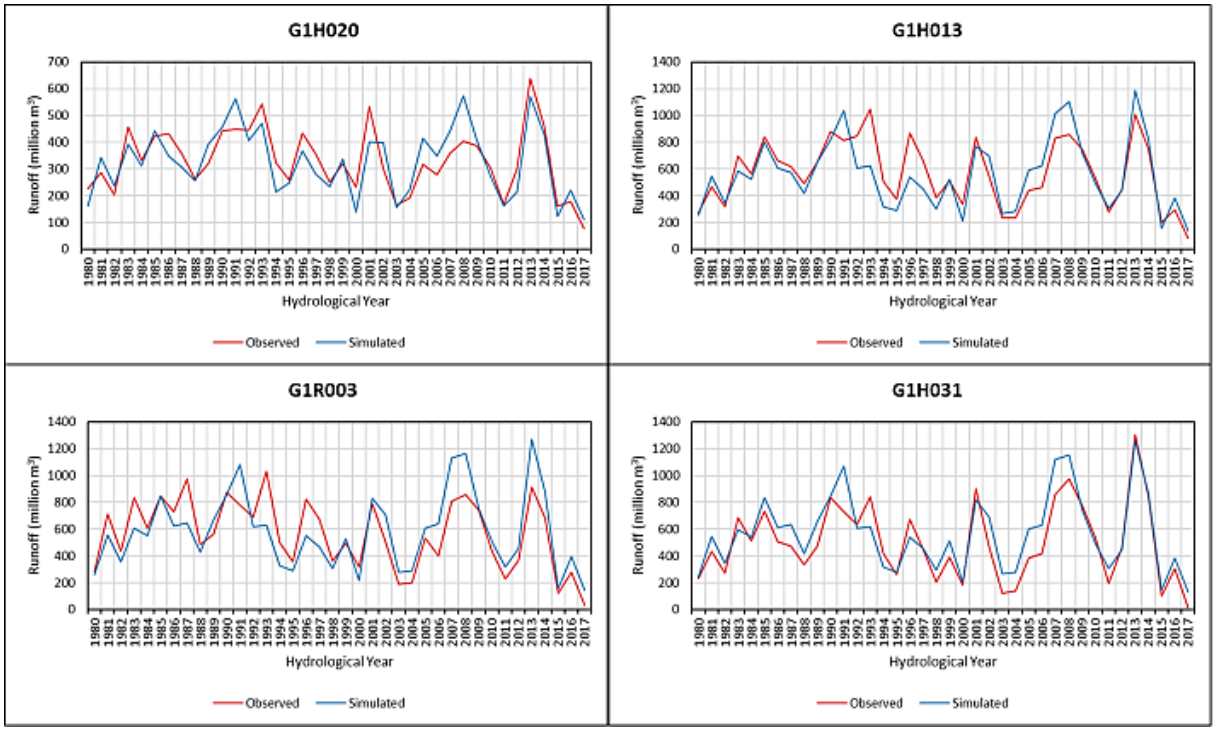

Figure 18. Annual hydrographs of modelled runoff and observed streamflow for 1980–2017 (Oct-Sep) at streamflow gauging stations along the Berg River.

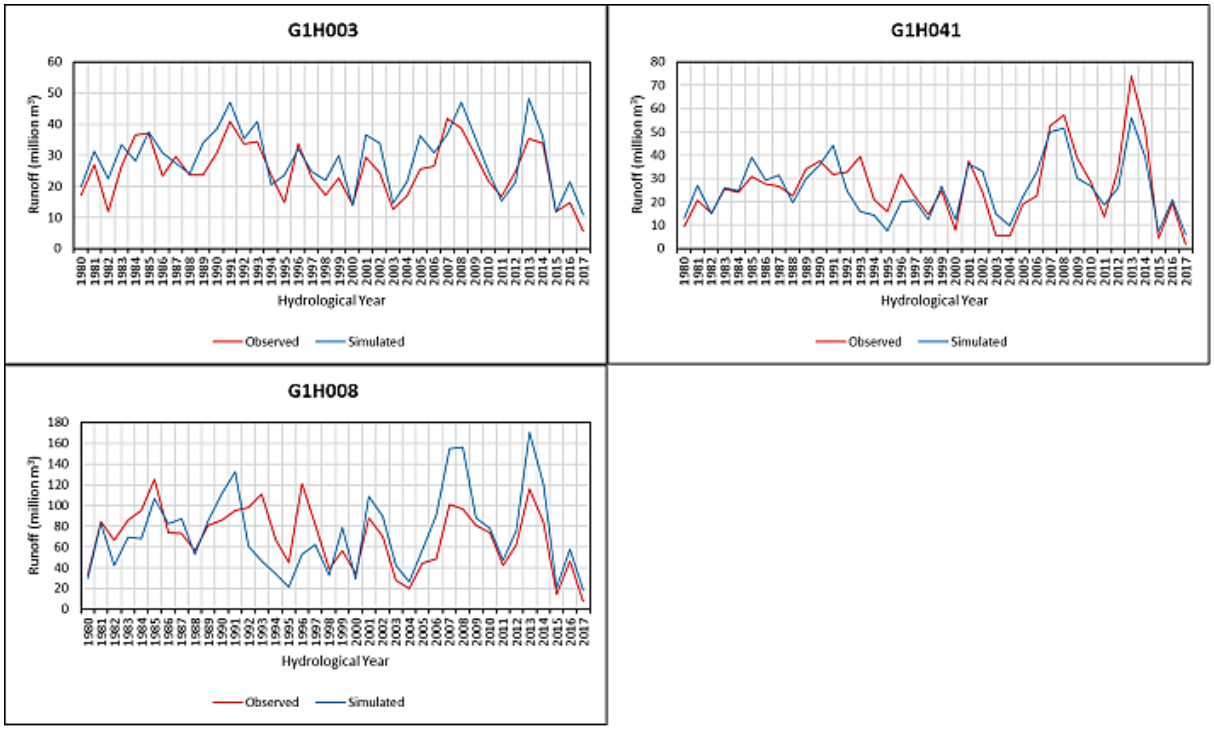

Figure 19. Annual hydrographs of modelled runoff and observed streamflow for 1980–2017 (Oct-Sep) at streamflow gauging stations located at tributaries of the Berg River.

Graphical analysis of scatter plots of annual streamflow depict that the model tends to overestimate flows during dry years along the Berg River (apart from gauging station G1H031) and its tributaries. This is offset by an under-simulation of runoff during wet years the model consistently underestimates runoff at gauging stations located along the Berg River (see Fig. 20). Whereas at the tributary gauging stations: G1H003 overestimates wet years, G1H041 greatly underestimates wet years and, G1H008 depicts no considerable difference between observed and simulated wet years (see Fig. 21). Overall, the model shows no consistent overall systematic bias of estimating wet years at the three tributary rivers.

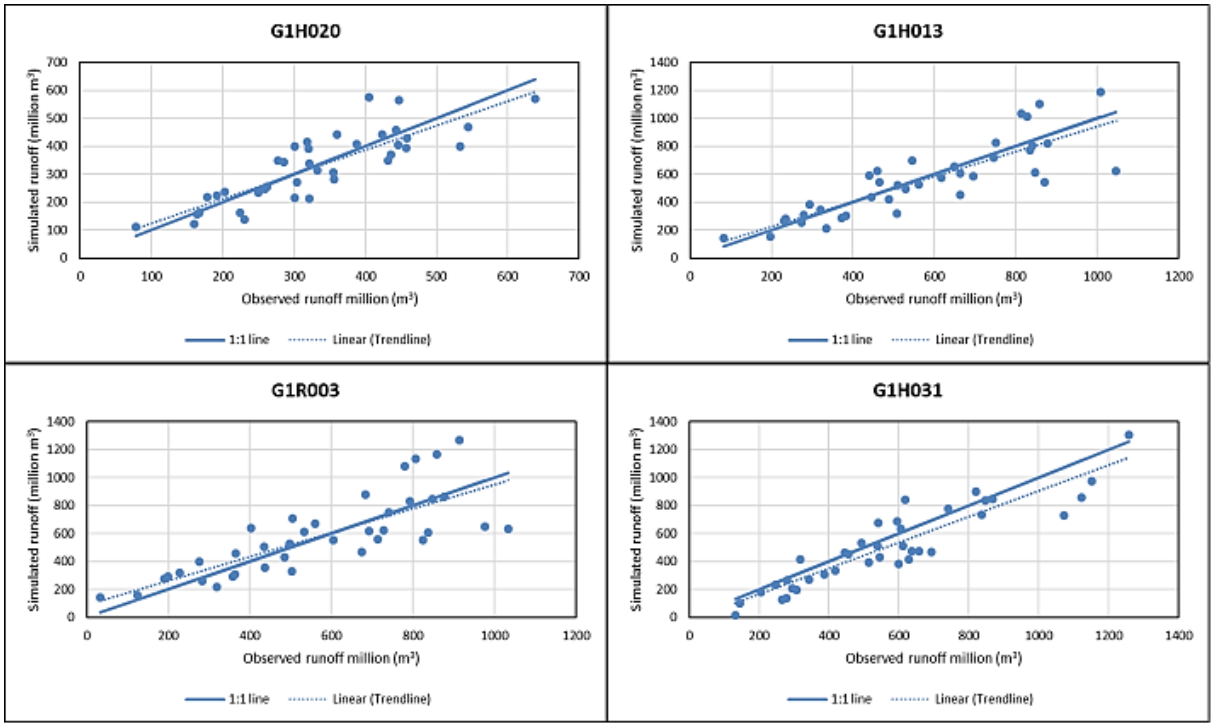

Figure 20. Scatter plots of annual modelled streamflow compared to observed runoff for 1980–2017 (Oct-Sep) at streamflow gauging stations along the Berg River.

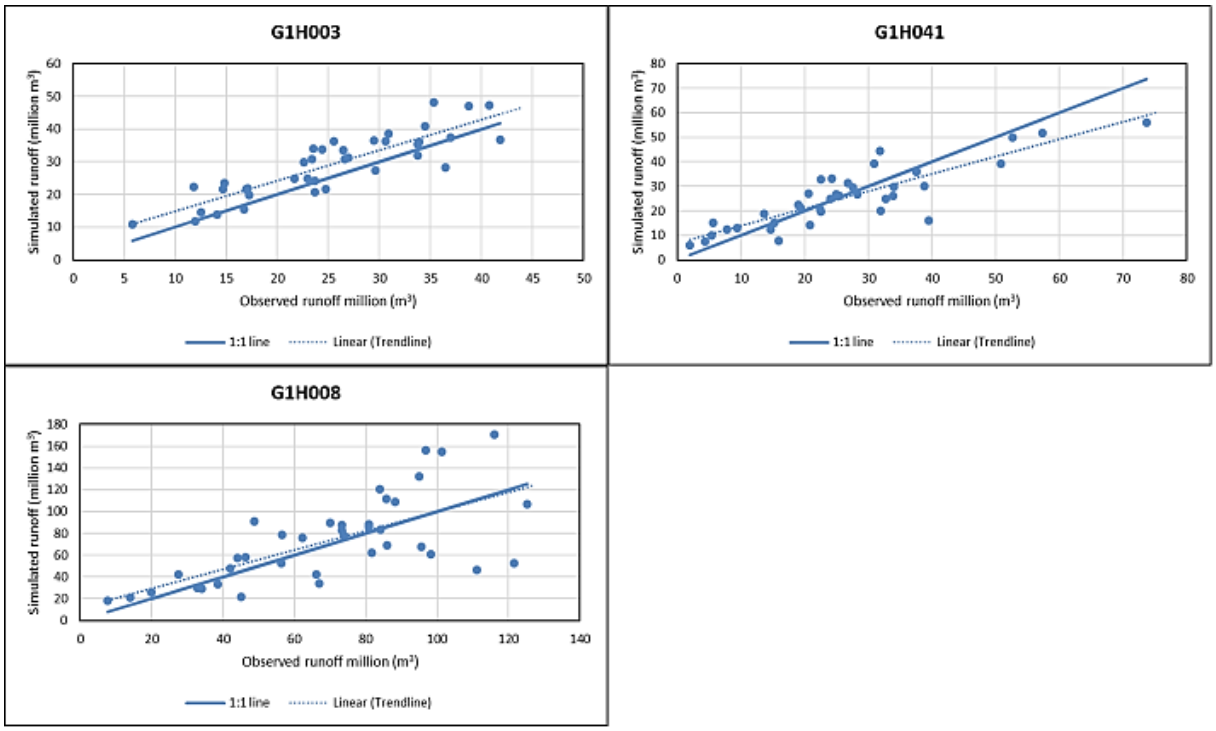

Figure 21. Scatter plots of annual modelled streamflow compared to observed runoff for 1980–2017 (Oct-Sep) at streamflow gauging stations located at tributaries of the Berg River.

Analysis of flow duration curves of monthly runoff confirms the biases noted above for annual flow, in that the model largely underestimates months of low streamflow (dry months) along the Berg River, particularly for exceedance probabilities higher than 60% (see Fig. 22). Note that streamflow gauging

station G1H031 the model simulates months of zero flow; which cannot be plotted on the log scale as the value is undefined.

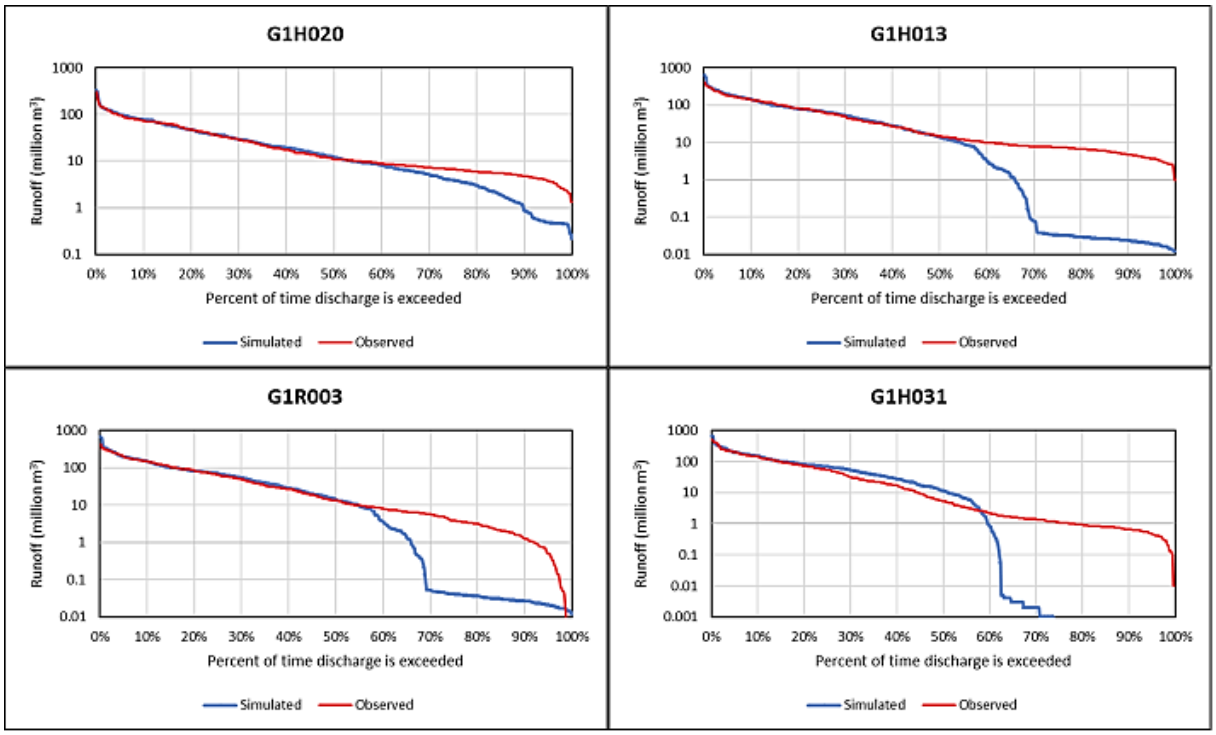

Figure 22. Flow duration curves of monthly and simulated runoff on a log scale for 1980–2017 (Oct-Sep) at streamflow gauging stations along the Berg River.

Monthly flow duration curves at gauging stations located along the Berg Rivers tributaries similarly illustrate overestimations of low flows months at G1H041 and G1H008 (see Fig. 23). In contrast, G1H008 illustrates under simulated runoff for low flow months. G1H041 is located along the Kompanjies River which is a non-perennial river; with months of zero flow during the dry season.

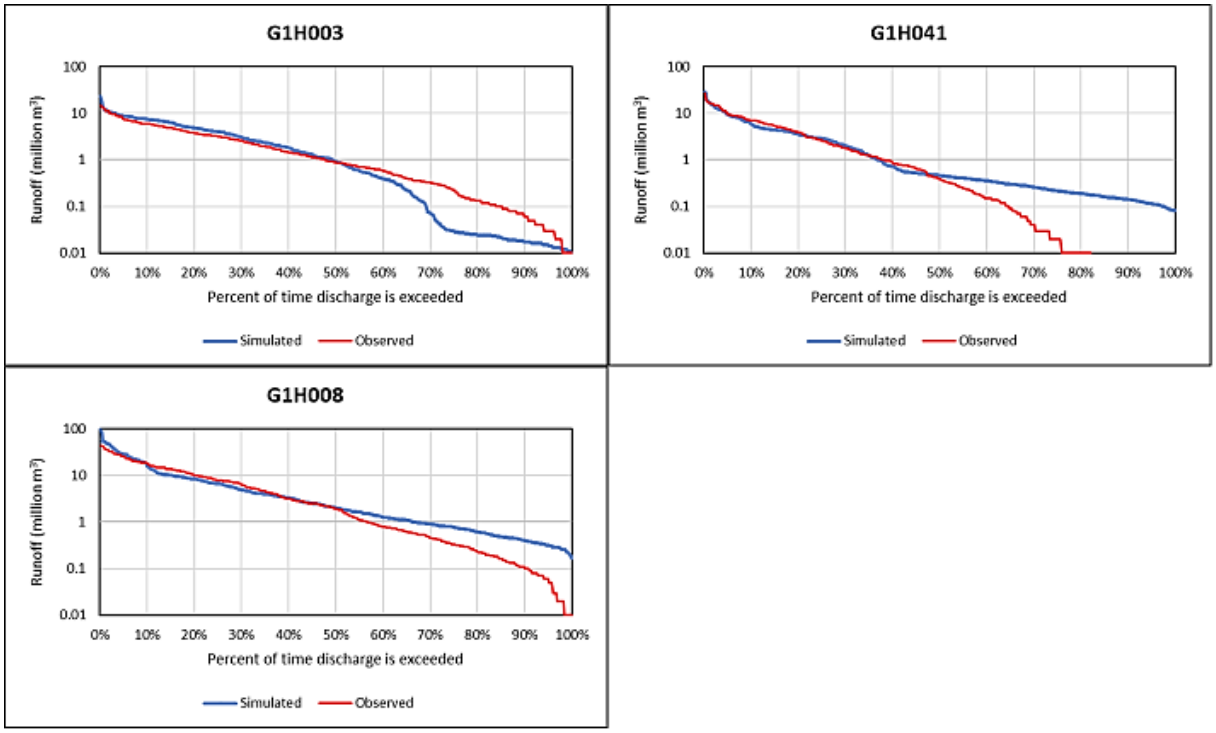

Figure 23. Flow duration curves of monthly and simulated runoff on a log scale for 1980–2017 (Oct-Sep) at streamflow gauging stations located at tributaries of the Berg River.

Mean monthly streamflow graphs indicate that the Pitman model, for most gauging stations located along the Berg River, typically underestimates months of low streamflow (Oct-Mar), see Fig. 24. Gauging stations located at the tributaries depict very little difference between observed streamflow and simulated runoff during months of low flow (see Fig. 25).

Months of high streamflow (Jul-Sep) are typically overestimated in three of the four gauging stations located along the Berg River (see Fig. 24). Gauging stations of tributaries of the Berg River show no consistent trend of over or underestimation during wet months (see Fig. 25).

The largest bias of overestimations of streamflow by the Pitman model occurs in August for most stations, apart from G1H020 and G1H003 where the largest bias occurs in July (see Fig. 24 & 25). The Pitman model performs best at gauging stations located along the Berg River in the months of May-July for gauging stations along the Berg River (see Fig. 24). Months of low flow are simulated more efficiently at gauging stations of tributaries as opposed to months of high flow (see Fig. 25).

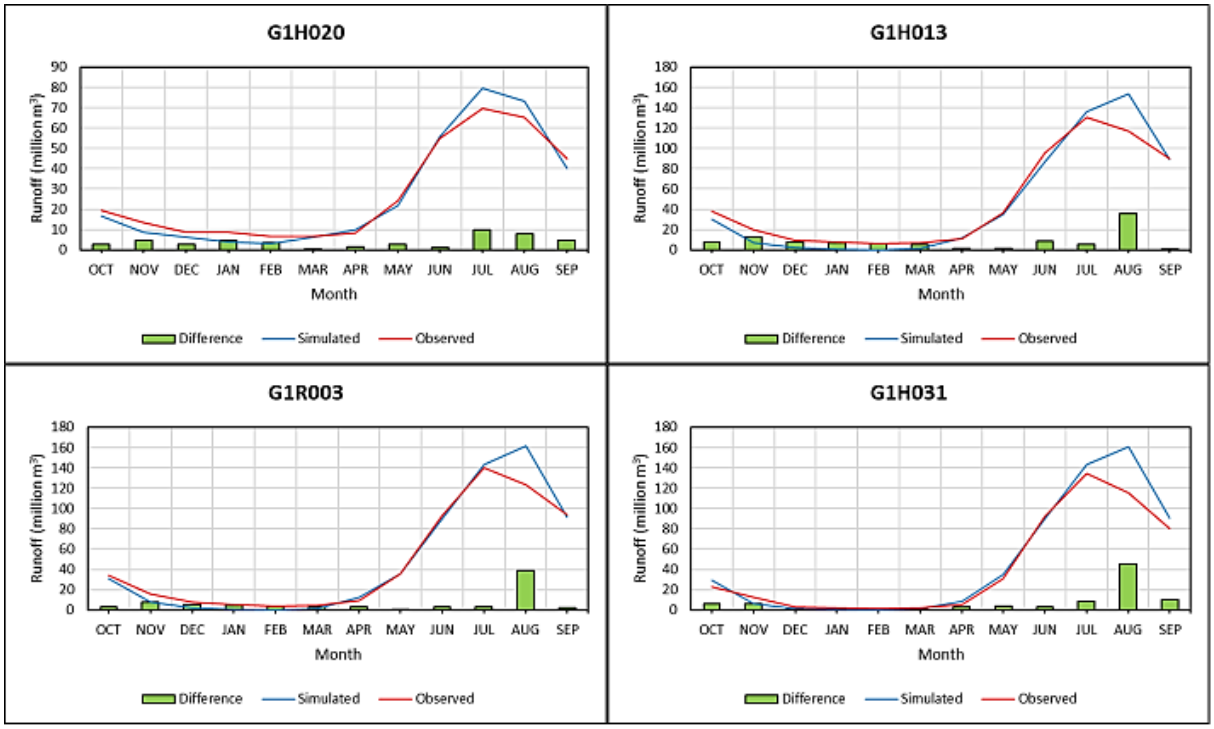

Figure 24. Mean monthly hydrographs of modelled runoff and observed streamflow for 1980−2017 (Oct –Sep) at gauging stations located along the Berg River. **Difference refers to absolute difference.*

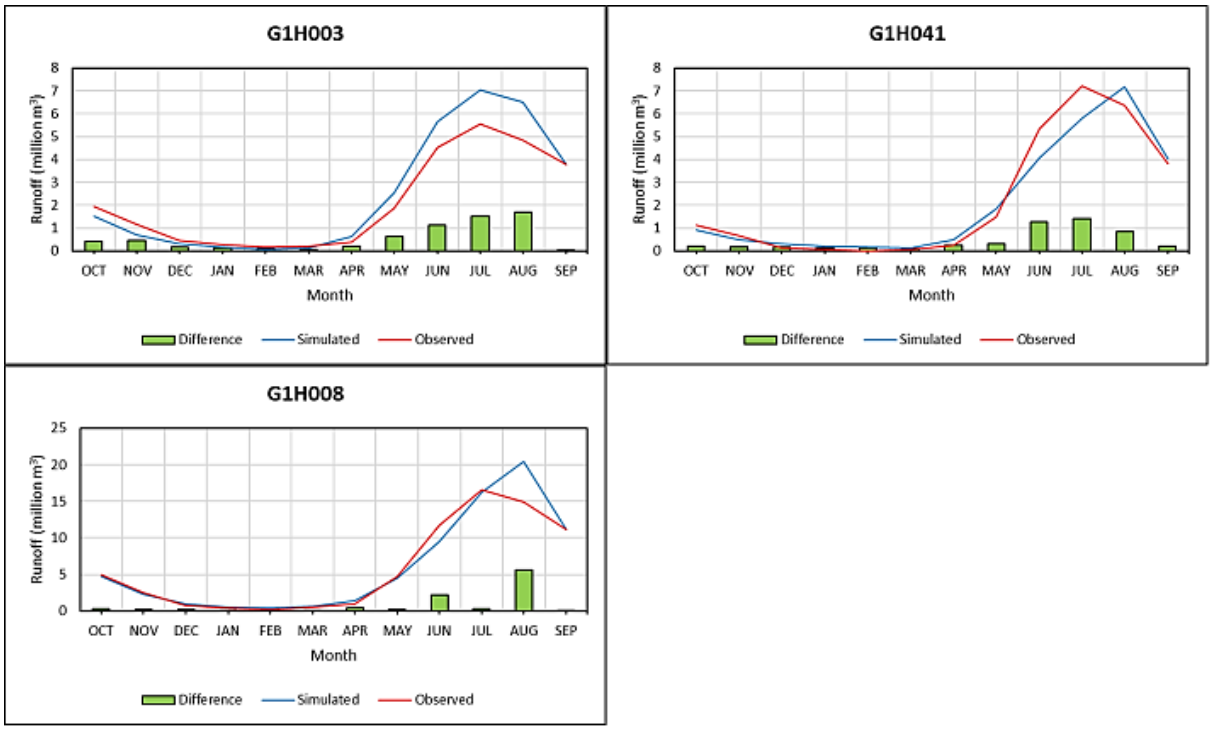

Figure 25. Mean monthly hydrographs of modelled runoff and observed stream for 1980−2017 (Oct –Sep) at streamflow gauging stations located at tributaries of the Berg River.**Difference refers to absolute difference.*

Based on the hydrological model evaluation the Pitman model was deemed suitable for application in this drought attribution study, as the model captures the 2015−2017 SWC drought. However, as runoff in the drought years 2015, 2016 and, 2017 is overestimated this may misrepresent, i.e. decrease the RR, the extent that anthropogenic climate change had on the drought event.

4.2 Rainfall and Runoff Characteristics in the BRC during the 2015–2017 SWC Hydrological Drought Event

This section focuses on annual and seasonal rainfall and runoff received during the three-year hydrological drought in the BRC as a whole and its 12 quaternary catchments. An analysis is undertaken on annual and seasonal rainfall (observed and model input rainfall) and modelled runoff, during the drought period (2015–2017) and is compared to the average (1980–2014) rainfall/runoff characteristics of the BRC and its 12 quaternary catchments. This was done to assess how the different rainfall and runoff time series vary in their representation of the drought event throughout the BRC.

a) Annual and Seasonal Rainfall

The mean over the recent period (1980–2014) for the BRC was calculated to be 608 mm. The lowest annual average rainfall values for the period analysed occurred during the 2015–2017 drought event, in 2015 (380 mm) and 2017 (366 mm), which were 62% and 60% respectively of the mean. While 2016 received nearly normal rainfall (96% of the mean), see Fig. 26.

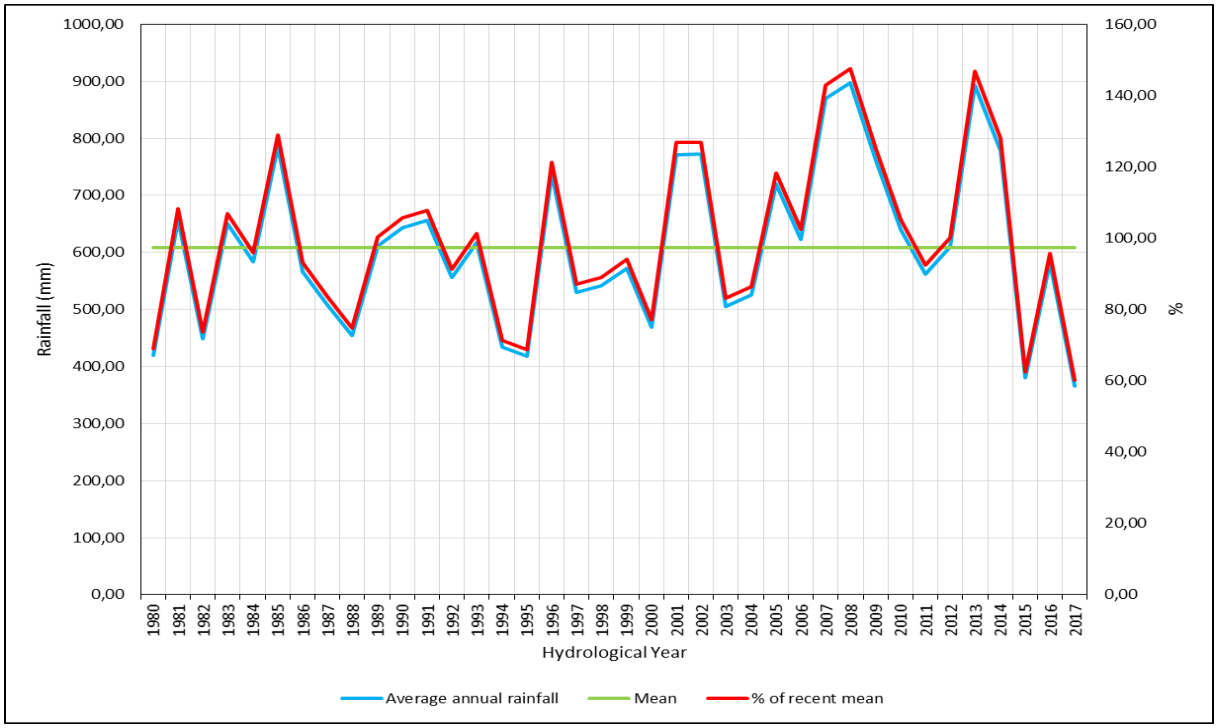

Figure 26. Average annual rainfall per year expressed as absolute values (mm) and as a percent of the mean over the recent period, (1980–2014) in the BRC.

The model rainfall inputs for each of the 12 quaternary catchments in the BRC show a similar pattern of very low rainfall in 2015 and 2017 (see Fig. 27). Wet and intermediately wet catchments (G10-A, -B, -C, -D, -E, -F and -G), received their lowest rainfall amounts during the analysed period (1980–2017) in 2017. The drier northern quaternary catchments of the BRC (G10-H, -J, -K, -L, -M) received their lowest amount of rainfall in 2015.

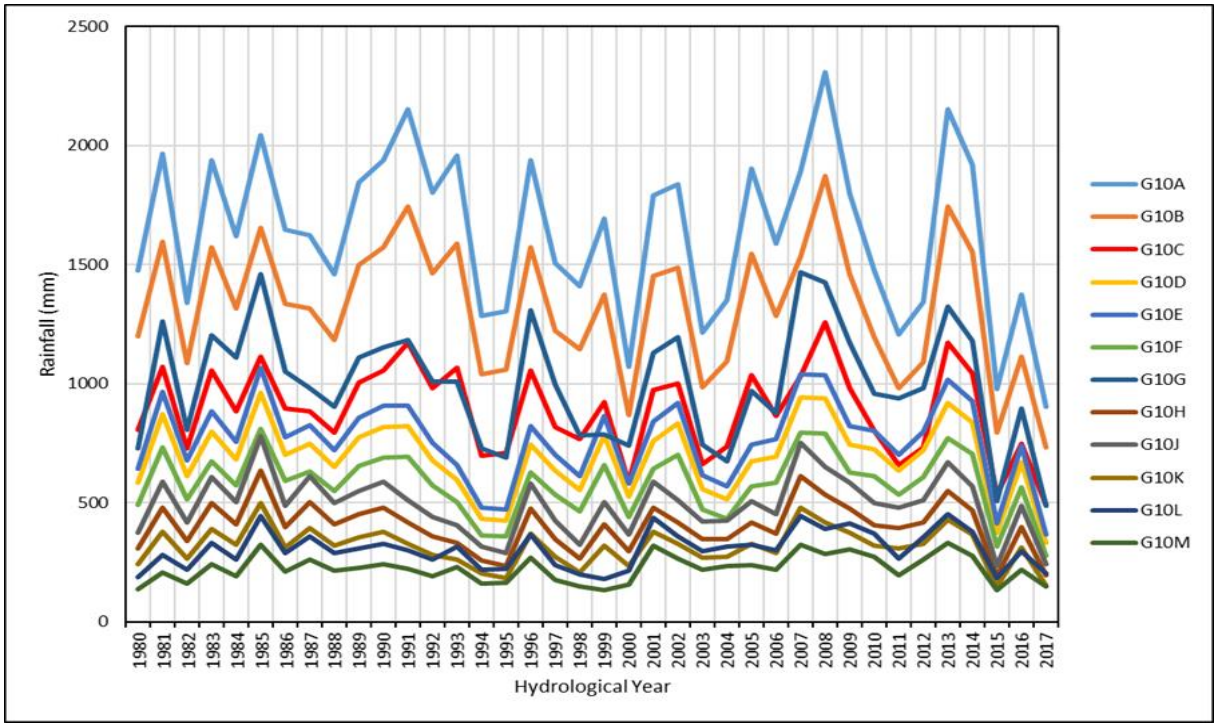

Figure 27. Model input annual rainfall of the 12 quaternary catchments in the BRC, 1980−2017.

Based on model input rainfall data, quaternary catchments G10-H and -K experienced the highest percentage of reduced rainfall in 2015 (see Fig. 28). While the wetter headwater catchments (G10-A, -B, -C) and the intermediately wet quaternary catchments (G10-D, -E, -F) experienced the largest percentage reductions in rainfall in 2016 and 2017, respectively. During the drought period (2015-2017), the mountainous wet quaternary catchment (G10G) experienced the largest reduction in the percentage of average rainfall received.

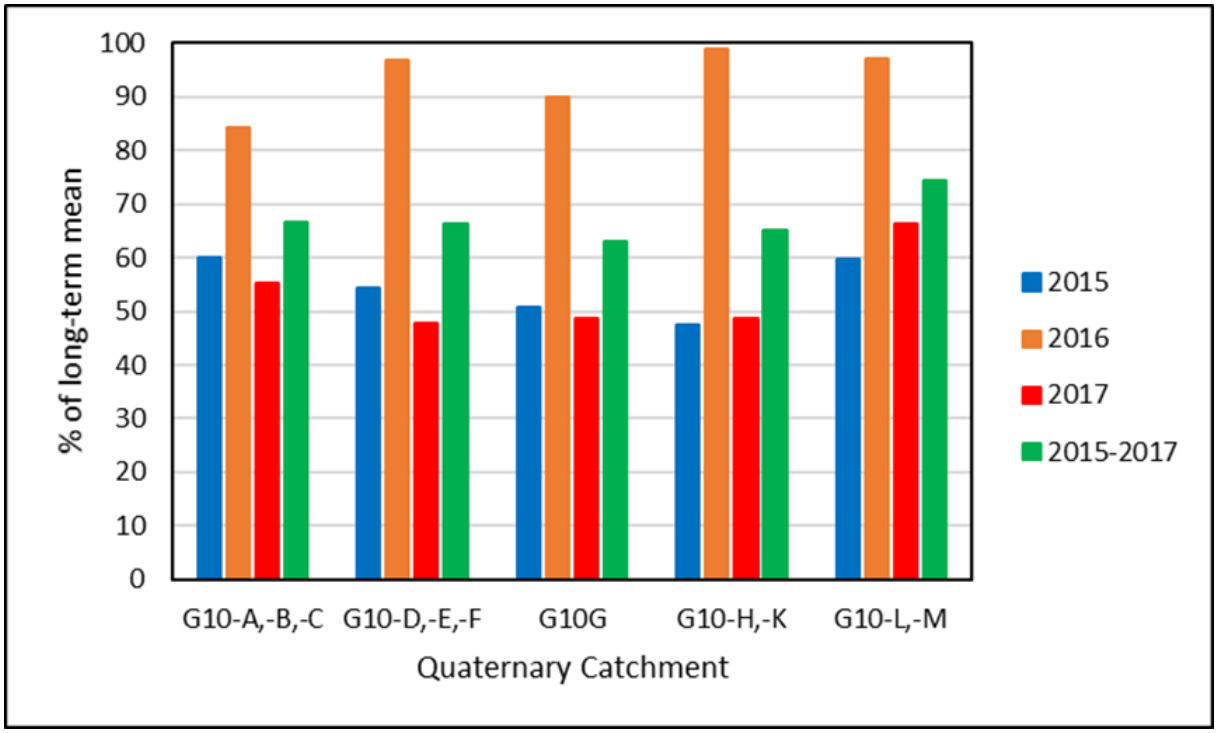

Figure 28. Model input rainfall of the drought period and individual drought years in the 12 quaternary catchments as a percentage of the mean (1980−2014).

Mean monthly rainfall for the BRC was calculated for the period 1980−2014 for the nine rainfall stations in the BRC and compared to mean monthly rainfall for the individual drought years (2015, 2016, and 2017) and the three-year average monthly rainfall of the hydrological drought period (2015−2017), see Fig. 29.

Analysis of precipitation during the drought event indicates that below-normal total rainfall in the BRC was the result of a strong precipitation anomaly observed during the shoulder months (March-May and August-October) of the individual drought years. During March-May rainfall was below-normal particularly in 2015 and 2017, whereas March and April were above-normal in 2016. The shoulder months of August-October received below-normal rainfall for all three individual drought years, particularly the month of October. These findings are in agreement with that of Otto et al. (2018), which found that one of the main drivers of the drought was the lack of precipitation during the aforementioned months.

During the drought period, the core of the winter rainy season, months of June and July, had nearly normal rainfall. The month of June received more rainfall during the drought period than the monthly mean, due to above-normal rainfall received in 2016 and 2017. Whereas, above-normal rainfall in July occurred in 2015 and 2016.

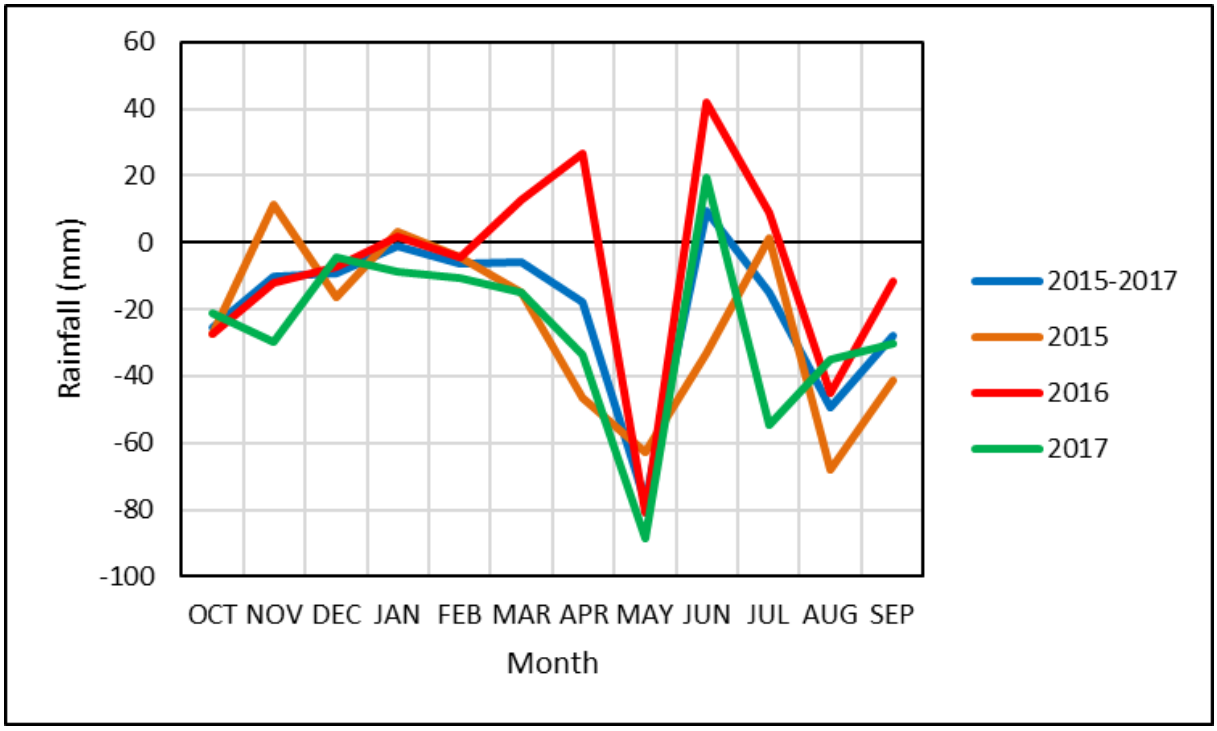

Figure 29. Monthly average rainfall received during the drought and individual drought years compared to monthly average rainfall (1980−2014) in the BRC.

Mean monthly model input rainfall for the 12 quaternary catchments in the BRC was calculated for the period 1980−2014 and compared to mean monthly rainfall for the individual drought years (2015, 2016, and 2017) and the three-year average monthly rainfall of the hydrological drought period (2015−2017), and described below:

2015: Wetter headwater quaternary catchments (i.e. G10-A,-B and-C) experienced the largest reductions in rainfall in June, these quaternary catchments received above-normal rainfall in July; while the drier northern quaternary catchments received largely just below- to normal- rainfall during the core of the winter rainfall season (see Fig. 30). The mountainous wet quaternary catchment (G10G), received slightly above-normal rainfall in June, but below-normal rainfall in July. The shoulder months of August-October and March-May received below-normal rainfall for all quaternary catchments, with the wettest quaternary catchments showing the greatest negative anomalies.

2016: The core winter rainfall months June and July received above-normal rainfall in all quaternary catchments, apart from the extreme-northern dry quaternary catchments (G10-L and -M) which were below-normal in July; with the wetter quaternary catchments showing greater positive anomalies than the drier northern quaternary catchments in the BRC (see Fig. 30). The wetter quaternary catchments show the greatest negative anomalies during the shoulder months of August-October. In the shoulder months of March-May, all quaternary catchments received above-normal rainfall in March and April, while May exhibits the greatest negative rainfall anomalies of all quaternary catchments in 2016, with the wettest quaternary catchments showing the greatest negative anomalies.

2017: All quaternary catchments received below-normal rainfall for much of the year, apart from June in which the wetter headwater catchments (G10-A, -B and -C) received above-normal rainfall (see Fig. 30). The most extreme negative rainfall anomalies occurred in May and July, particularly in the wetter headwater quaternary catchments of the BRC.

2015–2017: During the drought years, rainfall in all quaternary catchments was below-normal for most of the year, apart from July in which the drier northern quaternary catchments of the BRC received above-normal rainfall (see Fig. 30). Below-normal rainfall conditions were most extreme in the wetter headwater quaternary catchments. The highest negative rainfall anomaly occurred in May for all quaternary catchments. The drier northern quaternary catchments of the BRC received above-normal rainfall in July.

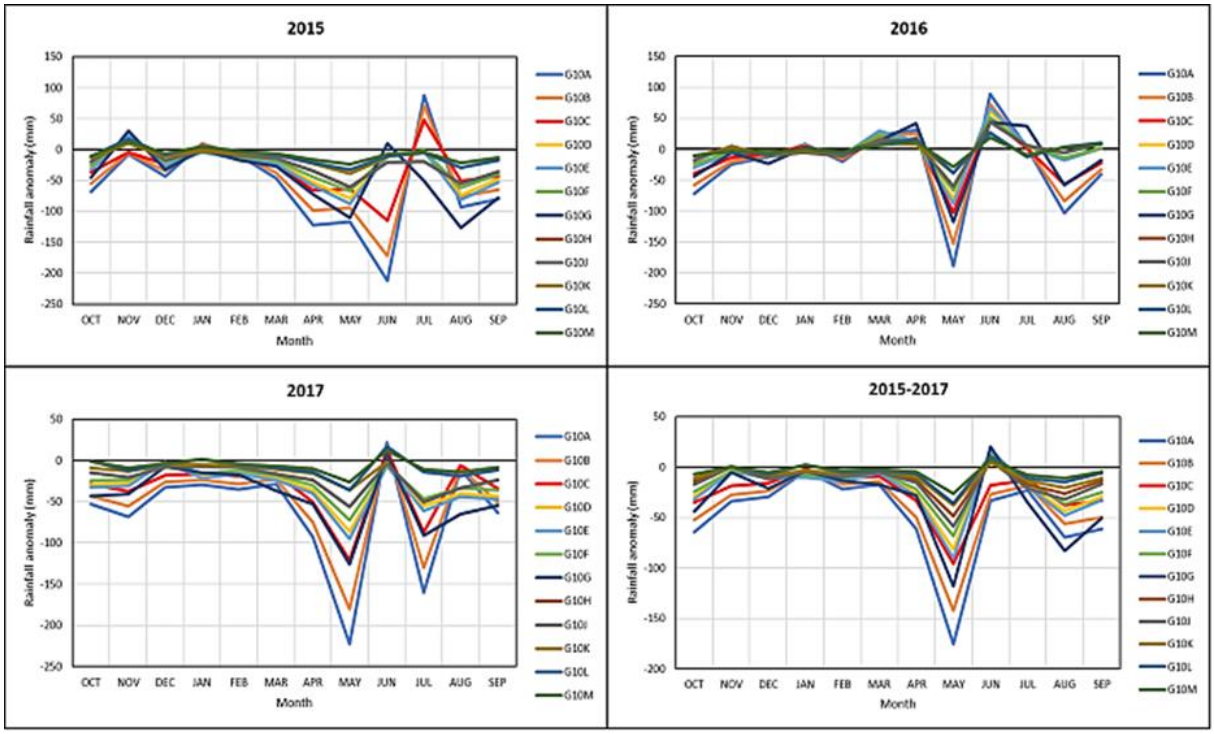

Figure 30. Monthly average model input rainfall received during the drought period and individual drought years compared to the monthly average model input rainfall (1980−2014) in the 12 quaternary catchments.

b) Annual and Seasonal Modelled Runoff

The average modelled runoff for the BRC for the period of 1980−2014 was calculated to be 700 million m^3 on average per annum. During the analysed period, runoff peaked in 2013 (1437 million m^3), while, 2017 received the lowest amount of runoff (261 million m^3) in the catchment (see Fig.31).

Analysis of runoff indicates a large reduction in total annual runoff beginning in 2015 (72% lower than runoff in 2014), see Fig. 31. The slight increase, although not substantial, in 2016 coincides with higher rainfall received in that year. In the drought years; 2015, 2016 and 2017, runoff was 40%, 71% and 37% respectively, of the mean.

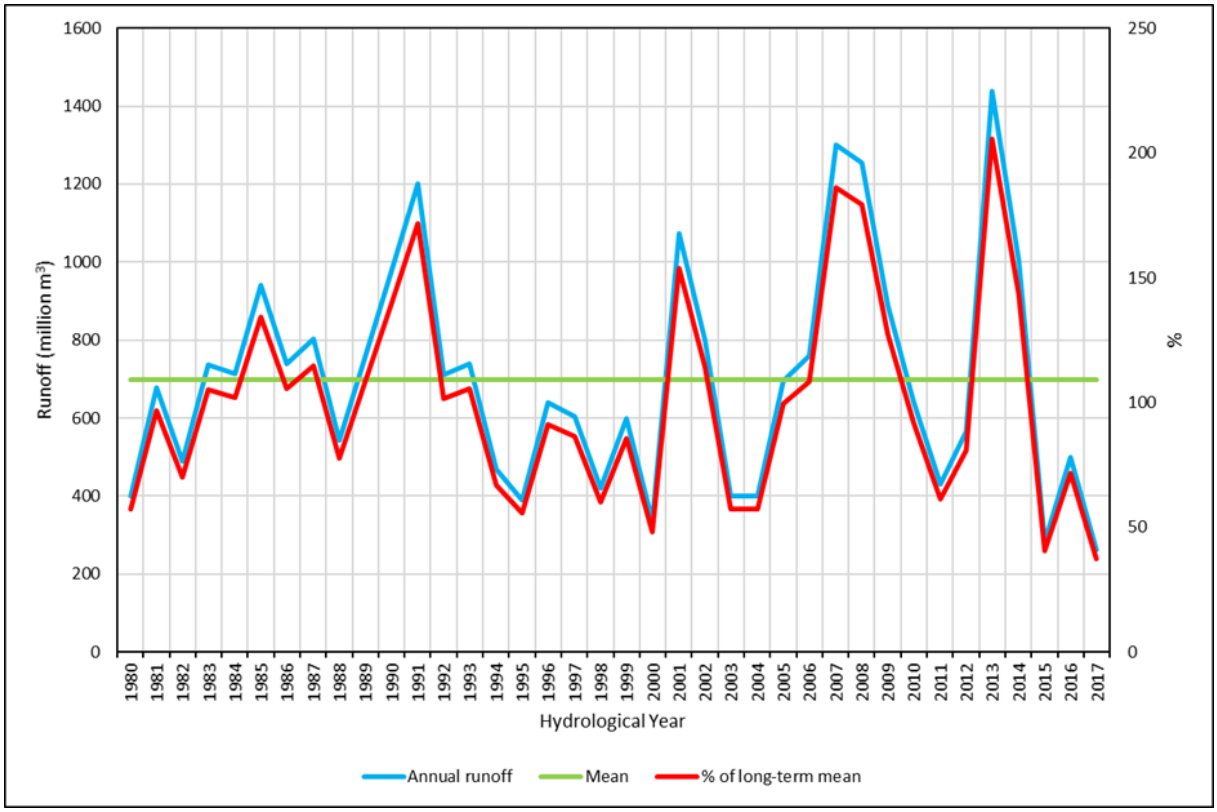

Figure 31. Annual hydrograph of total modelled annual runoff expressed as absolute values (million m^3) and as a percent of the mean for 1980–2014 in the BRC.

Runoff received in the 12 quaternary catchments in the BRC show similar patterns of decreases in runoff in 2015 and 2017, and a less severe reduction in runoff in 2016 (see Fig. 32). Mostly the wet and intermediately wet catchments (G10-A, -B, -C, -D, -E, -F and -G) received their lowest volume of runoff in 2017, within the analysed period. While the drier northern quaternary catchments (G10-H, -K, -L and M) received their lowest volume of runoff in 2015, apart from G10J which received its lowest volume of runoff in 2017. Quaternary catchments G10-A and -D contribute the largest volume of runoff in the BRC, while G10M contributes the least volume of runoff to the BRC.

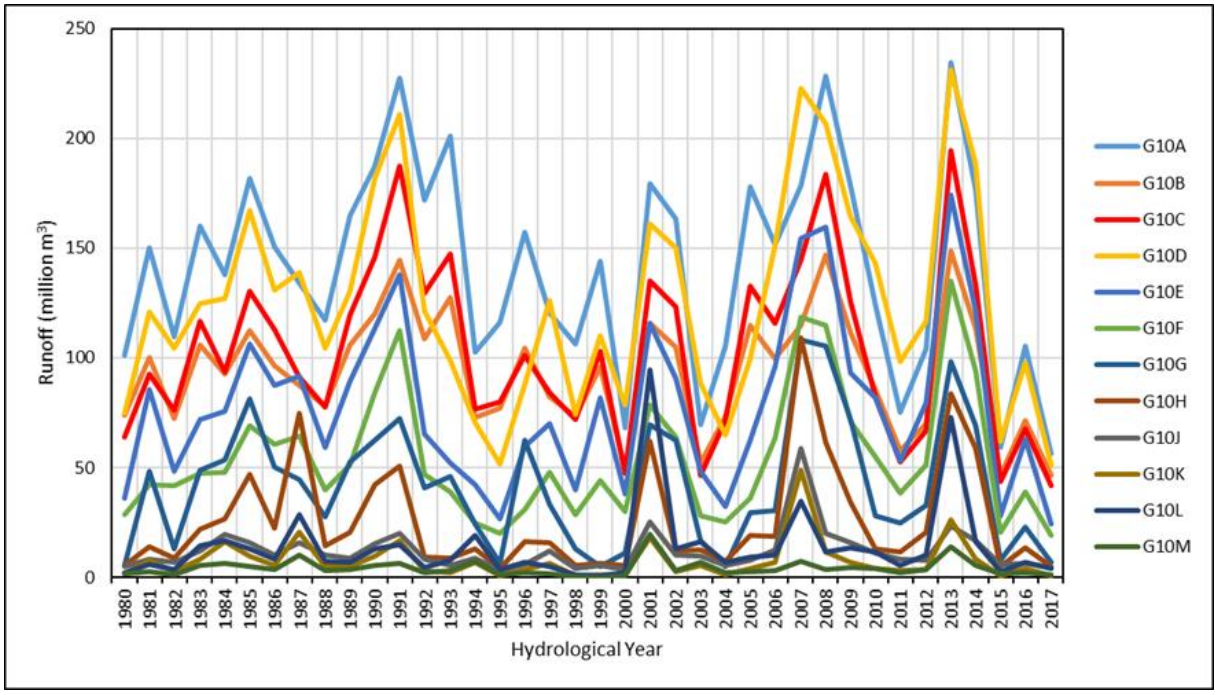

Figure 32. Modelled runoff received in the 12 quaternary catchments in the BRC, 1980−2017.

In 2015, reductions in the volume of runoff in the 12 quaternary catchments were between 8% and 50% (see Fig.33). 2016 showed lesser reductions in runoff volume received in the quaternary catchments, runoff was still below-normal (ranging from 49% to 81% of the mean across the quaternary catchments) in all the 12 quaternary catchments. 2017 showed substantial decreases in runoff in the quaternary catchments similar to that of 2015, in the range of 9% and 50%. During the drought period, G10K experienced the greatest reduction in runoff volume received.

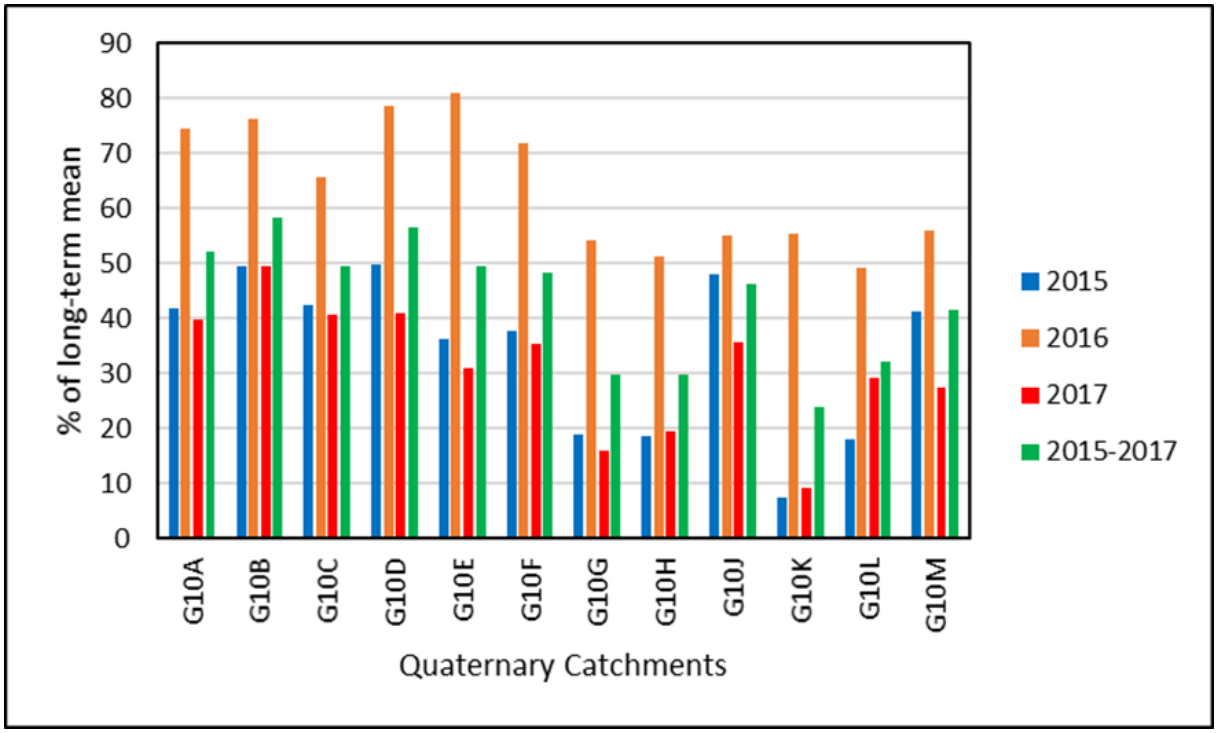

Figure 33. Modelled runoff received during the drought period and individual drought years in the 12 quaternary catchments as a percentage of the mean (1980−2014).

Mean monthly runoff for the BRC and it's 12 quaternary catchments was calculated for the period 1980–2014 and compared to mean monthly runoff for the individual drought years (2015, 2016, and 2017) and the three-year average monthly runoff of the hydrological drought period (2015–2017), see Fig. 34.

For all drought years (2015, 2016 and 2017), simulated runoff in October and November was below-normal, after which runoff began to steadily increase and was near normal in March (see Fig. 34). In May runoff volume received decreased substantially for all drought years. For the remainder of the year, 2015 and 2017 remained well below-normal, while 2016 was above-normal in June it was below-normal for the remainder of the year. During the drought period, runoff was below-normal for the entire year, particularly in August.

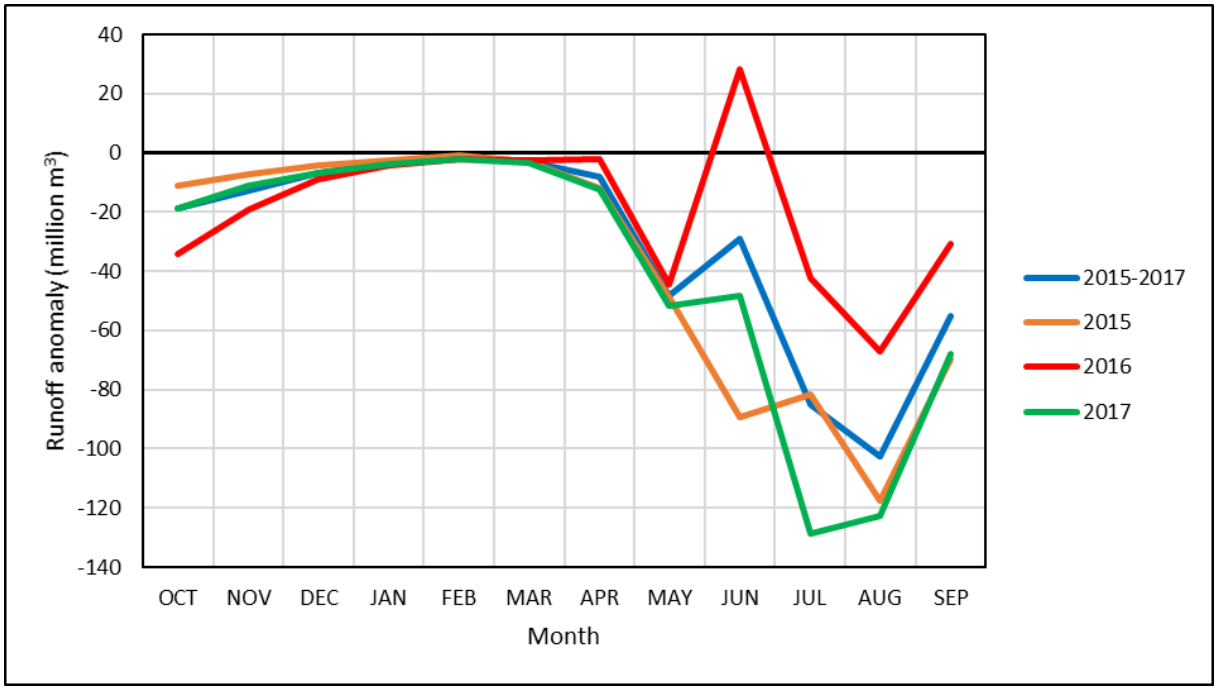

Figure 34. Monthly average modelled runoff received during the drought period and individual drought years compared to monthly average rainfall (1980–2014) in the BRC.

Monthly runoff received in the 12 quaternary catchments for the individual drought years and the drought period was compared to the monthly mean over the recent period and is described below:

2015: The largest reductions in runoff occurred in June in the headwater quaternary catchments (G10-A and -B); while the rest of the quaternary catchments experienced their greatest reduction in runoff volume in July (see Fig. 35). For the entire year, all quaternary catchments received below-normal to normal runoff volume, particularly quaternary catchments that produce high runoff volumes, apart from G10B which was slightly above-normal in July.

2016: All the quaternary catchments in the BRC received below-normal to normal volumes of runoff for the entire year, apart from July in which G10-A, -B, -D, and -E were greatly above-normal (see Fig. 35). The greatest reductions for most quaternary catchments occurred in May, and from July through to September, apart from G10D which received its lowest runoff volume in October.

2017: all quaternary catchments were below-normal or normal for the entire year. The largest reductions in runoff occurred in July; particularly for higher runoff quaternary catchments (see Fig.

35). Runoff in these quaternary catchments increased in August and September but was still largely below-normal.

2015–2017: During the drought period, runoff for most quaternary catchments is greatly below-normal from May-October (see Fig. 35). The greatest reductions in runoff volumes occurring in July and August.

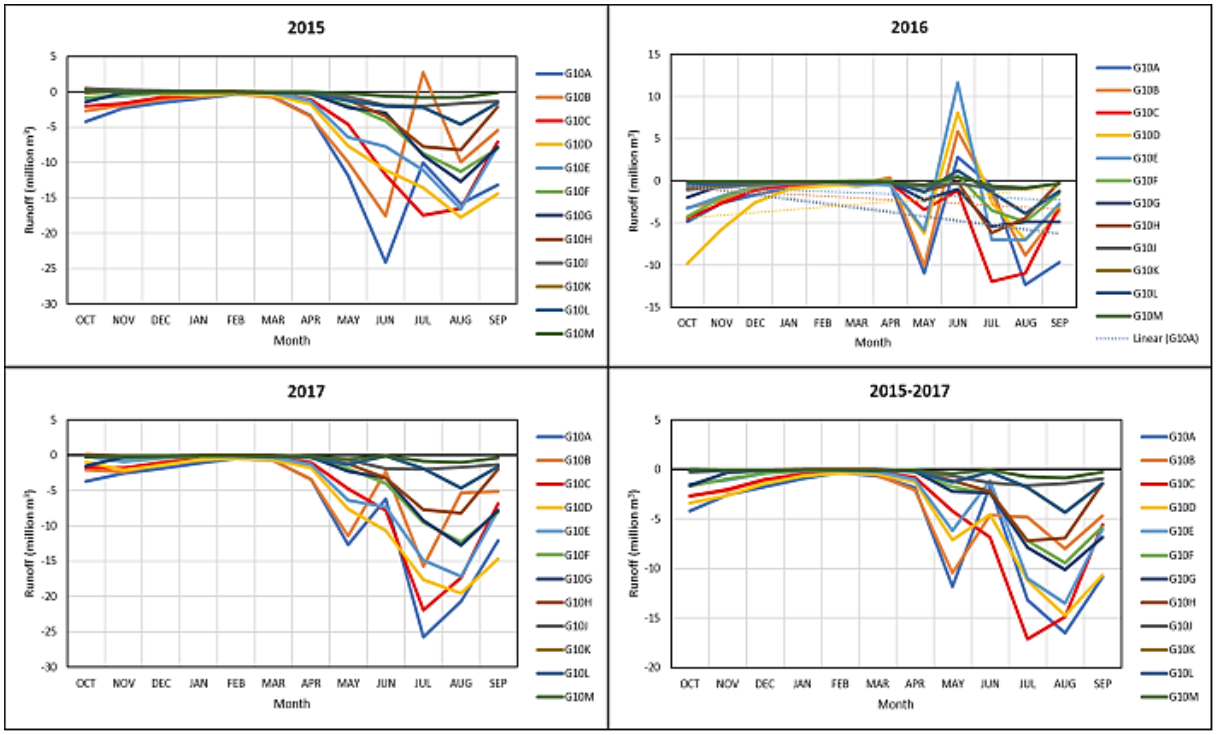

Figure 35. Monthly average modelled runoff received during the drought period and individual drought years compared to the monthly average modelled runoff (1980−2014) in the 12 quaternary catchments.

The annual average rainfall in the BRC, during the drought event, was lowest in 2015. The mountainous wet quaternary catchment (G10G), experienced the largest reduction in model input rainfall received during the three-year drought. During the drought period, the wetter headwater quaternary catchments (G10-A, -B and-C) and the mountainous wet quaternary catchment of the BRC experienced the largest reductions of model input rainfall, particularly in May.

The largest reduction in runoff received in the BRC during the drought event occurred in 2017. G10K (dry-northern quaternary catchment) experienced the largest overall reduction in runoff received during the drought period. In the greater BRC, the drought years experienced their greatest reductions in the winter months (June, July and August). Runoff was consistently below-normal for all drought years, apart from June in 2016. Seasonal runoff in the 12 quaternary catchments shows that quaternary catchments that receive higher runoff volumes experienced the greatest percentage reduction of runoff during the drought, particularly in the winter months of June and July.

4.3. Drought Definition Results

This section provides event definitions for the 2015−2017 meteorological and hydrological drought in the SWC for the 12 quaternary catchments that make up the BRC, and the BRC itself. Event definitions for the drought are based on observed rainfall data and modelled runoff.

Risk-based attribution requires that an extreme event be properly defined by a given threshold. As such, the 2015−2017 drought in the SWC will be defined in terms of observed rainfall and modelled runoff for the drought period in the BRC.

a) Rainfall

For rainfall, the event is defined in terms of the three-year observed MAP received in each of the 12 quaternary catchments during the hydrological drought period (2015−2017) and, the area-weighted average rainfall for the entire analysed region of the BRC (see table 16 below).

Table 16. Three-year (2015−2017) averages of observed rainfall values in the 12 quaternary catchments and the BRC used as thresholds for the attribution analysis.

Catchment	G10A	G10B	G10C	G10D	G10E	G10F	G10G	G10H	G10J	G10K	G10L	G10M	G10 (BRC)
3-year average (mm's)	1086.00	880.94	591.57	458.90	507.40	386.50	630.60	263.00	321.50	206.30	227.59	167.35	310.32

b) Runoff

For runoff, the event is defined in terms of the modelled MAR received during the hydrological drought period (2015−2017). The drought event magnitude in each of the 12 quaternary catchments was defined using modelled runoff because not all of the quaternary catchments have streamflow gauging stations. Modelled runoff values in the quaternary catchments for the three-year drought are in the range of 1.84−73.64 million m^3; while the entire BRC streamflow was calculated to be 347.87 million m^3. The event definitions for each of the 12 quaternary catchments (G10A-G10M) in the BRC, as well as for the BRC are provided in table 17 below.

Table 17. Three-year average modelled runoff values in the 12 quaternary catchments and the BRC used as thresholds for the attribution analysis.

Catchment	G10A	G10B	G10C	G10D	G10E	G10F	G10G	G10H	G10J	G10K	G10L	G10M	G10 (BRC)
3-year average (million m^3)	73.64	54.69	51.04	70.21	38.50	26.11	12.44	7.70	5.52	1.84	4.44	1.74	347.87

4.4 Attribution Results

This section presents the rainfall and runoff attribution data analysis results, as well as a comparison of the two RRs in the BRC. Furthermore, an explanation of hydrological parameters used in the Pitman model for the BRC and their influence on runoff RRs is presented.

a) Rainfall Attribution Results

The probabilities of the amount of rainfall received during the 2015−2017 drought event occurring under the pre-industrial climate rainfall scenario were consistently lower than that of the event occurring under the current climate rainfall for all 12 quaternary catchments in the BRC (see Table 18 and Fig. 36). Rainfall RRs for the 12 quaternary catchments in the BRC were between 11.5 and 41.0; while the calculated FAR was found to be between 0.91 and 0.98. The rainfall RRs for the quaternary catchments being significantly greater than 1 indicate that there is an increased risk of a drought event of this severity occurring under the current climate rainfall, compared to a climate without human influence.

For the average rainfall over the entire BRC, the probability of the 2015−2017 meteorological drought event occurring under the pre-industrial climate rainfall scenario is calculated to be 0.000026, while that for the current climate rainfall scenario is 0.00074, which indicates a more than 28-fold increase

of a meteorological drought event of this magnitude occurring due to anthropogenic climate change, implying an FAR of 0.96.

Table 18. Probabilities of the: i) current (P_1) and ii) pre-industrial (P_0) rainfall occurring; iii) Median RRs; iv) 95% CI RR range; and v) FAR's for meteorological drought for the 12 quaternary catchments and for the entire BRC.

Catchment	P_1	P_0	RR	2.5^{th}; 50^{th}; 97.5^{th} percentile RR	FAR
G10A	0.00030	0.00000073	41.0	36.1; 41.3; 48.8	0.98
G10B	0.00030	0.00000073	41.0	35.1; 41.4; 47.3	0.98
G10C	0.00030	0.00000073	41.0	36.6; 40.7; 46.1	0.98
G10D	0.00056	0.000021	26.2	22.5; 26.2; 30.1	0.96
G10E	0.00056	0.000021	26.2	22.3; 26.2; 30.5	0.96
G10F	0.00056	0.000021	26.2	22.6; 26.0; 29.1	0.96
G10G	0.00094	0.000059	16.1	12.5; 14.4; 17.8	0.94
G10H	0.00066	0.000028	23.5	21.0; 23.8; 26.0	0.96
G10J	0.00066	0.000028	23.5	20.5; 23.7; 27.4	0.96
G10K	0.00066	0.000028	23.5	20.3; 23.2; 26.2	0.96
G10L	0.015	0.0013	11.5	10.5; 11.5; 12.6	0.91
G10M	0.015	0.0013	11.5	10.7; 11.5; 12.4	0.91
G10 (BRC)	0.00074	0.000026	28.5	24.9; 28.5; 32.8	0.96

A previously undertaken attribution study by Otto et al. (2018) on the 2015−2017 SWC meteorological drought calculated a RR of 3.5 (95% CI: 2.7−4.1) using CMIP5 rainfall simulations (42 model simulations), while this study calculated a much higher RR of 28.5 (95% CI: 26.0−32.4) for the same event using CMIP5 rainfall simulations (77 model simulations).

One possible reason for these differences, among others (explained further below), could be that Otto et al. (2018) defined the 2015−2017 SWC meteorological drought as a 1 in 100 years event, based on the Climate Research Unit-Timeseries (CRU) 4.01 observed dataset. This return period was used by Otto et al. (2018) to calculate RRs from the CMIP5 simulated rainfall dataset for the 2015−2017 SWC meteorological drought event.

To control for this difference in this study, in which the drought event was defined based on a three-year average observed rainfall threshold, the 2015−2017 SWC meteorological drought event was redefined as a 1 in 100 years event. The RR for the entire BRC, calculated based on the event being a 1 in 100 years event, was still much higher (15.2, roughly 4.5 times larger), see table 19, than that of Otto et al. (2018). This could further be explained by the following:

Otto et al. (2018), extended CMIP5 historical simulations (1861−2005) with RCP 4.5 simulations (2006−2017), while this study extended CMIP5 historical simulations (1861-2010) with RCP 8.5 simulations (2011-2100), which was bias corrected based on observed rainfall station data.

To calculate current and pre-industrial risk, this study used time slices of the model rainfall data. This means that PDFs of rainfall were determined over a period meant to represent pre-industrial world conditions (1860-1890) and another period to represent current world conditions (2002-2031).

Otto et al. (2018) employed the multi-method approach of attribution analysis in their study. Each of the climate models taken from CMIP5 was given equal weight by using an ensemble from each of the 42 models, as in van Oldenborgh et al., 2013. Each model was then normalised multiplicatively to have the same MAP as the ensemble mean. The study used a single PDF of the model rainfall data, the year

1900 was chosen to represent pre-industrial conditions and 2015 to represent current world conditions, and parameters of the PDF were scaled with global mean surface temperature (GMST). This method is frequently used to analyse observations by the World Weather Attribution group (van Oldenborgh, 2007; Otto et al., 2012; van Oldenborgh et al., 2019).

In the method used in this study, the RR in effect reflects rainfall change between the pre-industrial and current period. In the method used by Otto et al. (2018), RR reflects only the fraction of that change that is co-linear with GMST.

In summary, the differences between the base datasets (RCP4.5 vs. RCP8.5) and differences in methodology have resulted in substantial quantitative differences between this study and that of Otto et al. (2018). Qualitatively, however, both results are similar, i.e. they indicate a significant positive RR.

Different scientifically valid approaches to studying the same event have been shown to produce different quantitative assessments of the role of anthropogenic climate change in attribution studies such as in: Rahmstorf and Coumou (2011) and Dole et al. (2009): The 2010 Russian heatwave; Cheng et al. (2016) and Diffenbaugh et al. (2015): The 2015 Californian drought; and Hauser et al. (2017): The 2015 European drought.

Table 19. Probabilities of the: i) current (P_1) and ii) pre-industrial (P_0) rainfall occurring; iii) Median RRs; iv) 95% CI RR range; and v) FAR's for a 1 in 100-year meteorological drought event for the 12 quaternary catchments and for the entire BRC.

Catchment	P_1	P_0	RR	2.5^{th}; 50^{th}; 97.5^{th} per centile RR	FAR
G10A	0.01	0.00057	17.6	16.2; 17.4; 19.1	0.94
G10B	0.01	0.00057	17.6	16.1; 17.7; 19.3	0.94
G10C	0.01	0.00057	17.6	16.1; 17.7; 19.2	0.94
G10D	0.01	0.00074	13.6	12.5; 13.5; 14.6	0.93
G10E	0.01	0.00074	13.6	12.4; 13.4; 14.5	0.93
G10F	0.01	0.00074	13.6	12.3; 13.7; 14.7	0.93
G10G	0.01	0.001	9.6	8.7; 9.6; 10.3	0.90
G10H	0.01	0.00081	12.3	11.2; 12.3; 13.3	0.92
G10J	0.01	0.00081	12.3	11.5; 12.4; 13.3	0.92
G10K	0.01	0.00081	12.3	11.3; 12.4; 13.2	0.92
G10L	0.01	0.00077	13.0	11.9; 12.9; 14.0	0.92
G10M	0.01	0.00077	13.0	11.8; 13.0; 13.9	0.92
G10 (BRC)	0.01	0.000658	15.2	14.0; 15.2; 16.6	0.93

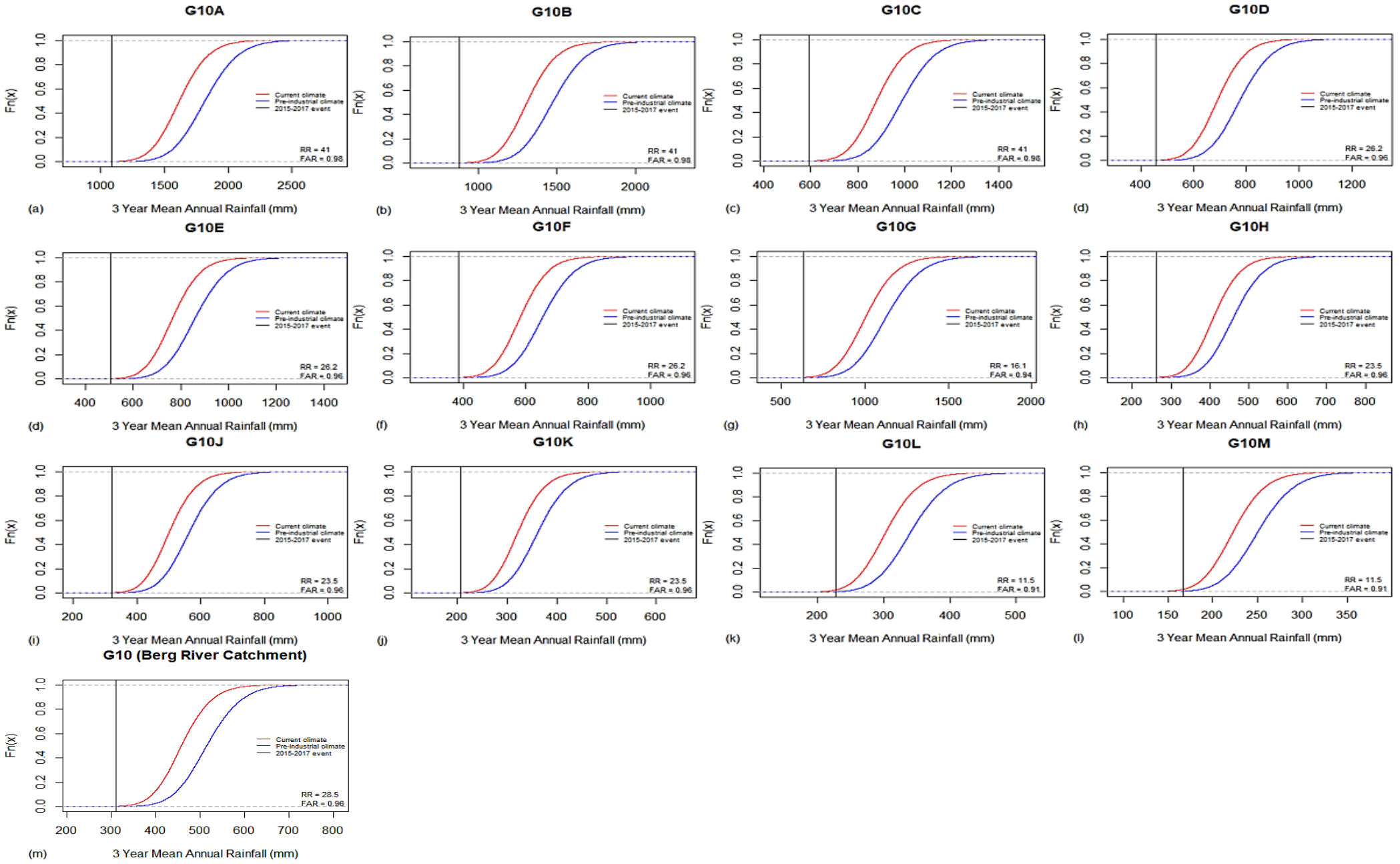

Figure 36. Cumulative distribution of current climate rainfall (red line) and pre-industrial climate rainfall (blue line) compared to observed rainfall of the drought event (black line) for catchments: a) G10A, b) G10B, c) G10C, d) G10D, e) G10E, f) G10F, g) G10G, h) G10H, i) G10J, j) G10K, k) G10L, l) G10M, and m) G10 (BRC).

b) Runoff Attribution Results

For each of the 12 quaternary catchments in the BRC, the probabilities of the 2015−2017 hydrological drought event occurring under pre-industrial climate scenario were significantly lower than those of the event occurring under current climate runoff. RRs for the 12 quaternary catchments in the BRC were between 2.7 and 60.2, while the calculated FAR was found to be in the range of 0.63 and 0.98 (see Table 20 and Fig. 37). The RRs for runoff being significantly greater than 1 indicate that there is an increased risk of the 2015−2017 hydrological drought event occurring under the current climate, compared to a climate without human influence.

For the average runoff received over the entire BRC, the probability of a hydrological drought event of this severity occurring under the pre-industrial climate scenario is 0.0011, while for the current climate is 0.012, which indicates a more than 11-fold increase of a hydrological drought of this magnitude occurring due to anthropogenic climate change, implying an FAR of 0.91.

Table 20. Probabilities of the: i) current (P_1) and ii) pre-industrial (P_0) runoff occurring; iii) Median RRs; iv) 95% RR CI range; and v) FAR's for hydrological drought for the 12 quaternary catchments and for the entire BRC.

Catchment	P_1	P_0	RR	2.5th; 50th; 97.5th percentile RR	FAR
G10A	0.00082	0.000014	60.2	51.63; 60.2; 70.7	0.98
G10B	0.0014	0.000045	31.1	28.1; 30.9; 34.7	0.97
G10C	0.0029	0.000090	31.2	28.1; 31.8; 35.3	0.97
G10D	0.023	0.0020	10.2	9.5;10.2; 11.2	0.90
G10E	0.023	0.0020	11.4	10.6; 11.4; 12.2	0.91
G10F	0.030	0.0044	6.9	6.5; 6.9; 7.3	0.85
G10G	0.018	0.00094	19.3	17.2; 19.1; 21.2	0.95
G10H	0.045	0.0063	7.2	6.8; 7.2; 7.6	0.86
G10J	0.072	0.023	3.1	3.0; 3.1; 3.2	0.68
G10K	0.039	0.012	3.3	3.1; 3.3; 3.5	0.70
G10L	0.13	0.049	2.7	2.6; 2.7; 2.7	0.63
G10M	0.19	0.063	3.0	2.9; 3.0; 3.14	0.67
G10 (BRC)	0.012	0.0011	11.3	10.5; 11.4; 12.2	0.91

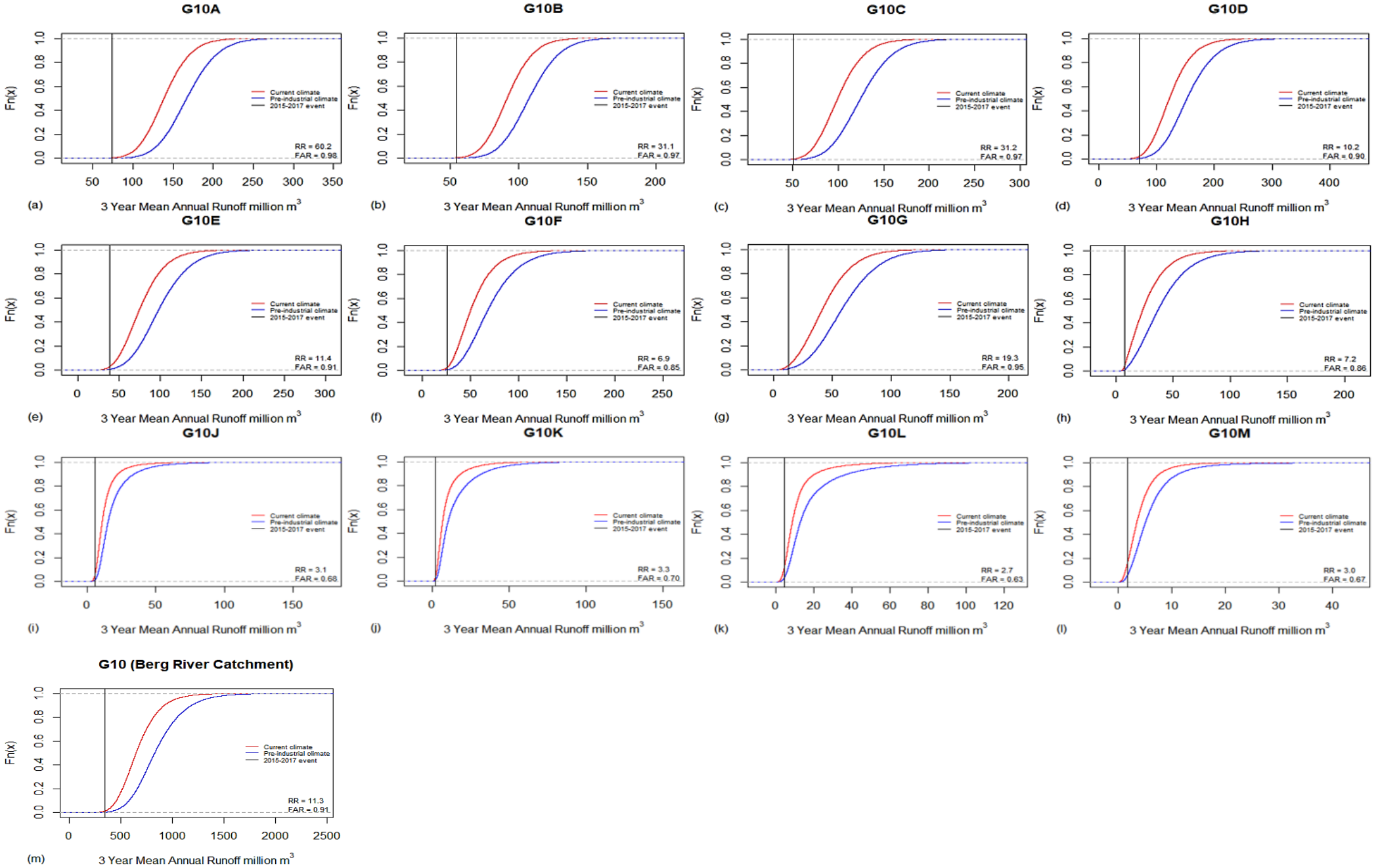

Figure 37. Cumulative distribution of current climate runoff (red line) and pre-industrial climate runoff (blue line) compared to observed runoff of the drought event (black line) for catchments: a) G10A, b) G10B, c) G10C, d) G10D, e) G10E, f) G10F, g) G10G, h) G10H, i) G10J, j) G10K, k) G10L, l) G10M, and m) G10 (BRC).

c) Comparison of Rainfall and Runoff RRs in the BRC

Runoff RRs were found to vary considerably across the quaternary catchments that make up the BRC. Furthermore, quaternary catchments with the highest rainfall RRs do not always correspond to those with the highest RRs for runoff. To understand the variability of the runoff RRs and the correlation between rainfall and runoff RRs, a stepwise regression was done to investigate whether parameters in the model, as well as the rainfall RR themselves, have any effect on the runoff RRs.

For catchments G10-A and -G, the RR of rainfall is amplified in runoff (see Fig. 38); these catchments are in the headwaters and mountainous regions of the BRC, respectively, where MAP is high. In contrast, catchments G10-B, -C, -D, -E, -F, -H, -J, -K, -L, and -M, show a decrease in RRs from rainfall to runoff, particularly in drier quaternary catchments in the northern regions of the BRC. These increases and decreases occur as a result of the rainfall to runoff conversion.

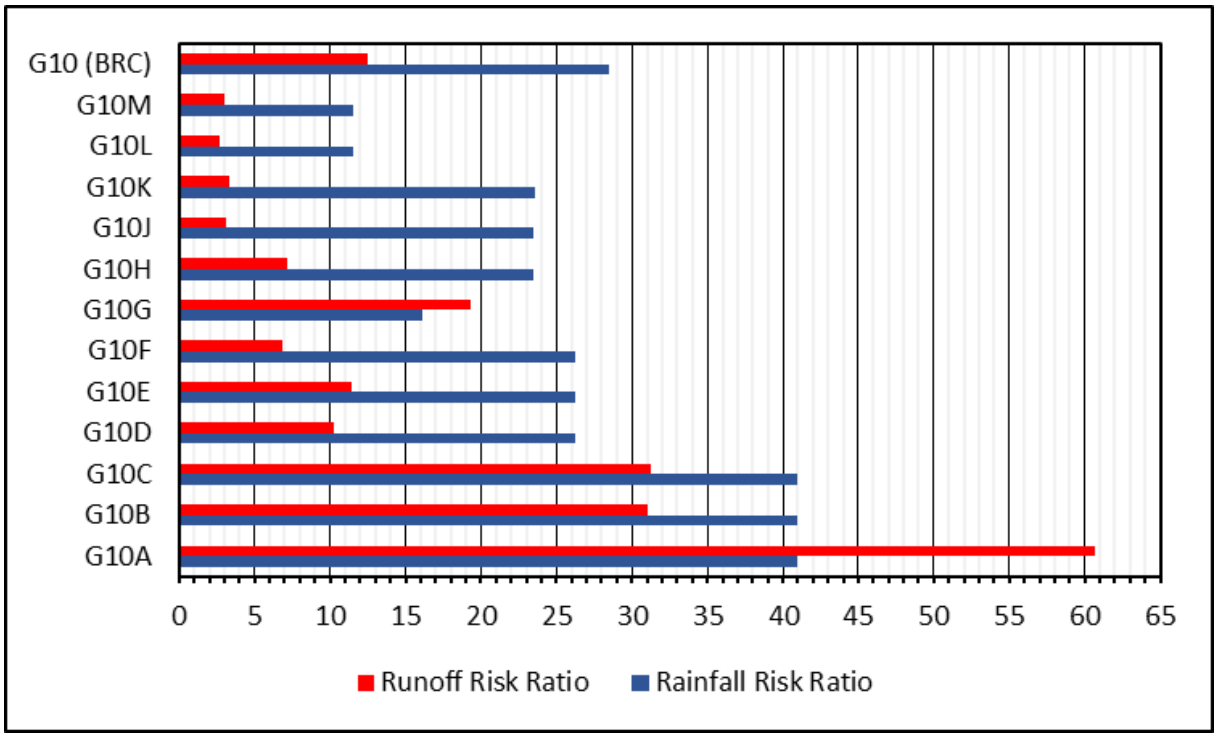

Figure 38. Catchment rainfall RRs compared to runoff RRs.

Based on the stepwise linear regression model (see Table 21 and Appendix B), MAP has the strongest relationship with the associated runoff RR and 86% of the variance in runoff RR can be explained by MAP. MAP is also the most statistically significant predictor of runoff RRs with a p-value of 0.000012. To confirm that these results reflect the full data set, rather than just the effect on the largest RR, log (RR) was used in the calculation and the results qualitatively remain the same as there are no real outlier RR values.

Table 21. Linear regression of individual hydrological parameters and rainfall RRs against runoff RRs in the BRC, full model.

Explanatory Variables vs Runoff RR	Coefficient of Determination (R^2)	p-value
MAP	0.86	0.000012
Rainfall RR	0.60	0.0032
HGGW	0.45	0.016
FT	0.30	0.067
MAE	0.11	0.29
ST	0.06	0.45
TL	0.03	0.59
Zmin	0.00	0.88
Zmax	0.00	0.94

According to the regression model analysis, MAP, MAE, Zmin and ST explain the largest amount of variance, in that order, and are significantly ($p \leq 0.1$) correlated to the quaternary catchment runoff RRs (see Table 22 and Appendix C). All other parameters used in the Pitman model (TL, Zmax, HGGW and FT) as well as the rainfall RRs for the quaternary catchments were found to explain very little variation and have a non-significant ($p > 0.1$) relationship with the catchment runoff RRs.

Based on the linear regression, HGGW and FT have a high individual correlation to runoff RRs, they are not significant in the stepwise linear regression as a result of collinearity. This is because HGGW and FT are already correlated ($R^2 = 0.57$ and 0.41, respectively) to MAP (see Appendix B).

Resultantly, the multiple regression model with the four predictors, MAP, MAE, Zmin and ST produced $R^2 = 0.98$, $p < 0.0000076$, and AIC = 67.96. The model is:

RR = 153.95 + 0.038(MAP) - 0.11(MAE) + 0.18(Zmin) - 0.02(ST)……..Equation 15

MAP and Zmin have a positive correlation with runoff RRs, indicating that as these two parameters increase catchment runoff RR increases. MAE and ST have negative significant correlation weights, meaning that as these parameters increase catchment runoff RR decreases.

Table 22. Stepwise regression of hydrological parameters and RRs in BRC, where column i) is the RR correlated against multiple explanatory variables; column ii) is the coefficient of multiple determination of the model; column iii) is the p-value of the model; column iv) is the AIC value of the model; column v) is the p-values of all each explanatory variable within the model; and column vi) is the model equation.

Runoff RR Against:	Coefficient of Multiple Determination (R^2)	p-value	AIC	Coefficient p-values	RR Estimate ($\hat{y}$)
MAP+MAE+Zmin+ST	0.98	0.0000076	67.96	0.0000016, 0.00078, 0.0081, 0.096	153.95 +0.038(MAP) -0.11(MAE) +0.18(Zmin) -0.02(ST)
MAP+MAE+Zmin+Rainfall RR	0.97	0.000016	70.47	0.00010, 0.0017, 0.022, 0.24	143.67 +0.032(MAP) -0.10(MAE) 0.13(Zmin) 0.24(Rainfall RR)
MAP+MAE+Zmin+TL	0.97	0.000025	72.09	0.0000060, 0.0021, 0.030, 0.48	156.69 +0.035(MAP) -0.11(MAE) +0.13(Zmin) -0.48(TL)
MAP+MAE+Zmin+Zmax	0.97	0.000027	72.41	0.0000053, 0.0024, 0.041, 0.56	156.86 +0.035(MAP) -0.11(MAE) +0.14(Zmin) -0.0066(Zmax)
MAP+MAE+Zmin+HGGW	0.97	0.000032	72.95	0.00019, 0.0030, 0.050, 0.85	150.30 +0.035(MAP) -0.11(MAE) +0.13(Zmin) -0.24(HGGW)
MAP+MAE+Zmin+FT	0.97	0.000033	73.01	0.000084, 0.0037, 0.071, 0.95	149.54 +0.035(MAP) -0.11(MAE) +0.13(Zmin) -0.0050 (FT)

MAP in the quaternary catchments of the BRC is between 225-1610 mm. In the Pitman model, MAP is the primary contributor to runoff. During dry years, higher (lower) rainfall will increase (decrease) MAR, through increasing (decreasing) overland flow from impervious surfaces, satisfying catchment absorption rates more (less) frequently resulting in an increase (decrease) in the occurrence of runoff events in the catchment. Higher (lower) precipitation will exceed soil moisture-holding capacity more (less) often increasing (decreasing) subsurface flow and decreasing (increasing) the moisture available for evaporation, as well as increasing (decreasing) baseflow and groundwater recharge.

Wetter (higher MAP) quaternary catchments have higher runoff RRs and are more sensitive to regional climate change than dryer (lower MAP) quaternary catchments. This is because the analysis is done on the driest rainfall years, which are the lowest runoff years (i.e. the left tail of the three-year MAR distribution). In drier (lower MAP) quaternary catchments, the rainfall-runoff conversion in dry years is very low, regardless of whether it is the pre-industrial or current climate scenario runoff; much of the rainfall is used in evaporation in both climate scenarios. The differences in rainfall in dry years in the current against that of the pre-industrial are modulated downwards by what is known as a low

elasticity of runoff response, which is the ratio of the percentage change in rainfall to the percentage change in runoff. In wetter catchments, with a higher runoff coefficient, the effects of the driest rainfall years are amplified, as these correspond to amounts of rainfall where the catchment water balance is the most sensitive to unit changes in rainfall (Chiew, 2006). In drier quaternary catchments, the fact that potential evaporation is higher in the northern (warmer, lower elevation) quaternary catchments of the BRC exacerbates this effect.

MAE in the quaternary catchments of the BRC is between 1460-1640 mm. In the Pitman model, MAE depletes soil moisture and interception storage. During dry years, higher (lower) evaporation will reduce the amount of moisture in the soil store (will reduce the amount of moisture returned to the atmosphere form the soil store), reducing (increasing) subsurface runoff. More (less) of the precipitation lost to interception will be returned to the atmosphere, ultimately decreasing (increasing) MAR.

MAE is higher in wetter quaternary catchments because there is a soil moisture constraint on evaporation. In wetter catchments, if MAE is higher (after accounting for rainfall) it moves that catchment more towards a dry water balance, therefore producing a lower RR because the rainfall-runoff conversion is lower.

ST in the quaternary catchments of the BRC is between 160-670 mm. In the Pitman model, ST is the amount of water that the soil in a catchment can hold. Soil moisture contributes to MAR through sub-surface flow only when the soil water store is exceeded as well as contributing to groundwater recharge through gradual drainage. Soil moisture is depleted by evaporation and drainage into the groundwater store. During dry years, higher (lower) ST values have a decreased (increased) likelihood of soil moisture storage being exceeded. A larger (smaller) proportion of rainfall will be absorbed and held by the soil, decreasing (increasing) subsurface runoff and increasing (decreasing) groundwater. Evaporation losses are increased (decreased) as there is more moisture available to be partitioned back into the atmosphere (as there is level moisture available in the soil). Overall decreasing (increasing) MAR. Quaternary catchments that have lower soil moisture storage capacity are more sensitive to regional climate change than quaternary catchments that have higher soil moisture storage capacity due to the amplified reduction in subsurface flow during dry years.

Zmin in the quaternary catchments of the BRC is between 0-100 mm. In the Pitman model, Zmin is the minimum catchment absorption rate and can be considered as a wetting-up threshold in the model. Only when monthly rainfall exceeds the monthly sub-catchment value of Zmin in the model is surface runoff produced, as well as contributing to both soil moisture storage and groundwater recharge. During dry years, higher (lower) Zmin values have a decreased (increased) likelihood of exceeding the minimum catchment absorption rate, decreasing the (increasing) frequency of surface runoff events and MAR. A higher (lower) proportion of the rainfall is partitioned into the soil, with increasing (decreasing) baseflow and groundwater flow, as well as decreasing (increasing) overland flow. Actual evaporation is increased (decreased) so that more (less) water is lost from the catchment through evaporation. Quaternary catchments that have higher Zmin values are more sensitive to regional climate change, as less rainfall is available to be converted to surface runoff.

CHAPTER 5: SUMMARY, KEY FINDINGS AND LIMITATIONS

The recent three-year compound hydro-meteorological drought in the SWC combined with an increasing population and demand for water led to extreme water shortages, particularly impacting the ~3.7 million residents in the CoCT. As water supply to residents was set to fail at the beginning of 2018, commonly known as the Day-Zero crisis, restrictions on water-usage for residents and agriculture were put in place. The 2015−2017 SWC hydro-meteorological drought was the worst drought to occur in the region in over 100 years. Rainfall deficits manifested into low runoff into, among other, important catchments that form part of the WCWSS, the BRC. A multi-method impact attribution analysis is applied to the drought event to determine the extent to which human influence on the climate from fossil fuel emissions has changed the likelihood of a hydro-meteorological drought of this magnitude occurring in the SWC. This chapter provides a summary of the approaches used in this impact attribution study. This is followed by the key findings, implications as well as limitations of the study and possibilities for further work.

5.1 Summary of Approach

The aim of this study was to determine the extent to which anthropogenic climate change contributed to the likelihood of the 2015−2017 hydro-meteorological drought event that occurred in the SWC. This aim was achieved through the following objectives listed below.

Objective I: To set up the Pitman hydrological model to realistically simulate hydrological responses in the BRC driven by attribution experiment data from GCM simulations.

This was achieved by evaluating the Pitman hydrological model to simulate runoff in the BRC using observed rainfall station data as an input into the model. This was done to determine the suitability of using bias corrected GCM rainfall data as an input into the model in attribution mode to generate current and pre-industrial runoff realisations for climate impact attribution experiments in the BRC.

Objective II: To generate attribution inputs for the model from GCM simulations.

In achieving objective two, attribution experiments were generated by extending historical (1861−2010) with RCP 8.5 (2011−2100) for 77 rainfall simulations taken from CMIP5, to create 150-year rainfall time series. The periods 1860−1890 and, 2002−2031 were selected to represent pre-industrial and current climate conditions, respectively. Five stochastic time series were then generated for each of the 77 simulations conditioned on observed rainfall characteristics to account for differences in GCM climates (385 in total each for the pre-industrial and current world climate).

Objective III: To implement attribution experiments with the Pitman model setup for the BRC.

To generate the climate impact attribution runoff experiments, the Pitman model was automated and each of the bias corrected rainfall realisations were then used as inputs to 'drive' the Pitman model in attribution mode. This generated 385 pre-industrial and current climate time series of runoff realisations spanning 150-years long each.

Objective IV: To analyse the attribution outputs and assess possible reasons for variation in RR across the Berg River quaternary catchments.

To meet the fourth and final objective of the study, the risk-based approach to attributing extreme climatic events was applied to both the rainfall and runoff attribution experiments. The meteorological/hydrological drought event was defined in terms of the three-year mean annual rainfall/runoff received for each quaternary catchment and the greater BRC region. The probabilities of these three-year averages occurring in the pre-industrial and current world scenarios were then estimated and used to calculate RR and FAR values for each quaternary catchment and the greater BRC region. This was done to determine the change in the probability that anthropogenic climate

change had in a meteorological/hydrological drought event with the same magnitude as the 2015−2017 SWC drought occurring. To assess the variability of the runoff RRs produced across the BRC a stepwise regression was undertaken to investigate whether parameters used in the Pitman hydrological model, as well as the rainfall RR themselves, have any effect on the runoff RRs.

5.2 Key Findings

A summary of the main findings that have emerged from this impact attribution study on the 2015−2017 SWC drought based on the results in Chapter 4 are presented in the following sections below:

5.2.1 Pitman Hydrological Model Evaluation for the BRC

- Overall, annual runoff simulated by the Pitman model in the BRC was found to be satisfactory to very good in six of the seven gauging stations based on NSE and PBIAS model evaluation guidelines.
- Along the Berg River, annual runoff is underestimated by the model during wet years, while dry years are overestimated by the model. During dry years the model consistently overestimates runoff of the tributary rivers of the Berg River, while years of high flow show no consistent overall systematic bias.
- The Pitman model largely underestimates months of low streamflow along the Berg River and overestimates months of high streamflow along the tributaries of the Berg River.
- For seasonal flows along the Berg River, the largest bias was found to occur during Oct-Mar underestimating low flows and overestimating high flows between Jul-Sep. The runoff simulated by the model of the tributaries of the Berg River shows very little bias in estimating months of low and high flows.
- The simulation of runoff by the Pitman model for the 2015−2017 BRC drought was deemed acceptable for the purpose of the study, as simulated runoff followed a similar pattern of substantial decreases in streamflow of the gauging stations during the hydrological drought years of 2015, 2016 and, 2017.

5.2.2 Rainfall and Runoff Characteristics in the BRC during the 2015−2017 Hydrological Drought Event

- During the three-year drought annual average rainfall received was lowest in 2015; wetter quaternary catchments experienced the largest reductions in model input rainfall received, particularly in May.
- Runoff received during the three-year drought was the lowest in 2015; quaternary catchments which receive higher annual average runoff volumes experienced the greatest reductions in the volume of runoff received during the drought, especially in the winter months.

5.2.3 Attribution of the 2015−2017 Meteorological Drought in the BRC

- The probabilities of the meteorological drought occurring under the pre-industrial world scenario were consistently lower than that of the event occurring under the current world scenario in the 12 quaternary catchments and the greater BRC.
- The risk of a meteorological drought of this magnitude occurring in the BRC was significantly increased by more than 28-fold (95% CI: 24.9−32.8), but more than 11- to 41- fold in the 12 quaternary catchments, as a result of human influence on climate from fossil fuel emissions.
- The results of this study were qualitatively similar to that of Otto et al. (2018), as both show an increase in risk attributed to human influence on the climate for the 2015−2017 BRC meteorological drought; as both studies produced a RR > 1. However, they are quantitatively different as this study produced a RR much higher than that of Otto et al. (2018).

5.2.4 Attribution of the 2015−2017 Hydrological Drought in the BRC

- The probabilities of the hydrological drought occurring under the pre-industrial world scenario were consistently lower than that of the event occurring under the current world scenario in the 12 quaternary catchments and the entire BRC.
- The risk of a hydrological drought event of this magnitude occurring in the BRC was increased by more than 11-fold (95%: 10.5−12.2), and more than 2- to 60- fold in the 12 quaternary catchments of the BRC, due to human influence on climate from fossil fuel emissions.

5.2.5 Comparison of Rainfall and Runoff RRs

- Rainfall RRs were lower than runoff RRs in the wetter southern quaternary catchments, while they were higher than for rainfall in the drier northern quaternary catchments. As such human influence on the meteorological drought appears to have been amplified in the quaternary catchments most important to the WCWSS.
- MAP was found to have the greatest influence on the calculated runoff RRs. Higher (lower) MAP produces an enhanced (reduced) RR. This was because the analysis was done on the three driest rainfall years. The differences in rainfall in dry years in the current climate against that of the pre-industrial climate are modulated downwards by a low elasticity of runoff response in drier quaternary catchments. In wetter catchments, which have a higher runoff coefficient, the effects of the driest rainfall years are amplified.

5.3 Implications of the Study

The increasing risk of extreme climatic events such as the 2015−2017 SWC hydro-meteorological drought in South Africa highlights the crucial need for climate impact attribution studies to determine if and how this risk has been altered due as a result of human influence on the climate. Work in the impact attribution field has the potential to suggest how the trend of current increases in frequency and magnitude of drought and other extreme climatic events will continue into the near-future and become what many consider to be the 'new normal' state of the climate. Attribution assessments that focus primarily on meteorological aspects are not enough to make informed decisions and better protect people and the environment; there is a need for increased impact attribution studies that directly tie a change in risk of an extreme event to societal and environmental impacts.

A clear link has been established between the majority of continental-scale temperature impact attribution studies highlighted in the AR5 and human-induced climate change. However, very few multi-method climate impact attribution studies exist which explicitly link precipitation changes and their associated impacts to anthropogenic climate change. Furthermore, very few studies use hydrological models for drought impact attribution analysis. This study fills this gap identified by Hansen and Stone (2016), by quantitatively directly linking changes in precipitation to a reduction in runoff as a result of anthropogenic forcing in the SWC.

5.4 Limitations and Further Work

i) The study used rainfall from the multi-model CMIP5 experiment; using multi-model ensembles has been known to assist in characterizing model uncertainty (NSM, 2016). To provide a more robust assessment drawing on multiple experiments the study could have used bias corrected rainfall time series as inputs for the Pitman hydrological model from the following:

1. Atmospheric model attribution simulations such as weather@home and Climate of the Twentieth Century Project (C20C) experiments.
2. Dedicated coupled model attribution experiments such as European Community-Earth (EC-Earth).
3. CMIP6 experiments, which is an update of the CMIP5, using the same methods.

4. Observational approaches, as used by van Oldenborgh et al. (2019), where rainfall data are modelled with temperature as a covariate.

ii) The use of multiple climate models has the potential to improve the results of the attribution experiments presented in this study. However, due to the computational time it takes to run the Pitman model for a single simulation, this was not included in the scope of the study. The drawback of using multiple GCM's in attribution studies is that the number of downscaled, bias corrected time series from each GCM would have to be reduced due to time constraints.

iii) An evaluation of the bias corrected rainfall ensembles from CMIP5 against that of station rainfall data would help to understand the uncertainty and any limitations arising from the downscaling approach used. However, for the purposes of this study and time constraints, the bias corrected rainfall CMIP5 ensembles were deemed suitable to produce reliable results, as the CMIP5 models have been previously used in rainfall climate change projections and attribution studies of drought in the southern African region (Niang et al., 2014; Otto et al., 2018; Jury, 2018). Additionally, CMIP5 has been proven to be suitable for analysis of extremes occurring over a large spatial area, such as drought (NSM, 2016).

iv) The Pitman model is a monthly time-step water balance model, with quite simplistic conceptual hydrology; the study does not explore how this has influenced the runoff RRs produced. With additional time and resources other hydrological models already set up for the BRC, such as the Agricultural Catchments Research Unit (ACRU), could have been used to explore how the results vary according to the hydrological model used. Moreover, the study does not assess whether potential evaporation has changed; and how this would alter the hydrological response in the BRC.

v) In calculating the RRs this study considered the lowest three-year average rainfall/runoff values from a stochastic time series of 150 years. Other alternative approaches could have been undertaken to calculate the RRs for the 12 quaternary catchments and the greater BRC. Such as, analysing the entire distribution of values generated under a given climate. The implication in this is that it considers the distribution of all possible values (events) in a given climate which can be considered unconditioned attribution. By selecting the three lowest years of rainfall/runoff this was essentially a conditioned attribution study (only a sub-sample of possible events were analysed), as such the calculated probabilities cannot be directly translated into return intervals for the 2015–2017 SWC drought event.

vi) In addition to the impact attribution analysis, climate model projections could have also been used to assess how the probability of the 2015−2017 SWC hydro-meteorological drought might change in future decades, or at different levels of projected global warming as a result of human influence on the climate.

vii) This impact attribution approach could also be applied to the full WCWSS catchments, which would include at least the Upper Riviersonderend (Theewaterskloof) and the Steenbras; and could also include the Table Mountain reservoirs. This would improve the understanding of the impact of the hydro-meteorological drought on the entire SWC.

REFERENCES

Agri SA. A Raindrop in the Drought. Agri SA's status report on the current drought crisis'. Pretoria, South Africa. Available: http://www.greenagri.org. za/assets/documents-/Water-efficiency/Agri-SA-Drought-Report-24-Feb-2016.pdf. [2017, February 06].

Akaike, H. 1973. Information theory and an extension of the maximum likelihood principle. *Proceedings of the 2nd International Symposium on Information Theory*. B. Petrov and F. Csaki, Eds. Budapest, Akademiai Kiado. 267-281.

Allen, M. R. 2003. Liability for climate change. *Nature.* 421(6926): 891-892. DOI: 10.1038/421891a.

Andersson, L., Wilk, J., Todd, M.C., Hughes, D.A., Earle, A., Kniveton, D., Layberry, R. & Savenije, H.G. 2006. Impact of climate change and development scenarios on flow patterns in the Okavango River. *Journal of Hydrology*. 331(1-2): 43-57. DOI: 10.1016/j.jhydrol.2006.04.039.

Bae, D.H., Jung, I.W. & Lettenmaier, D.P. 2011. Hydrologic uncertainties in climate change from IPCC AR4 GCM simulations of the Chungju Basin, Korea. *Journal of Hydrology*. 401(1): 90-105. DOI: 10.1016/j.jhydrol.2011.02.012.

Bailey, A.K. & Pitman, W.V. 2005. *Proceedings of the 12th SANCIAHS Symposium*. 5-7 September. Eskom Convention Centre, Midrand, South Africa: Managing Water for People and the Environment.

Bailey, A.K. & Pitman, W.V. 2016. Water Resources of South Africa, 2012 Study: WRSM/Pitman Model Theory Manual. (WRC Report TT 690/16). Pretoria, South Africa: Water Research Commission.

Bates, B. C., Kundzewicz, Z. W., Wu, S. & Palutikof, J. 2008. Climate change and water. (Technical paper of the Intergovernmental Panel on Climate Change). Geneva, Switzerland: IPCC Secretariat.

Beck, L. & Bernauer, T. 2011. How will combined changes in water demand and climate affect water availability in the Zambezi river basin?. *Global Environmental Change*. 21(3): 1061-1072. DOI: 10.1016/j.gloenvcha.2011.04.001.

Behera, S.K. & Yamagata, T. 2001. Subtropical SST dipole events in the southern Indian Ocean. *Geophysical Research Letters*. 28(2): 327-330. DOI: 10.1029/2000GL011451.

Benson, C. & Clay, E. 1994. The Impact of drought on sub-Saharan African economies: A preliminary examination. (Working Paper 77). London: Overseas Development Institute (ODI).

Bergström, S., Carlsson, B., Gardelin, M., Lindström, G., Pettersson, A. & Rummukainen, M. 2001 Climate change impacts on runoff in Sweden—assessments by global climate models, dynamical downscaling and hydrological modelling. *Climate Research*. 16(2) 101-112. DOI: 10.3354/cr016101.

Beven, K.J. 1989. Changing ideas: The case of physically based models. *Journal of Hydrology*. 105(1-2): 157-172.

Beven, K.J. 2005. Rainfall-runoff modelling: Introduction. New York: John Wiley and Sons.

Bhend, J. & von Storch, H. 2008. Consistency of observed winter precipitation trends in northern Europe with regional climate change projections. *Climate Dynamics*. 31(1): 17-28. DOI: 10.1007/s00382-007-0335-9.

Bindoff, N.L., Stott, P.A. AchutaRao, K.M., Allen, M.R., Gilett, N., Gutzler, D., Hasingo, K. & Hegerl, G. et al. 2013. Detection and Attribution of Climate Change: from Global to Regional. In Climate Change 2013: The Physical Science Basis. (Contribution of Working Group I to the Fifth Assessment Report of

the Intergovernmental Panel on Climate Change). C.B. Field, V. Barros, T.F. Stocker, D. Qin, D.J. Dokken, K.L. Ebi, M.D. Mastrandrea, K.J. Mach, G.-K. Plattner, S.K. Allen, M. Tignor, & P.M. Midgley, Eds. Cambridge, United Kingdom and New York, NY, USA: Cambridge University Press, USA. 867-952

Blamey, R.C. & Reason, C.J. 2007. Relationships between Antarctic sea-ice and South African winter rainfall. *Climate Research*. 33(2): 183-193. DOI: 10.3354/cr033183.

Boken, V.J., Cracknell, A. & Heathcote, R. 2005. Monitoring and predicting agricultural drought: A global study. Oxford: Oxford University Press.

Boko, M., Niang, I., Nyong, A., Vogel, C., Githeko, A., Medany, M., Osman-Elasha, B., Tabo, R. & Yanda, P. 2007. Africa: Impacts, adaptation and vulnerability. In Climate Change 2007. (Contribution of Working Group II to the Fourth Assessment Report of the Intergovernmental Panel on Climate Change). M.L. Parry, O.F. Canziani, J.P. Palutikof, P.J. van der Linden & C.E. Hanson, Eds. Cambridge, UK: Cambridge University Press. 433-467.

Botai, C.M., Botai, J.O., de Wit, J., Ncongwane, K.P. & Adeola, A.M. 2017. Drought characteristics over the Western Cape Province, South Africa. *Water*. 9(876): 1-16. DOI: 10.3390/w9110876.

Botai, C.M., Botai, J.O., Dlamini, L.C., Zwane, N.S. & Elewani, P. 2016. Characteristics of droughts in South Africa: A case study of Free State and North West Provinces. Water. 8(439): 1-23. DOI: 10.3390/w8100439.

Bouwer, L. M., Aerts, J. C. J. H., Van de Coterlet, G. M., Van de Giesen, N., Gieske, A. & Mannaerts, C. 2004. Evaluating downscaling methods for preparing global circulation model (GCM) data for hydrological impact modelling. In Climate Change and Contrasting River Basins. J. C. J. H. Aerts & P. Droogers, Eds. Wallingford, UK: CAB International. 25-47.

Brink, E. 2016. Dust to dust. (A drought report). London: Solidarity Research Institute.

Brown, C., Greene A., Block, P. & Giannini, A. 2008. Review of downscaling methodologies for Africa climate applications. (Technical Report 08-05: IRI Downscaling Report). International Research Institute for Climate and Society IRI, Columbia University.

Bureau for Food and Agricultural Policy (BFAP). 2018. (Drought Policy Brief). Cape Town, South Africa: Western Cape Department of Agriculture and the Bureau for Food and Agricultural Policy.

Burke, E. J. & Brown, S. J. 2008. Evaluating uncertainties in the projection of future drought. *Journal of Hydrometeorology*. 9(2): 292-299. DOI: 10.1175/2007jhm929.1.

Burke, E. J. 2011. Understanding the sensitivity of different drought metrics to the drivers of drought under increased atmospheric CO2. *Journal of Hydrometeorology*. 12(6): 1378-1394. DOI: 10.1175/2011jhm1386.1.

Buytaert, W., Vuille, M., Dewulf, A., Urrutia, R., Karmalker, A. & Célleri, R. 2010. Uncertainties in climate change projections and regional downscaling in the tropical Andes: implications for water resources management. *Hydrology and Earth System Sciences*. 14(7): 1247-1258. DOI: 10.5194/hess-14-1247-2010.

Calow, R.C., MacDonald, A. M., Nicol, A.L. & Robins, N.S. 2010. Ground water security and drought in Africa: linking availability, access and demand. *Ground Water*. 48(2): 246-256. DOI: 10.1111/j.1745-6584.2009.00558.x.

Cameron, D. 2006. An application of the UKCIP02 climate change scenarios to flood estimation by continuous simulation for a gauged catchment in the northeast of Scotland, UK (with uncertainty). *Journal of Hydrology*. 328(1-2): 212-226. DOI: 10.1016/j.jhydrol.2005.12.024.

Centre for Research on the Epidemiology of Disaster (CRED). 2016. Poverty & death: Disaster mortality 1996 – 2015. Geneva: United Nations office for Disaster Risk Reduction.

Chen, T., van der Werf, G.R., de Jeu, R.A.M., Wang, G. & Dolman, A.J. 2013. A global analysis of the impact of drought on net primary productivity. *Hydrology and Earth System Sciences*. 17(10): 3885-3894. DOI: 10.5194/hess-17-3885-2013.

Cheng, L., M. Hoerling, A. AghaKouchak, B. Livneh, X.-W., & Eischeid, J. 2016. How has human-induced climate change affected California drought risk?. Journal of Climate. 29(1): 111-120. DOI: 10.1175/JCLI-D-15-0260.1.

Chiew, F., 2006. Estimation of rainfall elasticity of streamflow in Australia. *Hydrological Sciences Journal*. 51(4): 613-625. DOI: 10.1623/hysj.51.4.613.

Chikoore, H. 2016. Drought in southern Africa; structure, characteristics and impacts. Ph.D. Thesis. University of Zululand.

Christensen, J.H., Hewitson, B., Busuioc, A., Chen, A., Gao, X., Held, I., Jones, R. & Kolli, W. et al. 2007. Regional Climate Projections. In Climate Change 2007: The Physical science basis. (Contribution of Working Group I to the Fourth Assessment Report of the Intergovernmental Panel on Climate Change). S. Solomon, D. Qin, M. Manning, Z. Chen, M. Marquis, K.B. Averyt, M. Tignor, & H.L. Miller, Eds. Cambridge, UK, and New York, NY: Cambridge University Press, USA. 849-926.

Christidis, N. & Stott, P. A. 2012. Lengthened odds of the cold UK winter of 2010/11 attributable to human influence. In Explaining Extreme Events of 2011 from a Climate Perspective. *Bulletin of the American Meteorological Society*. 93(7):1060-1062. DOI: 0.1175/BAMS-D-11-00021.1.

Christidis, N., Stott, P.A., Scaife, A.A., Arribas, A., Jones, G.S., Copsey, D., Knight, J.R. & Tennant, W.J. 2013. A new HadGEM3A-based system for attribution of weather- and climate-related extreme events. *Journal of Climate.* 26(9): 2756-2783. DOI: 10.1175/JCLI-D-12-00169.1.

City of Cape Town (CoCT). 2017. Water Dashboard. Available: http://resource.capetown.gov.za/documentcentre/Documents/City%20research%20reports%20and%20review/damlevels.pdf [2017, November 20].

City of Cape Town (CoCT). 2018a. Day Zero FAQs. Available: http://resource.capetown.gov.za/documentcentre/ Documents/Procedures%2C%20guidelines%20and%20 regulations/Day%20Zero%20FAQs.pdf [2019 May 29].

City of Cape Town (CoCT). 2018b. Think Water. Available: https://www.capetown.gov.za/Family%20and%20home/residential-utility-services/residential-water-and-sanitation-services/make-water-saving-a-way-of-life [2018, November 21].

City of Cape Town (CoCT). 2018c. Water Outlook 2018. (Report). Cape Town, South Africa: Department of Water and Sanitation and City of Cape Town.

City of Cape Town (CoCt). 2018d. Water Resources and the Cape Town Urban Water Cycle. Available: https://resource.capetown.gov.za/documentcentre/Documents/Graphics%20and%20educational%20material/Water%20Services%20and%20Urban%20Water%20Cycle.pdf [2018, November 22].

Conway, D. & Hulme, M. 1996. The impacts of climate variability and future climate change in the Nile basin on water resources in Egypt. *International Journal of Water Resources Development*. 12(3): 261-280. DOI: 10.1080/07900629650178.

Cook, C., Reason, C.J. & Hewitson, B.C. 2004. Wet and dry spells within particularly wet and dry summers in the South African summer rainfall region. *Climate Research*. 26(1): 17-31. DOI: 10.3354/cr026017.

Cook, K.H. 2001. A southern hemisphere wave response to ENSO with implications for Southern Africa precipitation. *Journal of Atmospheric Sciences*. 58(15): 2146-2162. DOI: 10.1175/1520-0469(2001)058%3C2146:ASHWRT%3E2.0.CO;2.

Cramer, W., Yohe, G.W., Auffhammer, M., Huggel, C., Molau, U., da Silva Dias, M.A., Solow, A., Stone, D. et al. 2014. Detection and attribution of observed impacts. In Climate Change 2014: Impacts, adaptation, and vulnerability. Part A: Global and sectoral aspects. (Contribution of Working Group II to the Fifth Assessment Report of the Intergovernmental Panel on Climate Change). C.B. Field, V.R. Barros, D.J. Dokken, K.J. Mach, M.D. Mastrandrea, T.E. Bilir, M. Chatterjee, K.L. Ebi, Y.O. Estrada, R.C. Genova, B. Girma, E.S. Kissel, A.N. Levy, S. MacCracken, P.R. Mastrandrea, and L.L. White, Eds. Cambridge, United Kingdom and New York, NY, USA: Cambridge University Press, USA. 979-1037.

Cullis, J., Alton, T., Arndt, C., Cartwright, A., Chang, A., Gabriel, S., Gebretsadik, Y., Hartley, F. et al. 2015. An uncertainty approach to modelling climate change risk in South Africa. United Nations University World Institute for Development Economics Research. WIDER Working Paper 2015/045.

Dai, A. 2011a. Drought under global warming: A review. *Wiley Interdisciplinary Reviews: Climate Change*. 2(1): 45-65. DOI: 10.1002/wcc.81.

Dai, A. 2011b. Characteristics and trends in various forms of the Palmer Drought Severity Index (PDSI) during 1900–2008. *Journal of Geophysical Research*. 116(D12). DOI: 10.1029/2010JD015541.

Dai, A. 2013. Increasing drought under global warming in observations and models. *Nature Climate Change*. 3(1): 52-58. DOI: 10.1038/NCLIMATE1633.

Daniels, A. E., Morrison, J. F., Joyce, L. A., Crookston, N. L., Chen, S. C. & McNully, S. G. 2012. Climate projections FAQ. (General Technical Report). Colorado, United States of America: Department of Agriculture, Forest Service, Rocky Mountain Research Station.

Davison, A. C. and D. V. Hinkley. 1997. Bootstrap Methods and their Application. Cambridge, UK: Cambridge University Press.

Davis-Reddy, C.L. & Vincent, K. 2017. Climate risk and vulnerability: A handbook for Southern Africa. 2nd ed. Pretoria, South Africa: Council for Scientific and Industrial Research (CSIR).

de Jager, E. 2016. SA rainfall in 2015 the lowest on record. Available: http://www.politicsweb.co.za/documents/sa-rainfall-in-2015-the-lowest-on-record--saws [2017, August 15].

Department of Agriculture Forestry and Fisheries (DAFF). 2018. Revised area and 1st production forecast for summer crops (2018) and Final production estimate for winter cereals. South Africa: Department of Agriculture Forestry and Fisheries.

Department of Environmental Affairs (DEA). 2013. Long-term adaptation scenarios flagship research programme (LTAS) for South Africa: Climate trends and scenarios for South Africa. Pretoria, South Africa: Department of Environmental Affairs.

Department of Environmental Affairs (DEA). 2014. Climate change adaptation, disaster risk reduction and management: Adaptation scenarios factsheet Series (3 of 7). Pretoria, South Africa: Department of Environmental Affairs.

Department of Environmental Affairs and Development Planning (DEADP). 2013. State of Environment Outlook Report for the Western Cape Province: Inland Water Chapter. Cape Town, South Africa: Western Cape Government.

Department of Water Affairs (DWA). 2013. National water resource strategy 2nd edition: Water for an equitable and sustainable future. Pretoria, South Africa: Department of Water Affairs.

Department of Water Affairs and Forestry (DWAF). 1994. Hydrology of the Berg River Basin. (DWAF Report No. PG000/00/2491). Prepared by R. R. Berg of Ninham Shand Inc. in association with BKS Inc. as part of the Western Cape System Analysis. Pretoria, South Africa: Department of Water Affairs and Forestry.

Department of Water Affairs and Forestry (DWAF). 2004. River Health Programme State-of-Rivers Report: Berg River System. Pretoria, South Africa: Department of Water Affairs and Forestry.

Department of Water Affairs and Forestry (DWAF). 2007. Berg River Baseline Monitoring Programme: Introduction to the BRC; Groundwater and Hydrology. (DWAF Report No. P WMA 19/G10/00/1707). Pretoria, South Africa: Department of Water Affairs and Forestry.

Department of Water and Sanitation (DWS). 2015a. Strategic overview of the water services sector in South Africa: Version 4. Pretoria, South Africa: Department of Water and Sanitation.

Department of Water and Sanitation (DWS). 2015b. Support to the continuation of the water reconciliation strategy for the Western Cape water supply system: status report October 2015. Pretoria, South Africa: Department of Water and Sanitation.

Department of Water and Sanitation (DWS). 2018. Pretoria, South Africa: Department of Water and Sanitation. Available: http://www.dwa.gov.za/Hydrology/Provincial%20Rain/Default.aspx [2018, February 01].

Dieppois, B., Rouault, M. & New, M. 2015. The impact of El Niño on Southern African rainfall in CMIP5 Ocean Atmosphere coupled climate models. *Climate Dynamics*. 45(9-10): 2425-2442. DOI: 10.1007/s00382-015-2480-x.

Diffenbaugh, N. S., Swain D. L. & Touma, D. 2015. Anthropogenic warming has increased drought risk in California. *Proceedings of the National Academy of Sciences*. 112(13): 3931-3936. DOI: 10.1073/pnas.1422385112.

Dole, R., Hoerling, M., Perlwitz, J., Eischeid, J., Pegion, P., Tao Zhang, Xu, T. & Murray, D. 2011. Was there a basis for anticipating the 2010 Russian heatwave?. Geophysical Research Letters. 38(6): L06702. DOI: 10.1029/2010GL046582.

Döll, P. 2009. Vulnerability to the impact of climate change on renewable groundwater resources: a global-scale assessment. *Environmental Research Letters*. 4(3):035006. DOI: 10.1088/1748-9326/4/3/035006.

Driver, P. & Reason, C. J. 2017. Variability in the Botswana High and its relationships with rainfall and temperature characteristics over southern Africa. *International Journal of Climatology*. 37(7-8): 570-581. DOI: 10.1002/joc.5022.

du Plesis, A. 2017. Freshwater challenges of South Africa and its Upper Vaal River: Current State and Outlook. Springer. DOI: 10.1007/978-3-319-49502-6.

Easterling, D.R., Evans, J.L., Groisman, P.Y., Karl, T.R., Kunkel, K.E. & Ambenje, P. 2000. Observed variability and trends in extreme climate events: A brief review. *Bulletin of the American Meteorological Society*. 81(30): 417-425. DOI: 10.1175/1520-0477(2000)081<0417:OVATIE>2.3.CO;2.

Easterling, D.R., Horton, B., Jones, P.D., Peterson, T.C., Karl, T.R., Parker, D.E., James Salinger, M., Razuvayev, V. et al. 1997. Maximum and minimum temperature trends for the globe. *Science*. 277(5324): 364-367. DOI: 10.1126/science.277.5324.364.

Easterling, D.R., Kunkel, K.E., Wehner, M.F. & Sun, L. 2016. Detection and attribution of climate extremes in the observed record. *Weather and Climate Extremes*. 11: 17-27. DOI: 10.1016/j.wace.2016.01.001.

Edwards D.C. & McKee T.B. 1997. Characteristics of 20th century drought in the United States at multiple timescales. (Climatology Report No. 97-2). Fort Collins, United Sates of America: Colorado State University.

El Chami, D. & El Moujabber, M. 2016. Drought, climate change and sustainability of water in agriculture: A roadmap towards the NWRS2. *South African Journal of Science*. 112(9-10). DOI: 10.17159/ sajs.2016/20150457.

Emergency Events Database (EM-DAT). 2017. The international disaster database. Available: http://emdat.be/emdat_db/. [2017, October 11].

Fauchereau, N., Trzaska, S., Rouault, M. & Richard, Y. 2003. Rainfall variability and changes in southern Africa during the 20th century in the global warming context. *Natural Hazards*. 29(2): 139-154. DOI: 10.1023/A:1023630924100.

Fekete, B.M., Looser, U., Pietroniro, A. & Robarts, R.D., 2012. Rational for monitoring discharge on the ground. *Journal of Hydrometeorology*. 13(6): 1977-1986. DOI: 10.1175/JHM-D11-0126.1.

Feyen, L. & Dankers, R. 2009. Impact of global warming on streamflow drought in Europe. *Journal of Geophysical Research*. 114(D17116). DOI: 10.1029/2008JD011438.

Food and Agricultural Office (FAO). 2004. Drought impact mitigation and prevention in the Limpopo River Basin: A situation analysis. (Land and Water Discussion Paper). Harare, Zimbabwe: FAO Subregional Office for Southern and East Africa.

Fowler, H. J., Blenkinsop, S. & Tebaldi, C. 2007. Linking climate change modeling to impacts studies: recent advances in downscaling techniques for hydrological modeling. *International Journal of Climatology*. 27(12): 1547-1578. DOI: 10.1002/joc.1556.

Frost, J. A., Charles, S. P., Timbal, B., Chiew, F. H. S., Mehrotra, R., Nguyen, K. C., Chandler, R. E., McGregor, J. L. et al. 2011. A comparison of multi-site daily rainfall downscaling techniques under Australian conditions. *Journal of Hydrology*. 4089(1-2): 1-18. DOI: 10.1016/j.jhydrol.2011.06.021.

Fung, F., Lopez, A. & New, M. 2011. Modelling the impact of climate change on water resources. Oxford: Wiley-Blackwell.

Funk, C., Husak, G., Michaelsen, J., Shukla, S., Hoel, A., Lyon, B., Hoerling, M.P., Liebmann, B. et al. 2013. Attribution of 2012 and 2003-12 rainfall deficits in eastern Kenya and southern Somalia. In Explaining Extreme Events of 2012 from a Climate Perspective. *Bulletin of the American Meteorological Society*. 94(9): S6-S9.

Gamble, D.W. 2017. Droughts and water shortages. In The International Encyclopaedia of Geography. John Wiley & Sons. DOI: 10.1002/9781118786352.wbieg0557.

Gannon, K. E., Conway, D., Pardoe, J., Ndiyoi, M., Batisani, N., Odada, E., Olago, D. & Opere, A. et al. 2018. Business experience of floods and drought-related water and electricity supply disruption in three cities in sub-Saharan Africa during the 2015/2016 El Niño. Global Sustainability: Cambridge University Press. DOI: 10.1017/sus.2018.14.

Garrick, D & Hall, J.W. 2014. Water security and society: risks, metrics, and pathways. *Annual Review of Environment and Resources*. 39(1): 611-639. DOI: 10.1146/annurev-environ-013012-093817.

Giannini, A., Biasutti, M., Held, I.M. & Sobel, A.H. 2008. A global perspective on African climate. *Climatic Change*. 90(4): 359-383. DOI: 10.1007/S10584-008-9396-y.

Gihle, Y.B. 2008. Development of a framework for an integrated time-varying agro-hydrological forecast system for southern Africa. Ph.D. Thesis. University of KwaZulu-Natal.

Gillett, N.P., Kell, T.D. & Jones, P.D. 2006. Regional climate impacts of the Southern Annular Mode. *Geophysical Research Letters*. 33(23): L23704. DOI: 10.1029/2006GL027721.

Goderniaux, P., Brouyère, S., Fowler, H.J., Blenkinsop, S., Therrien, R., Orban, P. & Dassargues, A. 2009. Large scale surface–subsurface hydrological model to assess climate change impacts on groundwater reserves. *Journal of Hydrology*. 373(1-2): 122-138. DOI: 10.1016/j.jhydrol.2009.04.017.

Grey, D. & Sadoff, C.W. 2007. Sink or swim? Water security for growth and development. *Water Policy*. 9(6): 545-571. DOI: 10.2166/wp.2007.021.

Groisman, P.Y., Knight, R.W., Easterling, D.R., Karl, T.R., Hegerl, G.C. & Razuvaev, V.N. 2005. Trends in Intense Precipitation in the Climate Record. *Journal of Climate*. 18(9): 1326-1350. DOI: 10.1175/JCLI3339.1.

Gudmundsson, I. & Senevirante, S.I. 2016. Anthropogenic climate change affects meteorology drought risk in Europe. *Environmental Research Letters*. 11(4): 044005. DOI: 10.1088/1748-9326/11/4/044005.

Gupta, H. V., Sorooshian, S. & Yapo, P.O. 1999. Status of automatic calibration for hydrologic models: Comparison with multilevel expert calibration. *Journal of Hydrologic Engineering*. 4(2): 135-143. DOI: 10.1061/(ASCE)1084-0699(1999)4:2(135).

Guttman, N.B. 1999. Accepting the standardized precipitation index: a calculation algorithm. *Journal of the American Water Resources Association*. 35(2): 311-322. DOI:10.1111/j.1752-1688.1999.tb03592.x.

Handmer, J., Honda, Y., Kundzewics, Z.W., Arnell, N., Benito, G., Hatfield, J., Mohamed, I. & Peduzzi, P. et al. 2012. Changes in impacts of climate extremes: human systems and ecosystems. In Managing the Risks of Extreme Events and Disasters to Advance Climate Change Adaptation. (A Special Report of Working Groups I and II of the Intergovernmental Panel on Climate Change). C.B. Field, V. Barros, T.F. Stocker, D. Qin, D.J. Dokken, K.L. Ebi, M.D. Mastrandrea, K.J. Mach, G.-K. Plattner, S.K. Allen, M.

Tignor, & P.M. Midgley, Eds. Cambridge, United Kingdom and New York, NY, USA: Cambridge University Press, USA. 231-290.

Hannah, D. M., Demuth, S., Van Lanen, H. A. J., Looser, U., Prudhomme, C., Rees, G., Stahl, K., & Tallaksen, L. M. 2011. Large-scale river flow archives: importance, current status and future needs. *Hydrological Processes*. 25(7): 1191-1200. DOI: 10.1002/hyp.7794.

Hansen, G. & Stone, D. 2016. Assessing the observed impact of anthropogenic climate change. *Nature Climate Change*. 6(5): 532-537. DOI: 10.1038/nclimate2896.

Hartmann, D.L & Lo, F. 1998. Wave-driven zonal flow vacillation in the southern hemisphere. *Journal of Atmospheric Science.* 55(8): 1303-1315. DOI: 10.1175/1520-0469(1998)055%3C1303:WDZFVI%3E2.0.CO;2.

Hastenrath, S., Polzin, D. & Mutai, C. 2011. Circulation mechanisms of Kenya rainfall anomalies. *Journal of Climate*. 24(2): 404-412. DOI: 10.1175/2010JCLI3599.1.

Hauser, M., Gudmundsson, L., Orth, R., Jezequel, A., Haustein, K., Vautard, R., van Oldenborgh, G.J. & Wilcox, L. et al. 2017 Methods and model dependency of extreme event attribution: The 2015 European drought. Earth's Future. 5(10): 1034-1043. DOI: 10.1002/2017EF000612

Hayes, M., Svoboda, M., Wall, N. & Widhalm, M. 2011. The Lincoln declaration on drought indices: Universal meteorological drought index recommended. *Bulletin of the American Meteorological Society*. 92(4):485-488. DOI: 10.1175/2010bams3103.1.

Hayes, M.J. 2007. Drought indices. (Intermountain West Climate Summary). Colorado: Western Water Assessment.

Hegerl, G.C. 2015. Use of models and observations in event attribution. *Environmental Research. Letters*. 10(7): 071001. DOI: 10.1088/1748-9326/10/7/071001.

Hegerl, G.C., Hoegh-Guldberg, O., Casassa, G., Hoerling, M.P., Kovats, R.S., Parmesan, C., Pierce, D.W.& Stott, P.A. 2010. Good practice guidance paper on detection and attribution related to anthropogenic climate change. In Meeting report of the intergovernmental panel on climate change expert meeting on detection and attribution of anthropogenic climate change. T.F. Stocker, C.B. Field, D. Qin, V. Barros, G.K. Plattner, M. Tignor, P.M. Midgley & K.L. Ebi. Bern: IPCC Working Group I Technical Support Unit.

Hegerl, G.C., Zwiers, F.W., Braconnot, P., Gillet, N.P., Luo, Y., Marengo Orsini, J.A., Nicholls, N., Penner, J.E. et al. 2007. Understanding and Attributing Climate Change. In Climate Change 2007: The Physical Science Basis. (Contribution of Working Group I to the Fourth Assessment Report of the Intergovernmental Panel on Climate Change). S. Solomon, D. Qin, M. Manning, Z. Chen, M. Marquis, K.B. Averyt, M. Tignor, & H.L. Miller, Eds. Cambridge, UK, and New York, NY: Cambridge University Press, USA. 665-744.

Heim, R.R. 2002. A review of twentieth-century drought indices used in the United States. *Bulletin of the American Meteorological Society*. 83(8): 1149-1165. DOI: 10.1175/1520-0477(2002)083<1149:arotdi>2.3.co;2.

Hering, J.G., Maag, S. & Schnoor, J.L. 2016. A call for synthesis of water research to achieve the sustainable goals by 2030. *Environmental Science and Technology*. 50(12): 6122-6123. DOI: 10.1021/acs.est.6b02598.

Hermes, J.C. & Reason, C.J. 2005. Ocean model diagnosis of interannual coevolving SST variability in the South Indian and South Atlantic Oceans. *Journal of Climate*. 18(15): 2864-2882. DOI: 10.1175/JCLI3422.1.

Herring, S. C., Hoell, A., Hoerling, M.P., Kossin, J.P., Schreck III, C.J. & Stott, P.A. 2016. Explaining extreme events of 2015 from a climate perspective. *Bulletin of the American Meteorological Society*. 97(12): S1-S145. DOI: 10.1175/bams-explainingextremeevents2015.1.

Herring, S.C., Hoerling, M.P., Kossin, J.P., Peterson, T.C. & Stott, P.A. 2015. Explaining extreme events of 2014 from a climate perspective. *Bulletin of the American Meteorological Society*. 96(12): S1-S4. DOI: 10.1175/bams-d-15-00157.1.

Hesse, C., Krysanova, V., Pazolt, J. & Hattermann, F.F. 2008. Eco-hydrological modelling in a highly regulated lowland catchment to find measures for improving water quality. *Ecological Modelling*. 218(1-2): 135-148. DOI: 10.1016/j.ecolmodel.2008.06.035.

Hewitson, B. & Crane, R. 1996. Climate downscaling: techniques and application. *Climate Research*. 7(2): 85-95. DOI: 10.3354/cr007085.

Hewitson, B.C. & Crane, R.G. 2005. Gridded area-averaged daily precipitation via conditional interpolation. *Journal of Climate*. 18(1): 41-57. DOI: 10.1175/JCLI3246.1.

Hirabayashi, Y., Kanae, S., Emori, S., Oki, T. & Kimoto, M. 2008. Global projections of changing risks of floods and droughts in a changing climate. *Hydrological Sciences Journal*. 53(4): 754-772. DOI: 10.1623/hysj.53.4.754.

Hoerling, M., Kumar, A., Dole R, Nielsen-Gammon, J.W., Eischeid, J., Perlwitz, J., Quan, X-W., Zhang, T. et al. 2013. Anatomy of an extreme event. *Journal of Climate*. 26: 2811-2832. DOI: 10.1175/JCLI-D-12-00270.1.

Hoffman, M.T., Cramer, M.D. Gillson, L. & Wallace, M. 2011. Pan evaporation and wind run decline in the Cape Floristic Region of South Africa (1974 – 2005): implications for vegetation responses to climate change. *Climatic Change*. 109(3-4): 437-452. DOI: 10.1007/s10584-011-0030-z.

Holloway, A. 2000. Drought emergency, yes...drought disaster, no: Southern Africa 1991–93. *Cambridge Review of International Affairs*. 14(1): 254-276. DOI: 10.1080/09557570008400341.

Holloway, A., Fortune, G., Zweig, P., Barret, I., Benjamin, A., Chasi, V., & de Waal, J. 2012. Eden & Central Karoo drought disaster 2009-2011 "the scramble for water". Stellenbosch University: Disaster Mitigation for Sustainable Livelihoods Programme.

Hughes, D. A., Kingston, D. G. & Todd, M. C. 2011. Uncertainty in water resources availability in the Okavango River Basin as a result of climate change. *Hydrology and Earth System Science*. 15(3): 931-941. DOI: 10.5194/hess-15-931-2011.

Hughes, D.A. & Metzler, W. 1998. Assessment of three-monthly rainfall-runoff models for estimating the water resource yield of semi-arid catchments in Namibia. *Hydrological Sciences Journal*. 43(2): 283-297. DOI: 10.1080/02626669809492122.

Hughes, D.A. 1995. Monthly rainfall-runoff models applied to arid and semiarid catchments for water resource estimation purposes. *Hydrological Sciences Journal*. 40(6): 751-769. DOI: 10.1080/02626669509491463.

Hughes, D.A. 1997. Southern African FRIEND – The application of rainfall-runoff models in the SADC region. (WRC Report No. 235/1/97). Pretoria, South Africa: Water Research Commission

Hughes, D.A. 2006. Comparison of satellite rainfall data with observations from gauging station networks. *Journal of Hydrology*. 327(3-4): 399-410. DOI: 10.1016/j.jhydrol.2005.11.041.

Hughes, D.A. 2013. A review of 40 years of hydrological science and practice in southern Africa using the Pitman rainfall-runoff model. *Journal of Hydrology*. 501: 111-124. DOI: 10.1016/j.jhydrol.2013.07.043.

Hughes, D.A., Mantel, S. & Mohobane, T. 2014. An assessment of the skill of downscaled GCM outputs in simulation historical patterns of rainfall variability in South Africa. *Hydrology Research*. 45(1): 134-147. DOI: 10.2166/nh.2013.027.

Hughes, D.A., Mantel, S. & Mohobane, T. 2014. An assessment of the skill of downscaled GCM outputs in simulating historical patterns of rainfall variability. *Hydrology Research*. 45(1): 134-147. DOI: 10.2166/nh.2013.027.

Hulme, M., Doherty, R., Ngara, T., New, M. & Lister, D. 2001. African climate change: 1900–2100. *Climate Research*. 17(2): 145-168. DOI: 10.3354/cr017145.

Intergovernmental Panel on Climate Change (IPCC). 2007. Climate change 2007: The Physical science basis. (Contribution of Working Group I to the Fourth Assessment Report of the Intergovernmental Panel on Climate Change). S. Solomon, D. Qin, M. Manning, Z. Chen, M. Marquis, K.B. Averyt, M. Tignor, & H.L. Miller, Eds. Cambridge, UK, and New York, NY: Cambridge University Press, USA.

Intergovernmental Panel on Climate Change (IPCC). 2012. Managing the risks of extreme events and disasters to advance climate change adaptation. (A Special Report of Working Groups I and II of the Intergovernmental Panel on Climate Change). C.B. Field, V. Barros, T.F. Stocker, D. Qin, D.J. Dokken, K.L. Ebi, M.D. Mastrandrea, K.J. Mach, G.-K. Plattner, S.K. Allen, M. Tignor, and P.M. Midgley, Eds. Cambridge, UK, and New York, NY: Cambridge University Press, USA.

Intergovernmental Panel on Climate Change (IPCC). 2013. Climate Change 2013: The Physical science basis. (Contribution of Working Group I to the Fifth Assessment Report of the Intergovernmental Panel on Climate Change). T.F. Stocker, D. Qin, G.-K. Plattner, M. Tignor, S.K. Allen, J. Boschung, A. Nauels, Y. Xia, V. Bex and P.M. Midgley, Eds. Cambridge, UK, and New York, NY: Cambridge University Press, USA.

IPCC, 2014: Climate Change 2014: Synthesis Report. Contribution of Working Groups I, II and III to the Fifth Assessment Report of the Intergovernmental Panel on Climate Change. R.K. Pachauri and L.A. Meyer, Eds. Geneva, Switzerland: IPCC.

Jacob, D. & van den Hurk, B. 2009. Climate Change Scenarios at the Global and Local scales. In Climate change adaptation in the water sector. F. Ludwig, P. Kabat, van Schaik. H & M. van der Valk. Eds. Earthscan UK and USA. 23-33.

Jewitt, G.P. & Görgens, A.H. 2000. Scale and model interfaces in the context of integrated water resources management for rivers of the Kruger National Park (WRC Report 627/1/00). Pretoria, South Africa: Water Research Commission.

Jiang, T., Chen, Y.Q., Xu, C.Y., Chen, X.H., Chen, X. & Singh, V.P. 2007. Comparison of hydrological impacts of climate change simulated by six hydrological models in the Dongjiang Basin, South China. *Journal of Hydrology*. 336(3-4): 316-333. DOI: 10.1016/j.jhydrol.2007.01.010.

Jiménez Cisneros, B.E., Oki, T., Arnell, N.W., Benito, G., Cogley, J.G., Döll, P., Jiang T. & Mwakalila, S.S. 2014. Freshwater resources. In Climate Change 2014: Impacts, adaptation, and vulnerability. Part A: Global and sectoral aspects. (Contribution of Working Group II to the Fifth Assessment Report of the Intergovernmental Panel on Climate Change). C.B. Field, V.R. Barros, D.J. Dokken, K.J. Mach, M.D. Mastrandrea, T.E. Bilir, M. Chatterjee, K.L. Ebi, Y.O. Estrada, R.C. Genova, B. Girma, E.S. Kissel, A.N. Levy, S. MacCracken, P.R. Mastrandrea, and L.L.White, Eds. Cambridge, UK, and New York, NY: Cambridge University Press, USA. 229-269.

Jones, G.S., Stott, P.A. & Christidis, N. 2013. Attribution of observed historical near–surface temperature variations to anthropogenic and natural causes using CMIP5 simulations. *Journal of Geophysical Research Atmospheres.*118(10): 4001-4024. DOI: 10.1002/jgrd.50239.

Jury, M. R. 2018. Climate trends across South Africa since 1980. *Water SA*. 44(2): 297-307. DOI: 10.4314/wsa.v44i2.15.

Jury, M.R. & Mwafulirwa, N.D. 2002. Climate variability in Malawi, part 1: dry summers, statistical associations and predictability*. International Journal of Climatology*. 22(11): 1289-1302. DOI:10.1002/joc.771..

Jury, M.R. 2019. South Africa's Future Climate: Trends and Projections. In The Geography of South Africa, World Regional Geography Book Series. J. Knight, C. M. Rogerson, Eds. Springer. DOI: 10.1007/978-3-319-94974-1_33.

Kane, R.P. 2009. Periodicities, ENSO effects and trends of some South African rainfall series – an update. *South African Journal of Science*. 105(5-6): 199-207. DOI: 10.4102/sajs.v105i5/6.90.

Kapangaziwiri, E. 2010. Regional application of the pitman monthly rainfall-runoff model in southern Africa incorporating uncertainty. PhD Thesis. Rhodes University

Kay, A. L., &. Davies, H.N. 2008. Calculating potential evaporation from climate model data: A source of uncertainty for hydrological climate change impacts. *Journal of Hydrology*. 358(3-4): 221-239. DOI: 10.1016/j. jhydrol.2008.06.005.

King, A. D., van Oldenborgh, G.J., Karoly, D., Lewis, S.C. & Cullen, H. 2015. Attribution of the record high Central England temperature of 2014 to anthropogenic influences. *Environmental Research Letters.* 10(5): 054002. DOI: 10.1088/1748-9326/10/5/054002.

King, A.D., Lewis, S.C., Perkins, S.E., Alexander, L.V., Donat, M.G., Karoly, D.J. & Black, M.T. 2013. Limited evidence of anthropogenic influence on 2011–12 extreme rainfall over southeast Australia. In Explaining Extreme Events of 2012 from a Climate Perspective. *Bulletin of the American Meteorological Society*. 94(9): S55-S58. DOI: 10.1175/BAMS-D-13-00085.1.

Knutson, T. R., Zeng, F. & Wittenberg, A.T. 2013. Multimodel assessment of regional surface temperature trends: CMIP3 and CMIP5 twentieth-century simulations. *Journal of Climate*. 26(22) 8709-8743. DOI:10.1175/JCLI-D-12-00567.1.

Knutson, T., J.P. Kossin, C. Mears, J. Perlwitz. & M.F. Wehner, 2017: Detection and attribution of climate change. In: Climate Science Special Report: Fourth National Climate Assessment, Volume I. D. Wuebbels, D. Fahey, K. Hibbard, D. Dokken, B. Stewart & T. Maycock, Eds. Washington, DC: U.S. Global Change Research Program. 114-132 DOI: 10.7930/J01834ND.

Kogan, F.N. 1997. Global drought watch from space. *Bulletin American Meteorological Society*. 78(4): 621-636. DOI: 10.1175/1520-0477(1997)078<0621:gdwfs>2.0.co;2.

Kruger, A.C. & Sekele, S.S. 2013. Trends in extreme temperature indices in South Africa: 1962–2009. *International Journal of Climatology*. 33(3): 661-676. DOI: 10.1002/joc.3455.

Kruger, A.C. & Shongwe, S. 2004. Temperature trends in South Africa: 1960-2003. *International Journal of Climatology*. 24(15): 1929-1945. DOI: 10.1002/joc.1096.

Kruger, A.C. 2006. Observed trends in daily precipitation indices in South Africa: 1910–2004. *International Journal of Climatology*. 26(15): 2275-2285. DOI: 10.1002/joc.1368.

Krysanova, V., Kundzewicz, Z. W. & Piniewski, M. 2016. Assessment of climate change impacts on water resources: Handbook of applied hydrology 2nd edition. V. P. Singh, Ed. New York: McGraw-Hill.

Kundzewicz, Z. W., Krysanova, V., Benestad, R. E., Hov, O., Piniewski, M., & Otto, I. M. 2018. Uncertainty in climate change impacts on water resources. *Environmental Science Policy*. 79: 1-8. DOI: 10.1016/j.envsci.2017.10.008.

Kusangaya, S., Warburton, M.L., van Garderen, E.A. & Jewitt, G.W. 2013. Impacts of climate change on water resources in southern Africa: A review. *Physics and Chemistry of the Earth*. 67-69: 47-54. DOI: 10.1016/j.pce.2013.09.014.

Leung, L. R., Quin, Y., Bian, X. M., Washington, W. M., Han, J. & Roads, J. O. 2004. Mid-century ensembles regional climate change scenarios for the western United States. *Climatic Change*. 62(1-3): 75-113. DOI: 10.1023/b:clim.0000013692.50640.55.

Lewis, S.C. & Karoly, D.J. 2013. Anthropogenic contributions to Australia's record summer temperatures of 2013. *Geophysical Research Letters*. 40(14): 3705-3709. DOI: 10.1002/grl.50673.

Lindesay, J., 1998. Present climates of Southern Africa. In Climates of the Southern Continents: Past, present and future. J.E. Hobbs, J.A. Lindesay. & H.A. Bridgman, Eds. Chichester: John Wiley & Sons. 297-345.

Liu, C. & Allan, R.P. 2013. Observed and simulated precipitation responses in wet and dry regions 1850–2100. *Environmental Research Letters*. 8(3):034002. DOI: 10.1088/1748-9326/8/3/034002.

Lott, F.C., Christidis, N. & Stott, P. A. 2013. Can the 2011 East African drought be attributed to human-induced climate change?. *Geophysical Research Letters*. 40(6): 1177-1181. DOI: 10.1002/grl.50235.

Lynch, S.D. 2004. Development of a raster database of annual, monthly and daily rainfall for southern Africa. (WRC Report 1156/1/04). Pretoria, South Africa: Water Research Commission.

Lyon, B. & Mason, S.J. 2007. The 1997–98 summer rainfall season in Southern Africa. Part I: observations. *Journal of Climate.* 20(20): 5134-5148. DOI: 10.1175/JCLI4225.1.

MacKellar, N., New, M. & Jack, C. 2014. Observed and modelled trends in rainfall and temperature for South Africa: 1960–2010. *South African Journal of Science*. 110(7-8):1-13. DOI: 10.1590/ sajs.2014/20130353.

Mahlalela, P.T., Blamey, R.C. & Reason, C.J. 2018. Mechanisms behind early winter rainfall variability in the southwestern Cape, South Africa. *Climate Dynamics*. 53(1-2): 21-39. DOI: 10.1007/s00382-018-4571-y.

Mantel, S.K., Hughes, D.A. & Slaughter, A.S. 2015. Water resources management in the context of future climate and development changes: A South African case study. *Journal of Water and Climate Change*. 6(4): 772-786. DOI: 10.2166/wcc.2015.098.

Marshall, G.J. 2003. Trends in the southern annular mode from observations and reanalyses. *Journal of Climate.* 16(24): 4134-4143. DOI: 10.1175/1520-0442(2003)016%3C4134:TITSAM%3E2.0.CO;2.

Masih, I., Maskey, S., Mussá, F. & Trambauer, P. 2014. A review of droughts on the African continent: a geospatial and long-term perspective. *Hydrology and Earth System Sciences*. 18(9): 3635-3649. DOI: 10.5194/hess-18-3635-2014.

Mason, S. J. & Jury, M. 1997. Climatic variability and change over Southern Africa: a reflection on underlying processes. *Progress in Physical Geography.* 21(2): 23-50. DOI: 10.1023/A:1023630924100.

Mason, S.J., Waylen, P.R., Mimmack, G.M., Rajaratnam, B. & Harrison, J.M. 1999. Changes in extreme rainfall events in South Africa. *Climatic Change*. 41(2): 249-257. DOI: 10.1023/A:1005450924499.

Matondo, J.I. 2012. *Proceedings of the World environmental and water resources congress 2012: crossing boundaries*. 20-24 May 2012. 20-24 May 2012. Albuquerque, New Mexico United States of America: American Society of Civil Engineers.

Mavromatis, T. 2012. Changes in exceptional hydrological and meteorological weekly event frequencies in Greece. *Climatic Change*. 110(1): 249-267. DOI: 10.1007/s10584- 011-0095-8.

Mazvimavi, D., Meijerink, A.M., Savenije, H.H. & Stein, A. 2005. Prediction of flow characteristics using multiple regression and neural networks: a case study in Zimbabwe. *Physics and Chemistry of the Earth*. 30(11): 639-647. DOI: 10.1016/j.pce.2005.08.003.

McKee, T.B., Doesken, N.J. & Kleist, J. 1993. The relationship of drought frequency and duration to time scales. *Proceedings of the 8th Conference on Applied Climatology*. 17-22 January 1993. California: American Meteorological Society.

Meadows, M. 2006. Global change and Southern Africa. *Geographical Research*. 44(2): 135-145. DOI: 10.1111/j.1745-5871.2006.00375.x.

Meehl, G.A., Tebaldi, C., Walton, G., Easterling, D. & McDaniel, L. 2009. Relative increase of record high maximum temperatures compared to record low minimum temperatures in the US. *Geophysical Research Letters*. 36(23): L23701. DOI: 10.1029/2009gl040736.

Meque, A. & Abiodun, B.J. 2015. Simulating the link between ENSO and summer drought in Southern Africa using regional climate models. *Climate Dynamics*. 44(7-8): 1881-1900. DOI: 10.1007/s00382-014-2143-3.

Midgley, D.C., Pitman, W.V. & Middleton, B.J. 1994. Surface water resources of South Africa 1990. Volumes I to VI. (WRC Report No's 298/1.1/94 to 298/1.6/94). Pretoria, South Africa: Water Research Commission.

Midgley, G.F., Chapman, R.A., Hewitson, B., Johnston, P., de Wit, M., Ziervogel, G., Mukheibir, P., van Niekerk, L. et al. 2005. A Status Quo, vulnerability and adaptation assessment of the physical and socio-economic effects of climate change in the Western Cape. (CSIR Report No. ENV-S-C 2005-073). Stellenbosch, South Africa: Western Cape Government.

Midgley, S. & Methner, N. 2016. Climate adaptation readiness for agriculture: Drought lessons from the Western Cape, South Africa. (African Institute of International Affairs Policy Briefing 154). Johannesburg: South African Institute of International Affairs.

Midgley, S., New, M., Spelman, SS. & Parker, K. 2014. The Food-Energy-Water-Land-Biodiversity (FEWLB) Nexus and Local Economic Development in the BRC: Framework and Description. African Climate and Development Initiative, University of Cape Town.

Min, S-K., Zhang, X. & Zwiers, F. 2008. Human-induced Arctic moistening. *Science*. 320(5875): 518-520. DOI: 10.1126/science.1153468.

Mishra, A., Singh, V. & Desai, V. 2009. Drought characterization: a probabilistic approach. *Stochastic Environmental Research Risk Assessment*. 23(1): 41-55. DOI: 10.1007/s00477-007-0194-2.

Mniki, S. 2009. Socio-economic Impact of Drought Induced Disasters on Farm Owners of Nkonkobe Local Municipality. Masters Thesis. University of the Free State.

Moriasi, D.N., Arnold, J.G., van Liew, M.W., Bingner, R.L., Harmel, R.D. & Veith, T.L. 2007. Model evaluation guidelines for systematic quantification of accuracy in watershed simulations. *Transactions of the ASABE*. 50(3): 885-900. DOI: 10.13031/2013.23153.

Mulenga, H.M., Rouault, M. & Reason, C.J. Reason. 2003. Dry summers over north-eastern South Africa and associated circulation anomalies. *Climate Research*. 25(1): 29-41. DOI: 10.3354/cr025029.

Murthy, C.S., Sesha Sai, M.V.R., Naresh Kumar, M. & Roy, P.S. 2009. Temporal divergence in cropping pattern and its implications on geospatial drought assessment. *Geocarto International*. 24(5): 377-395. DOI: 10.1080/10106040802601037.

Nash, J. E. & Sutcliffe, J.V. 1970. River flow forecasting through conceptual models: Part 1- A discussion of principles. *Journal of Hydrology*. 10(3): 282-290. DOI: 10.1016/0022-1694(70)90255-6

National Academies of Sciences, Engineering, and Medicine (NSM). 2016. Attribution of Extreme Weather Events in the Context of Climate Change. Washington, DC: The National Academies Press. DOI: 10.17226/21852.

National Drought Mitigation Centre (NDMC). 2006. Monitoring drought. The Standardized Precipitation Index. Interpretation of SPI Maps. National Climatic Data Centre.

National Oceanic and Atmospheric Administration (NOAA). 2008. Drought: Public fact sheet. National Weather Service.

National Oceanic and Atmospheric Administration (NOAA). 2012. Climate model. Top Ten: Breakthroughs. Available: https://celebrating200years.noaa.gov/breakthroughs/climate_model/welcome.html [2017, July 18].

National Oceanic and Atmospheric Administration (NOAA). 2017. Global analysis - annual 2016. Available: https://www.ncdc.noaa.gov/sotc/global/201613 [2017, September 10].

National Water Act (NWA). Act No. 36 of 1998. 1998. Government Gazette 398 (19182). 26 August. Governemnt no. 19182 . Cape Town, South Africa: Office of the President.

Ndiritu, J. 2009. A comparison of automatic and manual calibration using the Pitman model. Physics and Chemistry of the Earth. 34: 729-740. DOI: 10.1016/j.pce.2009.06.002.

Nel, W. 2009. Rainfall trends in the KwaZulu-Natal Drakensberg region of South Africa during the twentieth century. *International Journal of Climatology*. 29(11): 1634-1641. DOI: 10.1002/joc.1814.

New, M. n.d. Joint Attribution of Biophysical and Economic Impacts of Hydro-climatic Extremes. A grant request from the University of Oxford. Unpublished.

New, M., Hewitson, B., Stephenson, D.B., Tsiga, A., Kruger, A., Manhique, A., Gomez, B., Coelho, C.A.S. et al. 2006. Evidence of trends in daily climate extremes over southern and west Africa. *Journal of Geophysical Research.* 111(D14). DOI: 10.1029/2005JD006289.

New, M., Lister, D., Hulme, M. & Makin, I. 2002. A high-resolution data set of surface climate over global land areas. *Climate Research*. 21: 1-25. DOI: 10.3354/cr021001.

Niang, I., Ruppel, O.C., Abdrabo, M.A., Essel, A., Lennard, C., Padgham, J. & Urquhart, P. 2014: Africa. In Climate Change 2014: Impacts, Adaptation, and Vulnerability. Part B: Regional Aspects. (Contribution of Working Group II to the Fifth Assessment Report of the Intergovernmental Panel on Climate Change). C.B. Field, V.R. Barros, D.J. Dokken, K.J. Mach, M.D. Mastrandrea, T.E. Bilir, M. Chatterjee, K.L. Ebi, Y.O. Estrada, R.C. Genova, B. Girma, E.S. Kissel, A.N. Levy, S. MacCracken, P.R. Mastrandrea, and L.L. White, Eds. Cambridge, United Kingdom and New York, NY, USA: Cambridge University Press, USA. 979-1037.

Nicholson, S. E. & Kim, J. 1997. The relationship of the El Niño–southern oscillation to African rainfall. *International Journal of Climatology*.17(2), 117-135. DOI: 10.1002/(SICI)1097-0088(199702)17:2<117::AID-JOC84>3.0.CO;2-O.

Nicholson, S.E. 2000. The nature of rainfall variability over Africa on time scales of decades to millennia. *Global and Planetary Change*. 26(1): 137-158. DOI: 10.1016/s0921-8181(00)00040-0.

Nicholson, S.E., Kim, J. & Hoopingarner. J. 1988. Atlas of African rainfall and its inter-annual variability. Tallahassee, Florida: Department of Meteorology, Florida State University.

Niemeyer, S. 2008. New drought indices. In Drought management: scientific and technological advances. A. Lopez-Francois, Ed. International Centre for Advanced Mediterranean Agronomic Studies. 267-274.

Organisation for Economic Co-operation and Development (OECD). 2012. Environmental Outlook to 2050: The Consequences of Inaction. Paris: OECD Publishing. DOI: 10.1787/9789264122246-en.

Otto, F., James, R. & Allen, A. 2014. The science of attributing extreme weather events and its potential contribution to assessing loss and damage associated with climate change impacts. Oxford: Environmental Change Institute, University of Oxford.

Otto, F., Massey, N., van Oldenborgh, G.J., Jones, R.G. & Allen, M.R. 2012. Reconciling two approaches to attribution of the 2010 Russian heat wave. *Geophysical Research Letters*. 39(4): 1-5. DOI: 10.1029/2011GL050422.

Otto, F.E., Jones, R.G., Halladay, K. & Allen, M.R. 2013. Attribution of changes in precipitation patterns in African rainforests. *Philosophical Transactions of the Royal Society B*. 368(1625): 20120299. DOI: 10.1098/rstb.2012.0299.

Otto, F.E., Philip, S., Kew, S., Li, Sahn., King, A. & Cullen, H. Attributing high-impact extreme events across timescales—a case study of four different types of events. 2018. *Climatic Change*. 149: 399-412. DOI: 10.1007/s10584-018-2258-3.

Otto, F.E.L., Boyd, E., Jones, R.G., Cornforth, R.J., James, R., Parker, H.R. & Allen, M.R. 2015. Attribution of extreme weather events in Africa: A preliminary exploration of the science and policy implications. *Climatic Change*. 132(4): 531-534. DOI: 10.1007/s10584-015-1432-0.

Otto, F.E.L., Wolski, P., Lehner, F., Tebaldi, C., van Oldenborgh, G.J., Hogesteeger, S., Singh, R. & Holden, P. et al. 2018. The role of climate change in the 2015-2017 drought in the Western Cape of South Africa. *Environmental Research Letters*. 13(12): 124010. DOI: 10.1088/1748-9326/aae9f9.

Pall, P., Aina, T., Stone D.A., Stott, P.A., Nozwa, T., Hilberts, A.G., Lohmann, D. & Allen, M.R. 2011. Anthropogenic greenhouse gas contribution to flood risk in England and Wales in autumn 2000. *Nature*. 470(7334): 382-385. DOI: 10.1038/nature09762.

Palmer, W.C. 1965. Meteorological drought. (Weather Bureau Research Paper No. 450). Washington DC: US Department of Commerce.

Pappenberger, F. & Beven, K. 2006. Ignorance is bliss: or seven reasons not to use uncertainty analysis. *Water Resources Research*. 42(5): W05302. DOI: 10.1029/2005WR004820.

Pearce, F. 2016. El Niño and climate change: Wild weather may get wilder. Available: http://e360.yale.edu/feature/el_nino_and_climate_change_wild_weather_may_get_wilder/2960/. [2017, February 07].

Perkins, S.E, Pitman, A., Holbrook, A.J. & McAneney, J. 2007. Evaluation of the AR4 climate models' simulated daily maximum temperature, minimum temperature and precipitation over Australia using probability density functions. *Journal of Climate*. 20(17): 4356-4376. DOI: 10.1175/JCLI4253.1.

Perkins, S.E., Lewis, S.C., King, A.D. & Alexander, L.V. 2014. Increased simulated risk of the hot Australian summer of 2012/13 due to anthropogenic activity as measured by heat wave frequency and intensity. In Explaining Extreme Events of 2013 from a Climate Perspective. *Bulletin of American Meteorological Society*. 95(9): S34-S37. DOI: 10.1175/bams-d-15-00074.1.

Perks, L. A. & Schulze, R. E. 1999. Modelling the potential impacts of climate change on water resources in southern Africa. in: *Proceedings of the 9th South African National Hydrology Symposium. 29-30th November*. Cape Town, South Africa.

Peterson, T.C., Hoerling, M.P., Stott, P.A. & Herring, S. 2013. Explaining extreme events of 2012 from a climate perspective. *Bulletin of the American Meteorological Society*. 94(9): S1-S74. DOI: 10.1175/bams-d-13-00085.1.

Pharoah, R. Holloway, A., Fortune, G., Chapman, A., Schaber, E., and Zweig, P.2016. Severe weather events 2011-2014 and their impacts in the Western Cape Province, South Africa. (OFF the RADAR: Summary Report). Stellenbosch, South Africa: Research Alliance for Disaster and Risk Reduction, Department of Geography and Environmental Studies, Stellenbosch University.

Phillippon, N., Rouault, M., Richard, Y. & Favre, A. 2012. The influence of ENSO on winter rainfall in South Africa. *International Journal of Climatology*. 32(15) 2333-2347. DOI: 10.1002/joc.3403.

Pitman, W.V., Potgeiter, D.J., Middleton, B.J. & Midgley, D.C. 1981. Surface Water Resources of South Africa – Volume IV: Drainage Regions EGHJKL, The Western Cape. (HRUReport No. 13/81). University of the Witwatersand, Johannesburg, South Africa: Hydrological Research Unit.

Pretorius, C. & Smal, M. 1992. Notes on the macro-economic effects of the drought: Quarterly Bulletin. Pretoria: South African Reserve Bank.

Rahmstorf, S. & Coumou, D. 2011. Increase of extreme events in a warming World. *Proceedings of the National Academy of Sciences*. 108(44): 17905-17909. DOI: 10.1073/pnas.1101766108.

Ratnam, J.V., Behera, S.K., Masumoto, Y. & Yamagata, T. 2014. Remote effects of El Niño and Modoki events on the austral summer precipitation of Southern Africa. *Journal of Climate*. 27(10): 3802-3815. DOI: 10.1175/JCLI-D-13-00431.1.

Reason C, J., Allan R.J., Lindesay J, A. & Ansell, T.J. 2000. Enso and climatic signals across the Indian Ocean Basin in the global context: Part I, interannual composite patterns. *International Journal of Climatology*. 20(11): 1285-1327. DOI: 10.1002/1097-0088(200009)20:11<1285::aid-joc536>3.0.co;2-r.

Reason, C.J, Rouault, M., Melice, J-L. & Jagadheesha, D. 2002. Interannual winter rainfall variability in SW South Africa and large scale ocean-atmosphere interactions. *Meteorology Atmospheric Physics*. 80(1): 19-29. DOI: 10.1007/s007030200011.

Reason, C.J. & Jagadheesha, D. 2005. Relationships between South Atlantic SST variability and atmospheric circulation over the South African region during austral winter. *Journal of Climate*. 18(16): 3339-3355. DOI: 10.1175/JCLI3474.1.

Reason, C.J. & Rouault, M. 2005. Links between the Antarctic Oscillation and winter rainfall over western South Africa. *Geophysical Research Letters*. 320(7): 1-4. DOI: 10.1029/2005GL022419.

Reason, C.J. 2001. Subtropical Indian Ocean SST dipole events and southern African rainfall. *Geophysical Research Letters*. 28(11): 2225-2227. DOI: 10.1029/2000GL012735.

Reichler, T. & Kim, J. 2008. How well do coupled models simulate today's climate?. *Bulletin of American Meteorological Society*. 89(3): 303-312. DOI: 10.1175/BAMS-89-3-303.

Richard, Y., Fauchereau, N., Poccard, I., Rouault, M. & Trzaska, S. 2001. 20th Century droughts in southern Africa: spatial and temporal variability, teleconnections with oceanic and atmospheric conditions. *International Journal of Climatology*. 21(7): 873-885. DOI: 10.1002/joc.656.

Rind, D., Goldberg, R., Hansen, J., Rosenzweig, C. & Ruedy, R. 1990. Potential evapotranspiration and the likelihood of future drought. *Journal of Geophysical Research*. 95(D7): 9983-10004. DOI: 10.1029/jd095id07p09983.

Rouault, M. & Y. Richard. 2005. Intensity and spatial extent of droughts in southern Africa. *Geophysical Research Letters*. 32(15): L15702. DOI: 10.1029/2005GL022436.

Salas, J. 1993. Analysis and modeling of hydrologic time series. In Handbook of hydrology. New York: McGraw-Hill. 1-72.

Sawunyama, T. & Hughes, D.A. 2007. Assessment of rainfall-runoff model input uncertainties on simulated runoff in southern Africa. *Proceedings of Symposium HS2004 at IUGG2007*. July 2007. Perugia: International Association of Hydrological Science 313: 98-106.

Schulze, R.E. 2003. The Thukela Dialogue: Managing water related issues on climate variability and climate change in South Africa. (ACRUcons Report 44:152). Pietermaritzburg, South Africa: University of Natal, School of Bioresources Engineering and Environmental Hydrology.

Schulze, R.E. 2012. A 2011 Perspective on Climate Change and the South African Water Sector. (WRC Report TT 518/12). Pretoria, South Africa: Water Research Commission.

Seager, R., Ting, M., Held, I., Kushnir, Y., Lu, J., Vecchi, G., Huang, H.P., Harnik, N. et al. 2007. Model projections of an imminent transition to a more arid climate in southwestern North America. *Science*. 316(5828): 1181-1184. DOI: 10.1126/science.1139601.

Segui, P., Ribes, A., Martin, E., Habets, F. & Boé, J. 2010. Comparison of three downscaling methods in simulating the impact of climate change on the hydrology of Mediterranean basins. *Journal of Hydrology*. 383(1-2): 111-124. DOI: 10.1016/j.jhydrol.2009.09.050.

Seneviratne, S. I., Donat, M. G., Pitman A. J., Knutti, R. & Wilby, R.L. 2016. Allowable CO2 emissions based on regional and impact-related climate targets*. Nature.* 529(7587): 477-483. DOI: 10.1038/nature16542.

Seneviratne, S.I., Corti, T., Davin, E.L., Hirschi, M., Jaeger, E.B., Lehner, I., Orlowsky, B. & Teuling, A.J. 2010. Investigating soil moisture–climate interactions in a changing climate: a review*. Earth-Science Reviews*. 99(3-4): 125-161. DOI: 10.1016/j.earscirev.2010.02.004.

Seneviratne, S.I., Nicholls, N., Easterling, D., Goodess, C.M., Kanae, S., Kossin, J., Luo, Y., Marengo, J. et al. 2012 Changes in climate extremes and their impacts on the natural physical environment. In: Managing the Risks of Extreme Events and Disasters to Advance Climate Change Adaptation. (A Special Report of Working Groups I and II of the Intergovernmental Panel on Climate Change). C.B. Field, V. Barros, T.F. Stocker, D. Qin, D.J. Dokken, K.L. Ebi, M.D. Mastrandrea, K.J. Mach, G.-K. Plattner, S.K. Allen, M. Tignor, & P.M. Midgley, Eds. Cambridge, United Kingdom and New York, NY, USA: Cambridge University Press, USA. 109-230.

Sheffield, J. & Wood, E. F. 2008. Projected changes in drought occurrence under future global warming from multi-model, multi-scenario, IPCC AR4 simulations. *Climate Dynamics*. 31(1): 79-105. DOI: 10.1007/s00382-007-0340-z.

Sheffield, J., Wood, E. F. & Roderick, M. 2012. Little change in global drought over the past 60 years. *Nature*. 491(7424): 435-438. DOI: 10.1038/nature11575.

Sheperd, T.G. 2016. A common framework for approaches to extreme event attribution. *Current Climate Change Reports*. 2(1): 28-38. DOI: 10.1007/s40641-016-0033-y.

Shongwe, M.E., Van Oldnborgh, G.J., Van den Hurk, B.J.J., De Boer, B., Coelho, C.A. & Van Aalst. M.K. 2009. Projected changes in mean and extreme precipitation in Africa under global warming. Part I: Southern Africa. *Journal of Climate*. 22(13): 3819-3837. DOI: 10.1175/2009JCLI2317.1.

Shukla, S., Steinemann A. C., & Lettenmaier, D. P. 2011. Drought monitoring for Washington State: Indicators and applications. *Journal of Hydrometeorology*. 12(1): 66-83. DOI: 10.1175/2010JHM1307.1.

Sinclair-Smith, K. & Winter, K. 2019. Water demand and management in Cape Town: managing water security in a changing climate. In Mainstreaming climate change in urban development. D, Scott. H, Davies. & M. New, Eds. Cape Town: UCT Press. 100-133.

Singleton, A. T. & Reason, C.J. 2007. Variability in the characteristics of cut-off low pressure systems over subtropical southern Africa. *International Journal of Climatology*. 27(3): 295-310. DOI: 10.1002/joc.1399.

Smith, R.L. 1989. Extreme value analysis of environmental time series: an application to trend detection in ground-level ozone. *Statistical Science*. 4(4): 367-93. DOI: 10.1214/ss/1177012400.

Sousa, P.M., Blamey, R.C., Reason. C.J., Ramos, A.M. & Trigo, R.M. 2018. The 'Day Zero' Cape Town drought and the poleward migration of moisture corridors. *Environmental Research Letters*. 13(12): 124025. DOI: 10.1088/1748-9326/aaebc7.

South African Weather Service (SAWS). 2015a. General information: Maximum temperature record at Vredendal on 27 October 2015. Available: https://www.weathersa.co.za/Documents/Corporate/CLS-CI-GEN-INFO-099.2%20Vredendal%20Max%20Temp%20Record%2027%20Oct%202015.pdf [2017, August 8].

South African Weather Service (SAWS). 2015b. Heat wave conditions over Gauteng, Mpumalanga and western Limpopo. Available: http://www.weathersa.co.za/images/documents/275/Media%20release%206%20October%202015.pdf [2017, August 8].

Southern African Development Community (SADC). 1992. Regional Early Warning Unit: Quarterly Food Security Bulletin. Harare, Zimbabwe: Southern African Development Community Secretariat.

Southern African Development Community (SADC). 2016. Regional Humanitarian Appeal. Gaborone, Botswana: Southern African Development Community Secretariat.

Stainforth, D. A., T. Aina, C. Christensen, M. Collins, N. Faull, D. J. Frame, J. A. Kettleborough, S. & Knight, A. 2005. Uncertainty in predictions of the climate response to rising levels of greenhouse gases. *Nature*. 433(7024): 403-406. DOI: 10.1038/nature03301.

Statistical and Regional dynamical Downscaling of Extremes for European Regions (STARDEX). 2005. Downscaling climate extremes. Norwich, UK: Climate Research Unit, University of East Anglia.

Steinemann, A.C. & Cavalcanti, L. 2006. Developing multiple drought indicators and triggers for drought plans. *Journal of Water Resources Planning and Management*. 132(3): 164-174. DOI: 10.1061/(asce)0733-9496(2006)132:3(164).

Steyn M., Meissner R., Nortje K., Funke N. & Petersen C. 2019. Water Security and South Africa. In Understanding Water Security at Local Government Level in South Africa. R. Meissner, N. Funke, K. Nortje & M. Steyn, Eds. Basingstoke: Palgrave Pivot.

Stone, D. A. and M. R. Allen. 2005. The End-to-End Attribution Problem: From Emissions to Impacts. Climatic Change 71(3): 303-318. DOI: http://dx.doi.org/10.1007/s10584-005- 6778-2.

Stone, D., Auffhammer, M., Carey, M., Hansen, G., Huggel, C., Cramer, W., Lobell, D., Molau, U. et al. 2013. The challenge to detect and attribute effects of climate change on human and natural systems. *Climatic Change*. 121(2). 381-395. DOI: 10.1007/s10584-013-0873-6.

Stott, P.A., Christidis, N., Otto, F.E.L., Sun, Y., Vanderlinden, J.P., van Oldenborgh, G.J., Vautard, R., von Storch, H. 2016. Attribution of extreme weather and climate-related events. *Wiley Interdisciplinary Reviews: Climatic Change*. 7(1): 23-41. DOI: 10.1002/wcc.380.

Stott, P.A., Stone, D.A. & Allen, M.R. 2004. Human contribution to the European heatwave of 2003. *Nature*. 432(7017): 610-614. DOI: 10.1029/2001JB001029.

Tadross, M. & Johnston, P. 2012. Climate Change Projections for Cape Town: Adding value through downscaling. Cape Town, South Africa: ICLEI - Local Governments for Sustainability – Africa.

Tallaksen, L.M. & van Lanen, H.A.J. 2004. Hydrological drought: Processes and estimation methods for streamflow and groundwater. Amsterdam: Elsevier.

Tanner, J.L. & Hughes, D.A. 2013. Assessing uncertainties in surface-water and groundwater interaction modelling – a case study from South Africa using the Pitman model. In Assessing and managing groundwater in different environments. J. Cobbing, S. Adams, I. Dennis & K. Riemann, Eds. CRC Press. 121-134. DOI: 10.1201/b15937-10.

Taylor, K., Stouffer, R.J. & Meehl, G.A. 2012. An overview of CMIP5 and the experimental design. *Bulletin of American Meteorological Society*. 93(4): 485-498. DOI: 10.1175/BAMS-D-11-00094.1.

Teutschbein, C., Wetterhall, F. & Seibert, J. 2011. Evaluation of different downscaling techniques for hydrological climate-change impact studies at the catchment scale. *Climate Dynamics*. 37(9-10): 2087-2105. DOI: 10.1007/s00382-010-0979-8.

Theunissen, P. 2004. The economical impact of a drought. Bethlehem: Computus Management Information (PTY) LTD.

Thomas, D.S.G., Twyman, C., Osbahr, H. & Hewitson, B. 2007. Adaptation to climate change and variability: farmer responses to intra-seasonal precipitation trends in South Africa. *Climatic Change*. 83(3): 301-322. DOI: 10.1007/s10584-006-9205-4.

Thomas, H.A. & Fiering, M.B. 1962. Mathematical synthesis of streamflow sequences for the analysis of river basins by simulation. In: Design of Water Resources Systems. A. Mass Ed. Harvard University Press, Cambridge. 459-493.

Thompson, D.W.J. & Wallace, J.M. 2000. Annular modes in the extratropical circulation. Part I: month-to-month variability. *Journal of Climate.* 13(5):1000-1016. DOI: 10.1175/1520-0442(2000)013%3C1010:AMITEC%3E2.0.CO;2.

Thornthwaite, C.W. 1948. An approach toward a rational classification of climate. *Geographical Review*. 38(1): 55-94. DOI: 10.2307/210739.

Tirivarombo, S. 2012. Climate variability and climate change in water resources management of the Zambezi River basin. Ph.D Thesis. Rhodes University.

Trenberth, K.E., Fasullo, J.T. & Sheperd, T.G. 2015. Attribution of climate extreme events. *Nature Climate Change*. 5(8): 725-730. DOI: 10.1038/NCLIMATE2657.

Tsheko, R. 2006. Comparison between the United States Soil Conservation Service (SCS) and the two models commonly used for estimating rainfall-runoff in south-eastern Botswana. *Water SA*. 32(1):29-36. DOI: 10.4314/wsa.v32i1.5236.

Tshimanga, R., Hughes, D.A. & Kapangzawiri, E. 2011. Initial calibration of a semi-distributed rainfall runoff model for the Congo River basin. *Physics and Chemistry of the Earth*. 36(14): 761-774. DOI: 10.1016/j.pce.2011.07.045.

Tumbo, M. & Hughes, D.A. 2015. Uncertain hydrological modelling: application of the Pitman model in the Great Ruaha River basin, Tanzania. *Hydrological Sciences Journal*. 60(11): 2047-2061. DOI: 10.1080/02626667.2015.1016948.

Tyson, P. D. & Preston-Whyte, R. A. 2000. The weather and climate of Southern Africa 2nd edition. Cape Town, South Africa: Oxford University Press.

Tyson, P.D. 1987. Climatic change and variability in Southern Africa. Cape Town, South Africa: Oxford University Press.

Tyson, P.D., Dyer, T.G. & Mametse, M.N. 1975. Secular changes in South African rainfall: 1880 to 1972. *Quarterly Journal of the Royal Meteorological Society*. 101(4300): 817-833. DOI: 10.1002/qj.49710143008.

Unganai, L.S & Kogan, F.N. 1998. Drought monitoring and corn yield estimation in Southern Africa from AVHRR data. *Remote Sensing of Environment*. 63(3): 219-232. DOI: 10.1016/s0034-4257(97)00132-6.

United Nation (UN). 2017. Sustainable development goals: 17 Goals to transform our world. Available: http://www.un.org/sustainabledevelopment/sustainable-development-goals/. [2017, November 21].

United Nations Educational, Scientific and Cultural Organization (UNESCO). 2011. The Impact of Global Change on Water Resources. (The Response of UNESCO'S International Hydrology Programme). Paris, France: International Hydrological Programme.

United Nations Office for the Coordination of Humanitarian Affairs (UNOCHA). 2016. Southern Africa humanitarian outlook 2015/2016. (Special focus on El Niño report). Southern Africa Regional Inter-Agency Standing Committee.

United Nations-Water (UN-W). 2013. Water security and the global water agenda. (Analytical Brief). Ontario, Canada: United Nations University Institute for Water, Environment and Health (UNU-INWEH).

United States Agency International Development (USAID). 2014. A review of downscaling methods for climate change projections: African and Latin American resilience to climate change (ARCC). (Technical Report). Washington DC: Tetra Tech ARD.

University Corporation for Atmospheric Research (UCAR). 2017. Climate data guide. Available: https://climatedataguide.ucar.edu/climate-data/standardized-precipitation-evapotranspiration-index-spei. [2017, October, 12].

Uys, D. 2014. Climate Change Risks Require Combined Effort. Available: http://www.risksa.com/urgent-forum-on-climate-change-called/. [2017, October, 12].

Van Loon, A., Gleeson, T., Clark, J., Van Dijk, A., Stahl, K., Hannaford, J., Di Baldassarre, G. & Teuling, A. et al. 2016. Drought in the Anthropocene. *Nature Geoscience*. 9(2): 89-91. DOI: 10.1038/ngeo2646.

van Oldenborgh, G. J. 2007. How unusual was autumn 2006 in Europe?. *Climate Past*. 3(4): 659-668. DOI: 10.5194/cpd-3-811-2007.

van Oldenborgh, G. J., Stephenson, D.B., Sterl, A., Vautard, R., Yiou, P., Drijfhout S.S., von Storch, H. & van den Dool, H. 2015. Correspondence: Drivers of the 2013/14 winter floods in the UK. *Nature Climate Change*. 5(6): 490-491. DOI: 10.1038/nclimate2612.

van Oldenborgh, G.J., Doblas Reyes, F., Drijfhout, S. & Hawkins, E. 2013. Reliability of regional climate model trends. *Environmental Research Letters*. 8(1): 014055. DOI: 10.1088/1748-9326/8/1/014055.

Van Oldenborgh, G.J., Sjouke, P., Kew, S., Vautard, R., Boucher, O., Otto, F.E., Haustein, K. & Soubeyroux, J. et al. 2019. Human contribution to the record-breaking June 2019 heat wave in France. World Weather Attribution Group.

van Vliet, M.T., Franssen, W.H., Yearsley, J.R., Ludwig, F., Haddeland, I., Lettenmaier, D.P. & Kabat, P. 2013. Global river discharge and water temperature under climate change. *Global Environmental Change*. 23(2): 450-464. DOI: 10.1016/j.gloenvcha.2012.11.002.

Velázquez, J.-A., Schmid, J., Ricard, S., Muerth, M. J., Gauvin StDenis, B., Minville, M., Chaumont, D., Caya, D. et al. 2013. An ensemble approach to assess hydrological models' contribution to uncertainties in the analysis of climate change impact on water resources. *Hydrology and Earth System Sciences*. 17(2): 565-578. DOI: 10.5194/hess-17-565-2013.

Vicente-Serrano, S.M., Beguería, S. & López-Moreno, J.I. 2010. A multi-scalar drought index sensitive to global warming: The standardized precipitation evapotranspiration index. *Journal of Climate*. 23(10): 1696-1718. DOI: 10.1175/2009JCLI2909.1.

Vogel, C., Koch, I & Zyl, K.V. 2010. A persistent truth-Reflections on drought risk management in Southern Africa. *Weather Climate Society.* 2(1): 9-22. DOI: 10.1175/2009WCAS1017.1.

Vogel, C., Laing, M. & Monnik, K. 1999. Impacts of drought in South Africa 1980-94. In Hazards and disasters: a series of definitive major works. D.A. Wilhite Ed. Oxford, UK: Routledge Publishers.348-367.

Vogel, C.H. & Drummond, J.H. 1993. Dimensions of drought: South African case studies. *Geojournal.* 30(1): 93-98. DOII: 10.1007/BF00807832.

Vogt, J.V., Safriel, U., Von Maltitz, G., Sokona, Y., Zougmore, R., Bastin, G. & Hill, J. 2011. Monitoring and assessment of land degradation and desertification: towards new conceptual and integrated approaches. *Land Degradation and Development*. 22(2): 150-165. DOI: 10.1002/ldr.1075.

Wang, G. L. 2005. Agricultural drought in a future climate: Results from 15 global climate models participating in the IPCC 4th assessment. *Climate Dynamics*. 25(7): 739-753. DOI: 10.1007/s00382-005-0057-9.

Warburton, M.L., Schulze, R.E. & Jewitt, G.P. 2010. Confirmation of ACRU model results for applications in land use and climate change studies. *Hydrology and Earth System Sciences*. 14(12): 2399-2414. DOI: 10.5194/hess-14-2399-2010

Washington, R., Harrison, M., Conway, D., Black, E., Challinor, A., Grimes, D., Jones, R., Morse, A. et al. 2006. African climate change: taking the shorter route. *Bulletin of the American Meteorological Society* 87(10): 1355-1366. DOI: 10.1175/BAMS-87-10-1355.

Water Resource Commission (WRC). 2015. WRC Drought Factsheet 1: Background to current drought situation in South Africa. Pretoria: Water Research Commission.

Water Resources Group (WRG). 2012. Background, impact and the way forward. (Briefing report prepared for the World Economic Forum Annual Meeting 2012). Davos-Klosters, Switzerland: Water Resources Group.

Water Resources of South Africa, 2012 study (WR, 2012). Water Research Commission. Available: http://waterresourceswr2012.co.za/. [2017, June 08].

Water Services Act (WSA). Act, No. 108 of 1997. 1997. Government Gazette 390 (18522). 19 December. Government notice no. 18522. Cape Town, South Africa: Office of the President.

Watts G .2011. Water for people: Climate change and water availability. In Modelling the impact of climate change on water resources. F. Fung, A. Lopez & M. New, Eds. Wiley, Chichester, West Sussex: Blackwell Publishing. 86-127.

Western Cape Department of Agriculture (WCDoA). 2016. Western Cape Climate Change Response Framework and Implementation Plan for the Agricultural Sector. Cape Town, South Africa: Western Cape Government.

Western Cape Department of Environmental Affairs and Development Planning (WCDEDP). 2014. (Western Cape Climate Change Response Strategy). Cape Town, South Africa: Western Cape Government.

Western Cape Government (WCG). 2012. Western Cape Sustainable Water Management Plan. Pretoria, South Africa: Department of Water Affairs.

Western Cape Government (WCG). 2017. Informing the Western Cape agricultural sector on the 2015-2017 drought. (A drought fact sheet). Cape Town, South Africa: Western Cape Government.

Wheater, H. S. 2008. An introduction to the workshop. In Hydrological modelling in arid and semi-arid areas. H. Wheater, S. Sorooshian, & K.D. Sharma, K.D. Eds. Cambridge: Cambridge University Press.

Whitmore, J.S. 1971. South Africa's water budget. *South African Journal of Science*. 67(3): 166-176. DOI: 10520/AJA00382353_3636.

Wilby, R. L., Whitehead, P.G., Wade, A.J., Butterfield, D., Davis, R.J. & Watts, G. 2006. Integrated modelling of climate change impacts on water resources and quality in a lowland catchment: River Kennet, UK. *Journal of Hydrology*. 330(1-2): 204-220. DOI: 10.1016/j.jhydrol.2006.04.033.

Wilby, R.L. 2007. Decadal forecasting techniques for adaptation and development planning. (A briefing document on available methods, constraints, risks and opportunities).UK: Department for International Development.

Wilby, R.L., Troni, J., Biot, Y., Tedd, L., Hewitson, B.C., Smith, D.M., & Sutton, R. T. 2009. A review of climate risk information for adaptation and development planning. *International Journal of Climatology.* 29(9), 1193-1215. DOI: 10.1002/joc.1839.

Wilcox, L. J., Dong, B., Sutton, R.T. & Highwood, E.J. 2015. The 2014 hot, dry summer in Northeast Asia. In Explaining Extremes of 2014 from a Climate Perspective. *Bulletin of the American Meteorological Society*. 96(12): S105-S110. DOI: 10.1175/BAMS-D-15- 00123.1.

Wilhite, D.A. 2016. Droughts: A Global Assessment. Routledge Hazards and Natural Disasters.

Wolski, P. 2018. How severe is Cape Town's "Day Zero" drought?. *Significance*. 15(2): 24-27. DOI: 10.1111/j.1740-9713.2018.01127.x.

Wolski, P., Stone, D., Tadross, M., Wehner, M. & Hewitson, B. 2014. Attribution of floods in the Okavango basin, Southern Africa. *Journal of Hydrology*. 511: 350-358. DOI: 10.1016/j.jhydrol.2014.01.055.

World Economic Forum (WEF) .2014. Global Risks 2014: 9th edition. (Insight report). Geneva, Switzerland: World Economic Forum.

World Economic Forum (WEF). 2016. Global risks report 2016: 11th edition (Insight report). Geneva, Switzerland: World Economic Forum.

World Food Programme (WFP). 2016. El Niño: Undermining Resilience - Implications of El Niño in Southern Africa from a Food and Nutrition Security Perspective. (Analyses assessment). Johannesburg: Regional Bureau for Southern Africa.

World Meteorological Organization (WMO) and Global Water Partnership (GWP). 2016. Handbook of Drought Indicators and Indices. M. Svoboda, & B.A. Fuchs, Eds. Geneva. Switzerland: Integrated Drought Management Programme.

World Wide Fund South Africa (WWF-SA). 2016. Water: Facts & Futures. (Report) Cape Town, South Africa: World Wide Fund.

World Wide Fund South Africa (WWF-SA). 2018. WWF Agricultural Water File: Farming for a drier future. Available: http://awsassets.wwf.org.za/downloads/wwfwaterfiles_19july2018.pdf [2019 [2019, May 29].

Xu, C.Y. & Singh, V. P. 1998. A review on monthly water balance models for water resources investigation and climatic impact assessment. Water Resources Management. 12: 20-50.

Xu, C.Y. 2002. Hydrologic models. Sweden: Uppsala University, Department of Earth Science, Hydrology.

Xu, C.Y., 1999. Climate Change and hydrologic models. A review of existing gaps and recent research developments. *Water Resource Management*. 13(5): 369-382. DOI: 10.1023/A:1008190900459.

Yates, D.N. & Strzepek, K.M. 1998. Modeling the Nile basin under climatic change. *Journal of Hydrologic Engineering*. 3(2): 98-108. DOI: 10.1061/(asce)1084-0699(1998)3:2(98).

Zargar, A., Sadiq, R., Naser, B. & Khan, I. 2011. A review of drought indices. *Environmental Review*. 19(1): 333-349. DOI: 10.1139/A11-013.

Zhang, X., Zwiers, F.W., Hegerl, G.C., Lambert, F.H., Gillett, N.P., Solomon, S., Stott, P.A. & Nozawa, T. 2007. Detection of human influence on twentieth-century precipitation trends. *Nature*. 448(7152): 461-465. DOI: 10.1038/nature06025.

APPENDIX: A

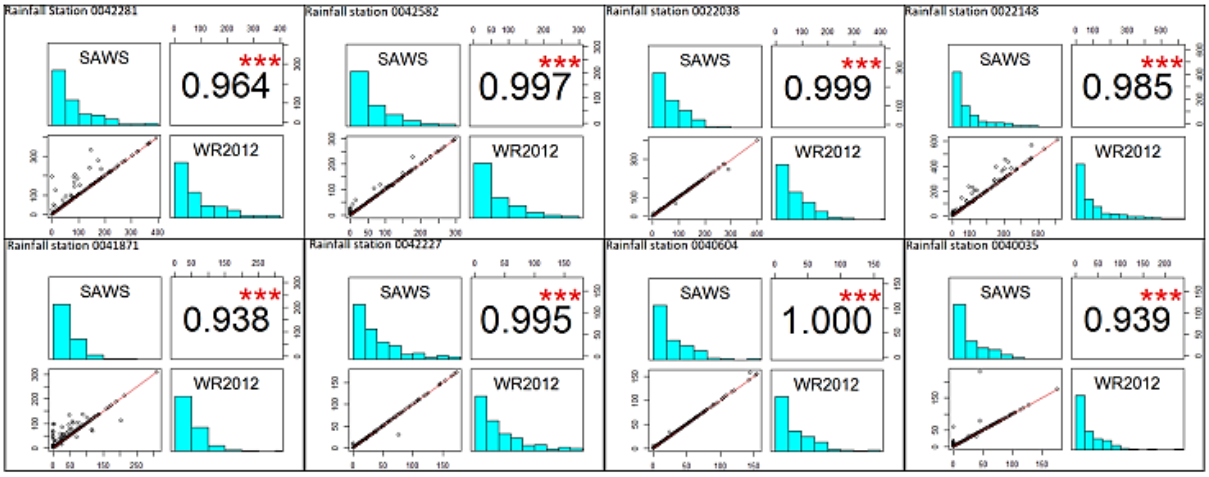

Figure 39. SAWS and WR, 2012 study rainfall station correlation (1979-2017).

APPENDIX: B

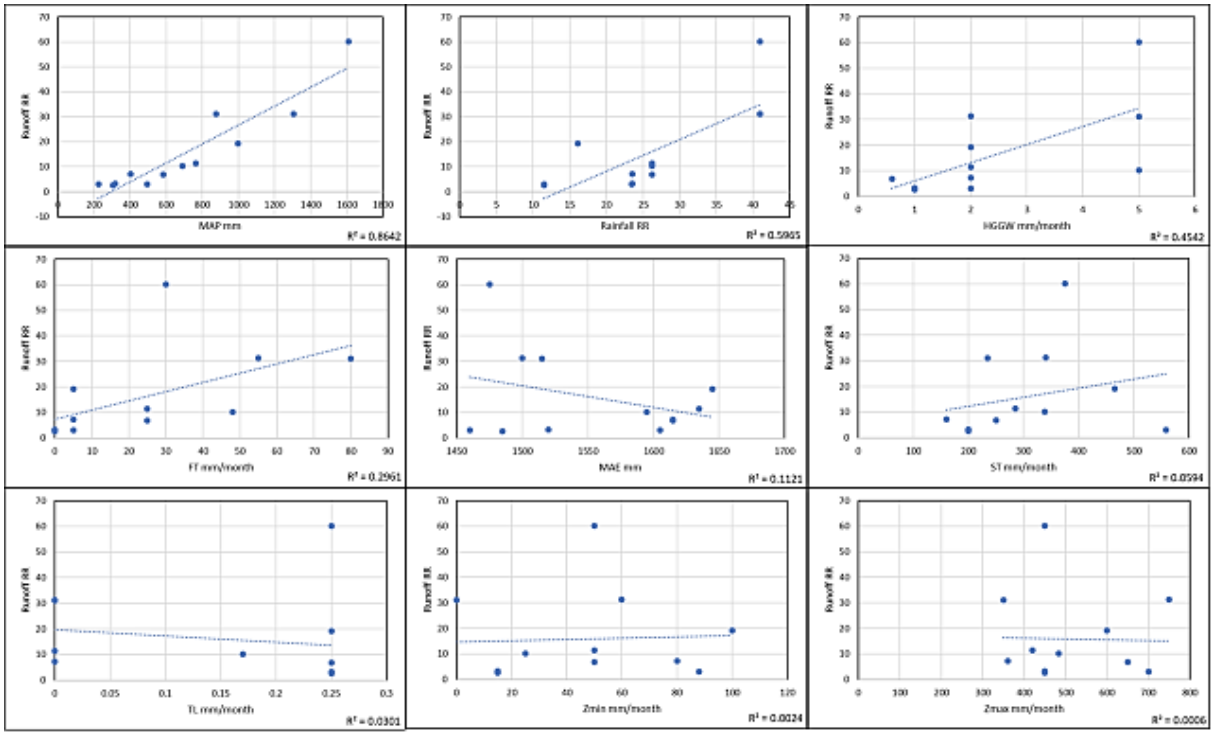

Figure 40. Linear regression of individual hydrological parameters and rainfall RRs against runoff RRs in the BRC, full model.

Table 23. Correlation coefficients between rainfall and runoff RRs and hydrological parameters of the BRC.

	Runoff RR	Rainfall RR	MAE	MAP	FT	HGGW	TL	Zmax	Zmin	ST
Runoff RR	1.00	0.60	0.11	0.86	0.30	0.45	0.03	0.00	0.002	0.06
Rainfall RR	0.60	1.00	0.03	0.58	0.65	0.41	0.26	0.01	0.00	0.02
MAE	0.11	0.03	1.00	0.01	0.01	0.01	0.02	0.03	0.41	0.12
MAP	0.86	0.58	0.01	1.00	0.41	0.57	0.05	0.00	0.01	0.13
FT	0.30	0.65	0.01	0.41	1.00	0.49	0.34	0.00	0.09	0.00
HGGW	0.45	0.41	0.01	0.57	0.49	1.00	0.07	0.10	0.03	0.05
TL	0.03	0.26	0.02	0.05	0.34	0.07	1.00	0.06	0.00	0.07
Zmax	0.00	0.01	0.03	0.00	0.00	0.10	0.06	1.00	0.27	0.41
Zmin	0.00	0.00	0.41	0.01	0.10	0.03	0.00	0.27	1.00	0.40
ST	0.06	0.02	0.12	0.13	0.00	0.05	0.07	0.41	0.40	1.00

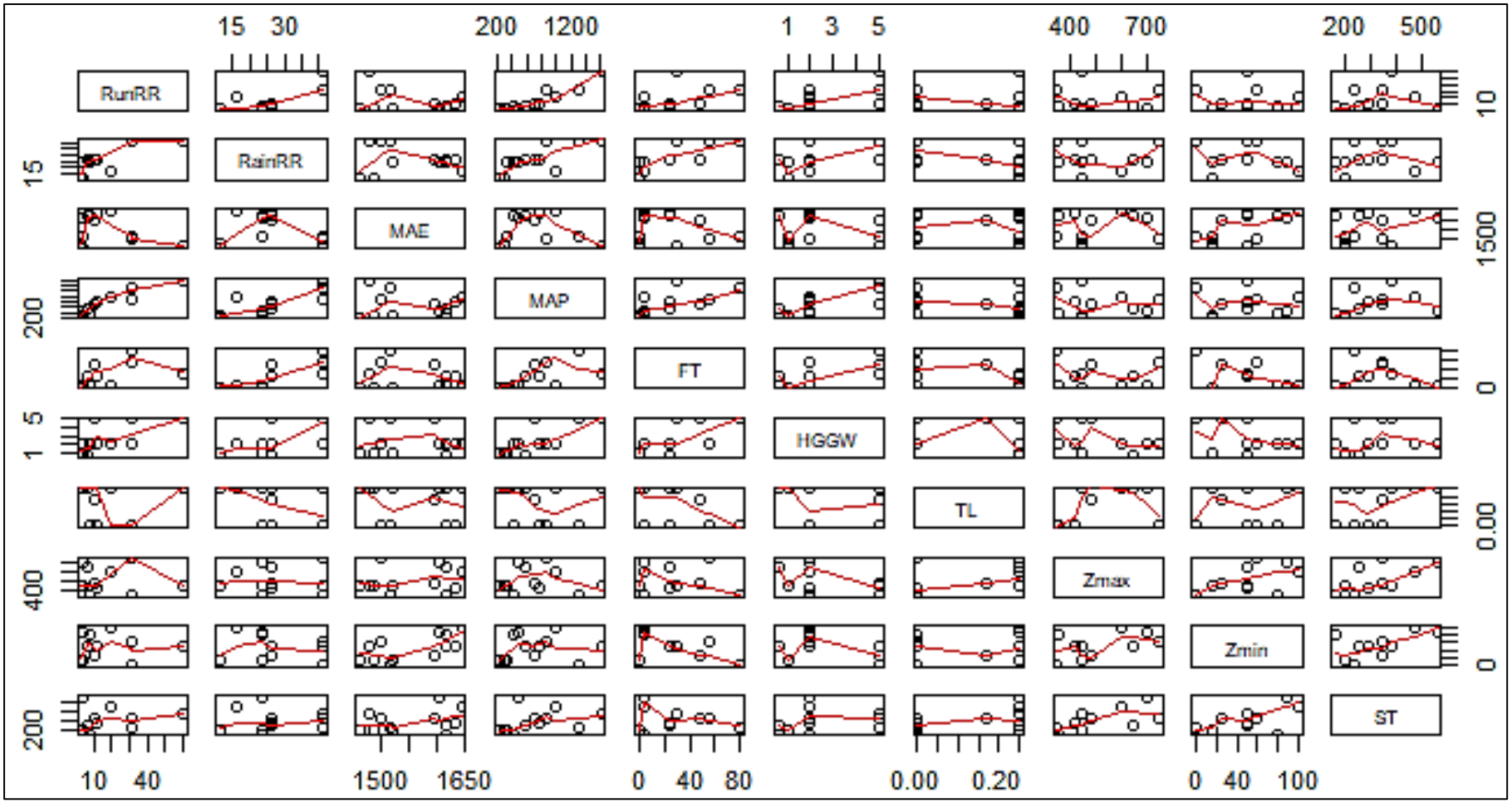

Figure 41. Correlation matrix of calculated runoff and rainfall RRs and hydrological parameters of the BRC.

APPENDIX: C

Table 24. Step one of the stepwise regression.

Runoff RR Against:	**Coefficient of Multiple Determination (R^2)**	**p-value**	**AIC**	**Coefficient p-value**
MAP+MAE	0.93	0.0000047	76.77	0.0000028 , 0.013
MAP+Rainfall RR	0.88	0.000087	84.56	0.0016, 0.41
MAP+ST	0.87	0.0000897	84.63	0.000032, 0.43
MAP+FT	0.87	0.00011	85.06	0.000144, 0.57
MAP+HGGW	0.87	0.0001163	85.32	0.000513, 0.71
MAP+TL	0.87	0.00012	85.45	0.000039, 0.8250
MAP+Zmin	0.87	0.00012	85.38	0.000033, 0.76
MAP+Zmax	0.86	0.00013	85.51	0.000034, 0.93

Table 25. Step two of the stepwise regression.

Runoff RR Against:	**Coefficient of Multiple Determination (R^2)**	**p-value**	**AIC**	**Coefficient p-value**
MAP+MAE+Zmin	0.97	0.0000037	71.02	0.000001, 0.0013, 0.027
MAP+MAE+Rainfall RR	0.94	0.00003468	78.05	0.00026, 0.021, 0.50
MAP+MAE+FT	0.94	0.0000243	76.97	0.000018, 0.012, 0.29
MAP+MAE+HGGW	0.94	0.000034	77.98	0.000081, 0.015, 0.48
MAP+MAE+Zmax	0.94	0.000035	78.05	0.000006, 0.015, 0.50
MAP+MAE+TL	0.94	0.000043	78.70	0.000010, 0.019, 0.84
MAP+MAE+ST	0.94	0.000044	78.77	0.000017, 0.026, 0.94

Table 26. Step three of the stepwise regression.

Risk Ratio Against:	Coefficient of Multiple Determination (R^2)	p-value	AIC	Coefficient p-values
MAP+MAE+Zmin+ST	0.9775	0.0000076	67.96	0.0000016, 0.00078, 0.0081, 0.096
MAP+MAE+Zmin+RFR	0.9722	0.000016	70.47	0.00010, 0.0017, 0.022, 0.24
MAP+MAE+Zmin+TL	0.9682	0.000025	72.09	0.0000060, 0.0021, 0.030, 0.48
MAP+MAE+Zmin+Zmax	0.967	0.000027	72.41	0.0000053, 0.0024, 0.041, 0.56
MAP+MAE+Zmin+HGGW	0.9659	0.000032	72.95	0.00019, 0.0030, 0.050, 0.85
MAP+MAE+Zmin+FT	0.9657	0.000033	73.01	0.000084, 0.0037, 0.071, 0.95

Table 27. Step four of the stepwise regression.

Runoff RR Against:	Coefficient of Multiple Determination (R^2)	p-value	AIC	Coefficient p-values
MAP+MAE+Zmin+ST +Rainfall RR	0.98	0.000038	67.31	0.000099, 0.0012, 0.0091, 0.12, 0.27
MAP+MAE+Zmin+ST +Zmax	0.98	0.000068	69.65	0.000014, 0.0025, 0.0019, 0.014, 0.71
MAP+MAE+Zmin+ST +HGGW	0.98	0.000056	68.88	0.00014, 0.0016, 0.014, 0.094, 0.48
MAP+MAE+Zmin+ST +FT	0.98	0.000072	69.91	0.000081, 0.0025, 0.024, 0.12, 0.89
MAP+MAE+Zmin+ST +TL	0.98	0.000073	69.95	0.000018, 0.0024, 0.016, 0.17, 0.97